Doctoral Dissertation
Doctoral Program in Energy Engineering (33rd Cycle)

Two-component grout in tunnelling applications

Carmine Todaro
* * * * * *

Supervisors
Prof. D. Peila
Dr. D. Martinelli

Doctoral Examination Committee:
Prof. A. Assis, Referee, University of Brasilia
Prof. J. Oh, Referee, University of New South Wales
Prof. D. Boldini, Università di Roma La Sapienza
Prof. R. Bruno, Università di Bologna
Prof. M. Cardu, Politecnico di Torino

Politecnico di Torino
February 29, 2021

I hereby declare that the contents and organisation of this dissertation constitute my own original work and do not compromise in any way the rights of third parties, including those relating to the security of personal data.

…….....

Carmine Todaro

Turin, February 29, 2123

Summary

The filling of the annular void created during the advancement of shielded machines is an operation of paramount importance although it occurs in a hidden area between the ring extrados and the excavated medium, not directly visible to operators. Nowadays, the most commonly used technology for this purpose is two-component grout, based on two fluids that, once mixed together, give rise to a gel in a few seconds, whereupon the hardening process starts, leading to a weak concrete suitable for the designed purposes of locking rings in the designed position, bearing the backup load, ensuring immediate support to the excavated medium and improving the waterproofing. Despite the current intensive use of two-component grout, very little information is at present available on this material. This lack concerns especially the unavailability of suitable standard regulations able to characterise the material. This has the result that different approaches are being adopted on different construction sites, where engineering issues have often been approached differently.

In this work, a standard procedure that is able to reproduce at laboratory scale a component A similar to the one produced on the construction site is provided. Furthermore, the mixing, casting and curing modalities of the two-component grout samples are also described. Thereafter, the mechanical characterisation is developed, focusing on the main parameters strongly required by engineers involved with the two-component field that to date have never been studied, namely the elastic properties and the shear strength. Furthermore, the issue of durability is addressed with an experimental approach based on the ageing of two-component grout samples cured in sand or subjected to the action of air and water. Speaking of water, a specific apparatus has been developed with the aim of studying the effect of water on the hardened two-component grout.

Finally, the effect of bentonite on the grout is investigated in depth and a procedure to guide engineers to the best choice of this raw material for the

production of component A is provided. Preliminary results of a two-component grout produced with an innovative raw material that is able to completely replace the use of bentonite are also presented.

Acknowledgement

Acknowledgements are mandatory when people outside the academic institution supported the development of the research that was performed in order to reach the conclusion of the doctorate program.

I would like to dedicate this thesis to my loving parents, my brother Michele and to my wife (draft)

Contents

List of Tables

List of Figures

Chapter 1

Introduction

The globalisation and the development of modern society have had a strong impact on the human life-style, mainly in the last years, concerning also the issue of transport. The necessity to travel towards places ever more distant from one's own dwelling place while having ever less time available is a common situation that arises not only for business reasons. The agile approach (i.e. smart working or virtual meetings) often cannot completely replace a face-to-face relationship, so the need to move quickly and safely is nowadays a requirement that our city structures must successfully satisfy.

Considering the modern view of cities, crowded and frequently gridlocked because of traffic jams, it has become clear that transferring entire traffic flows underground could guarantee a higher quality of life in the open spaces (Figure 1).

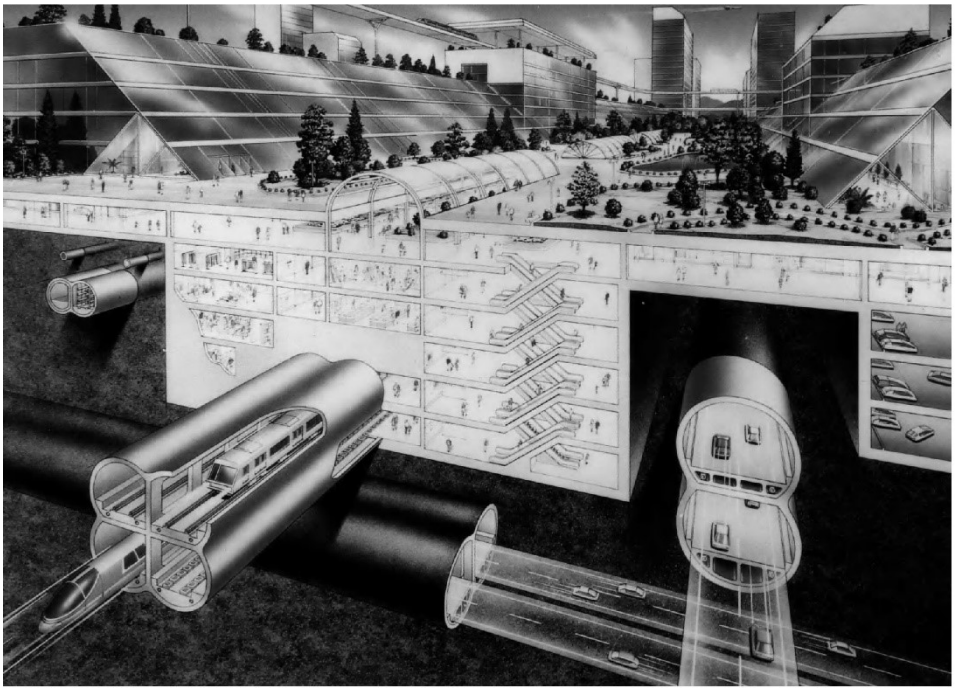

Figure 1 - Tunnelling activities in Japan 1990, Tokyo (Maidl et al., 2013).

In the last decades, traditional and mechanised methods have been successfully used in order to realise underground structures and the methodology choice is commonly linked to the work context, its peculiarities and economic reasons. Concerning tunnel projects in urban areas, the impact of the construction on open spaces has led engineers to prefer a full-face mechanised approach using shield machines. Although shield machines cannot be used for every tunnelling project, their different advantages are contributing to the widespread use of this construction methodology. Maidl et al. (2013) provided a concise and clear list of the main benefits of shield machines compared to other excavation methodologies. The key concepts are reported in the following:

- minimisation of the impact on the surface (in terms of noise, vibration and subsidence);
- high level of precision concerning the profile and the route;
- very high safety level for employers;
- possibility to work successfully also below the groundwater table;
- the full mechanisation of the process (excavation, front face stabilisation, mucking, support of the excavated cavity, final support) ensures a high rate of advancement.

This research is focused on a specific phase of the tunnelling construction proper of shielded machines: the backfilling. The backfilling phase involves different types of shielded machines. Specifically, all machines designed with an advancement system based on thrust cylinders and precast linings have integrated the backfilling phase in the excavation process. To give one example, Figure 2 depicts the scheme sections of a typical slurry machine (left) and an EPB machine (right), which are the most widely used and versatile machines currently available on the market. To describe briefly the excavation phase, the cutterhead rotates, the mucking circuit (in the case of a slurry machine) or the screw conveyor (in the case of an EPB) is active and guarantees the removal of muck from the excavation chamber, the thrusting cylinders provide the pressure necessary for penetration of the cutters and the friction to be overcome, while, simultaneously, an annular gap is left between the linings extrados and the excavated medium. It is in this exact context that the backfilling phase is framed.

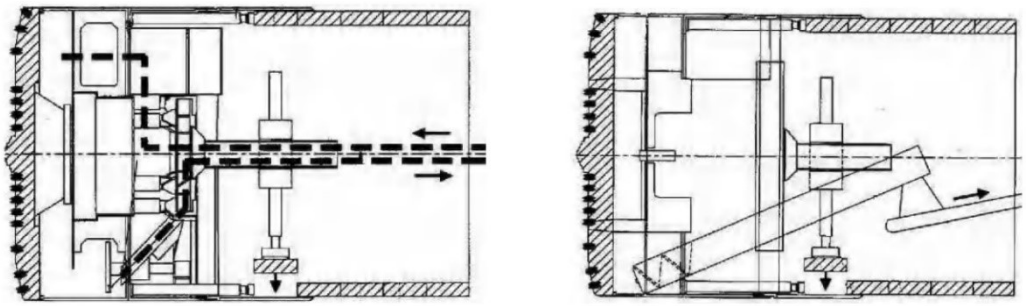

Figure 2 - Slurry and EPB schemes (Maidl et al., 2013).

The work performed is an in-depth investigation of different aspects of two-component grout material. In fact, it should be reported that the complete research path was not completely defined from the beginning but, once started, different issues were encountered and these new, unforeseen topics and the need to study them were also then involved in the research. Not all of the first ideas turned out to be correct, but, in my opinion, some of the unsuccessful experiences also contributed to increase my knowledge about the studied phenomena, contributing to increase my critical eyes. For this reason, in some chapters, a special paragraph named “additional information” has been inserted with the purpose of sharing with readers also the main, and no less important, unsuccessful experiences. Finally, in order to keep in mind the main results obtained, some sentences expressly written in italics called *“key concepts”* have been inserted in the text.

Chapter 2

Backfilling

2.1 Introduction to the backfilling issue

What is backfilling? This operation is strictly linked with the basic technology that shielded machines use for excavating and building tunnels. When a shielded machine advances, linings are continuously transported and assembled in rings. The assembling process is carried out under the protection of a shield (Figure 3). Therefore, for geometrical reasons, the drilled diameter must be bigger than that of the outer rings.

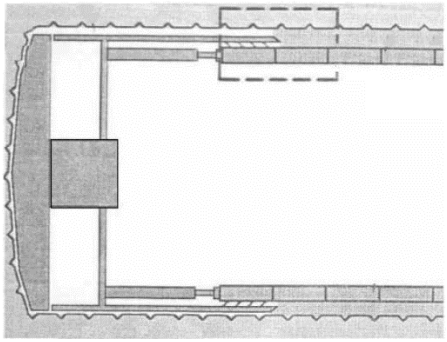

Figure 3 - Shielded machine showing the difference between drilled diameter and ring outer diameter. Modified from Peila et al. (2011)

The circular crown that is obtained is a gap called the *annulus* (Peila et al., 2011). The annulus filling operation is named the backfilling process.

Four factors should be analysed, the sum of whose thicknesses provides the amount of the gap (t_g).

1. The overcut (t_{oc})

Taking into account the head of any machine, the last level of disk cutters (the farthest from the centre) located circumferentially is characterised by an application angle that diverges from 90°. These kinds of disks are called “overcut

disks" or simply "overcuts". In this way, assuming that the bearings of each disk are properly designed (taking into account also transversal forces due to a non-orthogonal application), a drilled diameter bigger than the head diameter can be obtained.

2. The shield conicity (t_{sc})

Immediately after removal of the medium material and the progressive advancement of the machine, the convergence phenomenon starts to progressively reduce the hole diameter (Ye et al., 2015). The conicity is designed in order to reduce friction between the shield and the medium mainly during curved advancing.

3. The shield thickness (t_s)
   properly designed as a function of the machine diameter and the geology.
4. The tail brushes (t_{tb})

The gap between the ring extrados and the shield intrados must be sealed in order to avoid external material reaching the internal part of the machine (for instance, if operators mismanage the advancement of the machine, the conditioning process or the backfilling process, injected materials can flow along the shield and enter the abovementioned gap). The sealed system is composed of tail brushes (usually made of steel), arranged circumferentially usually in three lines (Figure 4).

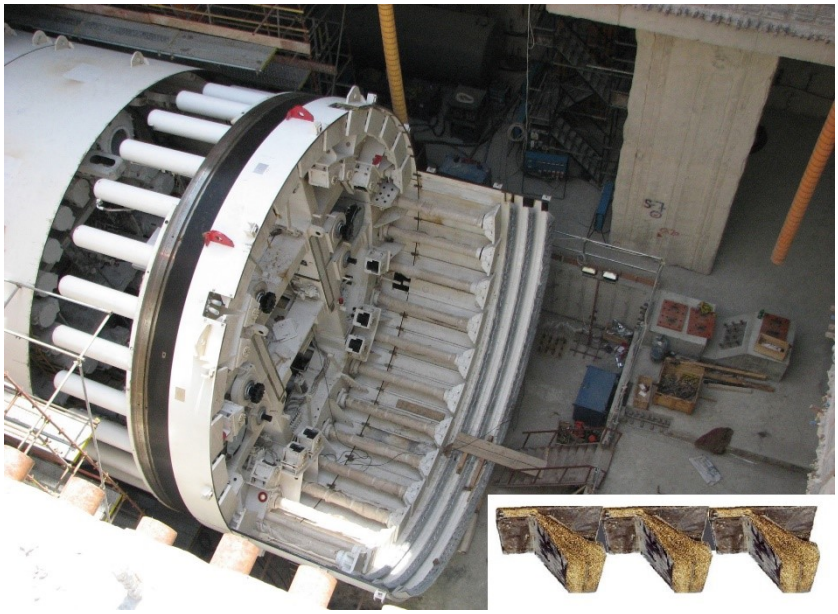

Figure 4 - Tail brushes of a shielded machine. The three circumferential lines are clearly visible. The photo is property of UTT Mapei. (Richard Schulkins master lecture, 2020).

The circular space between the external circumferential lines and the centre one is continuously filled with special grease. The cooperation of the grease and

tail brushes creates a perfect seal system that permits every external flow to be blocked in a certain range of pressure.

Thus, the comprehensive thickness of the annulus can be calculated as:

$$t_g = t_{oc} + t_{sc} + t_s + t_{tb} \quad (1)$$

In Figure 5 a scheme graphically represents Equation (1).

The value of t_g usually ranges between 130 and 180 mm, as discussed by Thewes and Budach (2009).

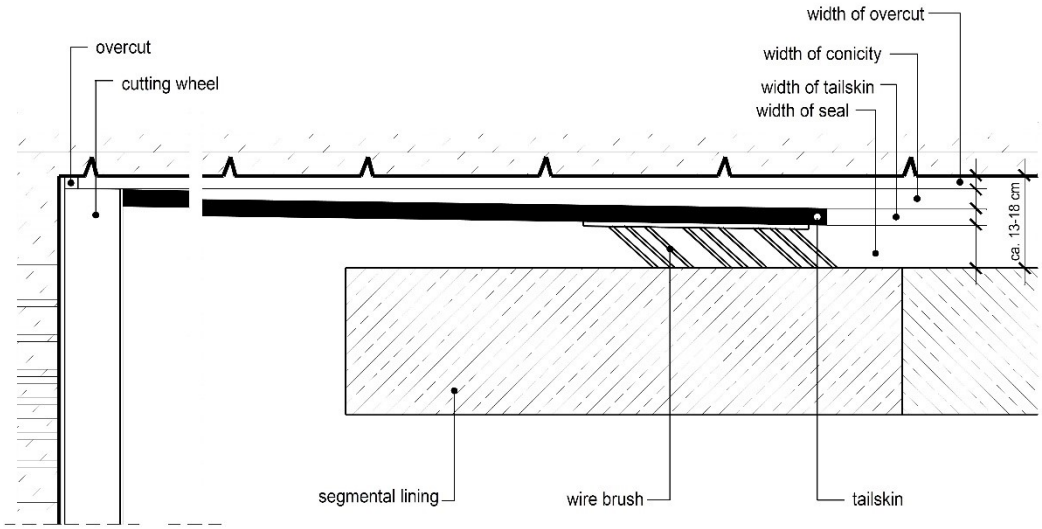

Figure 5 - Scheme of a longitudinal section related to a shielded machine and focus on the factors of the annulus thickness (Thewes & Budach, 2009).

Another factor that should be taken into account is the minimum radius of curvature that the machine must be able to overcome. Thereby the final annulus thickness that should be considered can be further increased (Guglielmetti et al., 2007).

2.2 The reason

At this point of the scientific processing it is clear that by using shielded machines, the creation of an annulus cannot be avoided. But why is the backfilling process considered so important? Different authors have addressed the topic and in the following the main reasons analysed in the scientific literature will be reported.

The first information can be found in EFNARC (2005), where it is required for the backfilling material to be a bond between the ground (or the rock) and rings. Specifically, it should:

- prevent rings flotation and heave;
- prevent surface subsidence;

- prevent rings misalignment;
- link soil (or rock) and rings into one single medium.

Bezuijen et al. (2005) have added some further information, particularly regarding subsidence. More specifically, the paper explained the role played by the injected material in reducing surface settlements over the tunnel. Taking into account that the tail void ranged between 3% and 16% of the whole internal tunnel volume, it was clearly highlighted how an incomplete filling operation could lead to non-negligible surface settlements. Still concerning subsidence, Ye et al. (2015) stated that the tail void grouting is considered the most likely factor leading to huge surface settlements.

Peila et al. (2011) and Pelizza et al. (2012) have highlighted the paramount importance of the backfilling process, providing more details regarding the requirements that should be satisfied. Firstly, the filled annulus should block segments into the design position, avoiding flotation and heave due to segments' self-weight and thrust forces applied by the machine. Secondly, the injected material should bear the backup machine load, ensuring uniform contact between the medium and the linings and avoiding punctual loads. Furthermore, the waterproofing action that a well performed backfilling should ensure to the comprehensive "linings + gaskets" system is also introduced. Thewes (2013), Youn & Breitenbücher (2014), Boscaro et al. (2015) and Dal Negro et al. (2017) confirmed the role of backfilling in the tunnelling sealing. Ivantchev & Dal Rio (2015) introduced also the phenomenon of the reduction of leakage through the tail-brushes due to an optimal injection.

Although different authors have considered an active role for the backfilling in the waterproofing aspect, only Youn & Breitenbücher (2014) investigated the topic in depth, performing dewatering tests by using mixes made up of various fineness of cement, fly ash, limestone and different dewatering pressure. Concerning the interaction between the backfilling operation and the groundwater, ITATech (2014) introduces the problem of the grout dilution. It was reported that the single-component technology seems to be affected more strongly than the two-component one. It is also suggested to add specific anti-washout agents in order to limit or avoid this issue.

2.3 Methods

The backfilling process can be carried out by using two different modalities, differing substantially according to the location of the injection points. In particular, the backfilling grout can be injected in the annulus:

- through linings;
- through the shield.

As will be carefully discussed in the next paragraphs, different materials can be used for a backfilling operation, but not every material can be injected in both modalities.

2.3.1 Injection through linings

Backfilling grouting carried out through the linings is the most traditional method.

In order to use this method for filling the annulus, linings must be designed and realised expecting a suitable hole for the injection, which is commonly closed during the installation with plugs or specific valves. When a complete ring is assembled, the injection can be performed only when the shield has completely passed the linings (or at least when the last row of steel brushes has passed the ring). This time lapse could allow small collapses of material from the excavated tunnel contour that might lead to settlements, which are non-negligible in the case of shallow tunnels. On the other hand, the risk of clogging is minimal (ITATech, 2014). Usually just one single injection is designed for each ring, whereby the crown of the annulus should remain allegedly empty. Roughly, by using this injection modality, the thickness of the empty area can be considered as 1/100 of the machine diameter (Thewes & Budach, 2009).

2.3.2 Injection through the shield

The abovementioned drawback concerning the potential subsidence that may occur by using a backfilling methodology through the linings has been overcome with the introduction of injection nozzles at the end of the shield tail. The mortar flows along pipes with energy supplied by specific pumps and, at the end, through special nozzles, it is injected directly into the annulus (Figure 6).

This methodology makes it possible to carry out the backfilling process continuously, drastically reducing the subsidence. This positive result was highlighted for the first time in 1982, after its introduction during the construction of Line 4 of the Osaka Subway, Japan (Hashimoto et al., 2005). In this specific case, a two-component grout was used and ground settlements of 50–100 mm were expected by using classic mortar grouting, but instead the actual ones were of 10–30 mm by using injection through the shield (Hirata, 1989).

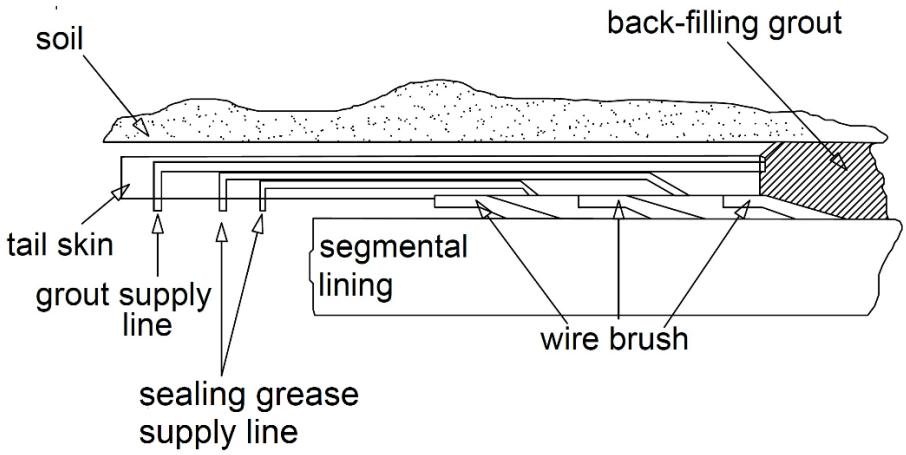

Figure 6 - Scheme of the backfilling injection system through the shield. Dimensions not in scale (Todaro et al.,2020).

2.4 Technical and operational features

In order to obtain a backfilling material that is able to satisfy all the requirements discussed in the previous paragraph, some further aspects were analysed by Peila et al. (2011). Firstly, the backfilling should ideally be carried out instantaneously, indeed only filling the annulus soon so that possible settlements and ring movements can be reduced or avoided. For this reason, especially in shallow tunnels, using shielded machines with the tail injection systems is preferred. Secondly, in order to ensure a good link between the rings and the surrounding medium, the annulus should be completely filled. As a third aspect, the reliability of the comprehensive backfilling system must be ensured, considering the whole process: starting from the delivery of raw materials (by raw materials suppliers), the batching station process (when expected for the technology used) and also during transportation, storage in the machine and finally during and after the injection. For the reliability of the whole process, the grouted material should be expressly designed in order to guarantee the constancy of the base parameters of the grout, such as the pumpability (when pumps are used), the workability for a certain time step (usually considered as 72 h, equal to the maximum ordinary maintenance duration) and the avoidance of a segregation phenomenon or the starting of setting before the injection. Besides, Pelizza et al. (2012) highlighted the necessity for the grouting material to gel quickly after injection (in this paper, also if not clearly declared, the reference to two-component technology seems obvious, being the two-component technology the only one characterised by a gelling process), but not so fast in order to avoid choking of the nozzles. Furthermore, the grouting material should permit the re-starting of the injection process when needed and should be homogeneous in terms of mechanical and physical properties at every point of the annulus. Lastly, considerations pertaining to the resistance against the washing action of groundwater are reported by authors. Youn & Breitenbücher (2014) introduced also a requirement concerning the fast development of the stiffness modulus and

the shear strength of the injected grout, which should be equal to those of the surrounding medium.

2.5 Materials

Different materials can be used for performing the backfilling.

In EFNARC (2005), two different classifications concerning the possible kind of materials are reported. The first classification is based on the specific ability of the grout to perform the hydration process. In other words, considering the cement as the most commonly used binder component, the first classification recognises classes as a function of the use and dosage of the cement. This classification includes:

- active grout: the injected material contains a binder that performs a full hydration process, for instance, Portland cement metered at more than 300 kg/m^3;
- inert grout: there is no cement inside the injected material. Pea gravel is a typical example;
- semi-inert grout: the injected material is composed of the same matrix as the inert grout plus a small amount of material able to generate a certain degree of hydration, for instance, Portland cement metered at less than 100 kg/m^3;

The second classification, undoubtedly simpler and mainly used by tunnelling engineers, is based on the number of components that are used in order to obtain the final grout for the backfilling. This classification includes:

- mono-component grout (or single-component grout);
- two-component grout.

2.5.1 Inert grout

Inert mixes are often used in tunnels excavated in hard rock. Pea gravel consists of washed gravel with particle diameters ranging between 8 and 12 mm (Thewes & Budach, 2009), but also sands transported in water are often used (Peila et al., 2011). The inert mix cannot be pumped through the shield, so the backfilling operation is performed through the segments, only after the shield is completely running ahead of the considered ring. In ITATech (2014) a scheme property of Robbins (Tunnel Segment Backfilling with Double Shield TBMs) shows a tunnelling section and the point of injection for the pea gravel, located in the upper part of the analysed ring (Figure 7).

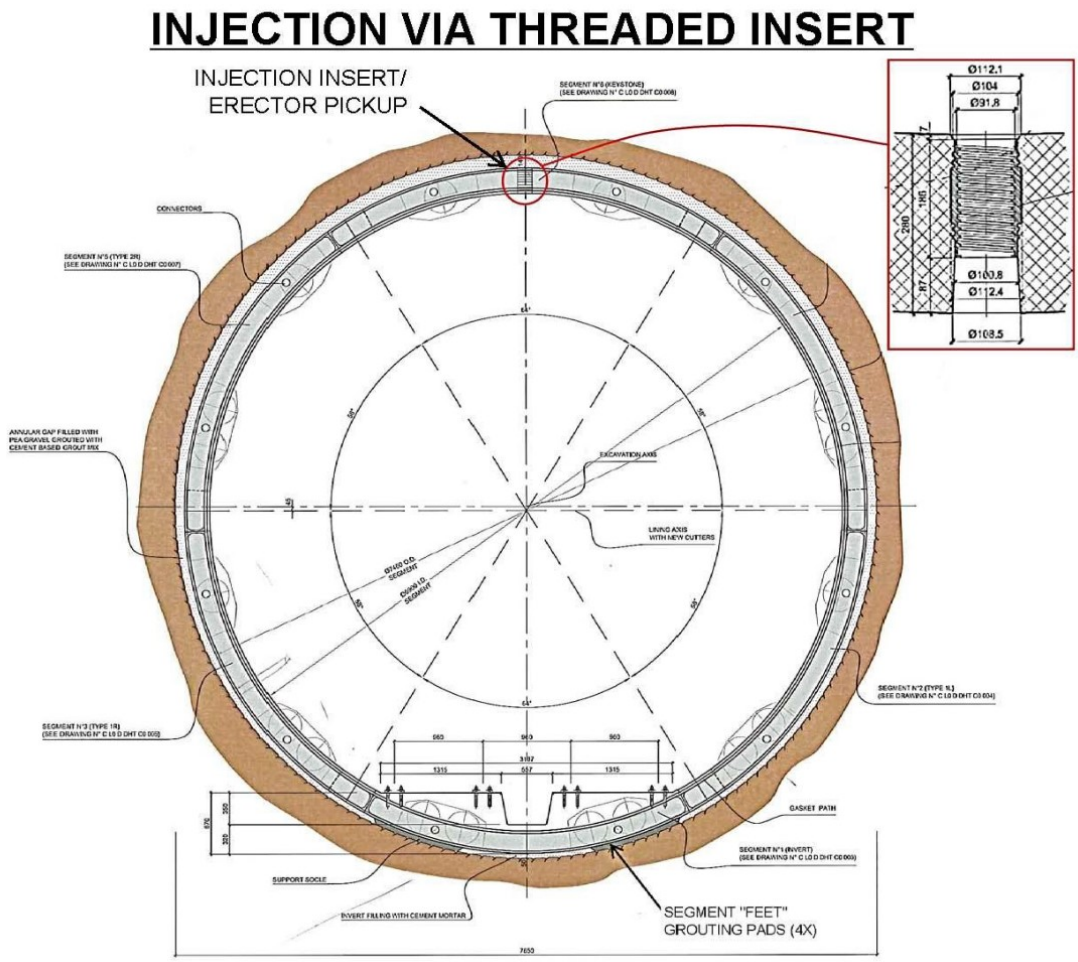

Figure 7 - Pea gravel injection through segments (Tunnel Segment Backfilling Double Shield TBMs, Robbins).

Home (2014) provided an operative scheme pertaining to the geometry along the tunnel axis, indicating that the annulus filling should be performed following the "angle of repose" criterion, from the top of the ring located a few metres back from the tail shield (Figure 9). Starting from the last assembled ring and following the angle of repose proper of the type of pea gravel used (45° in the example), it is possible to compute for how many rings after the last assembled one it is possible to operate the backfilling without risk of injected material flowing inside the machine head. In the Robbins brochure (Tunnel Segment Backfilling with Double Shield TBMs), the most useful kind of pump for this type of injection is recognised as the dry type rotary shotcrete pump (Figure 8).

Figure 8 - Rotary machine. The photo is property of the UTT Mapei. (Richard Schulkins master lecture, 2020).

Furthermore, in order to avoid choking and clogging phenomena, the minimum suggested insert diameter should be bigger than 70 mm while DN60 or DN70 should be used as hoses.

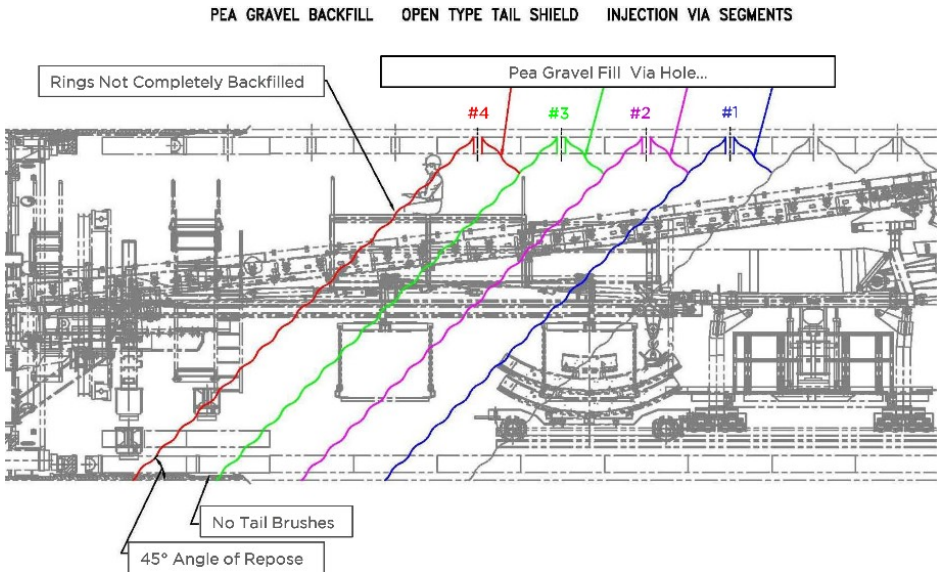

Figure 9 - "Angle of repose" criterion. In the schema reported, the backfilling injection is carried out through the 4th chronologically assembled lining (Home, 2014).

Often, the annulus filled with pea gravel can be re-injected with a mortar, in order to fill all the empty spaces between the particles and provide a certain level of strength and waterproofing. Figure 10 shows an example of the final backfilling material after the secondary injection phase.

Figure 10 - Sample of pea gravel after a cement mortar secondary injection. The photo is property of UTT Mapei. (Richard Schulkins master lecture, 2020).

2.5.2 **Active and semi-inert grout**

Active and semi-inert grout are characterised by the presence of a binder in the elements composing the grout material, typically cement. These kinds of materials for the backfilling are made up of water, cement, bentonite and chemical components specifically added in order to reach the required specification, such as plasticisers or retarders (more details concerning the mortar specification will be explained in the following).

The injection can be performed either through the tail skin or through segments, taking into account that the mortar requirements and the final grout properties will be different for each case, as the pumping systems differ. Peila et al. (2011) and Pelizza et al. (2012) highlighted the strong connection between the mortar properties and the reliability of the raw materials used. Moreover, construction site experiences show how small variations of the raw material's technical properties can lead to choking of supply pipes and consequent long and expensive maintenance. Therefore, for example, the cement fineness, the salts concentration in the water or the silicate concentration in the accelerator are parameters that should be continuously and systematically checked (with an established frequency) in order to avoid drawbacks.

Table 1 reports different mix designs used in real construction sites. All of them refer to active grout, and specifically mono-component grout. According to the definition reported in the introduction of paragraph 2.5, it could be apparently wrong to classify the case histories from St. Petersburg and Toulouse as active grout, since the cement dosage is plainly lower than 100 kg/m^3. Actually, in these cases also the fly ash must be considered as a binder element, due to its

involvement in the cement hydration reaction and its non-negligible role in increasing the final performance of the grout.

Table 1 - Mix designs used in real construction sites. Guglielmetti et al. (2007) and Novin et al. (2015). The percentages values are intended by volume.

country	Russia	Portugal	Italy			United Kingdom	France	Iran			
Components (kg/m^3)	St. Petersburg	Porto	Torino	Bologna	Milano	Hastings	Toulouse	Shiraz	Esfahan	Tabriz	Aboozar
Cement	70	200	220	370	240	110	60	100	150	150	250
Water	260	230	250	270	300	255	240	520	270	350	494
Water lime	/	60	/	/	/	/	/	/	/	/	/
Silica fume	400	/	/	/	/	/	/	/	/	/	/
Fly ash	300	120	380	/	/	330	120	/	/	/	/
Filler		/	/	580	450	/	150	120	550	250	/
Aggregates	1380	1530	1250	880	1200	1305	1430	900	1200	1300	1300
Bentonite		/	/	/	/	10	16	33	45	50	20
Plasticisier	4,1 (%)	2 (%)	4 (%)	3 (%)	/	/	/	/	/	/	/
Retarder		0,1 (%)	/	/	/	/	/	2 or 3 L	4 L	2 L	2 L
Reference	Guglielmetti et al. (2007)					Novin et al. (2015)					

2.5.3 **Active grout: the two-component mix**

The two-component grout is based on two fluids that will be identified in this doctoral thesis as component A and component B. Component A is a mortar (cement-based suspension) while component B is an accelerator. This kind of technology has a wide versatility and it can be used in soil or rocks (Thewes & Budach, 2019). When the components are mixed, the material obtained gels in a few seconds and starts instantaneously to increase its mechanical properties.

As this PhD thesis is focused on this kind of technology, further information and more details will be provided in the next chapters.

2.6 Mono- or two-component grout?

Currently, mono-component grout and two-component grout are the main technologies used in the field of tunnelling backfilling. Although at this point in the thesis readers still do not have a thorough knowledge of the two-component grout technology, a brief paragraph concerning a comparison between these two valid backfilling systems is due.

ITAtech (2014) provided a complete analysis concerning a comparison of the two technologies, identifying eight key parameters that can be used for establishing grout selection criteria.

2.6.1 **Strength**

The grout strength depends on the mix designs but, generally speaking, mono-component grout offers a higher level of strength. The reason for the lower strength performance of two-component grout is the absence of aggregates and the higher water/cement ratio.

2.6.2 **Costs**

By choosing mono-component grout, the initial costs are lower although the convenience is not so marked if the necessary grout volume is taken into account in the cost estimation. Moreover, the costs are also strictly linked with the methodology of injection: injecting through segments does not require a bigger bore diameter. The major disadvantage of the two-component technology is that the tail tubes installed in the shield tail require a bigger bore diameter, with a consequent cost increase. Nevertheless, in counting the cost also the settlement control should be taken into account; this is easily managed with the two-component technology but hard to control using mono-component grout.

2.6.3 **Transportation**

The transportation has a strong impact on tunnelling construction and timing considerations. Single-component grout is usually transported by grout cars, while

two-component grout is directly pumped from the batching station. The best transportation approach should be estimated taking into account the volume of the material requiring injection, the tunnel length, depth and size.

2.6.4 Groundwater effects

The main problem of the action of groundwater on the backfilling grout is the potential dilution of the mortar. This effect is preliminarily recognised as having a higher impact on the mono-component grout. Two-component grout, injected at very high pressure, should shift the water, suffering less from the dilution phenomenon.

2.6.5 Early support of lining

Early support of linings is always required, since it locks the linings in the designed position and blocks the convergence phenomenon, reducing the surface settlements in shallow tunnels. In conclusion, early support is always required as soon as possible. The two-component grout easily satisfies this prescription, while mono-component grout has a slower setting time, a strong function of the speed of the cement's hydration reaction.

2.6.6 Pumpability/fluidity

The fluidity and the pumpability of the grout are very important in the transportation context and have an important role also in the injection phase. Higher fluidity means easier transportation and injection. Two-component grout is more easily transported, pumped and injected since, as will be better explained in the next chapters, these parameters are involved in the specific project of the two-component mix design.

2.6.7 Batching plant

No relevant differences can be highlighted between the two technologies.

2.6.8 Maintenance operations

The workability is a basic parameter used for the two-component mix designs project. This characteristic makes it possible to avoid line choking, which is statistically more frequent when using mono-component grout.

2.7 Conclusions

Although the above illustrated subdivisions are very useful in an academic approach, it is commonly the case that at real working sites more than one

technology or material is used in order to successfully complete the annulus filling.

Càmara (2018) reported the real case study of the "Legacy Way" in Brisbane (Australia). The backfilling phase was scheduled in two parts: the first based on a two-component mix injected through the tail shield aimed at filling the bigger part of the void, and the second one based on mono-component grout carried out through the segments with the aim of filling the crown. Both materials were active grout but the mix designs were completely different. Furthermore, the raw materials used could also be different and the requirements that the final grout should satisfy were normed by different specific documents. For example, in the specific case of the Legacy Way, after 28 days of curing a compression strength of 4 MPa was required for the two-component backfilling, while 12 MPa was expected for the mono-component one.

Another interesting example reported in Dal Negro et al. (2017) pertains to the construction site of the exploration tunnel for the new Turin–Lyons railway. In this case, the two-component backfilling was injected in a double way, namely first through the tail skin and then through the segments. According to the contractor's choice, the whole of the required grout was injected in different steps (some using the machine injection lines and some through ports appropriately located in the segments).

Concerning the use of inert and semi-inert grout, Thewes & Budach (2009) supplement the idea of using more than just one technology or material also concerning pea gravel. This paper highlights that a combination of mortar and gravel is commonly used as grout material for the backfilling. First the mortar is injected in the annulus at the bottom in order to lock the ring in the designed position, and secondly the gravel is inserted in order to avoid settlements. As a last step, the crown is filled from the top.

Also in ITATech (2014) it is reported that voids normally created between the gravel particles located in the annulus after the injection are commonly grouted by means of mono-component grout, usually performed a few segments back from the tail shield.

Finally, it is impossible and may be misguided to univocally define the best backfilling technology. On the contrary, in order to successfully design the backfilling operation of any tunnel project, it is crucial to know exactly the pros and cons of each backfilling technology and to schedule the backfilling phase by exploiting the potential advantages of each methodology.

Chapter 3

The two-component grout

In this chapter the basic operating principles of the two-component technology are described. The different areas of a typical construction site are introduced and described in respect of the backfilling process, with particularly detailed attention to the machine context. The strong technical specifications that the final grout should satisfy are listed and described and the mix design is introduced as the main tool for managing the grout properties. Finally, some information concerning the construction site tests and the maintenance operations is reported.

From this chapter, the injection of the backfilling grout is considered as being performed through the shield nozzles.

I declare under my accountability that the contents of this chapter are part of a number of different published papers: Todaro et al. (2019, 2020a, 2021).

3.1 General aspect

3.1.1 **Working principle**

The first certified use in a shielded machine of two-component grout as a backfilling technology dates back to 1982, in the construction of the No. 4 line of the Osaka Subway (Japan) (Hashimoto et al., 2005).

Two-component grout is made up of two different liquids, both stable from the physical and chemical point of view in order to guarantee their workability for all the backfilling process, starting from the batching station and ending with their injection through the tail shield nozzles.

The two liquids are named respectively component A and component B. Component A is a mortar composed of water, cement, bentonite and retarding/fluidifying agent, while component B (also named simply an accelerator) is commonly a sodium silicate solution.

It should be pointed out that also other components are now starting to be used for the manufacturing of component A. The case history reported in Càmara

(2018) concerning the Legacy Way (Brisbane, Australia) shows how fly ash was successfully added to the mortar in order to reduce the amount of cement. Furthermore, the addition of blast furnace slag, fly ash and metacaolin and their positive impact on the final two-component grout performance have been studied by Schulte-Schrepping & Breitenbücher (2019a).

In general, however, when component A and component B are mixed, the material obtained gels in a few seconds.

Definition 1: the gel time (or gelling time) is the elapsed time measured from the first contact between the two components till the obtained mix loses the liquid behaviour.

Definition 2: the gel time (or gelling time) is the elapsed time measured from the first contact between the two components till the obtained mix starts to exhibit shear strength.

Hashimoto et al. (2005) is the first reference that provides a graphical description of the working principle of the technology, integrated also with information concerning times and strengths (Figure 11). Obviously, the reported strength value of 0.1 MPa (assuming by reference to the uniaxial compressive strength but not specified on the chart) after 1 hour of curing should be considered in the context of a first construction site application of an experimental technology, realised with the available raw materials coming from the cement world not expressly designed for the purpose (as nowadays) and applied by employers without specific experience. Thereby, this strength value should not be compared with those that are currently easily obtained on construction sites.

However, it seems to be a valid starting point for explaining the different system phases and the technology. To better describe the chart and to avoid cumbersome text, however, numbering from 1 to 3 has been added on the timeline pertaining to the plant locations.

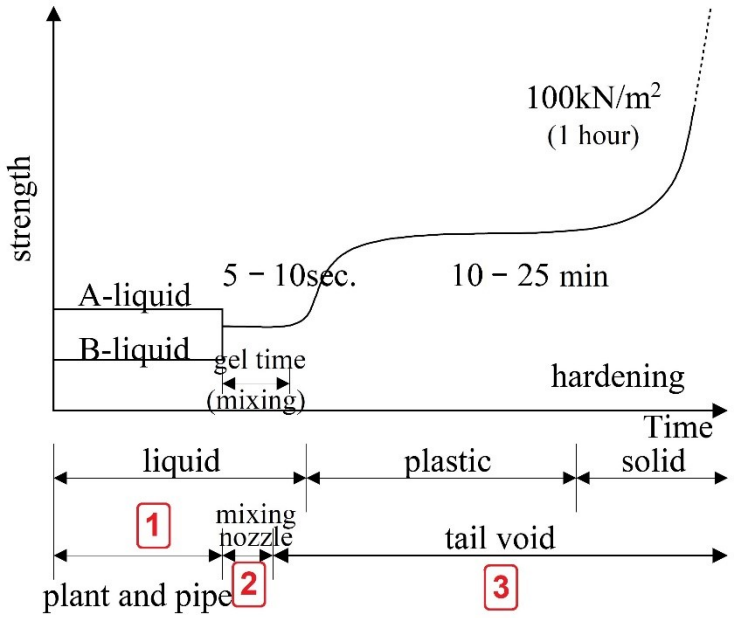

Figure 11 - Two-component technology working scheme. Modified from Hashimoto et al. (2005).

Before the description, a basic concept should be highlighted; indeed, failure to respect it can compromise the comprehensive working of the system:

KEY CONCEPT 1: For the correct application of the two-component backfilling technology, both components must be purposely designed to be chemically and physically stable for the whole of the time needed to cover the distances between the batching station and the injection points.

Once this concept is clear, and returning to Figure 11, two different lines pertain respectively to component A and component B (1 in Figure 11). These lines run separately until a few centimetres before the injection nozzles, where line B joins line A with a certain tilt angle or concentrically (Figure 12).

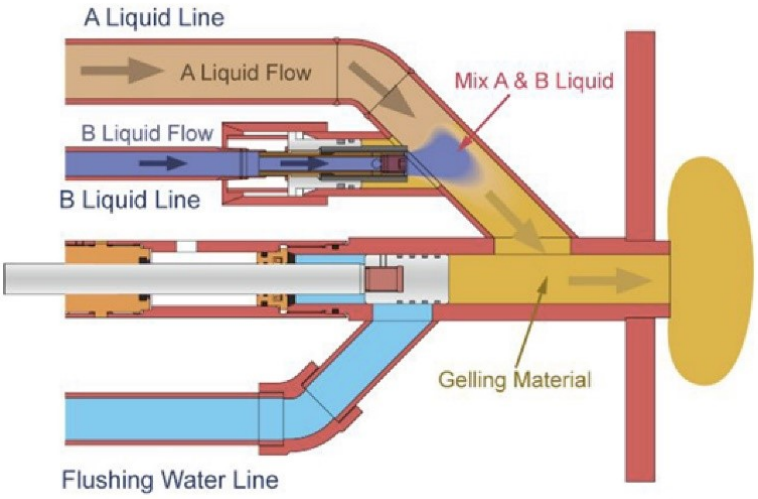

Figure 12 - Scheme of a two-component grout injection system. In the specific case, the component B flow enters the A flow with a certain tilt angle. TAC Corporation (Shah, 2017).

Each component is pumped with the appropriate pressure. These pressures allow mixing to occur turbulently, resulting in a homogeneous and unique material that starts to gel (2 in Figure 11). The duration graphically reported on the chart refers expressly to the analysed case history and should not be intended as an absolute range. At this stage, the two-component grout has finally been injected and the ring is completely embedded by the backfilling material. The curing reaction has started and the grout shows a plastic behaviour in the first minutes, followed by the hardening process that leads to a solid state (3 in Figure 11).

3.1.2 **The creation of an annular incompressible bubble**

Before introducing the theory expressed by Pelizza et al. (2010, 2012) and reconfirmed by Peila et al. (2011) concerning how the two-component grout behaves once injected in the annulus during tunnelling construction, some further information should be given pertaining to the ingredients used and their

corresponding dosages: the main raw material of the two-component grout dosage is the water.

Pelizza et al. (2012) stated that, as the two-component grout is mainly composed of water (usually about 800 litres for 1 m^3 of final grout), it can be considered an incompressible fluid, exactly like water. It can be affirmed consequently that the annulus void created due to the machine's advancement is a closed annular bubble that is instantaneously and continuously filled with an incompressible fluid. Hence, every ground convergence movement or every ring fluctuation, or generally speaking, every action that leads to an annulus volume reduction will create instantaneously a reaction pressure inside the fluid that will avoid all deformations. This results in the establishment of an incompressible zone, a bubble that perfectly confines the concrete rings. According to this theory, the long-term mechanical strength of the backfilling material does not have a practical meaning. This theory has been warmly welcomed by all the experts since its publication and is currently the most well-established in the scientific community. Nevertheless, thanks to the experience gained in the last decade, some additional aspects should now also be taken into account and the theory of the incompressible bubble should be integrated.

Firstly, the incompressible bubble can really work as an incompressible material only if the annulus is completely filled, without permeating the surrounding grout and without being changed by the action of external water. Unfortunately, experiences coming from construction sites prove that filling the annulus completely instantaneously with the advancement of the machine is impossible. A secondary grouting, and sometimes a tertiary grouting, must always be carried out (Shulkins, 2020). Nevertheless, despite the different injection phases, sometimes final investigations confirm the presence of unfilled parts in the annulus, commonly the upper part of the crown.

Secondly, as described in depth in the next paragraphs, the tail shield is not equipped with a huge number of nozzles. Commonly, as a function of the machine diameter, the number of nozzles ranges between 2 and 12. Therefore, in order to obtain a complete annulus filling, the gel time should be carefully managed: it should be long enough to allow the interpenetration of the two-component flows coming from different nozzles, producing a single layer of backfilling, but it should be short enough to lock the assembled lining in the designed position and to gel in the forecast position. From the experience gained at construction sites, the grout flows exiting from the nozzles are not always able to completely fill the space between them due to mismanagement of the gel time or choking of the nozzles.

In conclusion, it can be easily imagined that the incompressible bubble is in reality difficult to realise. But what might happen in the case of an incomplete backfilling operation? The linings tend to lean down on the tunnel's excavated profile and the two-component grout cannot be stressed triaxially (no lateral confinement). For this reason, although Pelizza's theory is widely accepted, currently the main parameter that is required for two-component grout in situation-specific technical requirements is the uniaxial compressive strength, at

short and long curing times. On the other hand, in the case of an incompressible bubble, only the stiffness parameters should be considered in the project; while these properties are starting to be considered recently by backfilling engineers, their use is not yet well established.

Finally, while the theory of the incompressible bubble is undoubtedly accepted and valid, it should be highlighted that it is a model that is hard to match in reality. According to this last concept, in all the different tunnel technical documents, the grout performance in terms of uniaxial compression is always required.

3.2 Technical and logistical aspects

This paragraph will describe the technical and logistical aspects pertaining to all the two-component grout paths, starting from the provision of raw materials in the construction yard and ending with injection through the shield nozzles. A concept that must be highlighted before starting the description is the following:

KEY CONCEPT 2: Each construction site can be organised in a different way as a function of the specific requirements that the final product must satisfy and as a function of the expected productivity. Many design choices may be valid but every design decision should be taken considering the final goal.

As a general guide, the capacity of the backfilling plant and the storage tanks are a function of the volume of the required backfilling grout. This volume should be sufficient at least for a complete ring injection without interruption (EEFNARC, 2005).

To generalise, considering a common tunnelling construction site, three macro areas can always be identified:

1 the batching station;
2 the transfer system;
3 the TBM.

In the following, the main information pertaining to these three areas and the proper operative/technical phases are described. Furthermore, a paragraph concerning the technical requirements introduces the strong provisions that are usually required for both components of this backfilling technology.

3.2.1 **Batching station**

ITAtech (2014) reports the crucial importance of the batching process, highlighting its potential effect on the final grout properties. The possibility of producing rapidly and suitably the required volume of grout is crucial for big

construction sites. Its productivity and its storage capacity have to be carefully chosen according to the expected machine productivity (Dal Negro et al., 2010).

The batching station, also commonly called “batching plant”, is always located outside the tunnel, in the construction yard. Here, enough space and suitably large streets allow the supply of raw materials that are collected by trucks from special silos (Figure 13).

Figure 13 - Raw materials for the two-component grout production. On the left, the construction yard of the “Variante di Valico”, Barberino di Mugello (IT). On the right, tanks for the component B storage relating to the Follo Line project (NO) (Dal Negro et al., 2017).

Commonly, a batching station is composed of a proper space for the batching plant operator, who interfaces with the computerised system to be able to follow and check the correct running of all the batching phases (Figure 14).

Figure 14 - Control panel of the batching plant and warning lights (top). Dosage setup display (bottom).

Close to the operator station are located all the associated equipment: the turbomixer, the agitator tank and pumps. An example of the whole batching area is shown in Figure 15.

Figure 15 - Working site batching station. Mont Cenis base tunnel, France (Dal Negro et al., 2017).

Regarding the production of the component A, usually the process is fully pre-programmed (Ivantchev & Dal Rio, 2015): raw materials are metered in an automatic way, usually with the mixer located on top of the load cells. Liquid raw material can also be dosed by volume. According to EFNARC (2005), the accuracy of batching should be to ±2% by weight for each ingredient used and

volume metering should be avoided. Drawing attention to these provisions, another key concept can be introduced:

KEY CONCEPT 3: Two-component backfilling is a "sensitive" technology. The adjective "sensitive" highlights that, once the batching procedure has been fixed as a function of the desired results, that procedure should be followed strictly, from the nature, quality and technical properties of the raw materials (that should be constantly checked also on the job site) to the metering and the mixing procedure.

The production of component A occurs in the turbomixer (colloidal mixer), which is able to provide volumes ranging between 0.5 and 2 m^3 for each batch. The capacity depends on the model. Figure 16 depicts a typical turbomixer (Team Mixing technologies SD1350) with high mixing performance named a "high shear colloidal mixer".

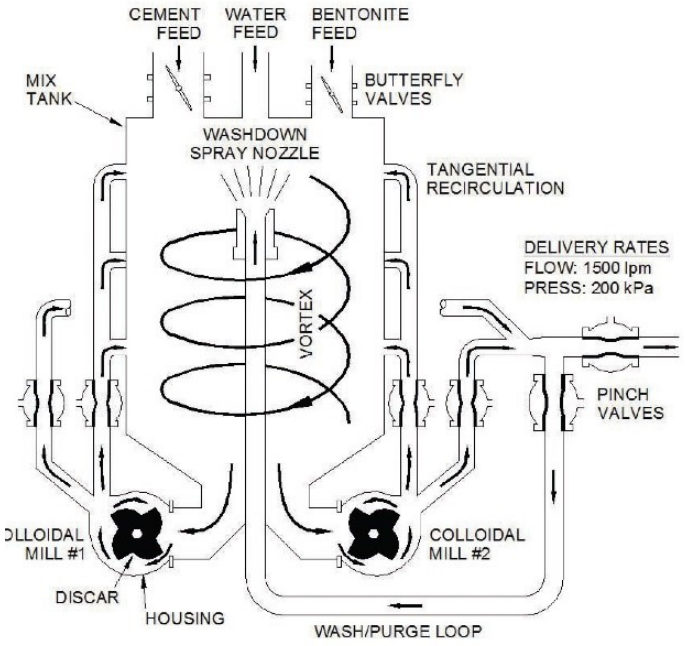

Figure 16 - Turbomixer scheme (Reschke & Noppenberger, 2011).

This very high-performing mixer was used at the working site of the Brisbane Airport Link (APL). Reschke & Noppenberger (2011) highlighted the crucial importance of achieving a proper mixing phase, recognising the mixer as the key element of the batching plant. In this specific case, two different mills were able to rotate at up to 2100 rpm, providing suitable turbulence to break down the dry cement particle clusters. The vortex created inside the turbomixer permitted the rapid assimilation of ingredients inside the water, obtaining a homogeneous and stable mortar. This paper, and only this paper, highlights the importance of the mixing phase concerning the final performance in terms of the uniaxial compressive strength achieved. As shown in Figure 17, a non-negligible

dependence between the mixing technology used and the UCS obtained was found.

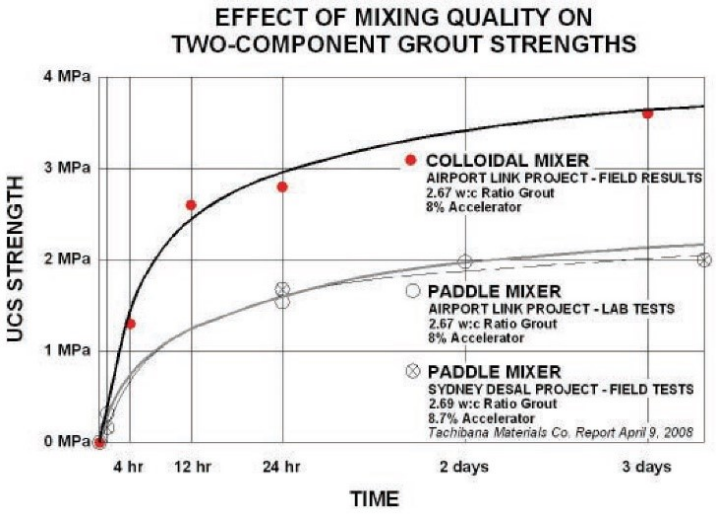

Figure 17 - Grout strength for two different mixers: colloidal and paddle technology (Reschke & Noppenberger, 2011).

Two different issues can be inferred from the chart in Figure 17:

- the test carried out in the laboratory underrated considerably the grout strength actually obtained at the construction site. Unfortunately, no further details are provided concerning the modality, equipment and procedure used for the laboratory component A manufacturing;
- speculating that laboratory tests meet the job-field specification, the unexpected rise in strength could lead engineers to reduce the concrete dosage, i.e. to save money.

Taking into account both issues, it is evident that there is a need to better calibrate the laboratory procedure in order to achieve more reliable outcomes, at least in terms of strength. Generally speaking, the aspect concerning the role of mixing on the final grout properties reported in Reschke & Noppenberger (2011) and the need to establish a detailed procedure for component A manufacturing at the laboratory scale, have been selected as a starting point for further investigations in the next chapters of this thesis work.

Coming back to the batching illustration process, and more specifically to the ingredients, they can be added in different orders and the mixing duration for each one can be different. Generally speaking, each construction site has its specific scheduled adding order and mixing durations. Table 2 reports the main batching information from four different construction sites.

Table 2 - The batching station: main design parameters and mixing procedure. Four case histories.

Reference	Ivantchev & Del Rio, 2015		Reschke & Noppenberger, 2011		Personal experience		Personal experience	
Construction site	North West Rail Link (Australia)		Brisbane Airport Link (Australia)		Mont Cenis base tunnel (France)		Italy	
Turbomixer volume	0.9 m^3		/		2 m^3		1 m^3	
Agitator tank	3 m^3		3.2 m^3		/		/	
Water	1°	0 s	1°	/	1°	0 s	1°	5 s
Bentonite	3°	90 s	3°	/	2°	120 s	2°	100 s
Cement	4°	120 s	4°	/	3°	10 s	3°	5 s
Retarding/fluidifying agent	2°	90 s	2°	/	4°	30 s	4°	15 s
Total necessary time (s)	300		/		160		125	

Regarding ingredients, two different types of information are reported. The first one (ordinal number) concerns the addition order, which ranges between 1 and 4. The second concerns the mixing duration and is expressed in seconds. Neglecting the differences in the capacities of the turbomixer and agitator tanks, it is interesting to note how, after adding the first ingredient, which is water for each site, the Australian sites foresee adding the chemical agent as the second ingredient, followed by the bentonite and cement, while the European sites foresee adding the bentonite, followed by the cement and only at the end adding the chemical ingredients. It could be interesting also to understand how each construction site differs from the others concerning the production time: for the North West Rail Link 300 seconds are required for producing less than 1 m^3 while in the Italian case, the same quantity is produced in half the time. These considerations do not mean that one plant is better than any other one. These remarks are intended only as proof of the wide-ranging possibilities for organising and projecting a batching station as a function of the individual requirements of each construction site and according to the available raw ingredients and the operator experience.

Returning to the batching process, after the mixing phase, the fresh component A is stored in the agitator tank and then pumped toward the machine. Commonly, piston pumps (Figure 18), peristaltic pumps and progressive cavity pumps (Thewes & Budach, 2009; Pellegrini & Peruzza, 2009; Reschke & Nopperberger, 2011; Càmara, 2018) are used for both components, but they operate through separate lines.

Figure 18 - Double piston pump for the component A transportation (left). Single piston pump for the component B transportation (right).

3.2.2 **Transfer system**

After the batching, both fluid components must be transferred from the construction yard towards the tunnel. Commonly, the transfer system is based on feeding pipes and pumps.

The batching plant is synchronised with the grout plant of the machine and when the automatic mode is active, the supply to the machine staging tanks is guaranteed in an automatic way; the pumps work till the upper tanks threshold is reached, whereupon the supply process is stopped. In addition, when required, the batching pumps can also be activated manually from the operator control panel.

Pipes run along the length of the tunnel, from outside to the machine backup for many kilometres (Figure 19), usually without any intermediate pumping stations (Boscaro et al., 2015). Pipe extension, as the machine advances, is carried out by proper employees with a daily frequency based on the machine advancement rate. However, each machine is equipped with hose reels, the hoses guaranteeing a sort of “lung” (in the jargon), permitting the reduction of the maintenance work needed for extension of the pipes.

A further detail, according to key concept 2 regards the possibility of not using pipes for transportation of the two components. Depending on the machine’s rate of advancement, the backfilling grout required for each stroke and the distance between the machine and the construction yard (Dal Negro et al., 2017), some construction sites choose to supply the grout components by trucks (named grout cars). While avoiding the pipes transport system, a potential downside is the impossibility of sufficiently shaking the component A. In this case, the bleeding phenomenon should be carefully taken into account in the design phase (taking into account the possibility of using the ingredients expressly realised).

Figure 19 - Provision tubes are clearly visible on the left of the photo. The machine backup is depicted in the centre.

3.2.3 **The TBM**

After the transportation, both component A and component B are stored in specific tanks located on the machine backup. The volumes that can be stored are commonly about 50% greater than the theoretical ones computed for one stroke. The component A is usually kept moving in a mechanical way in order to reduce the bleeding phenomenon and to maintain the homogeneity of the mortar.

3.2.3.1 The injection operation

The injections in the annulus are carried out by pumps located on the machine backup. Each line has one specific pump dedicated. Usually, not all the installed lines are used for the primary backfilling; indeed, commonly some lines are used for carrying out the secondary grouting, while other lines are simply spares.

Reschke & Noppenberger (2011) stated that small shielded machines are commonly equipped with two injection lines with nozzles located on the tail shield approximately at the 10 and 2 o'clock positions. Home (2014) confirms that for a shielded machine with a diameter less than 10 m, the two-component grout can be successfully injected with only 2 grout ports. Furthermore, considering that the two-component backfilling technology is successfully applied in both soil and rock, ITATech (2014) reports that the nozzle size is different in the case of a soil machine or rock machine. In the first case, ports can be located on the extrados of the tail shield and the nozzle size is not a critical issue. In the second case, ports should be embedded in the tail shield matrix and, preferably, the nozzles side should fit with the available annulus thickness, without requiring

further space. However, nozzles are generally located circumferentially on the tail shield and their number is substantially a function of the diameter.

Figure 20 shows two technical schemes pertaining to two EPB machines and their nozzle patterns. Regarding the one used in Beijing (China) with a diameter of 10.22 m, 5 injection lines were designed, respectively at 0°, 40°, 140°, 220° and 320° (considering 0° as the top of the shield). Concerning the machine used in Brisbane, with a diameter larger than 12 m, only 4 injection ports were used (A1, A2, A5 and A6), leaving 2 ports (A3 and A4) closed.

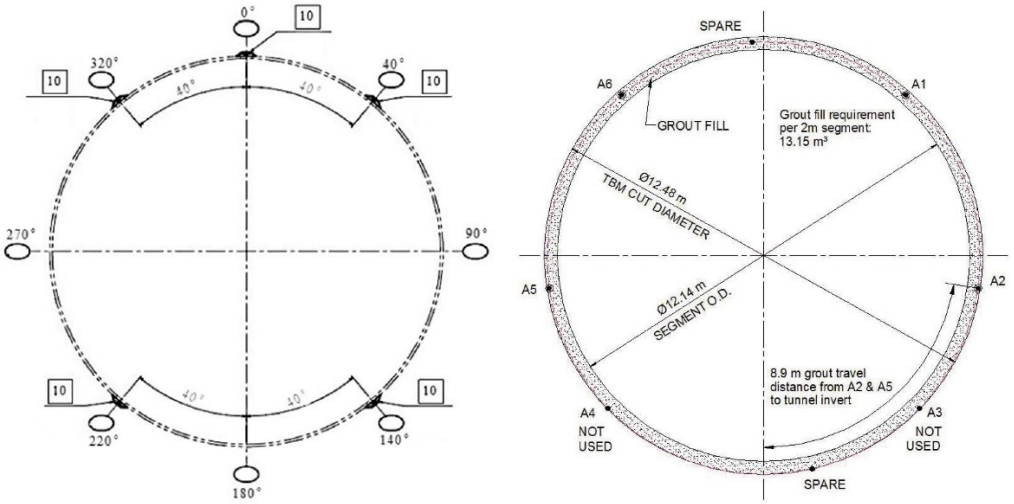

Figure 20 - Transversal section technical schemes of the EPB shield used in the Beijing subway construction (Li et al., 2004) (left) and in the Brisbane Airport Link (Reschke & Noppenberger, 2011) (right).

This example is given only to recall the abovementioned key concept 2, which can be easily applied also in the machine design: although the considered machines have different diameters, fewer nozzles have been used in the machine with the bigger diameter. Continuing with this comparison, it could be interesting to highlight how, for the Beijing machine, the grout is injected also from ports located in the lower part of the shield (140°–220°) while in the case of the Brisbane machine the lower ports used are located close to the horizontal diameter of the machine (A2 and A5). It is clear that in order to achieve the complete filling of the annulus, the gel time design was approached differently, being shorter in the case of Beijing and longer (leaving to the grout the time needed to flow downward) in the case of Brisbane.

Returning to analysing the injection operation, during the advancement, the pressures and flows of each line can be separately managed (Boscaro et al., 2015) according to the advance speed of the machine, with the purpose of injecting with each advance a grout volume at least equal to the theoretical one. As concerns the pressure that should be used during the injection, discordant information can be found in the scientific literature. Peila et al. (2011) and Pelizza et al. (2012) suggested that the backfilling injection should be carried out with pressures approximately 0.2 bar greater than the face support pressure. This pressure difference should be “balanced and controlled with the right equilibrium between

the pressure in the chamber and the backfilling one" in order to avoid the grout flowing through the gap, from the tail forward to the machine head or vice versa.

Thewes (2013) analysed both the flow directions that could affect the machine during the excavation process, providing the following criteria:

a) in order to avoid flows from the head backwards into the tail void, the grout pressure should be greater than the face support pressure by a minimum difference of 0.2–0.3 bar → $p_{grout} - p_{face} > 0.2–0.3$ bar;
b) in order to avoid grout flowing forwards into the excavation chamber, the grout pressure should be less than the face support pressure by a maximum 2–3 bar → $p_{grout} - p_{face} < 2–3$ bar.

Reschke & Noppenberger (2011) reported that the suggested injection pressure should be computed adding 1 bar to the groundwater pressure, without exceeding 5.5 MPa even if information concerning the face support pressure is provided. Dal Negro et al. (2014a) and Boscaro et al. (2015) state that the injection pressure should be 0.3–0.6 bar greater than the face support pressure, taking care of a further pressure rise of a few decimals of bar at the end of the stroke. Càmara (2018), concerning the Follo Line project despite the situation of 16 bars of hydrostatic pressure, highlighted that the target pressure for primary injection should be 0.5 to 1 bar (1 bar at the bottom line, 0.5 for the other lines). All the above-mentioned criteria can be considered valid; however, finally the author can provide some further information from personal experience of working on machines. Firstly, it is very uncommon to have fixed pressure values for all the injection lines, especially for machines with big diameters. Secondly, it should be highlighted that the pressure values are usually measured in pipes and they may not correspond to the real injection values measured at nozzles. Thirdly, in the scientific literature no one underlines that in order to guarantee the necessary mix turbulence between component A and B, the two lines cannot have the same pressure values. In order to summarise these concepts, Figure 21 shows an example of the real machine parameters during a common EPB stroke. It is clearly seen that component B is injected with pressure values that are double or triple those of the corresponding A line. Furthermore, the average component A pressure is 3 bars greater than the face support pressure, while the average component B pressure exceeds the face support pressure by about 10 bars. In conclusion, considering just one pressure value can be simplistic since there are two components. Furthermore, it should be underlined that none of the equations provided in the scientific literature take into account the crucial importance of the high turbulence needed to obtain a high quality of the final grout. These details are clearer for expert workers who, on the actual construction site, increase the pressure value in order to obtain the high turbulence required for perfect mixing of the components.

3.2.3.2 *The injection management*

Once the stroke is started, the backfilling does not start immediately, but only when the first centimetres have been excavated (commonly 10–20 cm) (Dal Negro et al., 2017). Each machine is equipped with a special area for the machine backfilling management that is usually located on the backup but separately from the control cabin. The two-component control system usually displays all the main machine parameters concerning the backfilling process. Figure 21 shows an example from EPB Herrenknecht.

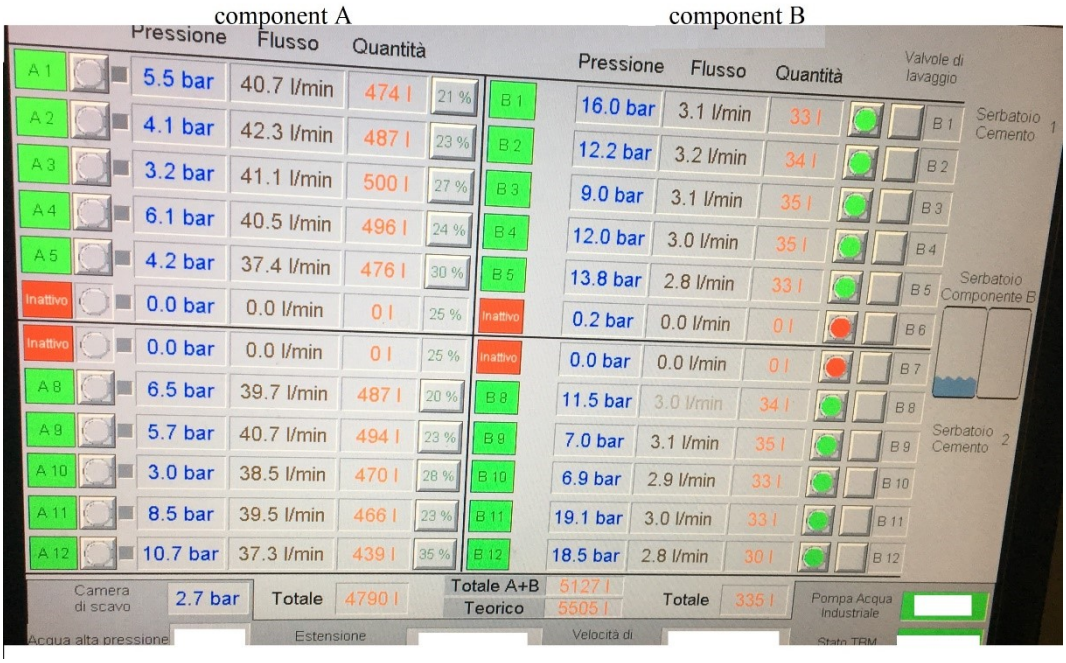

Figure 21 - Backfilling operative system on the machine backup.

In this specific case, the machine is equipped with 12 lines, which can inject with different pressure values. For each line, pressures, flows and injected volumes are displayed. On the right of the screen, the levels of components A and B in the machine tanks are shown, while at the bottom are displayed the pressure of the excavation face, the stroke advancement and the advancement rate. Furthermore, the theoretical volume foreseen and the injected comprehensive volumes are shown.

3.2.3.3 *Secondary grouting from the machine*

Commonly, during the backfilling injection performed by a shielded machine, to reach a perfect and complete annulus filling is very difficult while also taking care to use a specific mix design and formed employees. The gel time, expressly designed in order to have an order of magnitude of seconds, causes the injected grout to run downward, leaving the annulus crown empty. In order to avoid this drawback of the nature of the technology, a secondary grouting is commonly

scheduled. In some cases, this operation can be carried out from the machine backup, by using one line of the two-component backfilling system. Càmara (2018) reports the example of the Follo Line construction site, where secondary injection was performed every 2 or 3 rings from the backup. It is very interesting that the gel time was deliberately increased in order to be able to cover a distance of more than 2 rings.

In the literature, other examples pertaining to secondary grouting are reported in Ivantchev & Dal Rio (2015) and Li et al. (2004).

3.2.3.4 Some design aspects

The previous subparagraph mentions for the first time the "theoretical volume". This corresponds to the comprehensive amount of backfilling grout needed to completely fill the annulus created during one single machine stroke. The theoretical volume (V_t) can be calculated using the following equation:

$$V_t = \left(\frac{D_{exc}^2}{4} - \frac{D_{ext}^2}{4}\right) L_{ring} * \pi \qquad 2$$

where:

V_t is the theoretical volume;

D_{exc} is the excavated section diameter;

D_{ext} is the outer ring diameter;

L_{ring} is the length of the ring, or the stroke path.

According to Equation 2, the theoretical grout volume needed to fill the annulus is calculated as the difference between the whole volume excavated from the machine head and the extrados of prefabricated assembled linings. Once the theoretical volume has been calculated, the next design step is commonly to split this grout volume between the injection lines, regarding different annulus areas. Consequently, each line is characterised by its injection pressure, its comprehensive grout volume and, in certain cases, also by its specific gel time (the management of the gel time is quite complex).

Passing from the theory to the reality, which criteria can lead operators to stop the backfilling phase? In other words, when are we sure that the backfilling operation has been successfully accomplished? Dal Negro et al. (2014a, 2017) stated that there are two criteria for this purpose: the volume of injected material should be equal to the desired one (commonly equal to the theoretical volume increased by 10–20%) or the injection pressure should reach the established value. Consequently, regardless of the criterion used, the real injected backfilling grout volume will vary as a function of the specific situation encountered in the single stroke, such as the local permeability of the medium and the local convergence phenomenon (which reduces the annulus thickness). A grout volume slightly greater than the theoretical one is not regarded as a problem but, on the other hand, a grout volume that is significantly different should be considered as an

alarm for potential over-excavation conditions, which must consequently be verified (Guglielmetti et al., 2007). In order to accomplish a suitable backfilling operation, the machine advance speed may be adapted and calibrated to the backfilling one, in order to follow the foreseen pressure.

By way of example, Figure 22 shows the backfilled grout as a function of the machine advancement. The machine data are from the Arroy Maldonado Tunnel (Dal Negro et al., 2012).

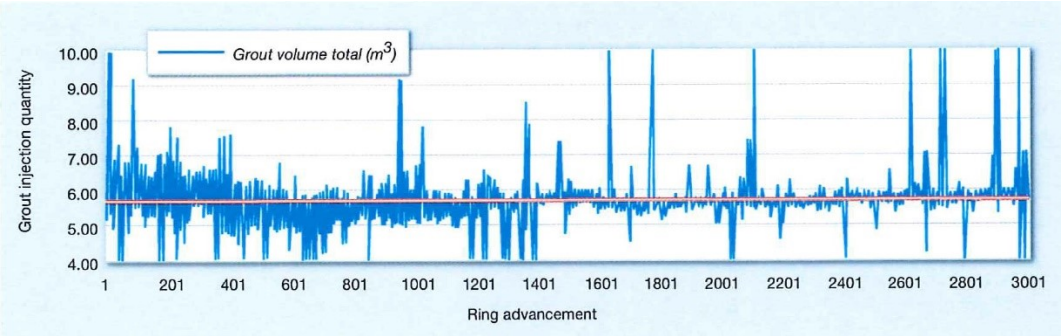

Figure 22 - Maldonado Tunnel – Buenos Aires (AR) (Dal Negro et al., 2012).

In this work, the theoretical volume V_t (the red line on the chart) was equal to 5.7 m^3 while the average of the real injected volume was slightly greater, at 6.1 m^3 per ring (an excess of 7%). The work was successfully completed with very low settlements, according to the construction site specification.

As mentioned above, this divergence between the theoretical volume and the real injected volume is normal. Also Càmara (2018), concerning the Legacy Way construction, reported a theoretical volume of 15.33 m^3 versus a real injected volume of 16.2 m^3. The excess of 5.7% was successfully correlated with drilling adjustments and other site observations.

3.3 The “specific” technical specification and the need for a careful design phase

As previously discussed, the choice of the two-component technology for the annulus backfilling involves the need for a careful design phase, concerning space management, the hydraulic design and the mix design.

In this context, we will focus strictly on the necessity to design in depth all aspects concerning the mix design. Describing the two components’ paths, from the batching station to the injection nozzles, the importance of operating with stable compounds (summarised in key concept 1) is clear.

At this point of the work, another key concept can be added:

KEY CONCEPT 4: The whole backfilling system (volume of component A produced, diameter of feeding pipes, numbers and flows of pumps, nozzles pattern with proper injection pressure and comprehensive injection volume and at least the strength performance of the grout) works assuming that the properties of both component A and component B are fixed.

In other words, components A and B must not only be stable but their technical properties must remain constant, since fluctuations could destabilise the whole backfilling system. As an example, Figure 23 depicts the classic case of tube choking, due probably to mismanagement of the dosages.

Figure 23 - Component A tube choking. The photo is property of the UTT Mapei. (Richard Schulkins master lecture, 2020).

The instrument used by backfilling engineers in order to guarantee certain properties of the components and of the final grout is the mix design.

Definition 3: The mix design is the core of the whole backfilling process. It is established after laboratory and job field test campaigns and includes information that is reported in official contract papers. It lists the raw ingredients, their commercial names and their dosage per 1 m^3 of hardened grout.

It should be reported that of the two components, only component A requires in depth analysis and tests, since component B is supplied directly by the manufacturer. Concerning the quality of component B, EFNARC (2015) suggests that building enterprises require a "Quality Assurance certificated" guarantee provided by the supplier. The following key concept completes the overview of the importance of the mix design:

KEY CONCEPT 5: The mix design project is a crucial phase that should be performed carefully in order to find the appropriate solution for each different job site, taking into account both technical and economic points of view. There is no two-component mix design that is suitable for every construction site.

Dal Negro et al. (2017) provide a careful analysis concerning all the aspects that should be taken into account for a two-component mix design project. Firstly, the ingredients and their respective dosages must be studied in depth. Considering that commonly the raw materials procurement is guaranteed by local suppliers, a deep knowledge of this aspect is the first step that should be verified. For example, different cements, despite belonging to the same strength class, may result in final grouts with different properties. Similarly, the type of bentonite also strongly affects the final results, as well as the water used.

For all the above-mentioned reasons, study of the mix design is strongly recommended, using the real raw ingredients that will be adopted at the job site. But now the question arises: what are the engineering requirements that can be used in order to calibrate the mix design for a certain construction site's requirements? In the following, the properties usually used as basic parameters for component A and the final grout, and the corresponding tests used (when available) for their assessment are listed. The list has been drawn up taking into account information from Bezuijen et al. (2005), Guglielmetti et al. (2007), Pellegrini & Peruzza (2009), Peila et al. (2011), Pelizza et al. (2012), Novin et al. (2015), Zarrin et al. (2015), and Todaro et al. (2019, 2021) that confirms a quite standardised and widespread approach:

1 **The pumpability and workability** are the basic concepts for the correct working of the transportation system based on pumps, pipes and nozzles. These components' features are assessed by means of the component A viscosity, measured instantaneously after the mortar manufacturing and then daily, up to 72 hours. The long workability required ensures first that pipe choking and system blocks in the case of long construction stops can be avoided and secondly that the grout production is independent of the excavation rate. Assessment of the pumpability and workability is usually carried out using the Marsh cone, which provides as output a time, expressed in seconds. This value, commonly called the flowability by Marsh cone, can be used to understand the pumping effort.

2 **The stability** is intended as the aptitude of component A to not segregate. Segregation can lead to different values of density when testing different parts of the considered volume. Since component A is a mortar, under the action of gravity all the cement particles tend to move downward, leaving the water above. This phenomenon is called bleeding and it must be avoided or, at least, restrained to a certain value. A small bleeding value minimises the risk of clogging pipes.

3 **The gel time** should be a few seconds. Study of the gel time must be related to the avoidance of nozzle choking, the avoidance of grout leaks through the tail brushes or through the ground, and the gelation of the grout in the designed position, so that the backfilling ensures the correct embedding of the rings inside the excavated medium. Assessment of the gel time is not standardised.

4 **Strength in the short and long term**. Usually job site specifications consider the uniaxial compressive strength, and it is only recently that sometimes the shear strength is also required. In the short term, the backfilling should lock the segments in the designed position and should bear the backup weight during the machine advancement. Furthermore, the filled annulus should always have a certain strength in order to ensure the avoidance of settlement. In general, the academic community favours the bubble theory, focusing on a short curing time, while at some construction sites, the specifications are focused also on the strength at medium/long curing times (7 and 28 days). Sometimes the strength at a long curing time can be calibrated as a function of the properties of the material that is being excavated (Zarrin et al., 2015).

5 **The washing-out resistance** indicates the grout's ability to seal the rings without being removed from the groundwater flow. Assessment of the washing resistance is not standardised.

Thewes & Budach (2009) highlighted also the importance of the stiffness modulus, which should be designed to be close to that of the medium being excavated (5–10 MN/m^2).

More detailed descriptions of specific tests aimed to assess the above-listed basic properties will be given in the next chapters.

3.4 After the project of the mix design

After having established a mix design at laboratory scale, the transition to full scale is another crucial step. This section is subdivided into four parts. In the first part the experiences at two construction sites are reported while the second part briefly describes the need for a backfilling checklist to be used after the machine launch. Finally, issues of maintenance and final checks are described.

3.4.1 The job field assessment

Commonly, a confirmed approach to the transition to the job field foresees repeating the comprehensive laboratory test pattern (performed using the component A produced in the laboratory) by using, this time, the component A produced at the construction site with the turbomixer (ITATech 2014; Dal Negro et al., 2014b; Todaro et al., 2021;). Tests are commonly performed in order to prove the correspondence between the laboratory outcomes (in terms of flowability, bleeding, density, gel time and strength) and job field outcomes. This praxis is nowadays used effectively everywhere.

However, sometimes the simple repetition of laboratory tests is not enough and more construction site tests can be required in order to test the real ability of the machine to backfill the annulus. As described by Dal Negro et al. (2014b),

regarding the Legacy Way project, once the laboratory tests had been successfully accomplished, proving the suitability of a certain mix design, a full-scale test was scheduled and performed, aiming to:

a) verify the design of the nozzles pattern and its suitability for the required backfilling performance;
b) verify the right grout properties in terms of the manufactured grout volume, flow rates for both component A and B and the gel time;
c) ensure that the technical properties of both component A and B found from the laboratory tests coincide with those at the construction site;
d) recognise and lessen potential issues affecting the whole backfilling phase, from batching to injection.

In the specific case, from practical aspects, the full-scale test was performed by assembling a suitable formwork around the machine. After that, the grout was injected, replaying the real scheduled injection sequence, namely first with injection at the inverter, secondly injection through the ports in the lateral segments and finally injection pertaining to the crown. Figure 24 shows photos of the results obtained.

Figure 24 - Hardened two-component grout after the full-scale test. Injection at the inverter and on the lateral part (left) and crown injection (right) (Dal Negro et al., 2014b).

From the positive results of performing this full-scale test, it was possible to verify all the main technical parameters pertaining to the machine backfilling phase prior to the machine launch. Analysing Figure 24, it is clear how a uniform layer of hardened grout was created. This result highlights and proves the successful interpenetration of the grout flows coming out of the different nozzles.

Ivantchev & Dal Rio (2015) reported a case history related to another Australian tunnel work, the North West Rail Link (NWRL). At this construction site also, after a careful project phase concerning the mix design study, full-scale tests were scheduled and performed. The first phase consisted of assessing the grout mixing process by manufacturing a copy of a grout mixing box. This equipment was set up by using equivalent size pipelines fed by the components A and B pumped in the same modality as the machine pumps (Figure 25).

Figure 25 - Trial grout mix box. On the top the component mixer is depicted (Ivantchev & Dal Rio, 2015).

This test confirmed the suitability of the previously studied mix design (at the laboratory scale) in terms of the gel time and above all in terms of the strength at a short curing time. After that, a full-scale test was performed with the aim of verifying that the chosen nozzle pattern and the backfilling plant were able to satisfy the requirement of backfilling more than 80% of the annulus during a prefixed time and machine advancement (1 minute and 570 mm of advancement). The test was successfully performed.

3.4.2 **The operative checklist**

Before starting work with the machine launch, an operative checklist should be designed in order to ensure the correspondence between the products used for the backfilling and the technical requirements. In order to do this, commonly two categories of grout testing should be designed. The first checklist should address regular grout testing, aiming to check both the component A properties and the hardened grout strengths. The second one should address restarting the grout test, aiming to understand if the components are still usable after the machine stops (since interruptions are not rare).

Regular tests should be carried out with a frequency depending on the outcomes obtained. In other words, a high discrepancy identified between the real time outcomes and the prescriptions will call for a higher checking frequency. Tests should be performed by highly trained operators. Commonly, this type of checklist foresees tests of the bleeding, viscosity, density, gel time and compressive strength at short curing times. Càmara (2018) states also the requirement for temperature measurements and shrinkage tests. Tests after a machine restart are usually scheduled if the component A is stored inside the machine tank for more than 12 hours. The most common tests relate to viscosity assessment.

3.4.3 **Maintenance**

Two-component backfilling can be considered a technology with a low maintenance frequency.

The only critical aspect that should be reported concerns the cleaning operation of the comprehensive injection plant. ITATech (2014) and Home (2014) highlighted that during the injection design phase, it is important to foresee an effective flushing system in order to prevent the nozzle choking and ensure easy pipe-cleaning operations. At every construction site, a daily cleaning operation is commonly scheduled in order to prevent more severe backfilling system maintenance. Ivantchev & Dal Rio (2015) commented on their own experience suggesting the use of low volume–high pressure pumps for a good flushing operation. In order to contextualise the flushing operation, Figure 26 reports an example of a scheme for the nozzle flushing system. The valve (open when the injection is running) is closed and the water flow allows cleaning of the component A line and of the nozzle of the component B line.

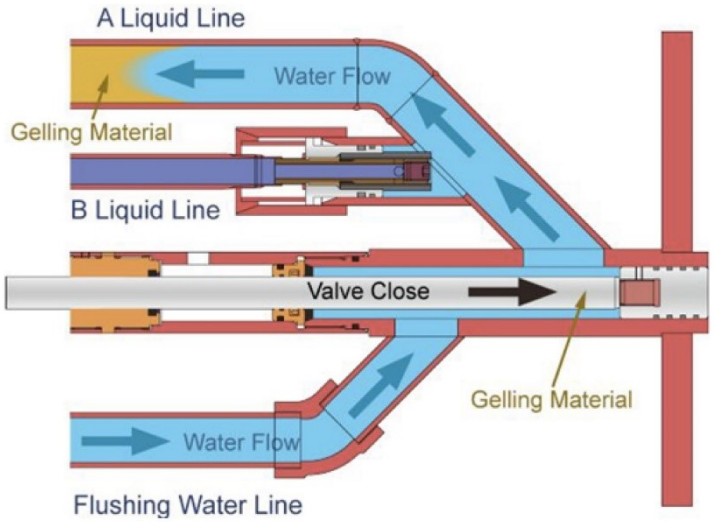

Figure 26 - Scheme of a two-component grout flushing phase. In the specific case, the nozzle valve is closed and the water flow cleans the pipe of component A. TAC Corporation (Shah, 2017).

Concerning the B liquid line, Reschke & Noppenberger (2011) reported that the accelerator is the most dangerous component for nozzle blockages. In order to avoid this inconvenience, they suggest stopping the accelerator injection 100 mm before the stroke end. Also Dal Negro et al. (2017) stated that the cleaning operation is crucial especially for the accelerator nozzle, which requires a suitable pressure in order to remove any hardened particles of component B.

3.4.4 **Has the backfilling been performed in the right way?**

Very few data are available regarding the checking of the backfilling grout after the complete machine passage, although it is known that the construction supervision should usually control the compliance of the operation with the situation-specific technical specification. Actually, the complete filling of the

annulus can be verified only when tunnel widenings are created and some of the tunnel rings are removed.

However, regarding the working site of Roma Metro C, Pelizza et al. (2012) reported that two different approaches could be used to verify the quality of the backfilling:

- Indirect approach: the filling of the annulus is verified indirectly, by monitoring the displacements around the tunnel and on the ground surface (this last condition can occur only in the case of shallow tunnels);
- Direct approach: the filling of the annulus is verified directly using georadar (Figure 27) tests or drilling the linings directly in order to extract a core of hardened grout.

Figure 27 - Georadar test in Roma Metro C construction site (Pelizza et al., 2012).

Pertaining to this last check modality and still concerning the construction site of Roma Metro C, Dal Negro et al. (2010) highlighted how the effective 360° filling of the annulus was inspected by extracting cores. Figure 28 shows the outcomes concerning the length of the two-component grout cores extracted.

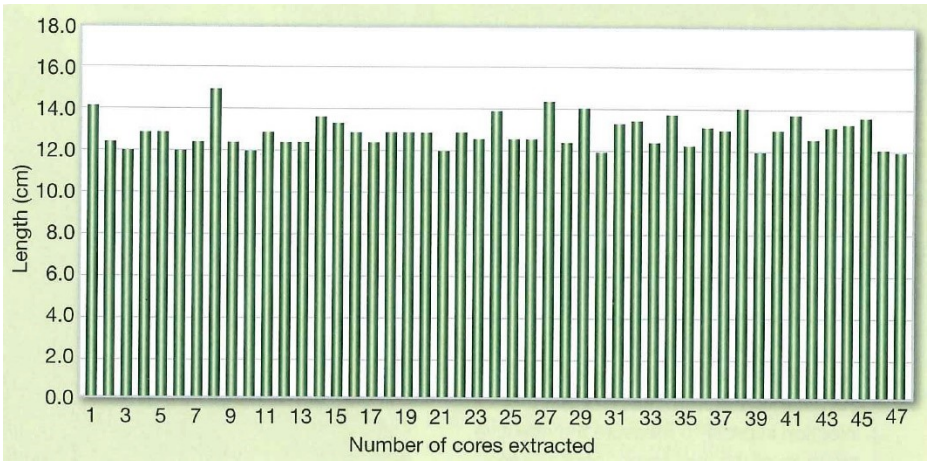

Figure 28 - Length of the hardened two-component backfilling cores extracted in the Roma Metro C tunnels (Dal Negro et al., 2010).

The expected core length of 130–150 mm was always achieved but unfortunately no information was provided concerning the space position (so it is

not known if the samples came from the crown or from other parts of the annulus).

In conclusion, as concerns the geophysical approach, Liu et al. (2012) highlighted the successful use of GPR (ground penetration radar) to estimate the thickness of the filled annulus in two tunnels in Shanghai (Yangtze River tunnel and Changjiang Road tunnel). Unfortunately, it was not clearly explained if the backfilling technology used was two-component or mono-component.

Chapter 4

Construction site case histories

Two-component backfilling is nowadays the most popularly used technology for the backfilling of the shielded machine but, unfortunately, it is not easy to find reliable information regarding the mix designs actually adopted at construction sites.

In this chapter, a collection of the main case histories available in the scientific literature will be presented, integrated with some personal experience. For each construction site, the mix design used is reported and correlated with the essential information regarding the technical requirements and, when known and available, other peculiarities are also referenced. Not every studied case is correlated with a complete set of information. All mix designs refer to the dosage of ingredients for 1 m^3 of final grout.

The purpose of the chapter is not to discuss each case history but to try to find conclusively some common aspects that can be used in order to generalise the nature of this backfilling technology.

4.1 Metro Rome Line C – Roma (Italy)

	Dosage range		Brand and/or type
Cement (kg)	320	350	/
Water (kg)	770	820	/
Bentonite (kg)	30	60	/
Retarder/fluidifying agent (L)	3	7	Mapei
Accelerator (L)	50	100	Mapei

References: Pelizza et al. (2010), Peila et al. (2011), Pelizza et al. (2012), Peila et al. (2015).

The technical specifications for the component A required 72 hours of workability and a gel time ranging between 5–15 s. Concerning the uniaxial compression strength:

1 h ≥ 50 kPa

8 h ≥ 100 kPa

24 h ≥ 450 kPa

This construction site was the only one where the provision for the permeability coefficient was formulated, with a maximum acceptable value of $1*10^{-8}$ m/s. Unfortunately, no information regarding the testing time for the permeability test was provided.

An interesting aspect that should be underlined is the complete absence of provisions concerning the strength at long curing times. This is not a design deficit, but rather the absence of any prescription for a long curing time is perfectly aligned with the theory of the incompressible bubble.

4.2 Oraki Main Sewer Hobson Diversion (OMSHD) – Auckland (New Zealand)

	Dosage	Brand and/or type
Cement (kg)	480	/
Water (kg)	730	/
Bentonite (kg)	30	/
Retarder/fluidifying agent (L)	1	Mapei
Accelerator (L)	50	Mapei
Super-plasticiser (L)	5	Mapei

References: Pelizza et al. (2010), Peila et al. (2011), Peila et al. (2015).

For this construction site the only available technical specifications concern the uniaxial compressive strength:

30 min ≥ 0.1 MPa

28 days ≥ 5 MPa

Two comments can be made:

- the final compressive strength obtained after 28 days of curing was 5.1 MPa, a very high value, considering the two-component technology;
- in order to satisfy the abovementioned requirement, a very high dosage of cement was used, requiring consequently the use of a super-plasticiser in order to permit the pumpability.

4.3 Metro Line in Sofia (Bulgaria)

	Dosage	Brand and/or type
Cement (kg)	290	/
Water (kg)	795	/
Bentonite (kg)	25	/
Retarder/fluidifying agent (L)	2.5	Mapei
Accelerator (L)	74	Mapei

References: Pelizza et al. (2010), Peila et al. (2011).

In this case history the technical specifications concerned the gel time, which must be equal to 12 s, and the uniaxial compressive strength:

1 h ≥ 0.03 MPa

24 h ≥ 1.5 MPa

Also in this case, no provisions concerning the strength at long curing times were reported.

4.4 Metro Line 1 in Brescia (Italy)

	Dosage	Brand and/or type
Cement (kg)	315	/
Water (kg)	816	/
Bentonite (kg)	42	/
Retarder/fluidifying agent (L)	3	/
Accelerator (L)	60	/

References: Pelizza et al. (2010), Peila et al. (2011), Peila et al. (2015).

4.5 Metro Line 2 in Warsaw (Poland)

	Dosage	Brand and/or type
Cement (kg)	300	IV B 32.5 N
Water (kg)	809	/
Bentonite (kg)	40	/
Retarder/fluidifying agent (L)	5	Mapei
Accelerator (L)	65	Mapei

Reference: Peila et al. (2015).

4.6 Hydraulic tunnel Maldonado in Buenos Aires (Argentina)

	Dosage	Brand and/or type
Cement (kg)	350	Type IV
Water (kg)	796	/
Bentonite (kg)	35	/
Retarder/fluidifying agent (L)	5	Mapei
Accelerator (L)	61	Mapei

Reference: Peila et al. (2015).

4.7 LTA tunnels – Singapore

	Dosage	Brand and/or type
Cement (kg)	230	Ordinary Portland
Water (kg)	810	/
Bentonite (kg)	30	/
Retarder/fluidifying agent (L)	4	/
Accelerator (L)	80	/

Reference: Peila et al. (2015).

4.8 Highway tunnel Sparvo between Bologna and Firenze (Italy)

	Dosage range		Brand and/or type
Cement (kg)	300	330	/
Water (kg)	795	810	/
Bentonite (kg)	40	45	/
Retarder/fluidifying agent (L)	4	5	MAPEQUICK CBS SYSTEM 1 - Mapei
Accelerator (L)	60	65	MAPEQUICK CBS SYSTEM 2 - Mapei

References: Dal Negro et al. (2014a), Peila et al. (2015).
The technical specifications regarding component A required a fluidity measured daily up to 72 hours, with the Mash cone value ranging between 30 and 45 seconds. The stability of the mortar was verified also by checking the unit weight (which must not change) and the bleeding, which must be lower than 3% after 3 hours. The gelling time must range between 5 and 20 seconds. Concerning the uniaxial compression strength:

1 h $\geq$ 0.1 MPa
24 h $\geq$ 0.5 MPa
28 days $\geq$ 2 MPa
It should be noted that the excavation was carried out above the water table.

4.9 Hydraulic tunnel STEP, Section II and III in Abu Dhabi (United Arab Emirates)

	Dosage range		Brand and/or type
Cement (kg)	280	300	/
Water (kg)	815	825	/
Bentonite (kg)	40	40	/
Retarder/fluidifying agent (L)	3	4	/
Accelerator (L)	60	65	/

Reference: Peila et al. (2015).

4.10 Personal experience (France)

	Dosage	Brand and/or type
Cement (kg)	230	Type I – 52.5 R - Buzzi Unicem
Water (kg)	853	From construction site
Bentonite (kg)	30	Bentonil CV15 - Clariant
Retarder/fluidifying agent (L)	3	MAPEQUICK CBS SYSTEM 1 - Mapei
Accelerator (L)	60	MAPEQUICK CBS SYSTEM 3 - Mapei

The author was personally involved in the backfilling assessment at both laboratory and construction site scales (a construction site in France).

The component A was characterised by a fluidity measured with the Mash cone, with results ranging between 34 and 51 seconds up to 72 hours. The stability of the mortar was verified by the unit weight, equal to 1.169 kg/L, and by the bleeding assessment, which was 1.05% at 3 hours and 2.09% after 24 hours. The calculated gel time was equal to 8 s. Concerning the compression strength:

1 h = 0.08 MPa

3 h = 0.35 MPa

24 h = 1.04 MPa

28 days = 1.64 MPa

4.11 Personal experience (Italy)

	Dosage	Brand and/or type
Cement (kg)	315	CEM IV A-P 42.5
Water (kg)	819	From construction site
Bentonite (kg)	35	SIPAG
Retarder/fluidifying agent (L)	4	MAPEQUICK CBS SYSTEM 1 -Mapei
Accelerator (L)	65	MAPEQUICK CBS SYSTEM 3 - Mapei

The author was personally involved (thanks to the availability of the construction site) in the backfilling assessment at both laboratory and construction site scales.

The component A was characterised by a fluidity measured with the Mash cone close to 33 seconds up to 72 hours. The stability of the mortar was verified by the unit weight, equal to 1.25 kg/L, and by the bleeding assessment, which was 1.02% at 3 hours and 1% after 24 hours. The calculated gel time was equal to 7 seconds. Concerning the compression strength:

1 h = 0.05 MPa

3 h = 0.15 MPa

24 h = 1.21 MPa

7 days = 1.89 MPa

28 days = 2.02 MPa

4.12 Brisbane Airport Link (APL), Brisbane (Australia)

	Dosage	Brand and/or type
Cement (kg)	337	General Purpose Cement (Sunstate Cement Ltd)
Water (kg)	783	/
Bentonite (kg)	40	Trugel (Unimin Australia)
Retarder/fluidifying agent (L)	6.7	Condat A Stabiliser L (Condat Lubrifiants)
Accelerator (L)	81	NG sodium silicate (PQ Australia Pty Ltd)

Reference: Reschke & Noppenberger (2011).

The component A was characterised by a fluidity measured with the Mash cone equal to 58 seconds. The stability of the mortar was verified by the unit weight, equal to 1.29 kg/L, and by the bleeding assessment, which was 2% at 3 hours and 6% after 24 hours. The calculated gel time ranged between 18 and 23 s. Concerning the uniaxial compression strength:

24 h = 0.36 MPa

48 h = 0.83 MPa

7 days = 1.4 MPa

A peculiarity of this case history regards the supplier's proposal to dilute the accelerator in a solution at 50% by volume. This operation was carried out in order to improve the gel time and permit a suitable filling operation.

4.13 Follo Line, Oslo (Norway)

	Dosage	Brand and/or type
Cement (kg)	340	GP cement - Norcem
Water (kg)	807	
Bentonite (kg)	30	MAPEQUICK CBS SYSTEM 7 - Mapei
Retarder/fluidifying agent (L)	5	MAPEQUICK CBS SYSTEM 1 Evo - Mapei
Accelerator (L)	7–6% by volume per 1 m^3	/

Reference: Càmara (2018).

The technical specification regarding the component A required a fluidity measured with the Mash cone ranging between 30 and 45 seconds. The stability of the mortar was verified also by checking the unit weight, greater than 1.25 kg/L, and by the bleeding assessment, required to be lower than 0.5% after 1 hour and lower than 1% after 2 hours. The gel time must range between 5 and 12 s. Concerning the uniaxial compression strength, tests carried out on cube samples satisfied the following requirements:

1 h ≥ 0.1 MPa

2 h ≥ 0.2 MPa

24 h ≥ 0.7 MPa

28 days ≥ 3 MPa

The peculiarity of this case history is the provision concerning the elastic modulus (E) in the situation-specific technical requirements, whereby E should satisfy the following values:

2 h > 20 MPa

4 h > 100 MPa

This case history describes a successful application of the two-component technology in rocks where in certain cases a water pressure up to 16 bars was reached.

4.14 Metro Line 7 (E-W lot), Tehran (Iran)

	Dosage	Brand and/or type
Cement (kg)	350	/
Water (kg)	872	/
Bentonite (kg)	35	/
Retarder/fluidifying agent (L)	3.5	/
Accelerator (L)	70	/

References: Novin et al. (2015, 2012).

4.15 Legacy Way, Brisbane (Australia)

	Dosage	Brand and/or type
Cement (kg)	40	GP cement (Wagner)
Water (kg)	766	
Bentonite (kg)	40	MAPEQUICK CBS SYSTEM 5 (Mapei)
Retarder/fluidifying agent (L)	5	MAPEQUICK CBS SYSTEM 1 (Mapei)
Accelerator (L)	9–10% by volume per $1m^3$	/
Fly ash (kg)	80	Millmeran Flyash (Wagner)

Reference: Càmara (2018).

In this site, the mix design was projected in order to obtain a component A that was stable in time, with a unit weight greater than 1.25 kg/L and bleeding values lower than 0.5% after 1 hour, lower than 1% after 2 hours, and lower than 2% after 4 hours. The flowability was assessed with the Marsh cone, with a required value of 35 seconds and a loss of viscosity lower than 0.5% after 24 hours. Concerning the uniaxial compression strength, tests carried out on cube samples satisfied the following requirements:

1 h ≥ 0.1 MPa

2 h ≥ 0.5 MPa

24 h ≥ 1.5 MPa

28 days ≥ 4 MPa

The gel time was equal to 11 seconds.

These technical specifications listed also the acceptable tolerance values concerning the assessment of the flowability and a gel time of ± 3 seconds.

The peculiarity of this case history is the provision concerning the shrinkage of the hardened grout, required to be less than 10000 micro-strain.

In conclusion, it should be highlighted the very high w/c ratio used could wrongly lead the author to expect a low strength performance. The reality shows how the addition of the fly ash had a strong impact on the strength development.

4.16 Bolaños-Campobecerros tunnel, NE-N High Speed Railway Line in Galicia (Spain)

	Dosage	Brand and/or type
Cement (kg)	600	/
Water (kg)	1668.6	/
Bentonite (kg)	70.8	/
Retarder/fluidifying agent (L)	6	Masterroc AGA925
Accelerator (L)	/	/

Reference: Càmara (2018).

Despite the significant lack of information on the mix design, this case history represents an interesting example of the two-component grout technology aimed at improving the waterproofing of tunnels. The tunnel was built through rocks, where at certain points the water pressure reached a pressure of 14 bar with a water flow up to 100 L/s. It was for that reason, as Càmara (2018) highlighted, that the two-component backfilling was chosen instead of the mono-component.

It should also be underlined that pre-hydrated bentonite (not less than 24 hours in water) was used in the batching plant in order to improve the sealing ability of the final grout. According to the author's personal experience, the systematic use of pre-hydrated bentonite is quite rare.

4.17 North West Rail Link (NWRL), Sydney (Australia)

	Dosage	Brand and/or type
Cement (kg)	292	80/20 FA Blended cement
Water(kg)	787	/
Bentonite (kg)	30	API 13A Drilling Bentonite
Retarder/fluidifying agent (L)	4.1	TAMCem 8BFG Retarder
Accelerator (L)	91	PQ TJH-135 Accelerator

Reference: Ivantchev and Dal Rio (2015).

At this working site, the mix design was projected in order to obtain a component A that was stable in time, with a bleeding value less than 5% after 24 hours. The gel time, required from the specification to be lower than 20 seconds, was assessed as close to 12–13 s, while the flowability obtained was equal to 34.3 s after 2 hours. Concerning the uniaxial compression strength, tests carried out on cube samples satisfied the following range of acceptance:

1 h = 0.12–0.15 MPa

6 h = 0.7–0.9 MPa

24 h = 1.5–1.7 MPa

28 days ≥ 5.5 MPa

Regarding this case history, the type of cement used should be highlighted. In fact, a cement composed of 20% fly ash was selected as a function of the excellent performance identified in preliminary tests that was able to satisfy the requirement concerning the strength at 1 hour.

4.18 Comments to case histories

After reading all the reported case histories, it should be clear that, at the moment, there exists no specific guideline that prescribes the targets that the two

components should meet, concerning the properties of both component A and the hardened grout. Obviously, recalling the key concept 2, it could partially explain such a wide and miscellaneous scenario but, in my opinion, there is no hiding the absence of a unique testing path that could be really helpful for all the stakeholders involved (the sample shape is not fixed, nor are the curing time and testing frequency).

However, not only differences but also similarities can be focuses that are useful for investigating the two-component backfilling technology in greater depth. Before that, I would just remark that the purpose of this paragraph is not to try to generalise all cases by forcing and fitting different scenarios into a single schema, but to try to provide an order of magnitude of the parameters that can enable us to characterise the backfilling grout.

First of all, the water/cement ratio (hereinafter w/c, computed as weight/weight) is taken into account. Usually this parameter ranges between 0.45 and 0.60 for concrete and close to 1 for mortar. But, as concerns the two-component technology, this value is higher. Table 3 summarises all the case histories, with their w/c values. In order to streamline the following analysis, also an ID has been added to each construction site, according to the paragraph numbers used above in sections 4.1 to 4.17. For construction sites characterised by a mix design without a unique dosage for each compound (but with a range), the average between the maximum and minimum values is reported.

Table 3 - W/c ratio of the reported case histories and their ID.

ID n°	Construction site	w/c
1	Metro Rome Line C – Roma (Italy)	2.37
2	Oraki Main Sewer Hobson Diversion (OMSHD) – Auckland (New Zealand)	1.52
3	Metro Line in Sofia (Bulgaria)	2.74
4	Metro Line 1 in Brescia (Italy)	2.59
5	Metro Line 2 in Warsaw (Poland)	2.7
6	Hydraulic tunnel Maldonado in Buenos Aires (Argentina)	2.27
7	LTA tunnels – Singapore	3.52
8	Highway tunnel Sparvo between Bologna and Firenze (Italy)	2.53
9	Hydraulic tunnel STEP, Section II and III in Abu Dhabi (United Arab Emirates)	2.83
10	Personal experience (France)	3.71
11	Personal experience (Italy)	2.6
12	Brisbane Airport Link (APL), Brisbane (Australia)	2.32
13	Follo Line, Oslo (Norway)	2.37
14	Metro Line 7 (E-W lot), Tehran (Iran)	2.49
15	Legacy Way, Brisbane (Australia)	19.15
16	Bolaños-Campobecerros tunnel, NE-N High Speed Railway Line in Galicia (Spain)	2.78
17	North West Rail Link (NWRL), Sydney (Australia)	2.7

Before moving to other considerations, it must be reported that the construction site ID n°15 will be excluded from further analysis because the relative mix design cannot be considered a classic two-component one. In fact, the addition of fly ash led to a strong reduction of the cement content, with a consequent great increase of the w/c ratio. The calculated w/c value of 19.15 is very high, rare, and out of line for the two-component technology. Strictly connected with this aspect is the flowability of close to 1 minute. Also the gelling

time, ranging between 18 and 23 seconds, is very long. From this point of view, construction site n°15 was unique, having used a dilute solution of accelerator that led to such a high value of gel time.

Regarding all the case histories that provide details of the grout parameters required from technical documents or simply measured during the backfilling study, some considerations can be made:

a) concerning the w/c, it emerges that the average value is 2.62, a very high value compared with the usual ones for normal concrete;
b) the gel time ranges between 5 and 20 seconds;
c) the flowability ranges between 30 and 58 seconds. Though not clearly mentioned everywhere, the test was assessed daily for up to 72 hours;
d) the unit weight ranges between 1.169 and 1.29 kg/L;
e) the bleeding is the first parameter that was not checked uniformly in time among the reported case histories. Generally, tests performed after 1, 2, 3, 4 and 24 hours are assessed. On the other hand, the range of acceptable values is very tight, namely between 1 and 5%.
f) the uniaxial compressive strength is the second parameter that is not checked uniformly in time. Furthermore, also the order of magnitude required at long curing times (28 days) among the reported case histories is variable. Concerning the testing times, assessments were performed after 0.5, 1, 2, 3, 6, 8, 24 hours, 7 and 28 days. However, the most commonly used testing times were 1 hour, 24 hours and 28 days. As concerns the different target of resistance at long curing times, construction sites adopting the incompressible bubble theory are clearly appreciable: the specified uniaxial compression strengths (UCS) at 28 days are lower than 2 MPa.
   For other cases, however, the required strength is higher. Concerning the UCS at short curing times, after 1 hour of curing the values range between 0.03 and 0.15 MPa.
g) only in one case (n°13), there is a provision related to the longitudinal elastic modulus. Unfortunately, the basic theory that led designers to require this value is unknown. If the requirement was as according to Thewes & Budach (2009), the value of E should be of the same order of magnitude as the excavated medium. Furthermore, no information regarding the standard procedure for the elastic modulus assessment is provided.

It should be remembered that the technical requirements, for very important and justified reasons, can be modified or integrated during the course of the tunnel construction.

Chapter 5

Ingredients

In this chapter the ingredients used for the production of the two-component grout are listed and described. Two different sections are presented: the first is related to the classic two-component application, while the second contains innovative ingredients that have been appearing in the two-component world in recent years. Generally, the working principle of the technology is still the same, namely the ingredients are always batched and components A and B are hence mixed together to obtain the grout.

5.1 Classic ingredients

First, it is necessary to provide a definition of "classic ingredients". According to the case histories of Table 3, the classic ingredients are: cement, water, bentonite, retarding/fluidifying agent and accelerator.

5.1.1 Cement

The cement usually adopted for component A production is ordinary Portland cement, which is composed of clinker and gypsum. The Portland cement clinker is made up of four different mineralogical compounds. Table 4 reports each component. The last column lists the chemical formula according to the Cement chemist notation (CCN).

Table 4 - Typical constituents of Portland clinker plus gypsum.

Component name	Chemical formula	CCN
Tricalcium aluminate	$(CaO)_3 \cdot Al_2O_3$	C_3A
Tricalcium silicate	$(CaO)_3 \cdot SiO_2$	C_3S
Tetracalcium aluminoferrite	$(CaO)_4 \cdot Al_2O_3 \cdot Fe_2O_3$	C_4AF
Dicalcium silicate	$(CaO)_2 \cdot SiO_2$	C_2S

The first two components are involved in the two fastest reactions, while in the development of the early strength the hydration of C_3S is the main actor (Youn et al., 2016).

Concerning the object of this research, in order to have good workability and pumpability, the w/c ratio plays a key role. By increasing the w/c, the viscosity decreases, which means the flowability increases. However, the bleeding phenomenon is proportional to the increase of the w/c, so an excessive increase of the water–cement ratio could lead to the occurrence of segregation problems. Furthermore, it should be highlighted that the higher is the Blaine value of the cement (cement particle fineness), the more strongly the water will be bonded to the cement particles, which means a more stable mortar. Finally, the designer should consider that by fixing all the mix design dosages, any change to the cement type will cause a consequent change in the gel time (Pellegrini & Peruzza, 2009).

Concerning the cement properties, EFNARC (2015) underlines also that the cement used should conform to EN 197-1.

5.1.2 **Water**

Water is the main element of the two-component backfilling technology. According to EFNARC (2015), the water used for component A production should be of potable quality or in accordance with EN 1008. It can also be acceptable to use water supplied from different providers, after the delivery of a conformity certificate, and after specific tests to prove the qualifying features.

From the author's personal experience, all the tunnelling construction sites have used and are using groundwater when it is present. At job sites characterised by a lack of water, a special cleaning treatment process can be foreseen in order to treat the available water.

In every case, the water quality is crucial for the success of the backfilling process. The potential presence of salts in the water can completely change the results in terms of both the component A performance and the final grout performance. The ingredient most sensitive to the water's chemical/physical variations is bentonite.

5.1.3 **Bentonite**

Bentonite is a natural clay mainly composed of montmorillonite, which is a soft phyllosilicate member of the smectite group.

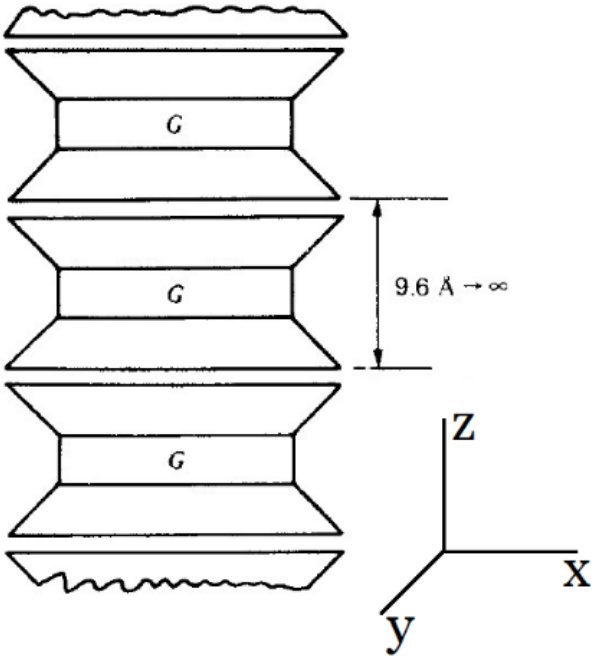

Figure 29 - Schematic diagrams of the structures of the smectite minerals: montmorillonite (Mitchell & Soga, 2005).

The particles are plate-shaped with an average diameter around 1 μm and a thickness of 0.96 nm made up of an octahedral sheet of gibbsite (octahedral sheet cations are mainly aluminium) sandwiched between two tetrahedral sheets of silica, as shown schematically in Figure 29. Montmorillonite forms continuous layers in the two main directions x and y that are stacked one above the other in the direction z. Van der Waals bonding and cations are the weak forces that bond successive layers. Therefore they can be easily separated by water or the adsorption of other polar liquids. The basal spacing in the z direction is variable, ranging from 9.6 A˚ to complete separation. The theoretical composition in the absence of isomorphous substitutions is $(OH)_4Si_8Al_4O_{20}$* n(interlayer)H_2O. The different types of bentonite are named as a function of the respective dominant element, such as potassium, sodium or calcium.

Bentonite is a natural material obtained from the alteration of volcanic ash due to weathering. It is used in engineering applications (in the natural state or after an industrial polymer addition process) for slurry production in excavation processes, for the realisation of seepage barriers or waterproofing layers in dumps. Bentonite is commonly characterised by Atterberg's liquid limit close to 500%. The process that leads the water absorption is named swelling.

Concerning the application of bentonite in the two-component technology, its role is strictly linked to the stability of component A, i.e., by using the right dosage the bleeding phenomenon can be satisfactorily controlled (Figure 30).

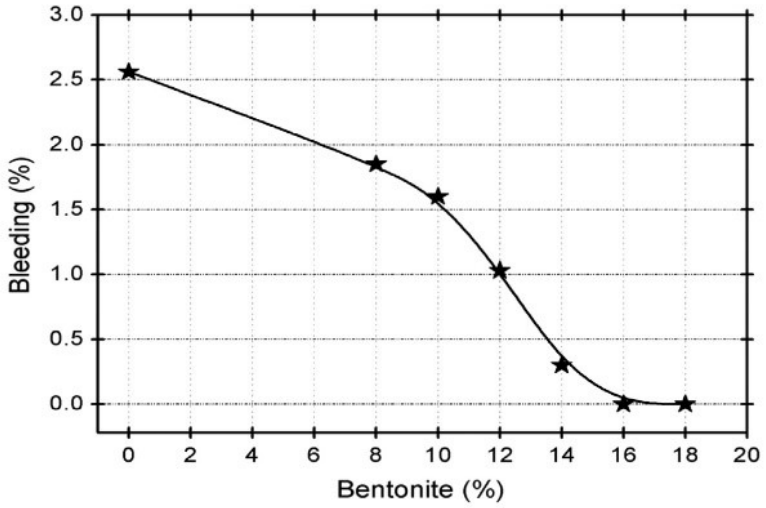

Figure 30 - Bleeding trend as a function of the bentonite increasing. Common Portland cement suspension (Mesboua et al., 2018)

This fundamental property has been explained in Mesboua et al. (2018). With an electrokinetic analysis, it has been determined that the zeta potential (ζ) (an electrokinetic potential that rules the colloidal dispersions) of the complex cement/bentonite fluid in aqueous medium is negative, dominated by the bentonite particles. Thereby, in this condition the repulsive forces prevail over the Van der Waals forces and the mortar is hence stable. A graphical and simplified view of the phenomenon is depicted in Figure 31.

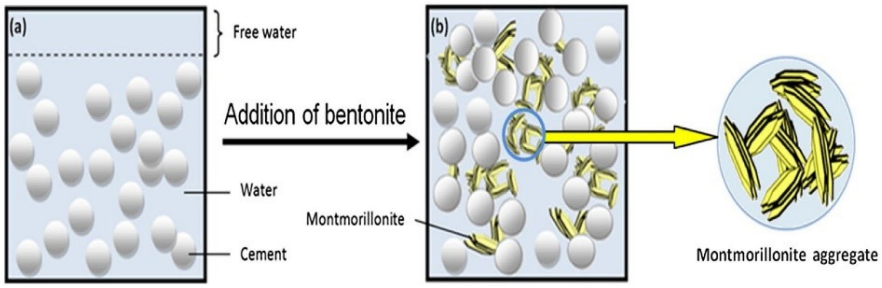

Figure 31 – Bleeding phenomenon. On the left (a) a common Portland cement solution; on the right (b) the same solution mixed with bentonite (Mesboua et al., 2018).

On the other hand, if the bentonite dosage is too high, the final mortar could reach flowability values not aligned with the technical specifications. Pelizza et al. (2010) highlighted also the role of the bentonite in the homogeneity of the mortar.

Regarding the type of bentonite in the two-component field application, natural sodium bentonite is most commonly used. The availability of this component is not ensured everywhere, so often the ion exchange process permits the conversion of other types of bentonites to sodium-activated ones with characteristics similar to natural sodium bentonite (Youn et al., 2016).

Càmara (2018) describes how the technical requirement for a more watertight action of two-component grout was achieved by using a pre-hydrated bentonite in the batching plant. The pre-hydration process in the specific case of the Bolaños-Campobecerros tunnel was of 24 hours duration.

5.1.4 **Retarding and fluidifying agents**

The purpose of this family of ingredients is to reduce the setting of the component A, to extend the workability up to 72 hours (this time lapse is considered the maximum break required for non-extraordinary machine maintenance) and to reduce the flowability.

The dosage of the retarding/fluidifying agent and the adding order in the procedure is very important and it should be carefully calibrated. For example, an excess in the dosage could lead to an accelerating effect (Youn et al., 2016), or changing the adding order in the procedure (without changing the dosage) can give strongly different results (personal laboratory experience). The most common products are based on phosphate, sucrose and phosphorous acid. A very interesting image is shown in Pellegrini & Peruzza (2009), where the authors stated that "natural sugar solution" was used as retarder.

The only problem with this ingredient is that chemical suppliers never divulge the real composition of their product.

5.1.5 **Accelerator**

The accelerator is the only ingredient of component B. In the backfilling technology, in my personal experience, only sodium silicate based accelerators are used. These types of accelerators are part of the wide group of alkaline silicate accelerators, also called water glass (Flores, 2015). On the market, different accelerators are available, composed of different water solutions of sodium silicate.

Adding an accelerator to the component A leads to a forced initiation of quick setting. Youn et al. (2016) introduced two different types of accelerator: the first brings forward the start of setting and the second boosts the initial hardening.

That research also highlights how, by increasing the volume percentage of the accelerator in the mix design (without changing the component A), the final strength of the grout increases too.

Sodium silicate based accelerators are used both in conventional excavated tunnelling (applied in the shotcrete) and in mechanised tunnelling (just used in the backfilling process). However, the products may be different: while the shotcrete process commonly uses alkali-free products, in the mechanised process stronger chemicals provide higher performance with lower dosages (due to the fact that the backfilling is performed mechanically, without the risk of worker injuries from contact with the accelerator, which is commonly strongly basic – pH≃13).

Unfortunately, the composition of these chemical products is covered by industrial secrecy. However, Table 5 summarises the information provided by Pellegrini & Peruzza (2009) concerning the accelerator product used in the Sao Paulo metro project. In this work, further information regarding the increase of the

gel time as a function of the increasing accelerator dosage is reported (seemingly illogical, this aspect will be examined in more depth in the next chapters).

Table 5 - Sodium silicate properties of accelerator used in Sao Paolo metro project (Pellegrini & Peruzza, 2009).

Density at 20 °C (° Baumé)	38
Viscosity at 20 °C (cP)	40
Content of solids (%)	34.4
SiO_2/Na_2O ratio	3.22
Unit weight (kg/L)	1.355

5.2 Innovative ingredients

In this paragraph innovative ingredients used in the two-component technology are analysed. Basically, all of them have come from the world of concrete, consequently their application is strictly for component A production. Concerning fly ash and stabilising polymers, the path from the laboratory experimentation to the construction site is completely covered, while for blast furnace slag the laboratory study is still ongoing.

5.2.1 **Fly ash**

Fly ash is an ingredient that came into the two-component technology directly from the classic concrete world. In concrete, fly ash operates both as a filler (physical contribution) and from a chemical point of view. Specifically, by replacing some part of common Portland cement with the addition of fly ash, the latter takes part in the concrete reactions, leading to better performance of the final grout in terms of:

a) less hydration heat: less Portland cement in the mix leads to less production of tricalcium aluminate and tricalcium silicate. These reactions produce the biggest part of the hydration heat;
b) higher waterproofing;
c) greater fluidity for fresh concrete, meaning the reduction of the w/c ratio by fixing a certain fluidity. Consequently, better performance in terms of strength is obtained.

As previously described, since tricalcium aluminate and tricalcium silicate are involved in the two fastest reactions, their reduction slows the development of strength at short curing times (1–7 days). Regarding this last statement, controversial information is reported in Ivantchev & Dal Rio (2015) in case history n°17. According to the authors, the choice to use a special cement with a certain percentage of fly ash in the matrix (20% fly ash and 80% Portland cement)

was made expressly in the light of the better performance at a short curing time (1 hour).

Furthermore, this paper also highlighted how the presence of fly ash in the cement matrix led to a slightly longer gel time (about 2 seconds). In the scientific literature, unfortunately only one case history reports the use of fly ash as a separate ingredient (i.e. not premixed with cement) in the two-component technology: Càmara (2018) in case history n°15 points out how, by using a dosage per cubic metre of fly ash equal to 80 kg and only 40 kg of cement, the grout performance is aligned with other case histories, it being understood that the uniaxial compressive strength of 4 MPa reached at 28 days of curing time is plainly above average.

5.2.2 **Stabilising polymer for cementitious grouts**

Nowadays, the use of polymers expressly designed for the stability of component A is starting to spread at specific construction sites. Specifically, in countries where for environmental or for logistical reasons the use of bentonite is impossible, these chemical products still permit the successful application of the two-component technology.

Obviously, the chemical nature of this ingredient is a commercial secret.

5.2.3 **Blast furnace slag**

The use of blast furnace slag as an ingredient in the two-component backfilling technology is not currently used. However, although the scientific literature reports no case histories using blast furnace slag, at the laboratory scale tests have started to be performed.

Schulte-Schrepping & Breitenbücher (2019a) highlighted that combining hydraulic cement and blast furnace slag leads to the formation of a hybrid binder that can be used for the backfilling process performed with the two-component technology. The authors report outcomes concerning the enormous increase in strength and stiffness compared to classic two-component grout based on cement. Furthermore, by using blast furnace slag the final grout shows better resistance to chemical attack and finally also the workability of the component A appears to be improved with respect to the classic technology.

5.3 Key concept

KEY CONCEPT 6: The two-component technology is based on the reaction between two components. Component A is made up of cement, water, bentonite and chemical agents (retarding/fluidifying agent), although in recent years also

fly ash and blast furnace slag are being tested in order to improve the final parameters of the grout. Also the study of replacing bentonite by using suitable polymers is ongoing. The component B is an accelerator composed of a silicate solution.

Although the hydration process plays a key role in the hardening of the two-component grout, no information concerning the exact chemical reactions between components A and B is available. Moreover, no information concerning the chemical compositions of the accelerator and the retarding/fluidifying agent is available.

Chapter 6

The experimental approach: the key for the two-component grout study

The purpose of this very short chapter concerns my desire to provide the clearest vision of the whole work performed during these last few years. This research covered different aspects concerning the two-component backfilling technology, often markedly different. The one concept that led me in this research was to "find something useful, find something that will help the backfilling stakeholders in their work".

In these years of research, I had the pleasure of analysing different numerical models concerning tunnels, and specifically regarding two-component grout. Very often I focused my attention on the parameters used for modelling the two-component grout: frequently the parameters were estimated according to analytical equations, without a real reference concerning any basic laboratory study; at other times the parameters were estimated according to the concrete (obviously better known, but completely different). In both cases, I always had doubts about the real validity of a perfect geometrical numerical model based on parameters pertaining to such an unknown material as two-component grout.

According to these concepts, I developed my tests and outcomes were obtained. In truth, the whole research path was not completely clear from the beginning, but the more time I spent working on the two components, the more interesting questions arose. Not all of them found answers: in certain cases there was not enough time, in other cases tests were scheduled and samples were produced, but Covid-19 meant that they were never performed (especially tests needing to be carried out after curing times longer than 1 year).

In conclusion, in this short chapter I wish only to point out the experimental nature of the work performed. The parameters that I decided to investigate, such as the elastic modulus or the shear strength, have never previously been studied.

The scarcity, and in certain cases, the complete absence of previous works led me to the difficult task of identifying, among the huge number of technical standards, those most suitable for two-component grout. On top of that, due to the evolutionary nature of the material studied, sometimes the same parameter was assessed according to different standards as a function of the short or long curing time.

In the next chapters, the experimental section of my PhD research will be presented. Three different main areas can be recognised:

1. preliminary tests – procedure validation: chapter 7;
2. pure experimentation: chapters 8, 9, 10, 11, 12 and 13;
3. greater depth concerning raw ingredients: chapters 14 and 15.

The first step was to establish a warranty aimed to ensure that all the subsequent developments were founded on "real" samples of two-component grout. After drawing up and testing a laboratory procedure that enabled me to produce a "real two-component grout" with properties comparable to those of a grout really produced on a construction site, I focused my attention on issues raised by all the two-component stakeholders and by my personal curiosity, issues currently without answers or with unsatisfactory answers in the scientific literature.

Each chapter is organised by introducing the scientific gap (or the lack), the idea for filling it, the tests performed and their results, and finally the discussion, followed by the key issues (very short sentences aiming to summarise briefly the new findings/innovation introduced). Specifically for chapters where innovative tests are addressed, a special paragraph named "Additional information" has been added, in order to provide, for potential future researchers, further details regarding tests, personal feelings experienced during the tests, failed tests etc. These paragraphs have been included in the thesis because, in my opinion, even unsuccessful research experiences should also be shared with the scientific community.

Before starting, some final information for readers: when not expressly reported, the curing time of 1 month is intended as 28 days.

Chapter 7

Production of a “real” two-component grout

The content of this chapter has been published in the papers Todaro et al. (2019) and Todaro et al. (2021). In this chapter all the results obtained during the first part of the research path are summarised. After the conclusion of this first preliminary phase, I developed a critical eye that has enabled me to better understand the issues concerning two-component grout that need to be investigated in greater depth.

7.1 The idea

Although the two-component backfilling system is becoming the most frequently used method for performing annulus backfilling, no standardised path for the grout assessment is yet available.

Taking into account the key concept 5 expressed in paragraph 3.3 and remembering the usual prescribed features that a suitable two-component mix should satisfy in terms of pumpability and workability (flowability), stability, gel time, and strength at both short and long curing times, a standard laboratory scheme that clearly expressed tests that should be performed is not provided in the scientific literature (1st gap). Furthermore, there is no information regarding a procedure that might be able to produce, at the laboratory scale, component A (2nd gap). It has been explained previously that component B is provided directly from the chemical industries supplier, whereas component A has to be produced in a batching phase. Thereby, another aspect should be addressed, namely how to produce a component A similar to the one produced at the construction site and what engineering instruments could be used for the comparison.

In conclusion, a research path was scheduled and can be summarised in 5 steps, as follows:

Step 1: draw up a laboratory procedure to obtain a good quality component A, starting from the necessary raw materials;

Step 2: draw up a test procedure able to assess the grout properties, according to the requirements described in paragraph 3.3 and the state of the art;

Step 3: choose at least 4 mix designs to perform a preliminary test campaign. Draw first considerations on the dependence of the parameters on the mix design dosages;

Step 4: carry out a construction site test campaign. The same mix design as in the laboratory was followed but component A was produced by using a turbomixer. The same tests described in Step 2 were performed;

Step 5: compare the laboratory procedure outcomes and those at the construction site in order to evaluate the reliability of the laboratory procedure to manufacture a component A similar to the one produced using the construction site turbomixers.

7.2 Development of a laboratory procedure for component A production

The importance of obtaining a component A with similar properties to the real component A produced at construction sites is considered of crucial importance, and may be the most sensitive phase of the whole research.

The first issue that has been taken into account concerns the mixing phase. Component A (water, bentonite, cement and retarding/fluidifying agent) requires a high mixing energy. For this purpose, an AM 20-D ARGOlab Overhead Stirrer (Figure 32) was selected as the laboratory mixer.

Figure 32 - AM 20-D ARGOlab Overhead Stirrer.

The second issue that was taken into account concerns a suitable impeller, with the appropriate shape and able to mix all the ingredients carefully, guaranteeing the right turbulence. Three different impellers were used and the choice of the best one was based on the quality of the results. The three impellers were tested by fixing the same parameters for each test in terms of:

a) the amounts of ingredients (in this phase only water and bentonite were used);
b) geometrical aspects (tank dimensions and the distance between the impeller and the tank bottom);
c) rotation speed of 2000 rpm;
d) duration of the mixing phase equal to 7 minutes.

Consequently, three different qualities of bentonite slurry were obtained. The choice was made by checking for the presence of lumps. Figure 33 depicts impellers that did not produce a suitable result, while Figure 34 shows the impeller that mixed the tested ingredients best, without the presence of lumps in the slurry obtained.

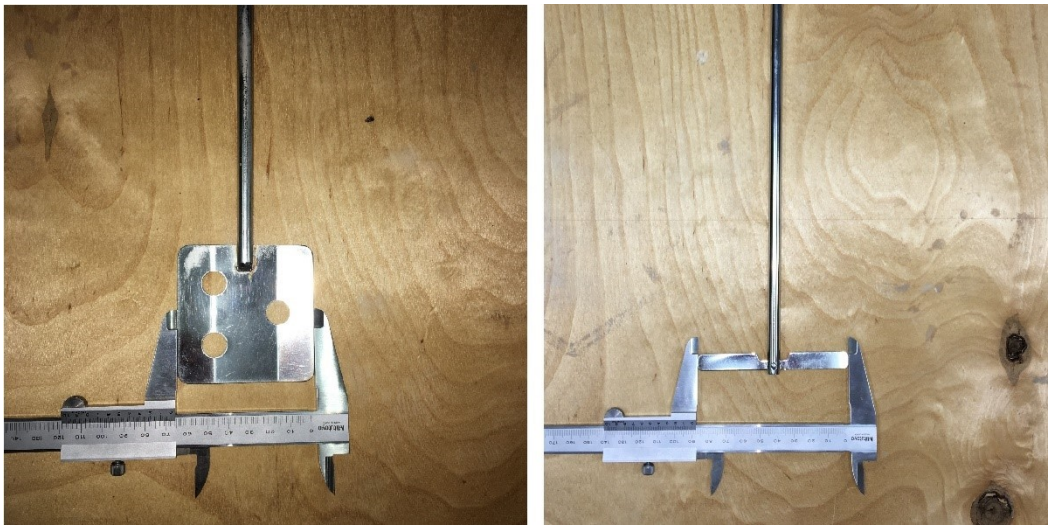

Figure 33 - Impellers discarded because of a low component A quality.

Its main geometrical dimensions, suitable for reproducing a similar impeller, are also reported in Figure 34.

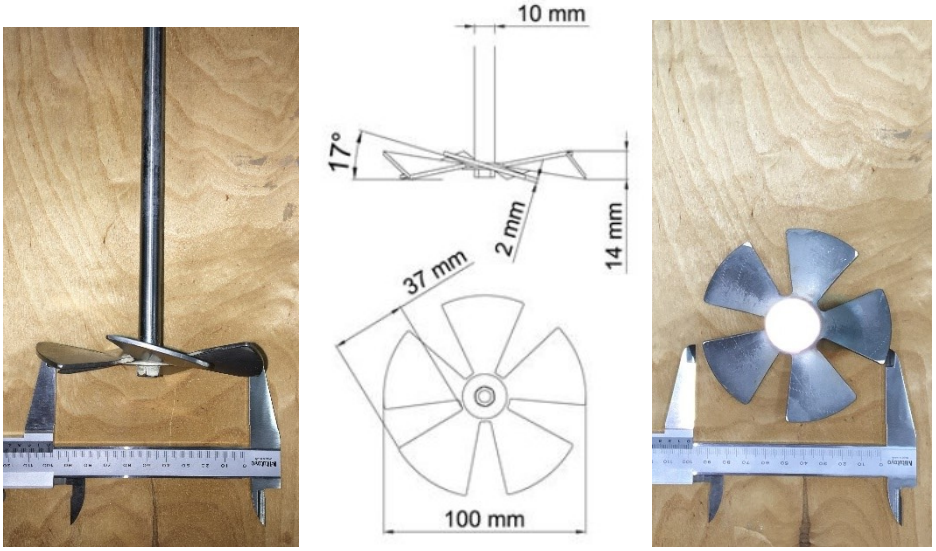

Figure 34 - Officially used impeller.

The duration and the order of each mixing step were defined following the advice of Mapei experts. Before listing the final procedure, some further details should be highlighted, resulting from a huge number of calibrating tests:

a) the bentonite must be dry, so no pre-hydration process was taken into account;
b) the mixing tank should have a diameter/height ratio not less than 0.66;
c) the ratio between the tank volume and the obtained mortar volume should range between 2 and 3;
d) the impeller should be able to create the right turbulence so as to homogenise the mortar properly. The impeller should be similar to the one

depicted in Figure 34, or in any case it should feature sloping blades that ensure a mixing with good turbulence;

e) the impeller must be fixed to the stirrer in such a way that the blade skims the tank bottom, without touching it;
f) the ratio between the impeller diameter and the mixing tank diameter should be close to 0.5.

In conclusion, in Table 6, the procedure defined for component A production is presented.

Table 6 - Procedure for component A production (Todaro et al., 2019).

Operation	Impeller rotation speed (rpm)	Duration (min)
Fill the tank with water and start the mixer	800	/
Add the bentonite, increasing the propeller speed at a constant rate	from 800 to 2000	0.5
	2000	6.5
Add the cement	2000	3
Add the retarding/fluidifying agent	2000	2

Beforehand, it is very important to weigh and prepare all the raw materials needed, according to the mix design under testing. Previously, the mixing tank with the right amount of water must be located under the stirrer, centrally, whereupon the impeller must be locked onto the stirrer. The best way to conduct this operation is to put the impeller in contact with the tank bottom and then raise it slightly, for a small space necessary only to avoid a scratching noise; after that the impeller can be locked in position. Initially, the stirrer engine can be activated, setting up a rotation speed close to 800 rpm. After that, the powdered bentonite can be added, dusting it constantly but not slowly, as this operation must be ended in 30 seconds. Before long, the rotation speed has to be increased to 2000 rpm; the activating phase of the bentonite is thus started, with a duration of 6.5 minutes. Subsequently, the concrete is added. It is suggested not to pour the whole amount in at once in order to avoid water spurts and impeller speed fluctuations. The mixing continues for a further 3 minutes, whereupon the retarding/fluidifying agent is added and the procedure ends after another 2 minutes of mixing. Finally, the stirrer engine is switched off. Figure 35 shows a photo of the mixing phase.

Figure 35 - Laboratory mixing phase.

With our equipment, no more than 3 L can be produced in one batching operation. The manufacturing of a larger amount of component A in a single batching operation was tested but unsuccessful because of inhomogeneous results.

The order of adding ingredients should be strictly followed. Since the bentonite must be the first ingredient used because of the time needed for the hydration process, the only possible order change is between the concrete and the retarding/fluidifying agent. Tests performed with this alternative order highlighted a non-negligible loss of fluidity and completely different outcomes in terms of the Marsh cone test.

7.3 Development of a testing procedure

The project of a mix design always starts in the laboratory. The first reports of tests were reported in Bezuijen et al. (2005) and in Bernett (2008), where a rough and poorly detailed list of potential assessments for testing the two-component grout are mentioned. EFNARC (2015) is the first reference to suggest the use of a Marsh cone for the component A workability and pumpability. Pellegrini & Peruzza (2009) introduced the prescription of the opening of the funnel, equal to 4.76 mm, and the volume of the cylinder for the bleeding assessment, equal to 250 cc. Antunes (2012) proposed a testing protocol based on ASTM international standards. He highlighted how the flowability could be assessed according to ASTM C939-10, but the prescribed funnel with an opening of 12.7 mm was in contrast with previous prescriptions. Also, for the gel time assessment, there are inconsistencies between different authors. Furthermore, information reported by Novin et al. (2015), Zarrin et al. (2015), Flores (2015), Dal Negro et al. (2014a), and Shah et al. (2018) concerning laboratory experiments was also taken into account.

The testing procedure set up was based on a comprehensive scientific literature review. The proposed tests were chosen taking into account the robustness of their application (how many authors used them in laboratory/construction sites) and the possibility of easily performing them at the construction site (without the "protection zone" typical of a scientific laboratory). This last aspect was of paramount importance, and in fact the need to repeat tests with a certain frequency in "hard conditions" was always kept in mind.
The testing procedure was organised in three groups:

- tests on component A;
- gel time assessment;
- tests concerning the gelled/hardened grout,

A specific paragraph has been dedicated to the samples production and the curing modalities.

7.3.1 Tests on Component A

7.3.1.1 Unit weight assessment

The unit weight assessment was the first test aimed to check expeditiously if a certain mortar had been manufactured according to a certain mix design. A large deviation between the expected value and the measured one highlights potential batching phase mismanagement or problems, or nonconformity of the raw materials with respect to the mix design.

The unit weight can be assessed using a mud balance. The instrument is composed of a steel rod, equipped with a cup on one side and a cursor weight on the other (Figure 36). When there is equilibrium between the cup full of mortar and the cursor, the unit weight can be red. The perfect horizontal alignment of the rod can be verified by a spirit level.

Figure 36 - Mud balance used.

Alternatively, mainly in the laboratory, the unit weight can be assessed also by using a volumetric flask and a high-precision scale. In our case, a 250 mL volumetric flask (Figure 37) and a Kern 572-39 scale (precision = 0.01 g) were used.

Figure 37 - 250 mL volumetric flask used for the component A unit weight assessment.

In this case, the flask was filled slowly till the liquid volume reached the notch. After that, a time lapse of 5 minutes allowed any air bubbles trapped in the mortar to rise and leave the liquid. Thereupon, a second volume check was carried out and, if necessary, further component A was poured till the notch was completely covered. Only after that, the weight could be measured and, considering the net weight, the unit weight was computed as the ratio on the volumetric flask volume.

Independently of the method used, at least three different determinations were performed. The tests were carried out on fresh mortar (component A is considered fresh if produced not more than 1 hour before).

7.3.1.2 Flowability assessment

The flowability is the parameter used to guarantee the pumpability and workability of the component A. According to UNI 11152:2005, paragraph 13, the flowability assessment performed using the Marsh cone provides an empirical value of the mortar viscosity, expressed as the time needed by 1 L of the mortar to flow through the Marsh cone. The exit hole has a diameter of 4.8 ± 0.1 mm.

Figure 38 - Marsh cone test.

Figure 38 depicts the test phases, starting from the left. First, the Marsh cone must be locked on its support stand. The cone is not equipped with an integrated spirit level, so its horizontality must be validated with an external level. After that, the component A should be slowly poured into the cone through the half circle equipped with the metal grid, taking care to plug the hole. If lumps are trapped in the grid, they must be removed. Only when the mortar level inside the cone touches the metal grid, the hole plug can be removed and the time count started. The tank under the cone has a marked notch highlighting the volume of 1L, and when the flowed mortar in the tank reaches this level, the time is stopped.

The procedure foresees four different determinations, carrying out tests on the fresh mortar, and after 24, 48 and 72 hours from manufacturing the component A.

Between one assessment and the next one (scheduled after 24 hours), the mortar should be stored in a closed tank. As concerns the tests performed at 24, 48 and 72 hours, before starting, special care should be taken over the homogenisation of the mortar, which must be tested as any bleeding phenomenon action will cause a clear separation between the water and the other ingredients of the mortar. The homogenisation operation must be performed manually, slowly stirring the mortar with a rod for about 1 minute. Mechanised mixing for the homogenisation was avoided because the potential effect of the strong energisation on the fluidity cannot be controlled.

7.3.1.3 Bleeding assessment

The bleeding test aims to assess the stability of the component A. According to UNI 11152:2005, paragraph 11, the bleeding value is a percentage value computed as the ratio between the volume of the bleeding water (in the upper part of the cylinder) and the mortar volume after a certain time of curing.

Beforehand, a suitable location protected from thermal shocks and mechanical vibrations has to be prepared. Then, the mortar to be tested is slowly poured into a graduated cylinder, till the 1L notch is reached, whereupon the cylinder is sealed

watertight. After a certain time, the bleeding of a certain volume of water (V_{water}) occurs and the bleeding index can be computed as follows:

$$Bleeding = \frac{V_{water}(mL)}{V_{mortar}\ (mL)} * 100 \qquad 3$$

The V_{mortar} must be equal to 1L, while the V_{water} must be measured.

The bleeding assessment was performed 3 and 24 hours after the component A production. In specific cases, due to the weak stability of the tested mortar, assessment at 1 hour was also carried out.

Figure 39 shows the beaker before sealing (on the left) and after the scheduled time lapse (on the right). The bleeding phenomenon is highlighted with the red arrow.

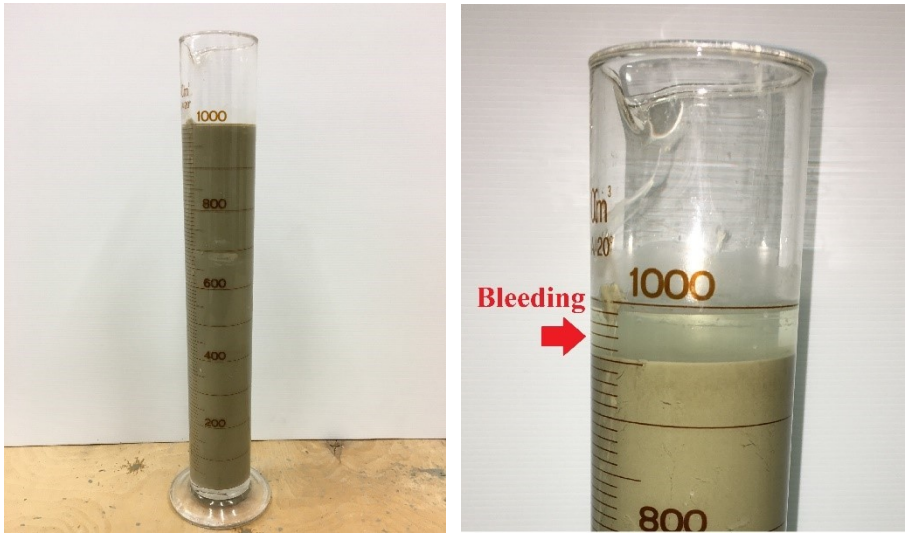

Figure 39 - Bleeding test. Before the counting starts (left) and after the scheduled time lapse (right).

7.3.2 **Gel time assessment**

The gel time evaluation is the first determination that foresees the use of component B. Its concept was introduced with *definition 1 or 2* in chapter 3. Currently, no standard procedure for the gel time assessment is available.

In this work, a new procedure has been introduced with the aim of making the operation easy and repeatable. Two plastic tanks with volumes of 0.4 L were used. Beforehand, a fixed amount of 200 g of component A and the same amount of component B (according to the mix design under study) are weighed and collected in suitable tanks. After that, the mixing starts by pouring the component A into the component B tank, and then the whole of the material from one tank to the other, till the mix obtained is no longer able to flow. The time measured from the first contact between the components to the loss of fluidity of the mix is the gel time. The mutual pouring operations must be performed quickly (not less than 2

emptyings per second). It is of crucial importance to start the test by pouring component A into component B, otherwise the required turbulence will not be reached. At least three different determinations must be performed, whereupon the average is computed.

During trial tests, bigger amounts of components were used for assessing the gel time but unsatisfactory results were obtained due to the inhomogeneous mixing which caused an inhomogeneous gelling process to occur.

After the assessment of the gel time was obtained following the mix design (i.e. the exact component B % reported in the mix design), a gel time test campaign must be performed, with the aim of covering all the possible construction site requirements. As several times underlined in earlier chapters, the backfilling project can require a more complex management of the gel time, foreseeing, for example, different gel times for different backfilling injection lines. In order to meet these needs, a fixed volume of 0.4 L of final grout was established as testing sample. Hence, components A and B were weighed according to the proper unit weights in order to obtain samples of hardened grout with the volume percentages listed in Table 7.

Table 7 - Percentages of both components used for the gel time campaign.

A (% by volume)	96	94	92	90	88	86	84	82	80
B (% by volume)	4	6	8	10	12	14	16	18	20

For each percentage combination (9 cases), at least three determinations must be carried out. Finally, a chart can be drawn up with all the outcomes, hereinafter called the “gelling function”.

7.3.3 **Samples production**

The samples production was based on the standard EN 196-1:05, according to which samples with dimensions of 40*40*160 mm were produced using specific moulds.

It should be underlined that the samples manufacturing is quite a complex process since the mould must be completely filled in a very short time, i.e. before the end of the gelling process. Furthermore, each sample must be cast in a single phase: if a double pouring is performed to completely fill the same mould, the two separate layers of grout will never bond together and the sample obtained must be discarded.

Beforehand, a sufficient quantity of component A and the computed amount of component B (according to the mix design) must be prepared in two tanks. Then, component A is poured into component B, the whole of the mixed liquid is poured again into the other tank (originally for component A) and finally it is poured into the mould. In Figure 40, four photos depict examples of the casting phases of a single sample.

Figure 40 - From left to right: component A poured into the component B tank, the mixed grout poured again into the previous tank and eventually the sample casting. In the last photo the residual material on the inner tank surfaces can be observed.

Concerning the calculation of the suitable amount of component A for a successful casting, it is strongly discouraged to use a volume of only 0.256 L (equal to the mould volume). It is suggested to increase the volume by at least 20% for two main reasons. Firstly, the turbulence generated from the mixing of the two components causes many air bubbles that naturally start to rise upwards (in the direction of the casting surface), but, due to the fast gelation process, could be trapped inside the mortar. It was checked that when using exactly 0.256 L, the casting surface was often characterised by different weak points due to the presence of bubbles. An example of this can be observed in Figure 41, which depicts a big bubble close to the casting surface. For this reason it is suggested to overfill beyond the mould edge with a surplus of cast material, creating a sort of "weak layer" on the top of the mould (where all the bubbles are concentrated).

Figure 41 - Example of a big air bubble trapped inside the medium, close to the casting surface. Sample discarded.

Secondly, another aspect that cannot be ignored regards the impossibility of pouring into the mould exactly all the material inside the tank, again because of the fast gelation process. Unavoidably, a gelled layer of grout (sometimes more than just a layer) will be stuck on the tank's inner surface (Figure 40, right).

To conclude, the two abovementioned drawbacks can be avoided by preparing a suitable volume of components, casting the sample and eventually scraping off the excess volume with a spatula (Figure 42), thus removing the weak layer characterised by a larger amount of bubbles. Trimming of the sample must be performed within 1 minute after the casting because scraping the sample after any longer time lapse can cause irremediable damage to the cast surface.

Figure 42 - Samples cast calculating a bigger total volume of components. Bubbles are clearly visible on the cast surface (left). Samples trimming performed with a spatula (right) allows the removal of the potential weak points due to the presence of bubbles.

Immediately after the scraping, the count for the curing time starts. The cast samples are sealed watertight using suitable plastic bags (in order to avoid dehydration), located and protected inside the mould, and set aside far from potential temperature shocks. If the scheduled curing time is less than 24 hours, the plastic bags are simply removed and the test performed. Instead, if tests have to be performed after 24 hours, after one day the samples are demoulded and immersed in water. The curing water temperature was 23 ± 2 °C, the same as in the laboratory.

7.3.4 **Tests on hardened grout**

Concerning tests on hardened grout, the compression strength was taken into account as a reference parameter. Because of the lack of proper specific standards for two-component grout, the standard EN 196-1:05, as mentioned in the previous paragraph, was selected as the base reference although different adaptations were needed due to the singular features of the two-component technology.

If a rigorous analysis is performed, EN 196-1:05 is not integrally applicable for the two-component technology. Firstly, it is clearly underscored that this standard cannot be used for mortar with a very short setting time. Secondly, the standard refers to mortars composed of concrete and sands, mixed mechanically by using certain specific kinds of mixers. Furthermore, a compaction process using a flow table is foreseen. However, it is considered that this standard:

- is easy to follow;

- is well-established and known in the tunnel engineering world (in fact, before the worldwide use of the two-component technology, the most frequently used backfilling technology was the mono-component, which is a mortar with fine aggregates, tested successfully following EN 196-1:05);
- despite the abovementioned incompatibility, is the one that normalises the mortar, the most similar material to the component A (which is the greater part of the hardened two-component grout);

In conclusion, for these three reasons, EN 196-1:05 has been used.

Concerning the technical prescriptions of the standard, two constraints have never been respected. The first one pertains to the curing temperature of the samples. Instead of 20 ± 2 °C, the laboratory and the curing water temperatures were 23 ± 2 °C. Secondly, tests were not performed in load control mode with a speed of 2400 ± 200 N/s, but all tests were performed in displacement control mode, with speeds differing as a function of the curing time (Table 8).

Table 8 - Compression strength test speeds.

Curing time	Displacement speed
3 hours	0.25 mm/min
≥ 24 hours	0.5 mm/min

Tests were performed using the frame for the compression strength test (hereinafter also called “comprimitor”) and the frame for the three-point bending tensile strength test (or alternatively, three-point flexural tests), as depicted in Figure 43.

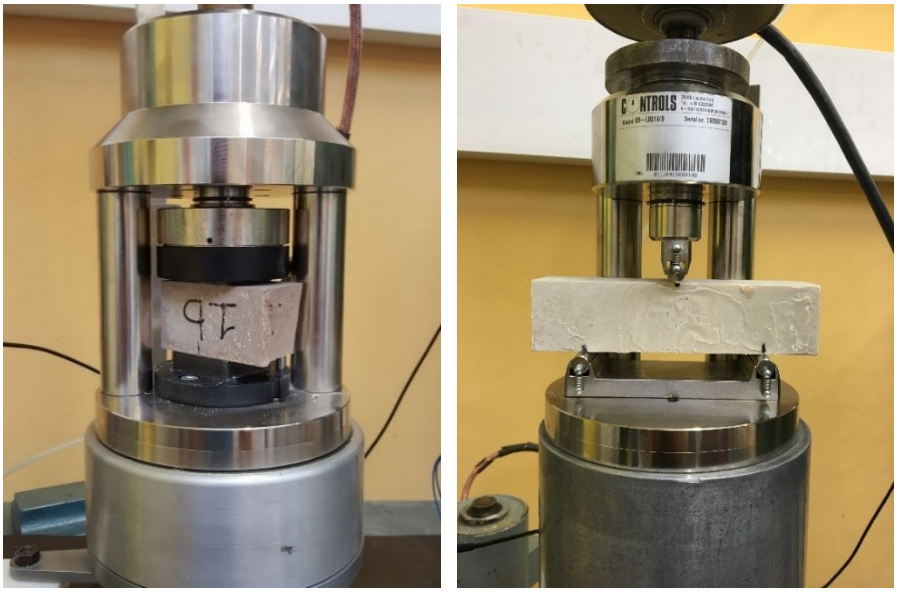

Figure 43 - “Comprimitor” (left) and frame for three-point flexural test (right) certified according to EN 196-1:05.

A load cell of 5 kN was used for the load recording for all performed tests.

EN 196-1:05 suggests performing first the three-point flexural test to obtain the indirect tensile strength and two half-samples. After that, both half-samples can be successfully tested under the comprimitor. The comprimitor is equipped with constraints to ensure that the sample is fixed exactly in position, with two platens with dimensions of 1600 mm^2, perfectly aligned, applying compression stress to the specimen.

Some considerations are relevant to the choice of the press and the relative test parameters. From the literature analysis and from the first preliminary tests, the evidence of dealing with a "weak" material (weak compared with the common cement mortar) was clear. Consequently, considering the load speed required by the standard and considering an application area of 1600 mm^2, in terms of strength, a rate of 1.5 MPa/s was judged much too high. Furthermore, there was evidence that the two-component hardened grout exhibited a behaviour similar to that of concrete only after 28 days, while for shorter curing times the material behaves as a compacted clay. For all the other tests, a clear peak is not easily identifiable on the stress–deformation graph; therefore, the modality of displacement controls was preferred.

The press was kindly provided by the Geotechnical Laboratory of DISEG (Politecnico di Torino).

From this point on, EN 196-1:05 is considered the standard, including the above-mentioned changes.

7.3.4.1 Short-term tests

"Short term" or "short curing time" is defined as the first 9 hours after the mixing phase (Todaro et al., 2020) although, with a view to mechanical tests, this range is commonly reduced to the first 3 hours of curing.

In this phase, the grout material is more similar to a hard clay than a weak concrete. According to this statement, ASTM D2166/D2166M-16 can be added as a further reference for the choice of 0.25 mm/min as the compression rate. In this regulation, the unconfined compressive strength of cohesive soil is normed, in terms of total stresses. The main requirements not respected concern the sample shape, which, according to the American standard, should be cylindrical (minimum diameter of 30 mm and height-to-diameter ratio ranging between 2 and 2.5) while the chosen compression rates respect the prescriptions guaranteeing that the test ends between 10 and 15 minutes.

For the short curing time, tests are performed 3 hours after casting of the samples. After different trial tests, it was established that it was impossible to demould samples before this curing period without irreparably damaging them. This problem was overcome by using a polystyrene mould, which it was simpler to destroy without stressing the sample.

Unfortunately, during the flexural test the samples were so weak that the supports indented the sample surface, without splitting it (Figure 44).

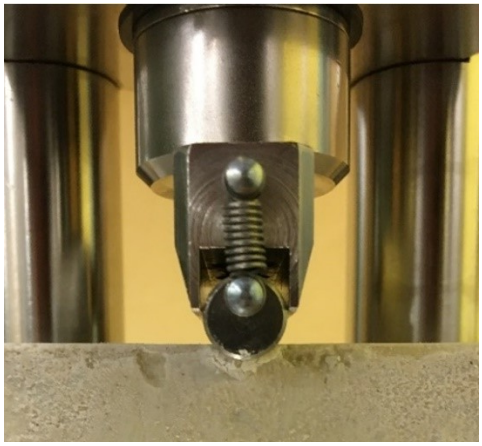

Figure 44 - Indentation phenomenon occurring on the central support of the flexural test frame.

Finally, in order to overcome all these drawbacks, it was decided to skip the splitting phase by manufacturing specific moulds, suitable for obtaining proper testing specimens after 3 hours (Figure 45).

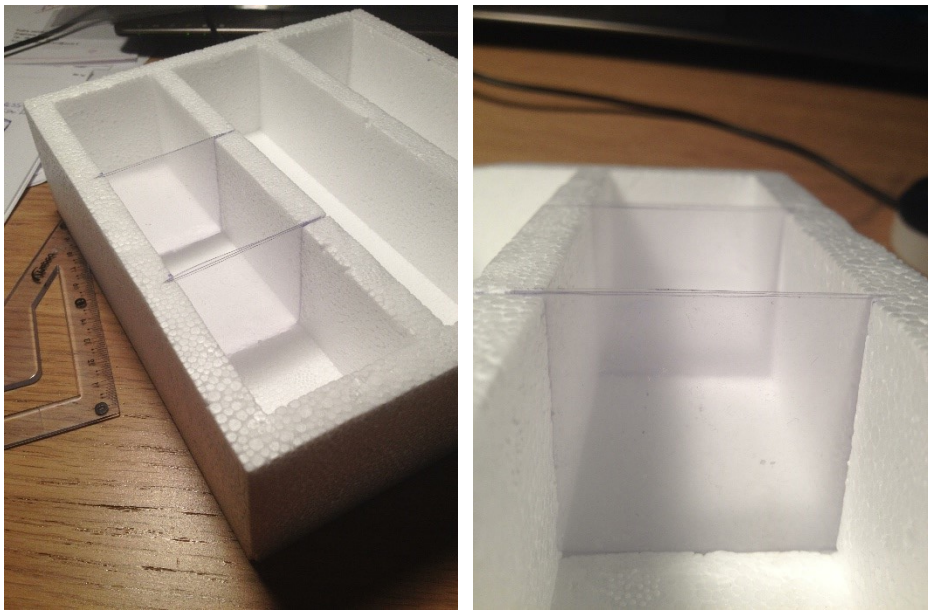

Figure 45 - Mould for compression strength at 3 hours of curing.

The location of the plastic layers along the sample can be carried out roughly. It is important only to be sure that at least the sample has a length longer than 40 mm. Consequently, not all the obtained samples had exactly the same lengths but this aspect did not affect the test quality.

After the 3 hours of curing, the samples were demoulded simply by breaking the mould. The specimens were tested and the uniaxial compression strength was assessed.

7.3.4.2 Tests after 24 hours

A curing time of 24 hours is not enough for carrying out the three-point flexural test successfully, just as the tests performed after 3 hours.

Therefore, the two half-samples were obtained just by cutting each sample with a blade. Then, the uniaxial compression strength was obtained.

7.3.4.3 Long-term tests

"Long term" or "long curing time" refers to tests performed after at least 28 days of curing, according to Todaro et al. (2020).

In this case, EN 196-1:05 was followed completely for the three-point flexural test.

7.4 Preliminary laboratory test campaign

The preliminary laboratory test campaign was developed on four different mix designs.

In the following paragraphs the outcomes of the previously introduced testing procedure are reported. Concerning EN 196-1:05 applied integrally for tests at 28 days, the frame for the three-point flexural test was used for splitting the sample, but the indirect tensile strengths were not computed.

Finally, some preliminary considerations on the dependence of the assessed parameters on the mix designs are reported and discussed.

7.4.1 **Mix designs**

The same type of water and a highly resistant cement (Buzzi CEM I 52.5 R) were used for all the mix designs. Two different kinds of sodium bentonite were used and three different chemical enterprises were contacted for provision of the chemical ingredients (retarding/fluidifying agents and accelerators). The mix designs 1 and 2, prepared using the retarding/fluidifying agent and the accelerator from the same supplier, differed only in the bentonite used. Table 9 summarises all the mix designs used.

Pertaining to the bentonites, both were sodium bentonite but the degree of purity (% of montmorillonite) was different (obviously not communicated by the suppliers).

Table 9 - Mix designs used in the preliminary test campaign.

Mix design	1	2	3	4
Cement (kg)	230	230	230	260
Bentonite (kg)	30 (type 2)	30 (type 1)	28 (type 1)	28 (type 1)
Water (kg)	853	853	819	819
Retarding/fluidifying agent (kg)	3.5	3.5	5	2.5
Accelerator (kg)	81	81	90	80

From the mix designs, the water/cement ratio and the percentage of the accelerator per 1 m^3 (considering the unit weights proper of each accelerator) can be computed. As previously stated (chapter 4), the w/c is computed by weight, while the accelerator dosage is computed by volume.

Outcomes are reported in Table 10.

Table 10 - W/c ratios and accelerator percentages per 1 m^3 (by volume) of the mix design used.

W/c	3.71	3.71	3.56	3.15
Accelerator (%)	6.00	6.00	6.57	6.01

7.4.2 **Unit weight**

Table 11 reports the measured unit weights for the four studied mix designs.

Table 11 - Average unit weights for the four studied mix designs.

Mix design	Unit weight (kg/L)
1	1.15
2	1.17
3	1.19
4	1.22

7.4.3 **Flowability**

Table 12 summarises the measured values of flowability. All the mix designs were tested just after the mix preparation and daily, up to 72 h.

Table 12 - Flowability assessed on the fresh mortar and on mortar collected 24, 48 and 72 hours after batching. Outcomes pertaining to the four studied mix designs.

	Flow time (s)			
Mix design	Fresh mortar	24 h	48 h	72 h
1	32	36.0	39.0	43.8
2	34.5	41.0	43.0	51.2

3	38	40.0	40.0	42.0
4	36	60.0	82.0	no flow

7.4.4 **Bleeding**

Table 13 reports the bleeding values assessed after 3 and 24 hours for the four studied mix designs.

Table 13 - Bleeding values assessed after 3 and 24 hours from the batching. Outcomes pertaining to the four studied mix designs.

	Bleeding (%)	
Mix design	3 h	24 h
1	0.52	2.80
2	1.04	2.09
3	0.70	2.40
4	1.21	8.50

7.4.5 **Gel time**

For the gel time results, Table 14 reports data related to the component B percentages for each mix design, i.e. the fixed amount of component A and B reported in the mix designs (Table 10). Figure 46 shows the outcomes pertaining to the four gelling functions.

Table 14 - Gel times pertaining to the four studied mix designs.

Mix design	Gel time (s)
1	11
2	8
3	10
4	7

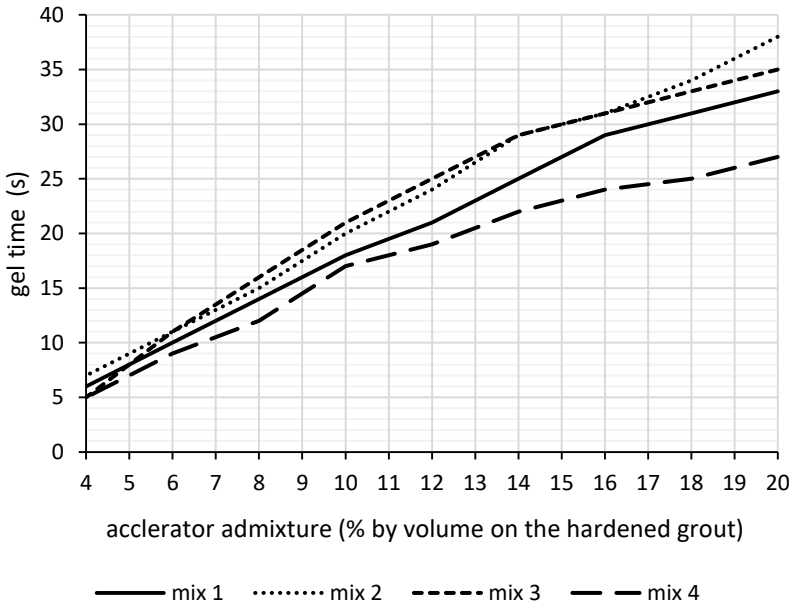

Figure 46 - Gelling functions.

7.4.6 **Uniaxial compression strength**

Table 15 reports the average UCS values assessed after 3, 24 hours and 28 days of curing related to the four studied mix designs. Figure 47 presents the outcomes graphically.

Table 15 - Average values of the uniaxial compression strengths assessed after 3, 24 hours and 28 days of curing.

	UCS (MPa)		
Mix design	3 hours	24 hours	28 days
1	0.32	1.04	1.50
2	0.35	1.04	1.64
3	0.24	1.05	1.52
4	0.23	1.09	1.21

Concerning the measurement precision, for all mix designs a standard deviation close to 0.01 MPa was computed for the tests performed at 3 and 24 hours of curing. Pertaining to the tests carried out at 28 days of curing, the outcomes were more scattered (irrespective of the mix considered), with a standard deviation of about 0.1 MPa.

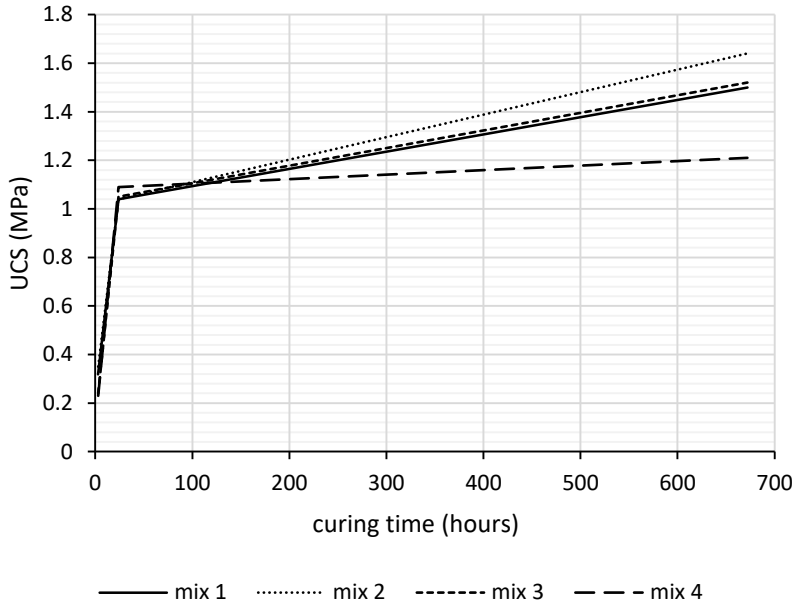

Figure 47 - Uniaxial compression strength of the tested mix designs.

7.4.7 **Comments**

The tests showed that the unit weight of the component A is fairly constant. However, there is a trend directly led by the w/c ratio, namely the lower the w/c, the higher the specific weight. Considering mixes 1 and 2 (which are exactly the same except for the kind of bentonite), it can be speculated that the bentonite plays a role in the unit weight assessment.

Considering the bleeding assessment, the outcomes show that, except for mix 4, all the other mixes behave in a quite similar way, with values ranging between 0.52% and 1.04% after 3 hours and between 2.09% and 2.80% after 24 hours. Comparing mixes 1 and 2, it is not possible to determine absolutely which is the better bentonite for bleeding control; whereas after 3 hours mix 1 seemed to be better, at 24 hours the result was reversed.

Concerning the flowability, it should first be noted that a variation of ± 1 second is not significant. Thereby, starting from mix design 3, it can be deemed that after a slight increase of the flow time in the first 24 hours, the mortar is stable and exhibits no further viscosity increase until the end of the test. Mix design 4, instead, exhibits a strong rise of the flow time in the first 24 hours and this growing trend is confirmed also in the subsequent assessment till failure of the test occurred after 72 hours. This could be explained by a wrong design of the mix, particularly concerning the volume ratio between the retarding/fluidifying agent and the cement. Taking into account mixes 1 and 2, it is possible to affirm that the quality of the bentonite plays a role also in the flowability, since the outcomes are different even though the mixes are substantially the same.

Regarding the uniaxial compression strength, the tests performed after 3 hours of curing show a substantial equivalence between the different grouts. After 24 hours all grouts show values close to 1 MPa. Nevertheless, at 28 days the

differences are marked, with a difference between the best mix (mix 2) and the worst mix (mix 4) of 0.43 MPa. This evidence indicates that the w/c ratio is not the only parameter that drives the UCS, and indeed the highest performance was reached by mix 2, with the highest w/c. Furthermore, from the comparison between mixes 1 and 2, it can be stated that the bentonite also plays a role in the UCS.

Referring to the gel time, it should be noted that a variation of ± 1 second is not significant. Mix design 4, as well as mix 2, showed the fastest gelation process, while the mix designs 1 and 3 are characterised by almost equal values of 10–11 seconds. Taking into account the gelling functions, it appears that while for small component B percentages the outcomes are compacted in a range of 3 seconds, for bigger component B percentages the range widens, up to more than 10 seconds for the highest B %. In the light of these comments, the concept expressed in key concept 5 seems clearer. A high w/c is not the only key for a good overall performance, since all the ingredients have to be correctly measured as a function of the desired result. The decision to test two mix designs that were identical other than in the different bentonites was taken in order to provide an example of key concept 3: replacing just one of the sample's ingredients (keeping the dosage constant) leads to different grout performances.

In conclusion, with the exception of mix 4, the other three were judged potentially suitable. However, only one mix design was chosen for the construction site test campaign. Because the UCS parameter was considered by the building enterprise to be the most important, mix 2 was chosen for the next research step.

7.5 Construction site tests

The test planning follows exactly the laboratory testing path, with one exception for the component A, which was prepared by using the construction site turbomixer. The raw materials used were taken from the silos located close to the batching station.

7.5.1 Construction site: the batching

Component B was taken from the proper silo, while component A was produced by using the batching station turbomixer. Figure 48 shows the turbomixer display. Beforehand, the batching parameters, clearly visible on the left of the display, were set up on the turbomixer, according to the dosages of mix design 2.

Figure 48 - Turbomixer display with mix design 2 set up.

The difference of 3 kg concerning the water dosage was set in order to balance internal dosage fluctuations of the water metering. However, the consequent divergence of 0.3% is negligible according to EFNARC (2005), which set the threshold at ±2%. Furthermore, the value of 0.3% is much lower than the 2.6% that was the threshold limit of the water dosage reported in Càmara (2018).

The turbomixer had a rotation speed of 1500 rpm. The metering was based on a weighting system for all the ingredients used for manufacturing component A. The volume produced for each batch was 1 m^3 (about 333 times the volume produced in the laboratory) in 160 s (less than ¼ of the time spent in the laboratory). Table 16 lists the batching steps and their durations.

Table 16 - Batching station procedure for the component A production.

Operation	Duration (s)
Water metering	/
Bentonite addition and turbomixer activation (start of the mixing process)	120
Cement addition	10
Retarding/fluidifying agent addition (end of the mixing process)	30

After the metering parameters were set up, a trial batching was performed, after which the component A to be used for testing was produced.

7.5.2 **Outcomes of tests on the construction site**

All tests regarding the construction site context were carried out by using the component A produced in the same batching operation. For the uniaxial compression strength tests, samples were sealed and transferred to the Politecnico di Torino laboratory, where the curing phase firstly and the testing phase secondly were performed according to the laboratory testing procedure previously described (paragraph 7.3). The bleeding test performed after 24 hours from the

batching was the only one not performed personally. The result was communicated by the engineers of the project management.

Table 17, Table 18 and Table 19 report the outcomes of the construction site campaign. In order to simplify the comparison, also the laboratory outcomes are reported.

Table 17 - Component A bleeding, gel time and unit weight assessments.

	Bleeding (%)			
Component A produced in:	3h	24h	Gel time (s)	Unit weight (kg/L)
Laboratory	1.04	2.09	8.0	1.17
Construction site	1.39	4.88	8.7	1.20

Table 18 - Component A flowability assessments.

	Flowability (s)			
Component A produced in:	Fresh mortar	24 h	48 h	72 h
Laboratory	34.5	41	43	51
Construction site	34	33	37	37

Table 19 - Uniaxial compression strength for hardened two-component grout.

	UCS (MPa)	
Two-component samples cast in:	24 h (MPa)	28 days (MPa)
Laboratory	1.04	1.64
Construction site	1.04	1.78

Concerning the measurement precision of the UCS tests, the standard deviation is close to 0.04 MPa for 24 hours of curing, while for 28 days the measurements are more scattered, with a standard deviation of about 0.1 MPa.

For reasons strictly linked to operative constraints, the uniaxial compression strength tests after 3 hours of curing were not assessed during the construction site test campaign.

7.6 Discussion

Starting from the component A assessment, it is possible to state that the mortars produced in the laboratory and at the construction site are similar but some differences are appreciable.

Considering the bleeding values, the component A produced in the laboratory shows more stability: starting with a bleeding value of 1.04% at 3 h, after 24 h the value doubles to 2.09%. For the mortar manufactured at the construction site,

instead, the bleeding starting point is barely higher, with a value of 1.39% that more than tripled at 24 h. The difference is confirmed also by the unit weight assessments, which show a slightly higher value for the construction site component A. Finally, the flowability assessment shows a considerably higher tendency of the mortar produced at the construction site to preserve the initial level of flowability and workability. The reason for these differences can be found in the different ways of mixing, namely the different volumes produced and the different mix durations. Considering that the bentonite is the main ingredient responsible for the mortar stability, it can be speculated that the longer activation process of the laboratory procedure leads to a more activated bentonite, namely a more stable mortar.

Pertaining to the uniaxial compressive strength, a marked match can be seen. Samples cured for 24 hours showed exactly the same UCS value, while those cured for 28 days had slightly different values, although this difference was less than 8%. However, it should be underlined that while for 28 days of curing the standard deviations were equal, with values close to 0.1 MPa, tests performed after 24 h on samples cast at the construction site exhibited a slightly more scattered distribution than the laboratory ones.

Regarding the gel time, considering the intrinsic test accuracy, the values are considered equal.

In conclusion, it can be summarised that the proposed laboratory procedure obtained, at the smaller scale, a component A that was considerably similar to the one produced in the batching plant of the construction site. The results obtained in terms of component A characterisation, gel time and UCS are similar, except for very slight differences that can be easily explained by, first, the completely different mortar manufacturing and secondly the different testing conditions (i.e. despite all efforts, conducting tests in an environment different from the laboratory undoubtedly affects the quality of the outcomes).

7.7 Additional information

7.7.1 The unregulated penetrometer test

The impossibility of performing uniaxial compression strength tests after 3 hours of curing at the construction site opened a new scenario, focused on the impossibility of ensuring that a certain mix design successfully fulfills the technical requirements at short curing times when operating at the job site scale (unless a suitable press is available at the job site). Furthermore, as reported in Chapter 4, at many construction sites the UCS is required after only 1 hour of curing.

This issue was overcome by introducing the penetrometer. The use of this device is covered in more detail in the next chapters, but, in this context, a brief introduction is provided and the outcomes obtained both in the laboratory and at the construction site are shown (Table 20).

The penetrometer is a load cell equipped with a circular bit. The force required to penetrate the grout surface divided by the bit area provides a strength value. Tests are performed at short curing times only (even if it is hard to carry out tests after 3 hours of curing), by pressing the bit perpendicularly on the grout to a depth of 5 mm. Samples are not demoulded but are tested inside their casting mould.

In this research phase, the penetrometer used was an IMADA DS2-1000N with a bit area of 134.7 mm^2 (Figure 49). At least three determinations were performed for each assessment.

Figure 49 - IMADA DS2-1000N used for the penetrometer assessment.

Table 20 - Penetrometer strength assessment for gelled two-component grout.

	Penetrometer strength (MPa)	
Two-component samples cast in:	1 h (MPa)	3 h (MPa)
Laboratory	1.00	1.38
Construction site	0.31	0.94

Considering the results reported in Table 20 and considering first the strength assessed after 1 hour, the laboratory value is about three times the job site value. Samples tested after 3 hours of curing show a smaller but basically non-negligible difference. The main reason for this discrepancy can be spotted in the different curing temperatures. In fact, while the samples tested in the laboratory were cured at 23±2 °C, at the construction site the temperature was about 10 °C less. Although proper references are not available in the literature, this temperature gap certainly influenced the strength development expressly at short curing times.

7.8 Key concept

KEY CONCEPT 7: The procedure proposed by Todaro et al. (2019) allows the production, at the laboratory scale, of a component A similar to the one produced with the turbomixers at the construction sites.

The component A can be studied by assessing: the unit weight, the flowability and the bleeding. The gel time assessment foresees the use of both components, while the hardened grout can be tested with a laboratory press computing the UCS.

From the preliminary results, it can be stated that, although in the scientific literature the UCS values have always been linked with the w/c values, also the bentonite plays a role in the compression strength, in addition to influencing the viscosity and the bleeding. Concerning the studied mix designs, three of them provided suitable results according to the situation-specific technical requirements, but the builder chose the one that exhibited the highest UCS at long curing times (the incompressible bubble theory did not determine the engineers' choice).

Chapter 8

Short-term uniaxial compressive strength

Once it was certain that a valid procedure for studying the two-component technology at the laboratory scale was established, an open point remained from the recently finished test campaigns: the uniaxial compressive strength at short curing times assessed by using the penetrometer.

The content of this chapter is partially taken from the published paper Todaro et al. (2020a).

8.1 The issue and the state of the art

The need to assess the uniaxial compression strength at short curing times is crucial if we take into account that during the continuous process of mechanised tunnel excavation, the ring just locked with the backfilling material must bear the weight of the successive segments and the weight of the machine backup, commonly in just 1–2 hours.

This concept is clearly expressed by all the requirements of the mix designs reported in Chapter 4, where a provision concerning the short curing time is present throughout. In order to fulfil these requirements, Peila et al. (2011) and Pelizza et al. (2012) suggested the use of a pocket penetrometer, but no more information is provided on how to use it, its advantages and/or limitations. Dal Negro et al. (2017) was the first work to clearly introduce the use of the penetrometer for assessing the mechanical strength at short curing times in a checking protocol. Antunes (2012) underlined that contractors and designers typically specify the early strength of the grout, but the operation is difficult as there is no directly applicable ASTM standard. However, nowadays the use of penetrometers is spreading at many construction sites, applied both in the mix design testing phase and in daily checking protocol, although its use is not officially regulated.

In general, the use of penetrometers is faster and simpler than a compression testing machine (a device also more commonly called a laboratory press, or simply a press). Furthermore, tests can be carried out on samples cast in moulds of different shapes. However, can the penetrometer replace the press? Can the penetrometer be successfully used for assessing the uniaxial compression strength at short curing times? These were the crucial issues. Moreover, Antunes (2012) stated that by comparing the two approaches for obtaining uniaxial compressive strength values using a penetrometer and a press, the outcomes are different. More particularly, it can be stated that the outcomes are different physical quantities although this aspect is often not recognised or is ignored. Often, the two types of test are considered similar, and consequently the outcomes are confused, overlapped or wrongly correlated. Furthermore, the absence of a clear standard procedure for the use of penetrometers on two-component grout should be highlighted.

8.2 The idea

Firstly, a procedure for the use of penetrometers was drawn up. Secondly, a double test campaign was scheduled using the penetrometer and a standard laboratory press, choosing the same curing time for both determinations. All samples were obtained following the same mix design and the outcomes were correlated. The desired result consists in computing a correlation factor that is able to provide an estimation of the UCS starting from penetrometer determinations.

8.3 Materials and test procedure

The component A and samples were manufactured according to the procedures set out in the previous chapters (paragraphs 7.2 and 7.3.3).

Starting from the official standard regulations for concrete, an innovative procedure for testing two-component grout at short curing times with the penetrometer was devised. Subsequently, a time testing path was scheduled: tests performed after a curing time of 60, 65, 70, 90, 100, 120, 125 and 180 minutes were programmed to be carried out following both the penetrometer procedure and the press procedure. The irregular time scheduling was for technical reasons (demoulding, sample checking and sample testing). Consistent with the available raw materials, five test campaigns were carried out. For the penetrometer tests, five samples were tested for each time, obtaining three assessments for each sample, i.e. 15 strength values for each curing time were available for computation of the average value. For the press tests, five samples were tested for each curing time, thus obtaining five strength values available for computation of the average value.

8.3.1 **Apparatus**

The test campaign was carried out using a penetrometer SAUTER GmbH Ziegelei 1 D-72336 Balingen digital model dynamometer (max force of 1000 N, 0.5 N of resolution) equipped with a flat circular bit, with a thickness of 5 mm and an area of 177.9 mm^2 (Figure 50).

Figure 50 - SAUTER GmbH Ziegelei 1 D-72336 Balingen digital model dynamometer (left) and bit details (right).

The compression testing machine used was a Wykeham Farrance, commonly used for clayey soil. The machine works in displacement control modality with a speed displacement ranging between 0.001 and 1 mm/min. An LVDT sensor was used for recording the vertical displacements, with the purpose of better identifying the peak of the obtained functions.

8.3.2 **Penetrometer tests: the surface compressive strength**

The penetrometer is not an innovation in the civil engineering field; indeed it is usually applied for assessing the setting time of concrete. So, beforehand, a study of the available material concerning the penetrometer used was performed in order to better understand if its application would be useful for our purpose.

ASTM C403/C403M-16 can be taken as reference. This standard refers to concrete, composed of cement and aggregates, and for testing concerning the setting time, it should be previously passed through a 4.75 mm sieve. It is evident that this provision is strictly linked to the nature of the concrete, but obviously it is not the only one. Indeed, for example, other prescriptions like the consolidation process of the mortar performed by stroking of the mould, or the removal of bleeding water from the casting surface during the curing time are clearly phenomena of the concrete itself (the mixed two-component grout does not require strokes for consolidation and never exhibits bleeding water on top of the casting surface after gelation). Furthermore, the technical standard does not foresee the use of only one kind of penetrometer bit (in the document these are called needles) but different dimensions are available and the choice is a function of the curing time (i.e. as a function of the expected strength).

It is known that two-component grout is a material different from standard concrete, but some prescriptions reported in ASTM C403/C403M-16 were adopted to devise an innovative procedure suitable for testing the two-component grout.

Some changes to the ASTM regulation were made about the bit area and its penetration thickness through the tested material. In particular, the required depth of 25 mm was reduced to 5 mm. This reduction was to avoid having to consider in the computation also the shear strength that potentially developed on the lateral bit surface. Furthermore, considering that the samples for testing must be cast in a mould according to EN 196-1:05 (mould thickness of 40 mm), by penetrating only 5 mm the negatively board effect due to the mould bottom can be successfully avoided (preliminary tests showed this).

After these preliminary but fundamental considerations (and divergences from ASTM C403/C403M-16), the test could be run. First, the mould containing the specimens to be tested must be located on a flat surface. Then, according to ASTM C403/C403M-16, the dynamometer is equipped with the bit and placed perpendicularly to the sample casting surface. Increasing pressure is applied manually, trying to apply this as far as possible at a constant advancement speed. The test ends after 10 seconds. During the test, the peak force ($F_{p\text{-}pen}$) is recorded. Finally, by computing the ratio between the peak force ($F_{p\text{-}pen}$) expressed in Newton and the bit area (A_b) expressed in mm^2, it is possible to obtain a physical quantity equal to the pressure, expressed in MPa (Equation 4). This quantity is herein called the SCS (surface compression strength).

$$SCS = \frac{F_{p-pen}}{A_b} \ (MPa) \qquad 4$$

In our case, $A_b = 177.9\ mm^2$.

Although ASTM C403/C403M-16 referred to the same quantity as "penetration resistance", it was decided to rename this pressure "surface compression strength" (SCS) in order to underscore the implicit differences adopted in the testing procedures. In particular, the ASTM procedures suggest the use of different bits that, inserted for a length of 25 mm, lead to diameter/depth ratios ranging between 1.14 and 0.18, while the adopted bit is flat and with a fixed diameter/depth ratio equal to 3 when penetrated for 5 mm. Consequently, it can be stated that the failure mechanisms are completely different: the shear strength plays a non-negligible role for the ASTM procedure, while in the case of the SCS the failure mechanism is more similar to a load-bearing capacity mechanism.

Some further practical information should be provided in order to carry out the penetrometer test successfully on the two-component grout. These suggestions are the result of a long trial and error preliminary study phase. In order to maximise the number of potential outcomes without affecting the data quality, considering each single cast sample according to EN 196-1:05, three different

tests distributed along the cast surface of the specimen can be performed. Figure 51 depicts the testing scheme.

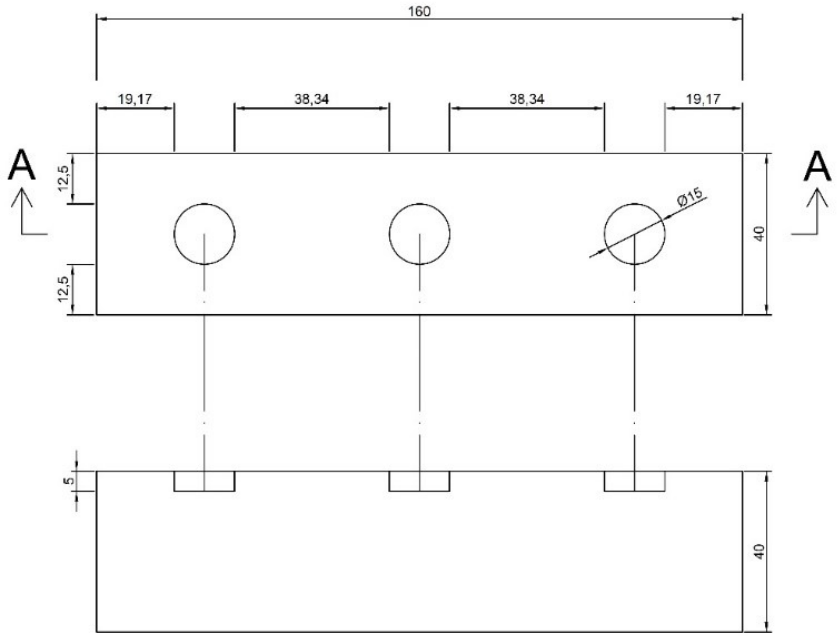

Figure 51 - Scheme of a sample tested with the penetrometer and geometrical disposition of the bit prints. Dimensions expressed in mm.

Although the central test has a bigger undisturbed space along the longitudinal direction, both the other tests (performed nearer to the mould boundary) did not show differences of value. In other words, the effect of the mould boundary on the final result can be considered constant and does not change between the central determination and the other two. In conclusion, for each sample three surface compression strength values can be successfully obtained.

In order to better control the penetration of the bit for 5 mm, two steel guides were designed and realised. Putting this steel guide across the testing sample and suitably calibrating the distance between the bit and the penetrometer body, it was possible to penetrate the grout for exactly the required length.

During the test campaign, the moulds used were made of rigid PVC. Generally, it is required to use a rigid mould in order to avoid any deformation due to the load application. Alternatively, polystyrene ones have been successfully used, equipped with a rigid frame aimed to prevent deformations. Figure 52 depicts a testing phase. In this specific case, the polystyrene mould is locked by the wood block device. Furthermore, the steel guide is visible.

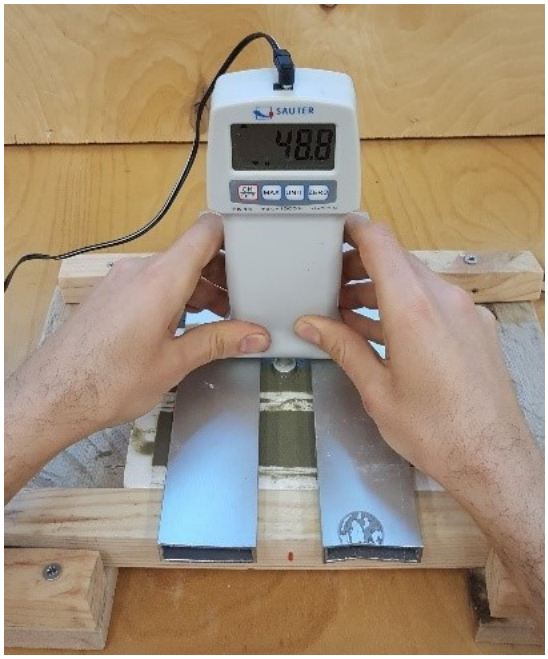

Figure 52 - Penetrometric testing phase. In this specific case, the mould in polystyrene is locked by the wood block device. The mould displacements are constrained. The steel guide leads the bit penetration to the wanted length.

8.3.3 **Press tests: the uniaxial compressive strength**

The press tests were performed according to the procedure introduced in paragraphs 7.3.4 and 7.3.4.1 (Todaro et al., 2020a).

In compliance with this procedure, the displacement rate was chosen as 0.25 mm/min. The outcomes of the tests were force–displacement graphs on which the peak force $F_{p\text{-}press}$ can be identified. Using Equation 5, considering the $F_{p\text{-}press}$ expressed in Newton, the UCS can be computed considering the comprimitor platens area of 40*40 mm^2.

$$UCS = \frac{F_{p-press}}{1600}\ (MPa) \qquad 5$$

8.3.4 **Mix design used**

The mix design used is reported in Table 21.

It is basically similar to mix design 2 of the previous chapter, but in this context the water used came from Turin's water network and the ingredients are identified also by their commercial names and producers.

Table 21 - Mix design used.

	Ingredients	Dosage (kg/m^3)
Component A	Water	853
	Bentonite Clariant Bentonil CV 15	30
	Cement Buzzi CEM I 52.5 R	230
	Retarding/fluidifying agent Mapei Mapequick CBS 1	3.5
Component B	Accelerator Mapei Mapequick CBS 3	81

8.4 Results

Table 22 reports the outcomes in terms of average values.

Figure 53 and Figure 54 report respectively the strength trends as a function of the curing time and the ratio between UCS and SCS, both as a function of the curing time.

Table 22 - Outcomes of the short-term test campaign.

Curing time (h)	Curing time (min)	SCS (MPa)	UCS (MPa)	SCS/UCS (-)
01:00	60	0.41	0.08	4.99
01:05	65	0.47	0.11	4.41
01:10	70	0.54	0.10	5.25
01:30	90	0.72	0.15	4.66
01:40	100	1.00	0.17	5.77
01:50	110	1.17	0.22	5.45
02:00	120	1.26	0.24	5.37
02:06	126	1.34	0.24	5.67
02:10	130	1.41	0.27	5.30
03:00	180	1.65	0.33	4.94

The tests performed with the penetrometer were characterised by a standard deviation ranging between 0.05 and 0.20 MPa, while the UCS exhibited smaller values, ranging between 0.01 and 0.05 MPa.

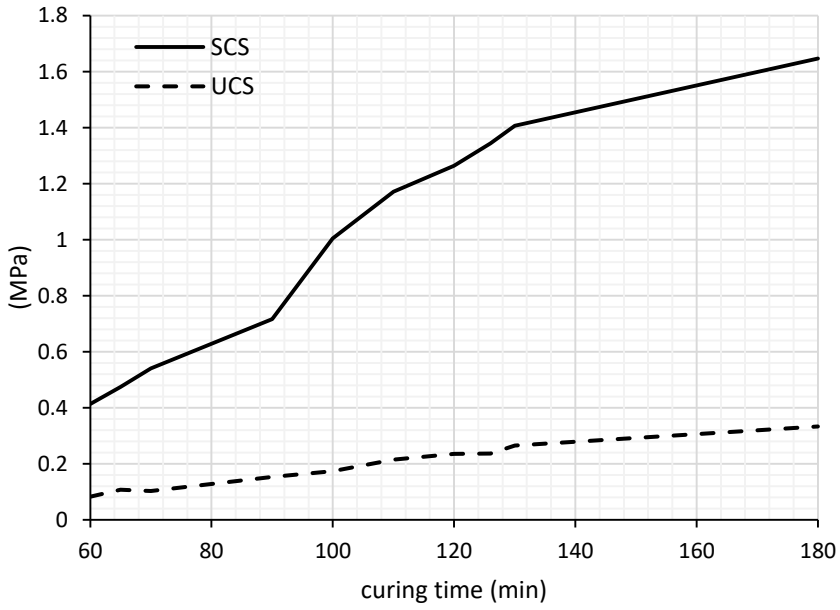

Figure 53 - UCS and SCS trends related to the curing time.

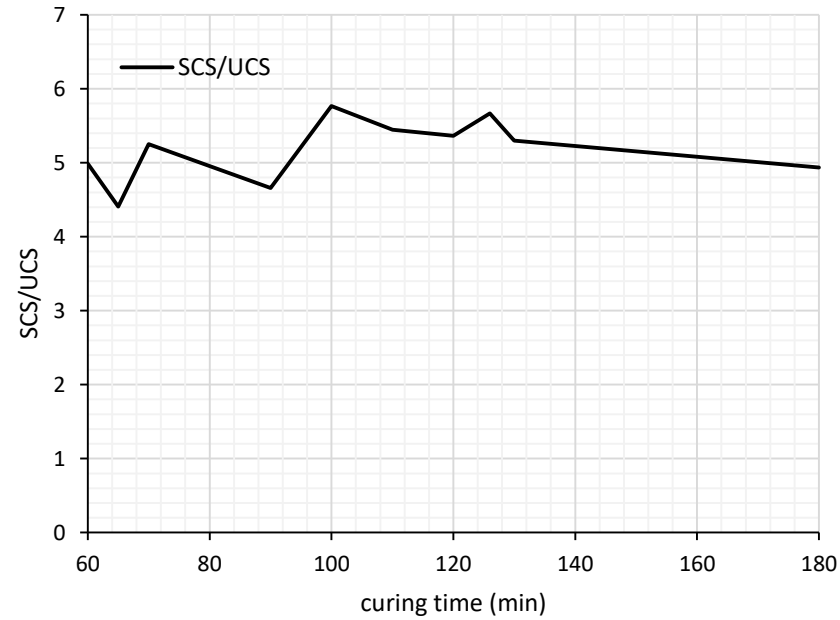

Figure 54 - Trend of SCS/UCS related to the curing time.

8.5 Discussion

Figure 53 clearly highlighted the marked difference between the functions of SCS and UCS.

The SCS function exceeds the UCS one for each testing time. The difference can be explained considering two aspects. Firstly, the failure mechanisms induced

by testing are different, i.e. samples are broken in a confined way for SCS while for the UCS there are no confinement forces.

Secondly, the SCS assessments were carried out on samples held in the mould (no stress for demoulding), while the UCS samples must be demoulded to be tested, and the demoulding operation, especially at very short curing times, could apply stresses capable of damaging specimens.

Considering the testing precision, the scattered distribution of the results pertaining to the SCS could be attributed to the smaller area of interest in the test. Although all the previously described precautions were always taken during the casting phase, it is evident that any hidden weak point near the testing area leads to fluctuation of the results. Considering that for the UCS the active area is about nine-fold larger, it is evident that the UCS is less sensitive to the possible presence of weak points.

Considering Figure 54, it can be stated that the ratio shows an almost constant trend, close to 5. This value is indirectly confirmed by Antunes (2012), referring to a curing time of 1 h. In that paper, the author tested three different mix designs to assess the UCS and the penetration resistance (according to ASTM C403-16). The outcomes were summarised in a table, but computing the ratio between the UCS and the penetration resistance confirmed the value of 5.

In conclusion, it can be stated that:

- the penetrometer is a useful equipment and simple to use both in the laboratory and at construction sites. However, no standards are available, so in order to perform reliable tests, the above-mentioned guidelines could be used;
- the SCS and the UCS are different physical quantities. They must not be confused and the results absolutely do not overlap;
- concerning this specific mix design, for curing times between 1 and 3 hours, the SCS and the UCS are correlated by a factor of 5. This value should not be used indifferently for all two-component mix designs, but it can be considered as a first reference value, in order to estimate expeditiously the order of magnitude of the UCS of a certain two-component grout.
- it is suggested that at least 15 tests should be performed using the penetrometer in order to obtain an average value.

8.6 Additional information

This paragraph reports some brief considerations regarding the dimensions of the samples used for assessing the UCS.

Before using the mould related to EN 196-1:05, bigger dimensions were tested, with the idea of completely avoiding boundary effects and trying to

perform tests without confinement effects. All the tests failed because the samples broke with punching collapse (Figure 55 and Figure 56). Furthermore, without the possibility of using a spatula, an additional difficulty was obtaining a suitable surface for the SCS assessment, with many weakness points and/or irregularly cast surfaces (Figure 56, right).

Figure 55 - Cubic sample (150*150*150 mm) of two-component grout, demoulded, tested with the penetrometer. Test failed.

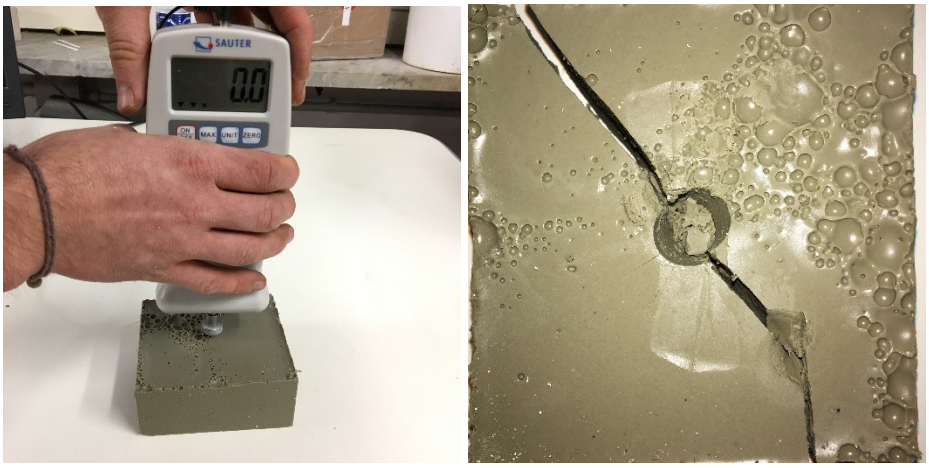

Figure 56 - Prismatic sample (100*100*40 mm) of two-component grout, demoulded, tested with the penetrometer. Test failed.

Only tests of samples held in the mould could be performed (Figure 57), but successful casting of 3.375 L of two-component grout was very difficult (one good sample per three attempts). Although such a big size ensures the absence of mould boundary effects on the SCS assessment, this possibility was discarded due to the unsustainability of the amounts of raw ingredients needed.

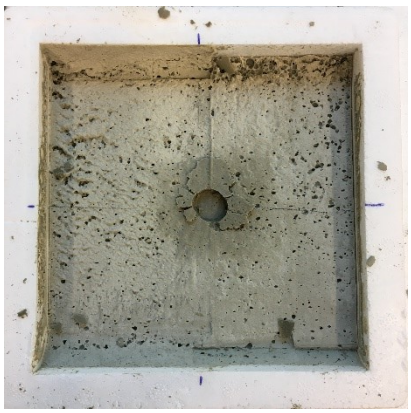

Figure 57 - Cubic sample (150*150*150 mm) of two-component grout, tested with the penetrometer.

In conclusion, it was decided that introducing other mould shapes was not advantageous and not aligned with the idea of a smart test performed using the penetrometer, so samples according to EN 196-1:05 were chosen.

8.7 Key concept

KEY CONCEPT 8: The use of a pocket penetrometer is fundamental for assessing the grout strength at short curing times (≤ than 3 hours), easily and quickly. The measured strength (SCS), obtained by penetrating the circular bit to a certain depth and shearing the peak force value on the bit area, is dimensionally a pressure, but should nevertheless not be confused with the UCS. For the studied mix design and by following the above-described procedure, the UCS can be estimated by penetrometer test assessment using the following equation:

$$UCS = SCS/5 \; t \leq 3 \; h$$

Chapter 9

Shear strength

In this chapter the test campaign related to the shear strength of the two-component grout hardened material will be described.

Two-component grout quickly changes its properties during the curing process but no-one has ever highlighted this peculiarity by using the direct shear test. The principal aim of the study is to develop a failure criterion that could evolve with time, which may be of interest for the various stakeholders.

A special thanks to the geotechnical laboratory of DISEG (Dipartimento di Ingegneria Strutturale, Edile e Geotecnica) of the Politecnico di Torino, especially Dr. Oronzo Pallara for help in the development of the laboratory tests and Prof. Guido Musso for suggestions on interpretation of the results.

9.1 State of the art

Shear strength can be considered as a recent issue in the study of two-component backfilling grout. Few authors in the last decade have addressed this topic and in the following the main concepts reported and a short review of their works are presented.

The first reference to the shear strength of two-component grout can be found in Antunes (2012). In this work, the author highlighted the crucial importance of assessing the properties of two-component grout in the short term, these being the information usually required by designers and contractors. The shear strength test was introduced as a valid approach for fulfilling that requirement, as a substitute or integration of the UCS or the penetrometer test; unfortunately, no results or testing methodologies were reported.

Thewes (2013), with reference to annulus backfilling but without specifying the technology, recognised the undrained shear strength as the most important property for providing an immediate support of the rings. Furthermore, this work underlines that the shear strength at short curing time never comes from the cement setting but is due to consolidation or chemical reactions. Eventually, as a

simple reference value for quick calculations, the value of 3–5 kPa of shear strength is suggested. This work was the first to suggest also how to conduct the tests, i.e., to present a methodology based on the cone-penetrometer.

Youn & Breitenbücher (2014), reporting typical parameters for cementitious grout applied to the annulus gap, listed a shear strength higher than 2 kPa, commonly in the range of 5–10 kPa, 24 h after the mixing. This range is considered as the minimal shear strength to ensure the avoidance of deformations caused by the buoyancy forces applied to the rings. This paper focuses on the influence of the dewatering phenomenon on the shear strength of mono-component grout (as a function of different binder element percentages and aggregates); however, very interesting information on the procedure for testing is provided. DIN 4094-4 is used as a technical standard and a shear vane was pre-installed in the testing sample at a depth of about 90 mm. Tests were carried out at programmed times, ranging between 5 and 480 min after the mixing phase.

Mähner and Hausmann (2017) explained clearly the importance of assessing the shear strength of the grout used for filling the annulus. They highlighted that a newly assembled tunnel ring tends to float upwards in the injected mortar, immediately after the injection, when the segments are out of the shield protection. A simple scheme of the phenomenon is depicted in Figure 58. Three areas can be identified: the machine (where the new ring is assembled), the mortar fluid hardening area and the hardened mortar area. In the second one, the flotation forces (uplift force) should be balanced by the ring dead load and the friction due to the cylinder thrusting forces. Additionally, a sufficient shear strength exhibited by the mortar should completely eliminate the flotation.

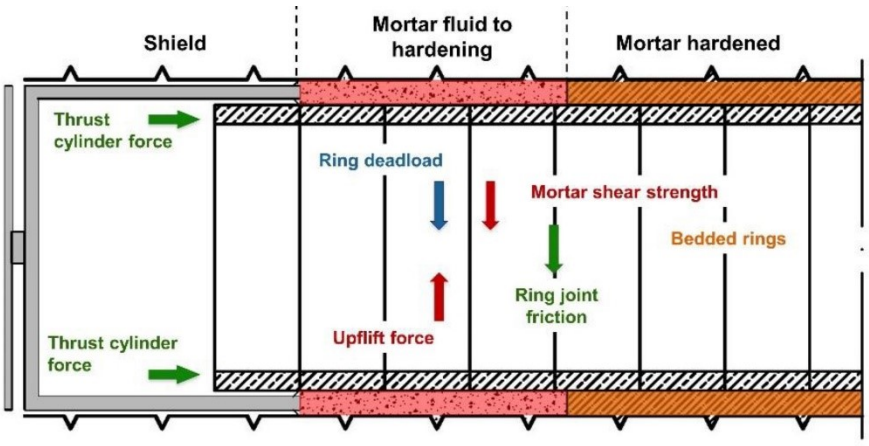

Figure 58 - Scheme of forces system for rings (Mähner and Hausmann, 2017).

These authors introduced a calculation algorithm that, taking into account the geometrical tunnel dimensions, mortar parameters and the machine advancement rate, provides the value of the shear strength that is able to avoid any stress on the ring joints. For the presented case study relating to a tunnel diameter of 10 m and a mono-component mortar used as backfilling technology, a shear strength of 2 kPa was obtained as the minimum value that should be guaranteed. In addition to the algorithm, the authors described also the laboratory study that was performed

according to DIN 4094-4, using a shear vane and testing samples cured for times ranging between 10 and 480 min after mixing. The value of 2 kPa was reached after 6–7 hours.

The last reference (chronologically) is a paper published by Schulte-Schrepping & Breitenbücher (2019b). These authors designed and developed a special device to simulate the annular gap grouting on a semi-technical scale. After the grouting phase was performed using a common two-component mix design, the shear strength was tested with a shear vane, according to DIN 4094-4:2002-01. The outcomes showed a shear strength of 23 kPa after 40–50 min and 52 kPa after 90 min.

9.2 The issue

Mähner and Hausmann (2017) explained better than other authors the importance of the shear strength of the material used for the backfilling. Their performed and published study focused on the short curing time, testing the grout by using a shear vane. However, no study has investigated a curing period of more than 8 hours. In general, all authors used the vane test, obtaining the values of the undrained shear strength.

The use of the vane test is certainly positive in allowing an easy procedure, and it can be considered as undoubtedly correct at very short curing times (i.e. up to 1 hour of curing). Nevertheless, some doubts arise considering longer curing times. The output of the vane test is the undrained shear strength, as the test is generally much too fast to ensure the dissipation of the water pressure. It can be consequently deduced that the measured stress is due to two factors: the strength of the material and the water pressure. Moreover, during the curing process, the conductivity of the two-component grout changes (it can be deduced indirectly by comparing the consolidation charts for different curing times). Consequently, the role of the water pressure has a different weight in the measured undrained shear stress as a function of the curing time. Therefore, vane tests performed at different curing times provide as their outputs undrained shear strengths where the roles of the water and hardened grout are not clearly separated.

In conclusion, the possibility was considered of finding a failure criterion for the two-component grout, with the classic geotechnical approach to the material. This research path was not chosen in order to cast a negative light on all the work performed by other researchers, yet this possibility was warmly welcomed by backfilling designers, who remarked on the utility of a failure criterion as an innovative instrument for better projecting and calibrating the mix design.

9.3 The idea

A mix design was chosen for performing tests, yet the basic aim of this chapter is not primarily to find numerical values but to try to devise a reliable procedure, a methodology that can be used in future applications.

The best approach for assessing the failure envelope of a material is to perform triaxial tests. However, in the preliminary program phase, it was decided to discard the triaxial tests, as the preparation and running time of this type of test was much longer than the hardening reaction velocity of the two-component grout, especially at short curing times. Consequently, the investigation of the failure envelope and its evolution in time was scheduled by using direct shear tests.

The last issue that required reflection was the modality to adopt for the shear tests referring to the neutral pressure. The shear test was developed for testing soils in drained conditions. Lancellotta (2001) stated that, as it is impossible to control the real drainage flow from the sample during the direct shear test (for technological reasons, the shear box is not equipped with pressure gauges), the shear rate must be chosen to guarantee a drainage condition. It is also underlined that if the drained condition is not guaranteed, the outcomes will be unreliable or hard to interpret. The Mohr–Coulomb model was chosen for drawing the failure envelope, this choice being made in view of the simplicity of use and interpretation by designers.

According to these statements, tests were planned in an effort to guarantee a drainage approach.

9.4 Materials and procedure

The component A and samples were manufactured according to the procedures set up in the previous chapters (paragraphs 7.2). The sample production was performed according to the procedure described in paragraph 7.3.3, with the exception of the mould shape. In this test campaign, cylindrical moulds with a diameter of 50 mm and a height of 30.54 mm were used. The mix design was the same as in the previous chapter, summarised in Table 21.

The shear tests were performed at 1, 3, 24 h and 28 days of curing time. Four different vertical stresses were used in order to consolidate (firstly) and test (secondly) the samples. In the absence of any references, the vertical strengths were chosen close to the uniaxial compression strength of the two-component grout cured for 3 hours (Table 23).

Table 23 - Vertical strengths used for assessing the direct shear tests.

	σ_v' (kPa)
1	49.96
2	99.92
3	199.85
4	299.77

9.4.1 **Apparatus**

For the shear test campaign, a Casagrande shear box with cylindrical samples was used (ϕ=50 mm). The shear machine was equipped with two different displacement transducers, to record both the horizontal and the vertical displacements of the sample. Two different acquisition programs were written, the first for the consolidation phase and the second for the shearing phase.

9.4.2 **Summary of the technical standard and procedure**

The direct shear tests were performed according to BS EN ISO 17892-10:2018.

The standard is applicable in undisturbed, remoulded, re-compacted and reconstituted soils. Depending on the type of the material, the standard allows also the specimen fabrication; therefore, for our particular case, samples were cast directly in the shear mould. Figure 59 depicts (from left to right): the moulds pattern and the two tanks with the correct proportional amounts of component A (the grey liquid) and component B (the transparent liquid), the samples covered after the casting and the same samples after 3 hours, just before testing. It can be seen that the uncovered material is completely cracked due to dehydration (the same phenomenon could occur also if the samples were not properly sealed).

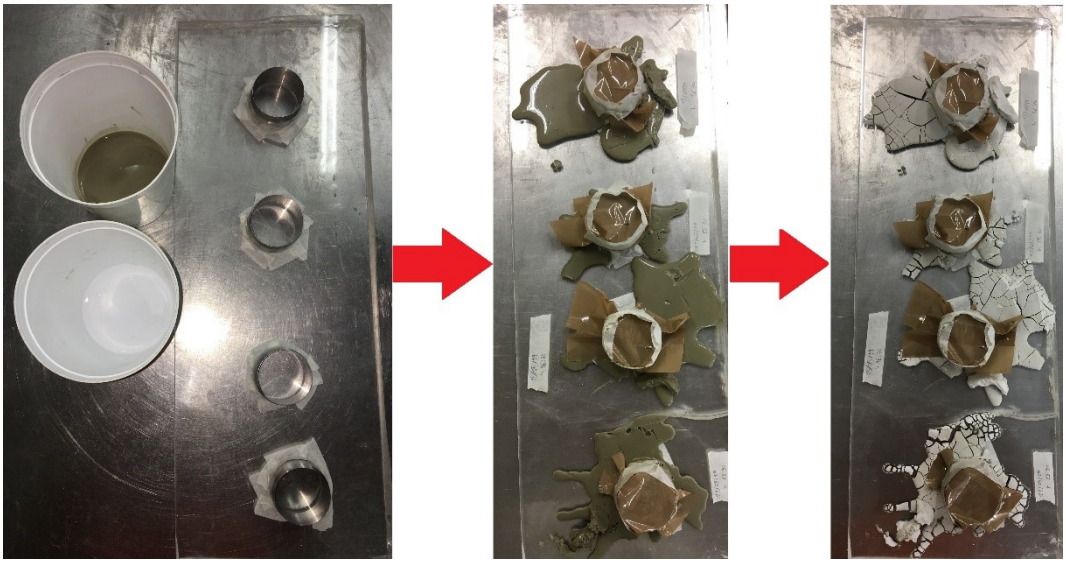

Figure 59 - From left to right: the moulds pattern and the component tanks, the samples covered after the casting and the same samples after 3 hours, just before testing.

Beforehand, measurements of the samples density were assessed. Since sample extrusion from the mould is difficult, the weights were measured without demoulding, subtracting retrospectively the mould tares from the gross weights. This operation was of paramount importance, being the only instrument (excluding the visual check) able to recognise potentially wrongly cast samples.

The next step was to put the sample into the shear box. This operation was performed particularly slowly and gently, with special care for samples tested

after only 1 hour of curing. Figure 60 shows photos concerning the demoulding and insertion of the sample in the shear box, including in particular the sample (1) in the shear box (2) and the push cylinder (3) under the pushing frame (4).

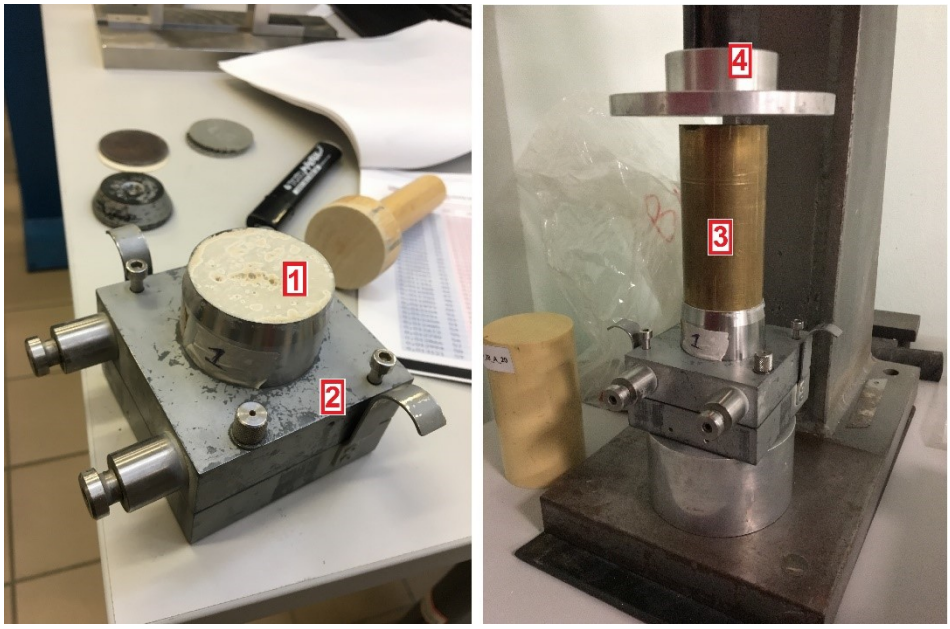

Figure 60 – Sample of two-component grout in the mould (left) and transferring phase of the sample from the mould into the shear box (right).

After the sample allocation inside the shear box, all the shear equipment was prepared: the shear box was fixed on the shear machine, the shear tank was filled with water (mainly to prevent the dehydration process), the weights needed for a certain axial strength were put on the load shaft (without yet applying the load on the sample) and the acquisition software was run. After that, the consolidation phase could be started, applying the load on the sample and running the acquisition software. The output of the consolidation phase consists in the determination of the maximum allowable rate of shear displacement (v_{max}). Drawing a graph of the vertical displacement (d) and the square root of the time, the time–settlement curve can be displayed. Recognising the two tangents on the two main linear parts of the function, the primary consolidation time can be assessed ($\sqrt{t_c}$) as the interception of the line extensions (Figure 61). t_c is the time that the water needs to drain from the tested sample.

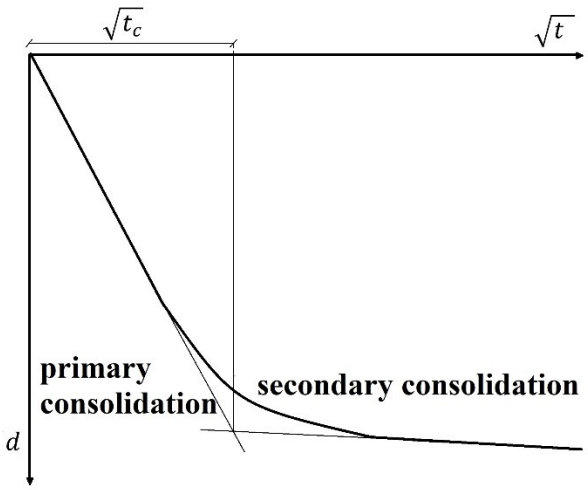

Figure 61 - Example of a time–settlement curve to determine the time for primary consolidation.

After that, the minimum time to failure t_f can be calculated by using Equation 6:

$$t_f = 13 * t_c \quad (6)$$

and consequently, with Equation 7, the maximum allowable rate of shear displacement v_{max} (mm/min) is obtained:

$$v_{max} = s_f / t_f \quad (7)$$

Some further consideration pertains to the value of s_f: this value indicates the horizontal shear deformation at failure, and, without experience on the tested material, can be chosen as equal to 1 mm. This value of 1 mm is confirmed also by ETC5-ISSMGE (1998), which suggests this value for marly clay (the most similar material listed in the technical rules).

After the choice of a shear rate (lower than v_{max}), the shearing phase can be started. After each test, the τ_{peak} is obtained as:

$$\tau_{peak} = \frac{T_{peak}}{A} \quad (8)$$

where T_{peak} is the maximum shear force recorded during the test and A is the integer sample area.

After each test, values of τ_{peak} and σ_v' allow the drawing of one point on the failure criterion chart.

9.4.3 Shear test: 3 hours, 24 hours and 28 days of curing

Shear tests were performed at 3, 24 hours and 28 days of curing using the same test parameters.

The calculation of the v_{max} was based on the consolidation phase pertaining to the case of 3 hours of curing, this being the youngest two-component grout characterised from the slower consolidation process.

After a consolidation phase duration of 10 minutes, the two different consolidation functions were clearly visible (Figure 62) for all the σ_v' and consequently the t_c was computed, ranging between 0.1 and 0.2. After that, considering an s_f equal to 1 mm, the v_{max} (choosing the more burdensome t_c) was computed equal to 0.43 mm/min. Finally, in order to compensate any possible speed fluctuation of the machine, a shear rate (v_s) of 0.132598 mm/min was set (one third of the maximum allowable value). The duration of each shearing phase until the shear peak ranged between 5 and 9 minutes.

After analysis of the outcomes, it was confirmed that the value of 1 mm used for s_f was realistic. The s_f values obtained ranged between 0.7 and 1.2 mm.

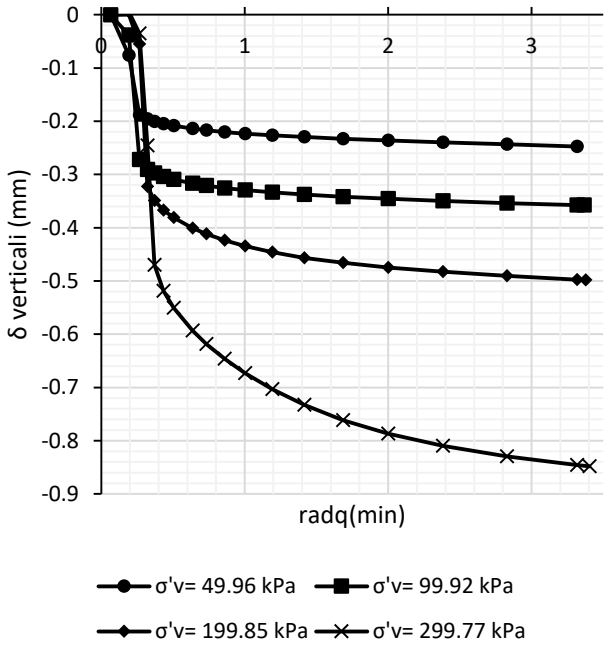

Figure 62 - Time–settlement curves related to samples cured for 3 hours.

9.4.4 **Shear test: 1 hour of curing**

Shear tests performed after 1 hour of curing were the most complex to perform. This short curing time was not simple to manage because of the following aspects:

- all the operations after casting had to be performed quickly;
- the samples were weak, so all the handling had to be carried out gently;
- the material was in the core time of evolution, namely the strength parameters were growing very quickly (proven by the previous test campaigns performed with the penetrometer and the press, chapter 8).

It was clear that for this curing time it was not possible to apply the same shearing rate used for the other cases. Consequently, the durations of both the consolidation phase and the shearing were fixed at 5 and 10 minutes respectively. The consolidation phase started after 55 min of curing time, whereupon the

shearing started. Considering for the shearing a maximum value of horizontal displacement of 5 mm (chosen arbitrarily), the v_s was calculated as equal to 5 mm/min.

The indirect approach for the determination of the shear rate was adopted in order to guarantee the completion of the tests in a time compatible with the required curing time of 1 hour. The possibility of carrying out tests potentially in an undrained condition was known, but in fact, analysing the time–settlement curve for 5 minutes duration, it was never possible to identify the $\sqrt{t_c}$. As an example, Figure 63 reports the time–settlement curve for the smaller σ_v'.

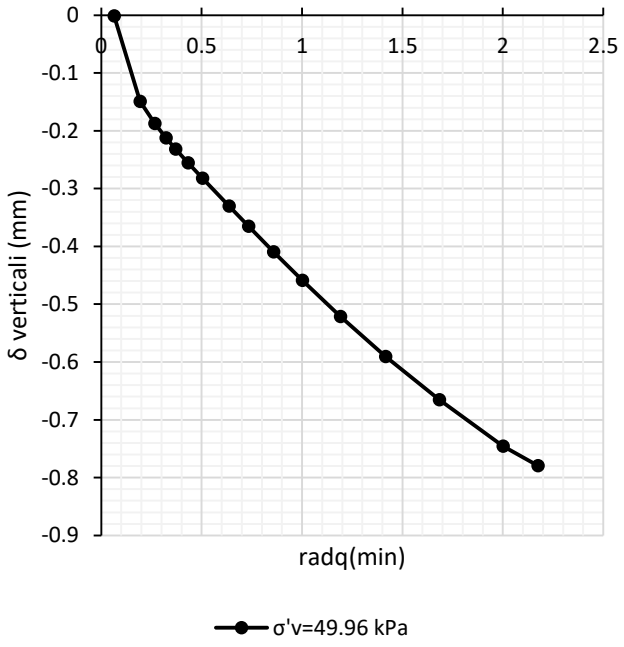

Figure 63 - Time–settlement curve concerning the test carried out on two-component sample cured for 1 hour and tested with a vertical stress of 49.96 kPa.

However, waiting until the right value of $\sqrt{t_c}$ could be spotted was not reasonable. For completeness, only one consolidation test was performed completely, and a value of v_{max} equal to 0.01 mm/min was computed. Simulating the use of this shear rate, also for a shearing distance of only 1 mm, a duration of 100 min was computed, which was plainly pointless for our purpose. Furthermore, the value of $\sqrt{t_c}$ was strongly affected by the curing evolution of the sample, so this approach cannot be successfully applied, as the system is in the fast evolution phase.

Summing up, for shear tests performed at 1 hour of curing, each test was accomplished in 10 minutes. The consolidation phase, with a duration of 5 minutes, was performed, starting after 55 minutes of curing. The shear rate was set equal to 0.5 mm/min.

9.5 Results

In this section the following symbols are used:

Table 24 - Symbols used.

Initial bulk density	ρ (kg/L)
Effective vertical strength	σ_v' (kPa)
Max shear stress	τ_{peak} (kPa)
Horizontal failure displacement	δ_{hf} (mm)

The initial bulk density (ρ) was calculated as the ratio between the sample weight and its volume, before starting the test. The horizontal failure shear stress displacement (δ_{hf}) is the displacement corresponding to the max shear stress (τ_{peak}) recorded during the shearing.

Each curing time has a dedicated paragraph below, which reports:

- a chart of the shear strength as a function of the horizontal displacements;
- a table summarising the outcomes obtained;
- a chart representing the Mohr–Coulomb failure envelope.

As concerns the last type of chart, the equation reported in the form $y = \alpha + \beta x$ was computed by using the linear regression method, which is able to provide as output a slope value β and *y*-intercept α. These values were used for the computation of the cohesion (c') and the friction angle (φ').

9.5.1 **1 hour**

After ending the tests performed according to the vertical strengths listed in Table 23, the shear test campaign related to 1 hour of curing was extended considering another three values of σ_v'. This choice was made after the unclear trend obtained by plotting the preliminary outcomes. Specifically, values equal to 74.96, 149.88 and 249.81 kPa were added as further values of σ_v'.

In the following, the horizontal displacement vs shear strength and the shear peaks values as a function of the corresponding effective vertical strengths are reported in Figure 64 and Figure 65 respectively. Table 25 summarises the outcomes obtained.

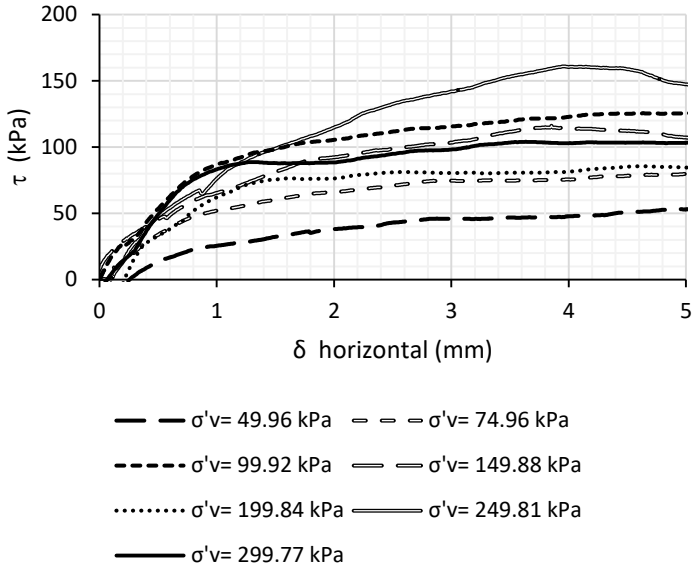

Figure 64 - Shear stress as a function of the horizontal displacement. 1 hour of curing.

In Figure 64, the first consideration is the absence of peaks of shear strength (the curves tend to asymptotes), while the second peculiarity concerns the chaotic nature of the different functions. In particular, the curve that reaches the highest values of shear strength can be seen to correspond to a vertical effective strength of 249.81 kPa, which is not the highest one. Continuing, the curve with the second highest values of shear strength corresponds to the vertical effective strength of 99.92 kPa, namely the third smallest value of σ_v'. Evidently, considering such a short curing time, the load applied during the consolidation phase and preserved during the shearing interacted significantly with the hardening process. As reported in Table 22, after a curing time of 1 hour the UCS is close to 80 kPa. Clearly, the mechanism of vertical loading during the consolidation phase is different, having in this case the lateral confinement. However, at the current state of the art it is impossible to neglect a priori the potential interaction caused by the vertical strength on the sample for 1 hour of curing.

Table 25 - Outcomes pertaining to the direct shear tests performed at 1 hour of curing.

	Test 1	Test 2	Test 3	Test 4	Test 5	Test 6	Test 7
ρ (kg/l)	1.20	1.18	1.20	1.19	1.20	1.20	1.21
σ_v' (kPa)	49.96	74.94	99.92	149,89	199.85	249.81	299.77
τ_{peak} (kPa)	54.60	81.76	126.80	116.05	85.70	160.97	106.39
δ_{hf} (mm)	/	/	/	/	/	/	/

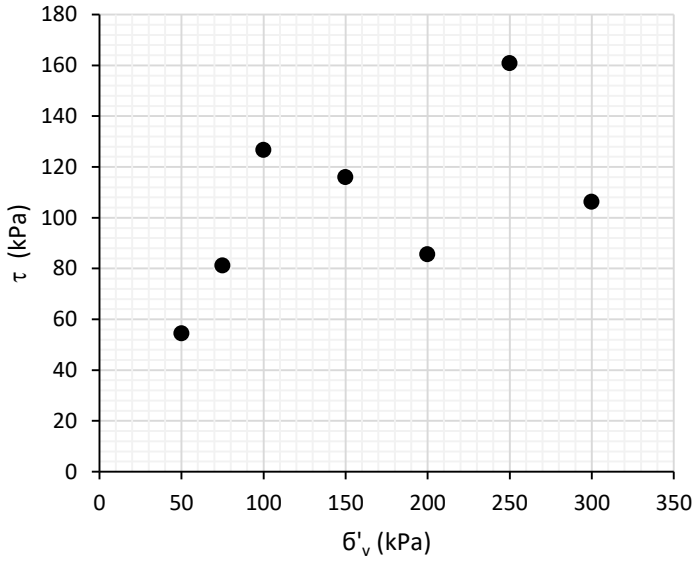

Figure 65 - Diagram of outcomes pertaining to the direct shear test performed at 1 hour of curing.

9.5.2 **3 hours**

In the following, the horizontal displacement vs shear strength and the failure envelope criterion are reported in Figure 66 and Figure 67 respectively. Table 26 summarises the outcomes obtained.

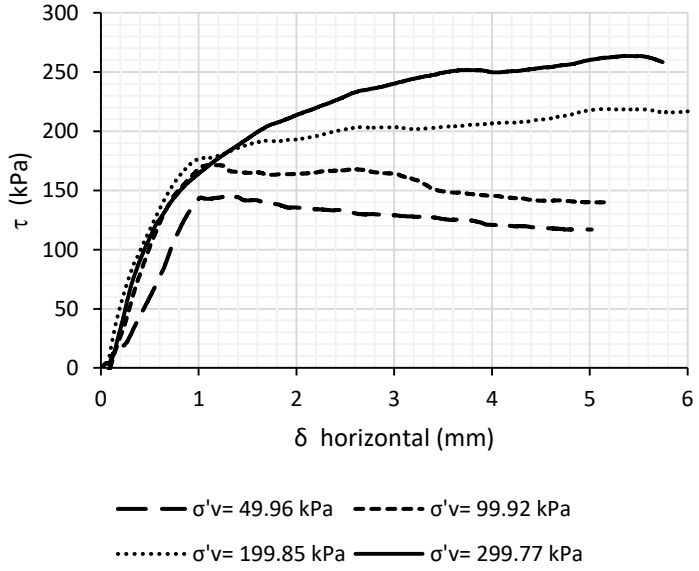

Figure 66 - Shear stress as a function of the horizontal displacement. 3 hours of curing.

In Figure 66, the transition from brittle to ductile behaviour, i.e. peaks, is clearly appreciable only for functions related to the smaller values of effective vertical strengths, i.e. 49.96 kPa and 99.92 kPa. On the other hand, considering the curve for σ_v' equal to 199.85 kPa, it can be observed that the curve tends to a constant value close to 200 kPa for horizontal displacements ranging between 2 and 4 mm. Right after that, it seems that the function tends to increase slightly

again, reaching the highest value of shear strength of about 219 kPa. Pertaining to the choice of the peak, the asymptotic value of 200 kPa was deemed more correct, and was consequently used for the Mohr–Coulomb failure envelope chart. A similar situation can be seen for the curve related to the vertical effective strength of 299.77 kPa, with a constant value close to 250 kPa reached in correspondence to a horizontal displacement ranging between 3.5 and 4.5 mm. As in the previously described case, the curve seems to rise for further displacements. The peak value of 250 kPa was thus used for the Mohr–Coulomb failure envelope chart.

Table 26 - Outcomes pertaining to the direct shear test performed at 3 hours of curing. For tests 3 and 4 the chosen τ_{peak} are the values reported after the arrows.

	Test 1	Test 2	Test 3	Test 4
ρ (kg/l)	1.19	1.19	1.20	1.20
σ_v' (kPa)	49.96	99.92	199.85	299.77
τ_{peak} (kPa)	145.30	171.58	218.79 → 200	263.70 → 250
δ_{hf} (mm)	1.00	1.15	/	/

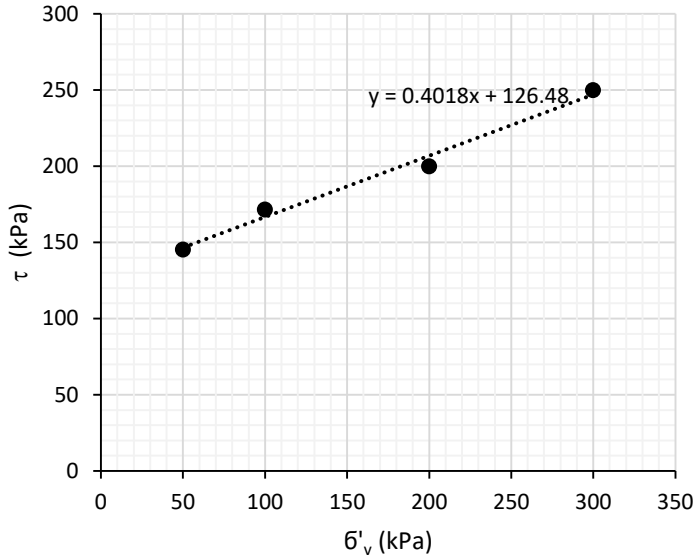

Figure 67 - Mohr–Coulomb failure envelope of the two-component grout at 3 hours of curing.

9.5.3 **24 hours**

In the following, the horizontal displacement vs shear strength and the failure envelope criteria are reported in Figure 68 and Figure 69 respectively. Table 27 summarises the outcomes obtained.

The function related to the vertical effective strength of 99.92 kPa was unfortunately not saved. However, the peak was manually recorded and consequently the Mohr–Coulomb failure envelope reported in Figure 69 is complete.

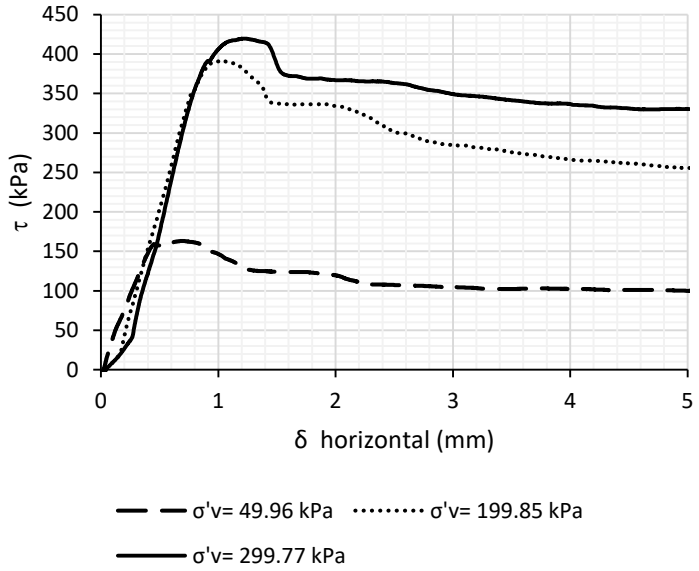

Figure 68 - Shear stress as a function of the horizontal displacement. 24 hours of curing.

Table 27 - Outcomes pertaining to the direct shear test performed at 24 hours of curing.

	Test 1	Test 2	Test 3	Test 4
ρ (kg/l)	1.15	1.14	1.19	1.19
σ_v' (kPa)	49.96	99.92	199.85	299.77
τ_{peak} (kPa)	163.25	282.41	391.78	419.68
δ_{hf} (mm)	0.69	0.97	1.04	1.21

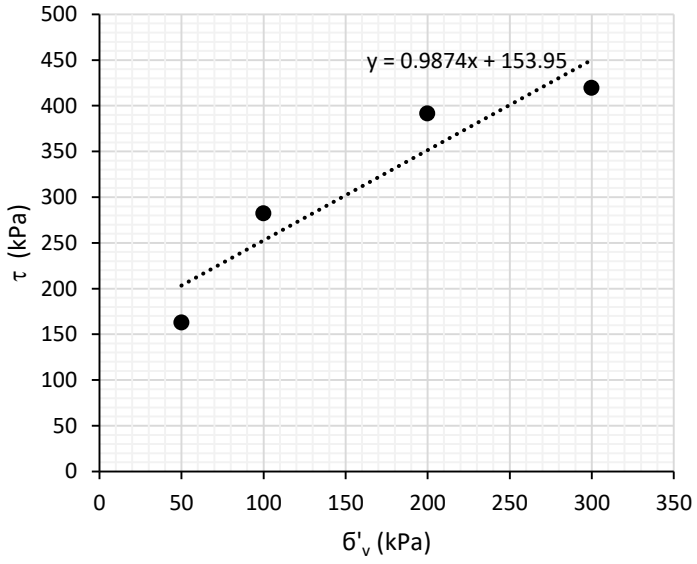

Figure 69 - Mohr–Coulomb failure envelope of the two-component grout at 24 hours of curing.

9.5.4 **28 days**

In the following, the horizontal displacement vs shear strength and the failure envelope criterion are reported in Figure 70 and Figure 71 respectively. Table 28 summarises the outcomes obtained.

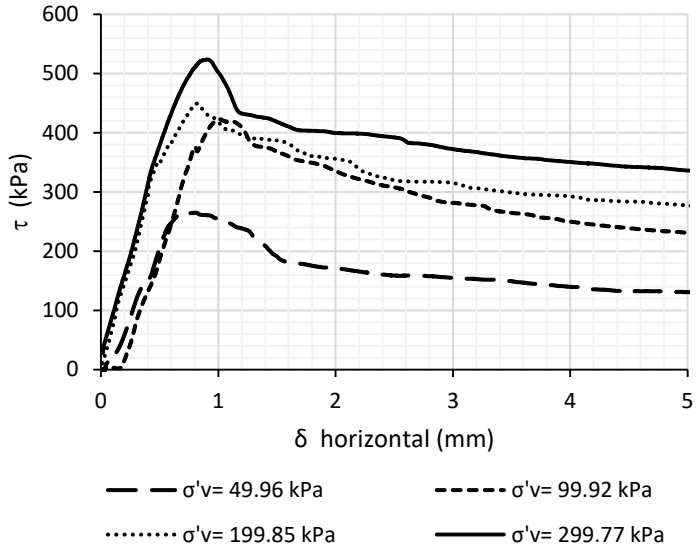

Figure 70 - Shear stress as a function of the horizontal displacement. 28 days of curing.

Table 28 - Outcomes pertaining to the direct shear test performed at 28 days of curing.

	Test 1	Test 2	Test 3	Test 4
ρ (kg/l)	1.17	1.19	1.18	1.20
σ_v' (kPa)	49.96	99.92	199.85	299.77
τ_{peak} (kPa)	266.10	422.74	449.66	523.81
δ_{hf} (mm)	0.72	1.01	0.82	0.90

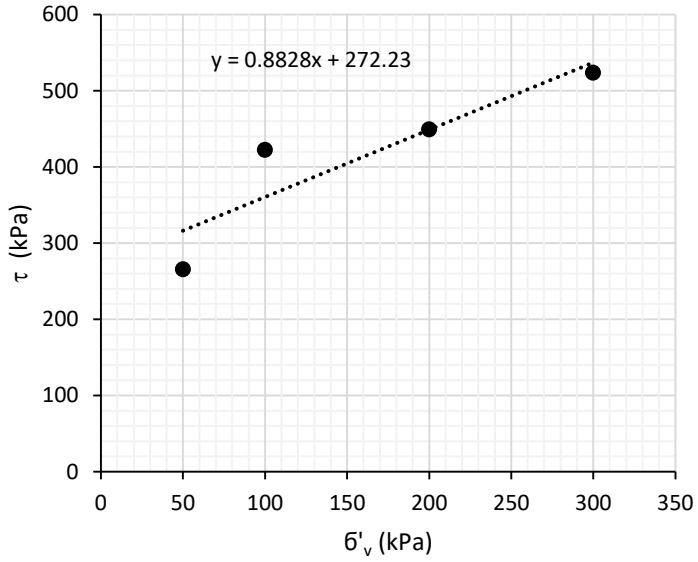

Figure 71 - Mohr–Coulomb failure envelope of the two-component grout at 28 days of curing.

9.6 Discussion

9.6.1 **1 hour**

The tests performed after 1 hour provided outcomes that were hard to interpret.

Firstly, considering Figure 62 and Figure 63, it can be stated that the t_c related to the sample cured for 1 hour should be higher than the one cured for 3 hours. However, as previously discussed, it was deemed appropriate to choose the strategy of a higher shearing rate (5 mm/min) with the purpose of accomplishing tests as close as possible to the right curing time.

Thereby, tests were not performed under the drained condition because of a shear rate higher than the suitable one. On the other hand, it is also incorrect to state that the tests were performed under the undrained condition because, in this last case, commonly the shear strength (constant independently by the considered σ_v') is close to half of the UCS value. In our case, speculating on the undrained condition, the average shear strength is about 104 kPa, a very high value compared to UCS/2 = 40 kPa.

Finally, it can be speculated that the shear tests performed after 1 hour of curing were carried out under a partially drained condition. No meaningful equation can be computed based on the outcomes obtained. The results are not reliable and cannot be used for any application.

9.6.2 **3 hours, 24 hours and 28 days of curing**

The outcomes for curing times of 3, 24 hours and 28 days highlighted the typical trend of the common shear tests under the drained condition.

The failure criterion pertaining to 3 hours of curing became wide in the diagram σ_v'-τ, highlighting an increasing strength performance as a function of the curing time. Figure 72 depicts the failure envelopes according to the Mohr–Coulomb model.

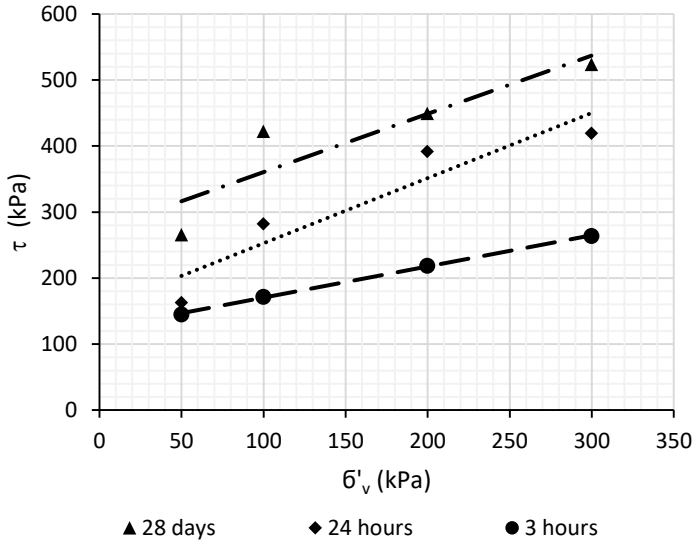

Figure 72 - Mohr-Coulomb failure criteria of the two-component grout as a function of the curing time. 3, 24 hours and 28 days.

The values of cohesion c' (kPa) and friction angle φ' (°) can be obtained from the equations reported on each chart, considering c' = α and φ'= arctan(β). Table 29 reports the final values.

Table 29 - Cohesion and friction angle of the two-component grout cured for 3, 24 hours and 28 days.

Curing time	c' (kPa)	φ' (°)
3 hours	126	22
24 hours	154	45
28 days	272	41

As expected, the two-component grout exhibits different values of cohesion and frictional angle as a function of the curing time. Three different materials were studied, each characterised by its specific failure criterion envelope. Considering the cohesion, the trend is not a linear increase: taking as the starting value the value assessed at 3 hours of curing, an increment of 25% was observed after 24 hours and subsequently a further increment of 77% was seen between 1 day and 28 days. Regarding the friction angle, after 24 hours of curing the material can be deemed to be ripe: the computed value of 45° is double the friction angle measured after 3 hours, whereupon it remains close to this value. However, the outcome of the last determination assessed after 28 days was a friction angle value slightly lower than the previous one.

9.6.3 **Final consideration**

In conclusion, it can be stated that, according to the scientific literature, the results obtained are decisively the first values of shear strength parameters obtained from the study of two-component grout material. The main result is the proposed procedure, which is quite easy to perform and can provide useful results for the designers. For the specific analysed material, the results are summarised in Figure 72 and Table 29. Concluding, the direct shear procedure successfully applied to the two-component grout material could be a useful instrument for tunnelling designers and all the stakeholders involved in the tunnelling world; namely, to have a failure criterion envelope as a function of the curing time could be successfully used to calibrate the mix design for the required performance during the design phase of a tunnelling project.

Considering the scientific literature, a comparison with the outcomes provided by the other authors cannot be easily done, since those results were expressed in terms of undrained shear values and were obtained from different mix designs.

9.7 Additional information

In the light of what was discussed in paragraph 9.6.1, it was decided to investigate the undrained shear strength (c_u) in greater depth, scheduling a test campaign by using the vane test on the two-component grout material cured for 1 hour.

A vane device consists of two main parts: the vane and the torque gauge (Figure 73). The vane is a device with four, flat and thin steel blades welded with angles of 90°. The torque gauge permits the measurement of the applied moment and is usually specifically designed to record the peak value during testing.

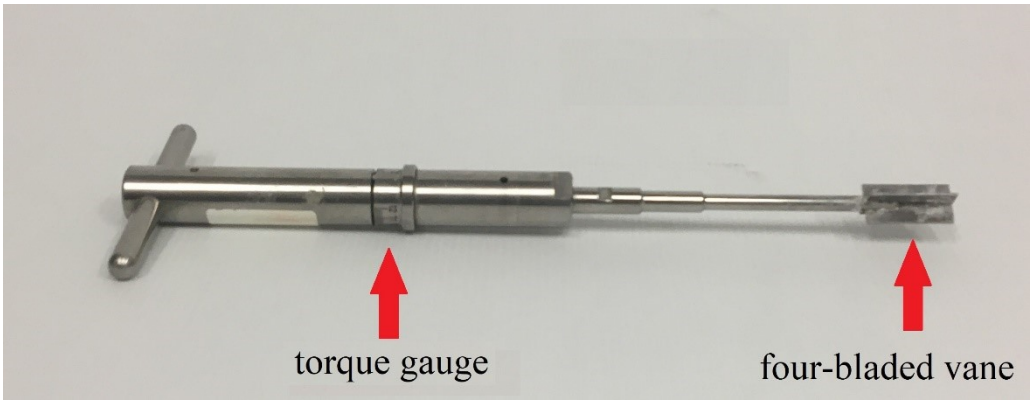

Figure 73 - Vane device used during the undrained shear strength assessment.

According to ASTM D2573/D2573M-18, the vane shear test involves inserting the four-bladed vane inside the intact material and rotating it from the surface. The required torque is manually and gently increased (6°/min) till the

sample is broken along a cylindrical surface determined by the vane dimensions. The peak torque is thereby converted to a shearing resistance of the failure surface by limit equilibrium analysis. Commonly, this test is used in order to assess the c_u of saturated fine-grained materials and clays in a variety of geotechnical explorations. Furthermore, it is also intensively used in the laboratory as a first analysis step, commonly followed by cone penetrometer tests and unconsolidated undrained triaxial compression tests.

The vane test device used for the test campaign (Figure 73) is a Model 16-T0174 produced by CONTROLS. The vane test device is composed of vanes of three different dimensions; after preliminary tests, the smallest one was chosen. The cylinder described by the four-bladed vane has dimensions of 16 x 32 mm.

According to Youn & Breitenbücher (2014), a first attempt at testing was carried out by pre-installing the vane in the grout. Operatively, the vane was manually suspended in the air at the chosen depth in the tank, after which the casting was performed (Figure 74).

Figure 74 - The vane pre-installed in the grout (left) and the assembled vane test device just before testing (right).

Although the torque gauge was fixed on the vane just before testing (in order to avoid any kind of unwanted stresses), the outcomes highlighted very small values compared with those obtained when exactly following ASTM D2573/D2573M-18 (namely by inserting the vane manually into the intact material). The reason for this significant discrepancy was found in the fast gelation process, which prevented the complete and perfect embedding of the four-bladed vane in the mortar before gelation. In light of this experimental observation, the procedure was changed: the grout was cast in the tank, after which the upper surface of the tank was sealed. After the curing time of 1 hour, the cover was removed and the vane (previously assembled on the torque gauge) was slowly and perpendicularly inserted into the grout until it reached about half of the grout thickness. Finally the test was performed. The tank dimensions

(average diameter of 104.2 mm) were chosen after a trial and error procedure, aiming to find the smallest dimensions able to avoid any kind of boundary effects.

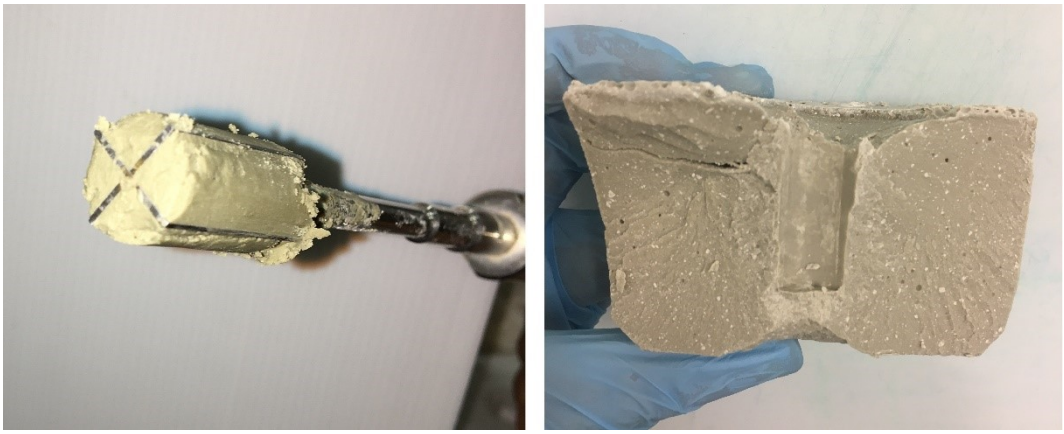

Figure 75 - Vane after the test and half-sample of the grout the day after testing.

As an example, Figure 75 depicts the vane immediately after testing (left) and the half-sample after testing (right). The cylindrical shape of the shearing surface is clear from both photos.

As concerns the outcomes, the average of the computed c_u was 44 kPa while the standard deviation was 3.3 kPa.

The first consideration is to compare the values of UCS/2 and c_u. The difference of 4 kPa is negligible and indicates the reliability of both the undrained shear test campaign and the UCS test campaign described in chapter 8. The second consideration is instead to compare the average of the peak shear strengths achieved after the direct shear test campaign, and the value of c_u. Assuming a undrained condition with the shear strength independent of the normal stresses applied, a shear strength close to 104 kPa was computed. Consequently, it is judged that this discrepancy of about 60 kPa proves the untruth of the undrained condition, and can instead be considered as the effect of the partial drainage process that affected the direct shear test. Figure 76, in terms of total stresses, provides a graphical representation to summarise all the stresses concerning the two-component grout after 1 hour of curing. The Mohr circle refers to the average value of the UCS test campaign, c_u is the average undrained shear strength obtained with the vane test campaign, and c_{pd} is the average of the peaks value obtained by testing the two-component grout with the direct shear test (the subscript pd stands for partially drained).

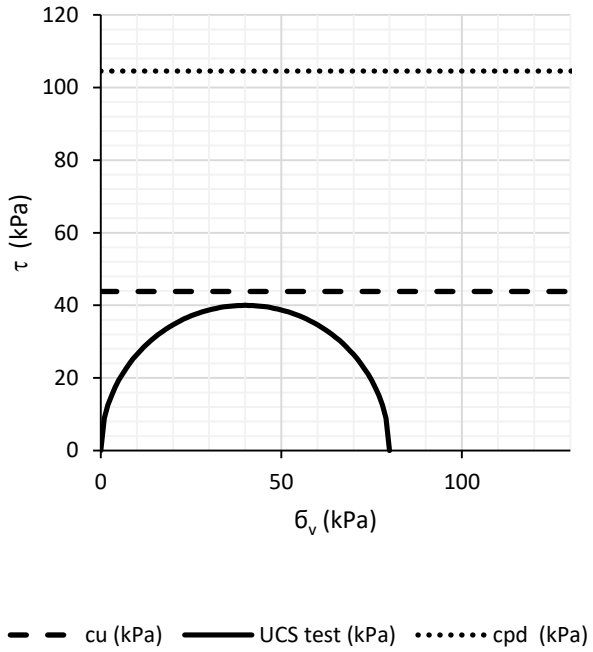

Figure 76 - Undrained stresses obtained studying the two-component grout after 1 hour of curing. The Mohr circle refers to the average UCS value, c_u is the undrained shear strength obtained by using the vane test and c_{pd} is the average of the peaks value obtained by testing the grout with the direct shear test.

Strictly speaking, the chart in Figure 76 is partially incorrect, because c_{pd} is an artificial stress and reporting it on a chart in terms of total stresses could be a forcing. In any case, the representation should be interpreted not strictly from a geotechnical point of view but only as a further vision of the discrepancy obtained between the two values of shear strengths.

9.8 Key concept

KEY CONCEPT 9: The evolution of the two-component grout's mechanical performance as a function of the curing time has been confirmed also from the shear strength assessment. In fact, the obtained Mohr–Coulomb failure envelope criterion widens in time, highlighting a growing trend of the cohesion and the friction angle of the material. The direct shear test provides reliable results for curing times equal to or longer than 3 hours, but it is inappropriate for testing younger grout. The procedure introduced can be integrated in the construction site testing protocol for checking the compliance of the grout with the technical specification. Furthermore, it can be a valid tool, alongside the UCS, in the preliminary phase of the mix design project for calibrating the ingredient dosages as a function of the desired performance.

Chapter 10

The elastic modulus

The elastic modulus is an “anachronistic” topic. The reason for this unusual adjective for an engineering thesis can be explained considering that in recent times tunnelling contractors and designers are eager to know about the elastic modulus of two-component grout. In the technical requirements the provision concerning this parameter is starting sometimes to be listed but, at the moment, no procedures able to assess it are available in the scientific literature. In other words, different tunnelling projects have prescribed different values of the elastic modulus for the backfilling material and, on the other hand, contractors need to assess if the two-component grout produced will satisfy the requirements, yet there is no methodology to help with this issue. Moreover, the lack of knowledge is not strictly linked to numerical values, which are obviously a function of the mix design, but to a standard approach that could provide reliable outcomes, at both short and long curing times.

In this chapter I thought about a simple way to start to understand the elastic parameters of the two-component grout. The section of this chapter related to the geophysics study has been published in the paper Todaro et al. (2020). Special thanks go to Prof. Alberto Godio who helped me with the data collection and analysis.

10.1 State of the art

In this work, the term “elastic modulus” means Young’s modulus, commonly indicated with the capital letter “E”. This is the parameter that provides information concerning the longitudinal stiffness of a material.

As concerns backfilling grout, very little information is available. Thewes & Budach (2009) stated that the material used for annulus filling should have a stiffness modulus similar to a soil that is suitable for a tunnel excavated with segment linings. The authors provide a numerical reference value of 5–10 MPa. Unfortunately, no time reference linked to this value is provided.

Mähner and Hausmann (2017) highlighted the major difficulties in assessing the elastic modulus when adhering strain gauges to the surface samples, and therefore used extensometers, linked to the cylindrical samples with steel blades. After a curing time of 24 hours, an E value of 1000–1200 MPa was determined (the studied material was a mono-component grout with fly ash).

Càmara (2018), referring to the Follo Line project, reports the design requirement for an elastic modulus higher than 20 MPa after 2 hours and higher than 100 MPa after 4 hours. It is interesting to highlight that, in this case, the elastic modulus was required at a short curing time, but unfortunately no further information concerning the test modality was provided and also the method for checking compliance with the technical documents is unknown.

Regarding the application of geophysical technology to two-component grout, Liu et al. (2012) reported the use of ground-penetrating radar (GPR) in an investigation of the mortar distribution in the annulus. Also, Pelizza et al. (2012) reported the use of a georadar for annulus investigation for the construction site of Rome Metro C. These two case histories are reported only to highlight that the application of geophysical technology is not an innovation in the tunnelling field, but the hidden potential of this technology in the study of the stiffness parameters has never been recognised.

10.2 The issue

In recent years, as explained in the previous chapter on shear analysis, tunnelling designers have started to project the backfilling grout assuming a certain value for its E. In some cases, the requirements pertain to a short curing time. However, the available information concerning laboratory test campaigns, methodologies and also the order of magnitude of the elastic modulus is very sparse.

10.3 The idea

The idea is to provide a laboratory procedure that is able to output reliable values of the elastic modulus. Firstly, the standards for testing hardened concrete were followed, but the technical rules were not suitable for the short curing time. Secondly, a geophysical approach was applied, initially only to investigate the short curing time, but later this methodology was extended also to long curing times. Once the geophysics procedure was set up, all the geophysical parameters were assessed and studied, including also the elastic modulus.

Beforehand, just a clarification: the application of the geophysical approach leads to a parameter different from the one obtained with the standard approach for concrete. Due to this difference, this chapter has been organised with two main parts, related respectively to the investigation of the elastic modulus performed “under the concrete rules” and “under the geophysical rules”.

10.4 The approach “under the concrete rules”

As the first step, it was decided to study the long curing times of the two-component grout.

According to Todaro et al. (2020), samples cured for more than 28 days were taken into account. Considering the outcomes obtained from the preliminary test campaign in terms of UCS (chapter 7), for the long curing time the two-component grout was considered as a weak concrete. Consequently, the first attempt at elastic modulus assessment was scheduled “under the concrete rules”. Samples were all produced at the same time, from the same batch of component A. The scheduled testing time foresaw monthly tests till ages of 2 years, but unfortunately, after 7 months, tests had to be stopped due to the impossibility of running further tests according to the chosen standard. Details are provided in the following.

Although it may sound strange, not all the characterisation was performed at the Politecnico of Turin. The elastic modulus assessments required a very long time, and especially concerning such a weak material, the standard approach used for concrete required special care, from samples handling to the compression testing machine recalibration. For this reason, it was decided to perform tests in the Utt Mapei laboratory, which readily and kindly offered the equipment and the technical support needed in order to accomplish the test campaign successfully. The only drawback regarded the trip: not always the taken cautions in terms of shocks protection or sealing for the dehydration saved the samples. Consequently, each E value obtained in this research was computed as the average of 2 or 3 samples, not more (during the trip between the Politecnico of Turin and Mapei’s laboratory in Milan, 1 or 2 samples were always lost).

10.4.1 Materials and test procedure

10.4.1.1 Apparatus

Tests were carried out in the Utt Mapei laboratory in Milan, by using a CONTROL press. The strains were measured with three extensometers. Suitable software, set up according to the standard followed, allowed computation of the elastic modulus.

10.4.1.2 Summary of the technical standard and procedure

EN 12390-13:2013 was taken as the technical standard although some adaptations were necessary. This European standard specifies the method for the determination of the secant modulus of elasticity in compression of hardened concrete on test specimens which may be cast or taken from a structure. Hereinafter, if expressly not specified, referring to elastic modulus, or E, the secant modulus of elasticity is intended.

The shape of 40*40*160 mm respects the standard requirement of a length/width ratio ranging between 2 and 4. The prescription of a curing of 20±2

°C was not respected. Moreover, exactly as described by Mähner and Hausmann (2017), it was impossible to link the strain gauges to the concrete surface, so extensometers were used. These were characterised by 4 steel bits, which, when slightly penetrating the sample surface, ensured reliable displacements readings.

Three extensometers were applied on each testing sample, fixing them by using an elastic wire (Figure 77).

Figure 77 - Extensometers applied on a two-component grout sample before testing.

EN 12390-13:2013 foresees that a single test consists of three pre-cycles followed by three loading cycles. The durations of the cycles and reference compression strength values are provided in the technical regulation (Figure 78).

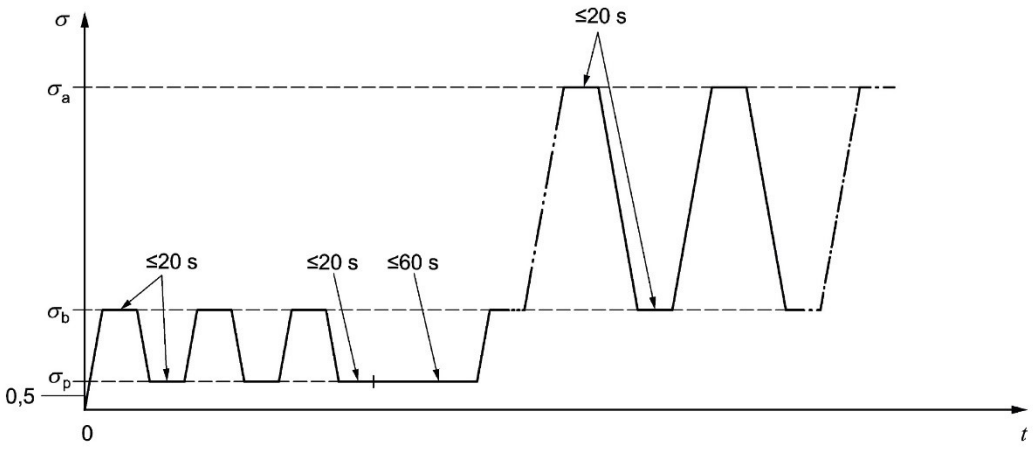

Figure 78 - Cycle for the determination of secant modulus of elasticity.

In Figure 78:

σ_a is the upper stress, computed as UCS/3;

σ_b is the lower stress, computed as UCS/10;

σ_p is the preload stress, ranging between 0.5 MPa and σ_b.

The standard allows the calculation of E taking into account only the first and the third cycle, according to Equation 9.

$$E = \frac{\Delta\sigma}{\Delta\varepsilon} \quad (9)$$

After trial tests, it was clear that EN 12390-13:2013 would not be applicable integrally, so some modifications were adopted. Firstly, the three pre-cycles were not performed. The two-component grout tested, according to the reference mix design, is characterised by UCS values that never exceed 2 MPa, so the σ_b values are always lower than 0.2 MPa. Thus, the requirement for 0.5 MPa $\leq \sigma_p \leq \sigma_b$ can never be respected.

Secondly, considering that the number of samples was limited, after a careful outcomes analysis, the elastic modulus was computed taking into account all three cycles. In reality, it is not clear what the reason was for discarding the data pertaining to the second load cycle, the values being perfectly aligned with the other two (experimentally proved).

Concerning the practical procedure, damaged samples were excluded from testing beforehand. After that, the UCS assessments were performed, being indispensable for computing the cycle stress ranges. Previously, the press had been programmed with the duration for each phase, according to Figure 78. Then, the extensometers were applied, ensuring they were stable on the sample. Before long, the press was switched on and the three cycles were carried out. The software provided as output only one chart, as a function of the average of the transducers acquisition. On the chart, considering the stress σ_a and σ_b and the corresponding strains, three values of E were calculated, the average of which was considered as the secant modulus of elasticity.

10.4.1.3 Samples manufacturing

The component A for the two-component grout was produced according to the procedure described in paragraph 7.2. The mix design used is reported in Table 21. Concerning the casting and the curing modality, the procedure described in paragraph 7.3.3 was followed.

10.4.2 **Results**

Figure 79, as an example, shows a photo related to the testing phase for the elastic modulus computation at 5 months of curing. As clearly shown, the image is related to the end of the second loading cycle (courtesy of Utt Mapei).

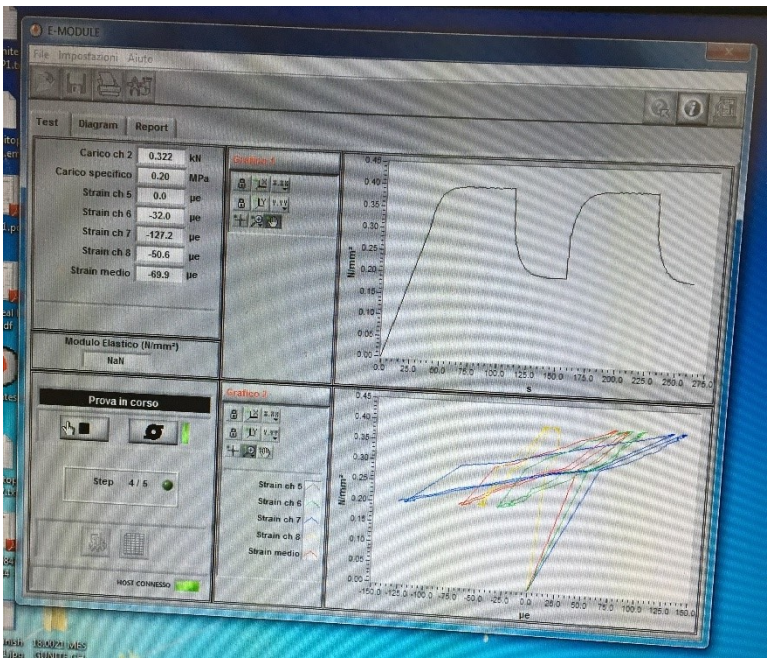

Figure 79 - Testing phase for the elastic modulus computation at 5 months of curing (courtesy of UTT Mapei). Stress in function of time (up) and stress in function of strain (down).

Table 30 and Figure 80 report results obtained from the test campaign. The samples cured for 4 months were not assessed because no integer specimens were available for testing.

Table 30 - Elastic modulus of the studied two-component grout at long curing time.

Curing time (months)	Curing time (days)	E (MPa)
1	28	1478
2	60	1659
3	90	1876
5	150	2199
6	180	1691
7	210	1447

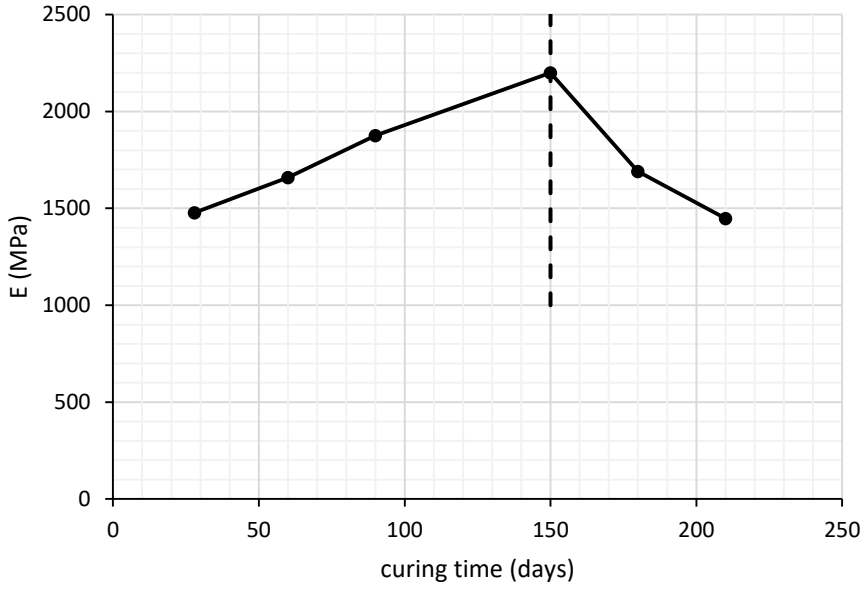

Figure 80 - Function of the elastic modulus of the studied two-component grout at long curing time.

10.4.3 **Discussion**

The outcomes highlighted a rising trend for the elastic modulus, until 5 months of curing.

The rising trend as a function of the material curing was plainly linear until the assessment performed at 5 months of curing time. However, the subsequent two scheduled testing times highlighted a decreasing of the E values. This decrease was due to the impossibility of recording the sample strains reliably during testing. A careful visual checking of samples tested after 6 and 7 months of curing showed the presence of a very thin layer of different grout on the sample surfaces, deteriorated and slimy. This layer affected the samples only superficially, to a depth of less than 2 mm, but it was sufficient to prevent correct coupling between the transducers and the samples. The extensometers' steel bits were completely uncontrolled and the outcomes were not reliable.

Unfortunately, after 6 and 7 months of curing, the layer was thin, without colour variation, so it was not possible to photograph it to be able to focus on the phenomenon. However, it was verified that the deteriorated layer was growing in depth with time. Figure 81, as an example, depicts a sample cured for 3 years. In this picture the phenomenon described has a bigger impact and is clearly visible (with the depth of 5–8 mm). The sample surfaces were so deteriorated that just swiping a finger caused removal of the grout (Figure 81, right).

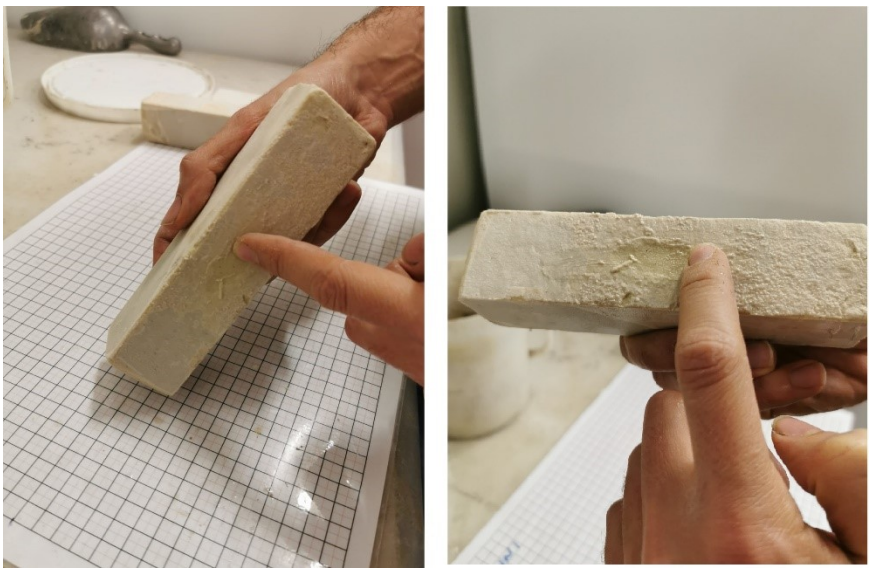

Figure 81 - Deteriorated external layer of the sample.

To complicate the situation, the distribution of this weak layer was seen to be inhomogeneous on the samples' surfaces, with a distribution that appeared random. This phenomenon halted the test campaign on long curing times. Furthermore, outcomes pertaining to 6 and 7 months of curing were discarded.

In conclusion, with the considered mix design, it can be stated that the "grout approach" permits reliable outcomes to be achieved in terms of the elastic modulus for curing times ranging between 1 and 5 months.

The trend obtained is linear only over the considered time lapse. Unfortunately, with this approach the impossibility of reliably investigating two-component grout younger than 1 month or older than 5 months was verified. If it were possible, probably a curve trend would be found.

For the considered time lapse, Equation 10 can be assumed:

$$E = 7t + 1314 \qquad 10$$

where:

E is the elastic modulus, expressed in MPa;

t is the time, expressed in days.

Finally, a comparison with the sparse information of the scientific literature was hard to perform. Considering the E value of 1000–1200 MPa after 24 hours achieved by Mähner and Hausmann (2017), in the first instance this referred to a mono-component grout (also an uncommon mono-component grout because of the presence of the fly ash) and in the second instance the time referred to was less than 24 hours, meaning that there is no possibility of comparison. Also the values of Càmara (2018) refer to short curing times. The values proposed by Thewes & Budach (2009) would to seem to be too low for a long curing time, so probably 5–10 MPa refers to a short curing time too.

10.4.4 **Additional information**

Tests performed according to EN 12390-13:2013 carried out on samples cured for less than 28 days were not excluded a priori. Due to the basic weakness of the material compared to standard concrete, the procedure prescribed an elastic range for the load cycle calibrated on very low values. Assuming a typical UCS value after 24 hours close to 1 MPa, by using EN 12390-13:2013 the range for the load cycle was between 0.1 MPa and 0.33 MPa, much too low for the compressive testing machine used.

Before fixing the sample shape conforming to EN 196-1:05 (prism dimensions of 40*40*160 mm), cylindrical ones were used. The sample had a diameter of 52 mm and a height of 130 mm (Figure 82). Consequently, the prescription of a length/width ratio ranging between 2 and 4 was respected. Tests were performed by using only two transducers for the strains, applied diametrically opposite each other on the sample. The transducers were different from those chosen for the official test campaign, without steel bits, but equipped with two steel blades. After the preliminary test, both the cylinder shape and the blade extensometers were discarded because of the major difficulties encountered with the reciprocal coupling adhesion problem. The low reliability of the outcomes achieved led us to change the sample shape and the type of transducer.

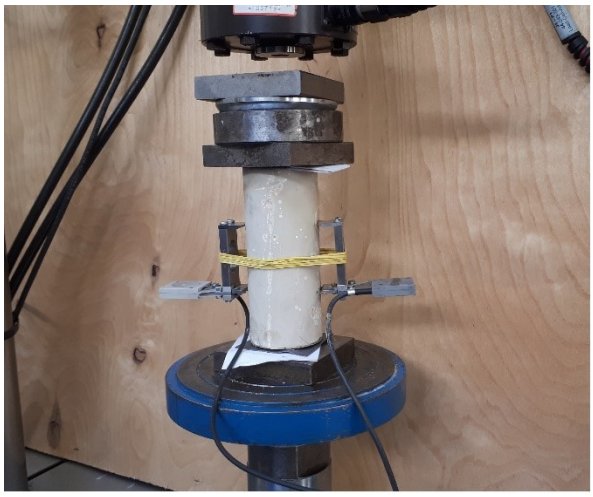

Figure 82 - Cylinder sample and transducers for the elastic modulus assessment. System discarded because of adhesion problems.

10.5 The geophysical approach

As the second step of the research, it was decided to study the two-component grout with a geophysical approach.

Once the geophysics test campaign was scheduled, it was decided also to proceed with the investigation of all the geophysics parameters, not only the elastic modulus. It should be highlighted that all the geophysics parameters are strictly linked and that, while seeking to avoid the other computations, it is not

possible to assess the elastic modulus without computing also all the other parameters. In this context, the elastic parameters are referred to as “dynamic” according to the geophysics discipline, in order to highlight that the tests are run stressing samples with infinitesimal deformations.

10.5.1 Materials and test method

10.5.1.1 Apparatus

The geophysical tests were carried out using a Pundit® PL–200, a fully integrated device specifically designed for performing ultrasonic velocity tests. The device was equipped with a pair of transducers, characterised by a natural frequency of 250 kHz (Figure 83).

Pundit® PL–200 incorporates a pulse generator, receiver, amplifier, a time measuring circuit and a touch display. Other authors (Zarei et al., 2019) have adopted a similar apparatus for testing concrete.

Figure 83 - Picture of Pundit® PL–200 (left) and the transducers used with a natural frequency of 250 kHz (right);

10.5.1.2 Summary of the technical standard and method

Before starting testing, a depth analysis of the technical standard pertaining to the geophysics approach was performed.

Basically, the method for assessing the ultrasonic longitudinal waves velocity in hardened concrete is set by the European Standard BS EN 12504. According to this technical regulation, the waves velocity can be analysed for assessment of the concrete’s uniformity, to recognise potential cracks or voids in the medium, to recognise changes in properties with time, and to assess the dynamic physical properties. In particular, BS EN 12504-4:2004 gives information concerning testing on fresh and hardened concrete or structural concrete: direct transmission (Figure 84a), semi-direct transmission (Figure 84b) and indirect transmission (Figure 84c) are described.

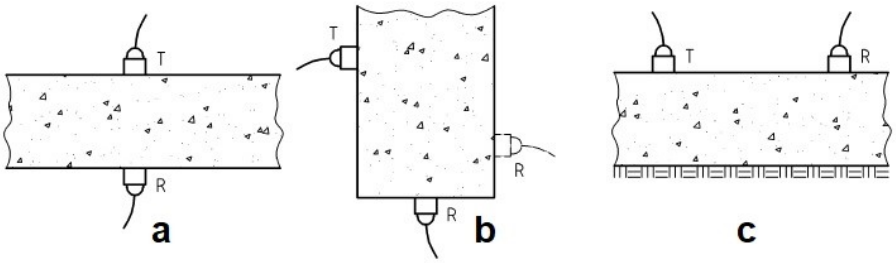

Figure 84 - Direct transmission (a), semi-direct transmission (b) and indirect transmission (c). BS EN 12504-4:2004.

Furthermore, additional information is provided concerning the main factor that can potentially affect the pulse velocity measurements and their correlation with the concrete strength.

In order to obtain wider knowledge, the American standards were also taken into account. ASTM C597-16 defines a standard for assessing the propagation velocity of longitudinal waves through concrete. However, this technical specification in fact overlaps the European one, so BS EN 12504-4:2004 was chosen as the base reference.

However, although the main well known and commonly used regulations concerning the geophysics approach to the properties of concrete have been studied in depth, no precise information on the sample–transducer coupling was found. Generally, both standards recommend ensuring "a sufficient coupling pressure". Unfortunately, from the preliminary tests, it was clear that one of the key parameters for reliably and successfully conducting this kind of test was the coupling pressure between the sample and transducers. Consequently, the scientific literature was searched further and some useful indications were found in ISRM (1977), a standard pertaining to the assessment of speed propagation in stones and rocks. According to ISRM (1977), the pressure of 0.1 MPa is considered as the minimum pressure coupling value between the two-component samples and transducers.

The method commonly known as ultrasonic pulse velocity (UPV) is a non-destructive one (Green, 1991) and it has been successfully used to assess the compressive strength of concrete and the presence of cracks or defects inside the tested structure (Sturrup et al., 1984). McCann et al. (2001) and Popovics (2003) published further results concerning applications of the UPV method. According to BS EN 12504-4:2004, the recording of the first arrival waves, both longitudinal and shear, correlated to the specific wave path, allows the computing of the dynamic mechanical properties of the tested material (Kahn et al., 2011).

The UPV method applied to concrete in construction sites foresees the use of transducers with a natural frequency ranging between 20 and 100 kHz, although the most commonly used ones are characterised by a frequency of 54 kHz. The test involves the application of both transducers on the sample surface (or the structure under testing), whereupon the transmission time of the waves is measured. The first transducer (T in Figure 84) generates the pulses while the second one (R in Figure 84) receives the vibrations and converts them into

electrical signals. The transit time is consequently measured. Knowing the waves path, the outcomes consist of the velocity values (v) relating to both the longitudinal wave (v_p) and shear wave (v_s).

Usually, at the laboratory scale, direct transmission is used (Figure 84a): the transmitter T and the receiver R are applied on two opposite faces of the sample (commonly a cylinder specimen, obtained by coring from a bigger structure). In laboratory conditions, transducers with frequencies ranging between 100 and 250 kHz can be successfully used.

Concerning the accuracy, the UPV method depends on different factors (Basu & Aydin, 2006; Aydin, 2014):

- the determination of the sample length;
- the quality of the coupling between the transducers and the testing sample;
- the potential presence of electronic noise;
- the determination of the material density.

10.5.1.3 Samples manufacturing

The component A for the two-component grout was produced according to the procedure described in paragraph 7.2. The mix design used is reported in Table 21. Concerning the casting and the curing modality, the procedure described in paragraph 7.3.3 was followed with the exception of the sample shape.

For the short curing time, cylindrical moulds made of PVC PN 16 were used (internal diameter of 52 mm, thickness of 5.4 mm and height of 130 mm), while for the long curing time standard prismatic ones were used. The introduction of the cylindrical mould was needed due to the specific testing condition of the short curing time. Specifically, the possibility of having two flat free surfaces of the cylinder available for applying the transducers enabled the test to be performed without demoulding the samples. This strategy allowed the samples to be handled without damaging them.

Figure 85 depicts an overview of the samples used for the geophysics test campaign. From left to right, the cylindrical mould and the cylindrical and the prismatic two-component grout samples are shown.

Figure 85 - From left to right: the cylindrical mould used, cylindrical and prismatic two-component grout samples. The background unit scale is 1 cm.

Considering the cylindrical shape, BS EN 12504-4:2004 recommended the minimal sample length of 100 mm for testing concrete characterised by aggregates with a nominal size of 20 mm. It is already clear that the two-component grout technology does not foresee aggregates in the concrete matrix, but the presence of air bubbles with maximum dimensions of 5 mm inside samples cast in the laboratory is not so uncommon. Consequently, it is reasonable to think about a parallelism between aggregates and air bubbles, both potential sources of wave propagation alterations. Thereby, moulds with a height of 130 mm were produced. Concerning the sample diameter, the chosen value of 52 mm respects annex B5 of BS EN 12504-4:2004 about the length/diameter constraint.

Regarding the density of the grout samples, the experience gained suggested that this physical quantity is not dependent on the curing time. Consequently, the large number of collected samples allowed the calculation of a density value equal to 1.206 ± 0.02 kg/L (where 0.02 kg/L is the standard deviation).

10.5.2 **Testing procedures**

Concerning the short curing time (i.e. curing time less than 9 hours), cylindrical samples protected inside the mould were tested.

The decision to avoid removing the mould made it possible on the one hand to handle the sample in simpler way, and on the other to avoid the possibility that the dehydration process (very fast during the short curing time, if no precautions are foreseen) affects the density of the material. A photo of the specimen during testing is depicted in Figure 86.

Using a laboratory press both transducers were successfully coupled with the sample. According to ISRM (1977), the coupling pressure of 0.3–0.4 MPa was applied.

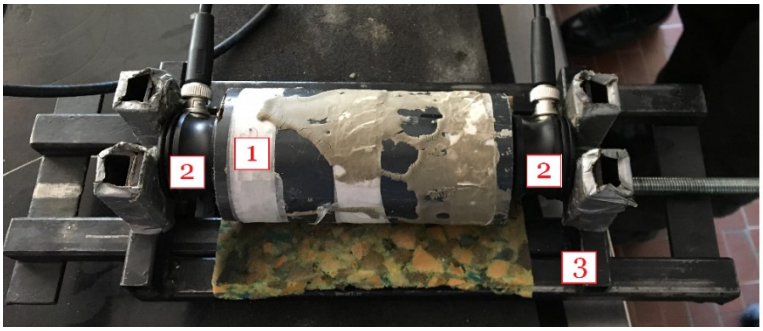

1. two component sample, covered by the PVC mold
2. transducers
3. laboratory manual press

Figure 86 - Photo of the pulse velocity test arrangement with direct transmission approach. Cylindrical sample for short-term analysis.

Beforehand, the two-component sample was weighed and the Pundit® PL–200 was assembled and switched on. After that, a calibration process was used to ensure accurate acquisition of the instrument. Then, a special coupling paste was applied on the surface of both the transducers (an operation of paramount importance mainly for the shear wave transmission). Finally the test was begun and the data recording started. Figure 87 shows a screenshot related to the data acquisition of the S-waves.

Figure 87 - Test running. The display is optimised for S-waves visualisation.

The geophysics test campaign consisted in measuring at different time steps the travel times of both the compression waves and the transversal waves. For analysis of the samples cured for a long time (more than 28 days), the same described procedures for the short-term analysis were followed, except for the shape of the sample, which was prismatic, and the coupling pressure, higher than 1 MPa.

For completeness, it should finally be highlighted that the study of the shear waves required some further precautions. In order to obtain a good quality of the signal (with the maximum intensity), both transducers must be perfectly aligned. This is due to the nature of shear, since the shear waves are generated in a single plane only. In any case, once the test has been started, perfect alignment can be assessed by fixing one transducer in position and gently rotating the other one,

observing on the display the shape of the wave, till the signal is maximised. The domain of rotation ranges between 0° and 90°: starting from a perfect alignment, the shear signal can be minimised or completely cancelled reaching an angle of 90° between the transducers.

10.5.3 **Data processing**

Although the Pundit® PL–200 has specially integrated software able to provide the values of elastic parameters directly as output, it was decided to approach the calculation in a more classic way in order to have broader control of the variables.

After the data recording performed during the tests, the raw outcomes collected consisted of wave signals that needed to be processed in order to obtain the velocity values relating to the longitudinal wave (also called the compression wave or P-wave) and the transverse wave (also called the shear wave or S-wave). However, the first step performed in the data processing procedure was the computation of the waves' travel times. The processing flow, carried out also by using a MATLAB application specifically created, was as follows:

- displaying the raw signal, commonly a wiggle trace;
- application of an automatic gain control to recover energy and tune the signal;
- application of a band pass filtering aimed at removing electrical noise;
- manual recognition of the "first arrival", namely the wave travel time.

Once all the travel times had been computed, the velocity v_p for the P-wave and v_s for the S-wave were easily computed as the ratio of the distance between the transducers, i.e. the sample length, and the travel time.

Taking into account the values of v_p and v_s, the dynamic bulk modulus (K) and the dynamic shear modulus (G) were computed, according to Equations 11 and 12 respectively:

$$K = \rho V_p^2 - \frac{4}{3}G \quad (11)$$

$$G = \rho V_s^2 \quad (12)$$

where:

ρ is the density of the material;

v_p is the pulse velocity of the P-wave;

v_s is the pulse velocity of the S-wave.

Poisson's ratio (υ) was calculated according to Equation 13 and its independence from the density parameter can be highlighted:

$$\nu = \frac{\left(V_p^2 - 2V_s^2\right)}{\left(2V_p^2 - 2V_s^2\right)} \quad 13$$

Once Poisson's ratio had been computed, the dynamic elastic modulus (E) was calculated according to Equation 14:

$$E = 2G\ (1 + \nu) \quad 14$$

Hereinafter, the reference to "geophysical parameters" must be understood as referring to the dynamic bulk modulus, the dynamic shear modulus, Poisson's ratio and the dynamic elastic modulus.

10.5.4 **Results**

In this paragraph the outcomes are presented. According to Todaro et al. (2020), the separation between short and long curing times should not be intended as an absolute division between two different materials, but is strictly linked to the different evolution trends of the two-component grout. The geophysics approach enables us to better highlight the nature of this "separation".

10.5.4.1 Short curing time

According to Todaro et al. (2020), the first 9 hours of curing were considered as a short curing time.

According to the information collected during the other test campaigns on the two-component grout (where the fast evolution of the geophysics parameters in the first hours of curing was forecast), the number of determinations was increased in the first hours after the mix. Unfortunately, before 45 minutes of curing time it was impossible to lock the sample using the laboratory press without irreparably damaging the sample, so no determinations were performed before 45 minutes. However, starting from 45 minutes of curing time, it was decided to perform determinations every 15 minutes up to 2 hours. After that, the testing times were extended to 30 minute intervals, up to 4 hours of curing time. After 4 hours, tests were performed every hour up to 9 hours.

The same sample was always used.

During the test campaign, and specifically after the test performed at 1 hour of curing, it was decided to check the coupling pressure between the sample and the transducers. Although the coupling was good, a second test was quickly planned and performed, 5 minutes after the previous one, just slightly increasing the coupling pressure (with a half-turn of the laboratory press screw block). Surprisingly, it was observed that although just 5 minutes had passed, the shape of

the wave had changed. Consequently, it was decided to collect both data (traces 2 and 3 respectively in Figure 88).

All the 16 recorded traces (also called seismograms in geophysics) are plotted in Figure 88. The seismograms show an overview of the work performed at short curing times. However, the depicted traces are quite raw data, so it is not possible graphically to determine exactly the first arrival times of the P-wave and S-wave.

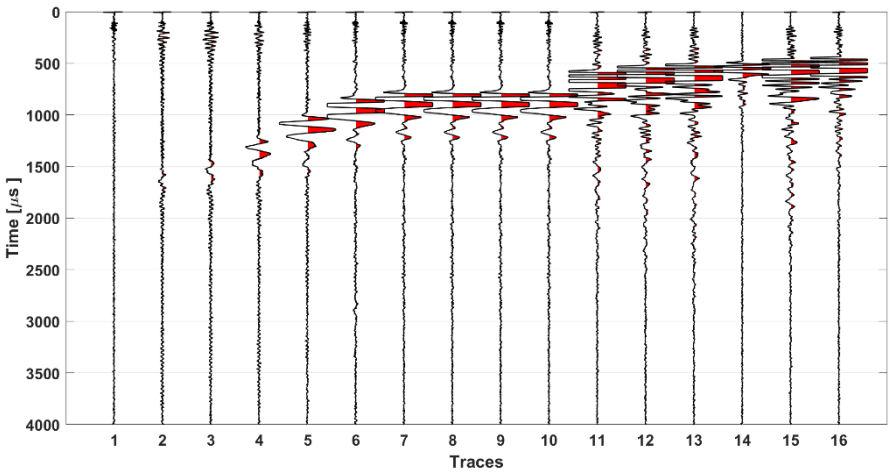

Figure 88 - Seismograms related to the geophysics test campaign at short curing time (trace 1 is related to 45 minutes of curing, while trace 16 is related to 9 hours). The most energetic signals, highlighted in red on the chart, refer to shear waves.

As previously described in the data processing flow, the signal amplitude was tuned and amplified. This operation was fundamental, especially for the shear wave analysis. Analysing Figure 88, it can be seen that the shear wave is recognised only after 1h 15' of curing time (trace 4). This is consistent with the nature of the shear wave: just after mixing, the grout is fresh and the water (remember that the water is the main ingredient of the two-component grout) is not yet involved in the cement hardening reaction, so it creates a barrier that successfully prevents S-waves propagation. Before long, due to the progress of the chemical reactions, the water becomes progressively linked to the grout matrix; thereby the shear waves begin to cross the material. However, after the complete data processing, shear waves were recognised also after 45 minutes of curing, even though the signal was very weak and not appreciable graphically in Figure 88.

Having obtained the travel times, the seismic velocity was computed, ranging from 80 m/s up to 300 m/s (respectively after 45 minutes and 9 hours of curing). After that, the values of the dynamic shear modulus (G) were calculated according to Equation 12. Figure 89 depicts the trend of G as a function of the curing time. G ranges between 8 and 105 MPa.

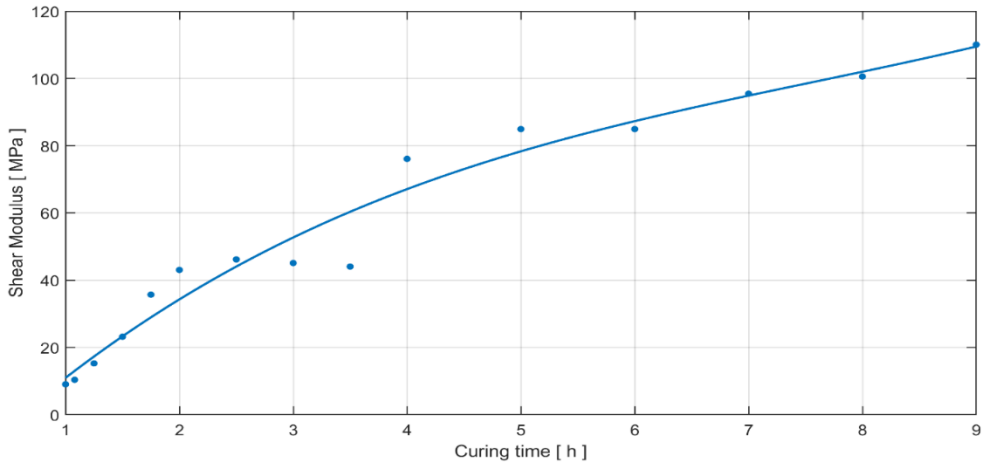

Figure 89 - Dynamic shear modulus (G) trend as a function of the curing time.

It should be underscored that the calculated values between 2.5 and 3.5 hours of curing time are similar (traces 8, 9 and 10 in Figure 89). This drawback was probably due to the shrinkage phenomenon, which was wrongly underestimated. During these tests, the checking of the coupling pressure was not assessed successfully, so the slight shrinkage of the sample was enough to cause a poor contact between the transducers and the sample, thus obtaining inaccurate travel time determinations (and consequently, inaccurate values of seismic velocity and G).

Concerning the P-waves, the travel time was assessed as stable in time, close to a value of 90 μs. This is consistent with the nature of compression waves, dominated by the water in the sample. By converting the travel time into seismic velocity, a value close to 1500 m/s was assessed as constant, independent of the curing time.

Once v_p and v_s had been assessed for all the curing times, the other geophysical parameters were computed according to Equations 11, 13 and 14. Table 31 reports the outcomes concerning the short curing times.

It should be noticed that v_p is affected by an uncertainly of ±15 m/s due to the travel time measurements. Thereby, K is affected by a marginal fluctuation (<5%) while ν is not significantly affected. Consequently, E is relatively stable.

Table 31 - Geophysical parameters concerning the short curing times.

	45 minutes of curing	9 hours of curing
v_p (m/s)	1500	1500
v_s (m/s)	80	300
υ	0.50	0.48
G (MPa)	8	105
K (MPa)	2703	2570
E (MPa)	24	312

10.5.4.2 Long curing time

The long curing time, identified as a period longer than 28 days after sample casting, was defined by Todaro et al. (2020). The tested samples were prismatic.

Samples cured for 1, 2 and 3 months were tested and the seismograms obtained are depicted in Figure 90.

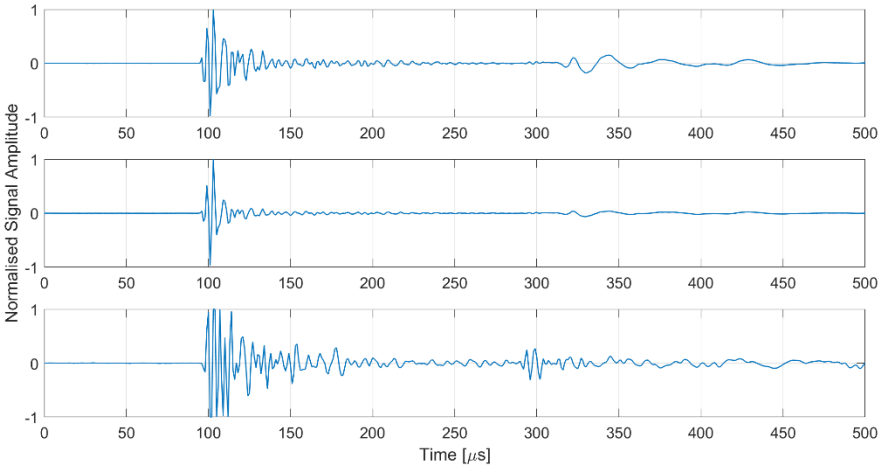

Figure 90 - Seismograms concerning samples cured for 1, 2 and 3 months (from top to bottom respectively).

From a graphical analysis, the travel time concerning the P-waves is clearly visible in each chart (close to 90 μs), while the S-waves are strongly attenuated, barely recognised in the sample cured for 1 month and clearly marked only in the sample cured for 3 months. According to the trend spotted in the short-term analysis, the S-waves' travel time is still decreasing; indeed, after 3 months of curing the travel time is recognised as close to 300 μs. According to Equations 11, 12, 13 and 14, the geophysical parameters were calculated. The outcomes are reported in Table 32.

Table 32 - Geophysical parameters concerning 1 and 3 months of curing.

	1 month	3 months
v_p (m/s)	1685	1685
v_s (m/s)	510	533
υ	0.45	0.445
G (MPa)	314	343
K (MPa)	3000	2964
E (MPa)	909	990

Unfortunately, it was impossible to accomplish the analysis concerning 2 months of curing time due to the unclear dataset.

It can be stated that after one month of curing the material is ripe. Considering the v_p characterised by a constant value, the slight increase of the v_s recognised at 3 months of curing produced just a small variation of υ, G, K and E. Considering the previously described uncertainty due to the measurement, neglecting the abovementioned slight parameter fluctuations need not be considered a mistake. Consequently, under a geophysics approach, the properties of two-component grout samples ranging between 1 and 3 months can be considered equal.

Finally, the last step of the geophysics research concerned the analysis on samples cured for 3, 4 and 6 months. The test at 3 months was repeated in order to verify that the outcomes overlapped with the previous test campaign. The seismograms obtained are reported in Figure 91.

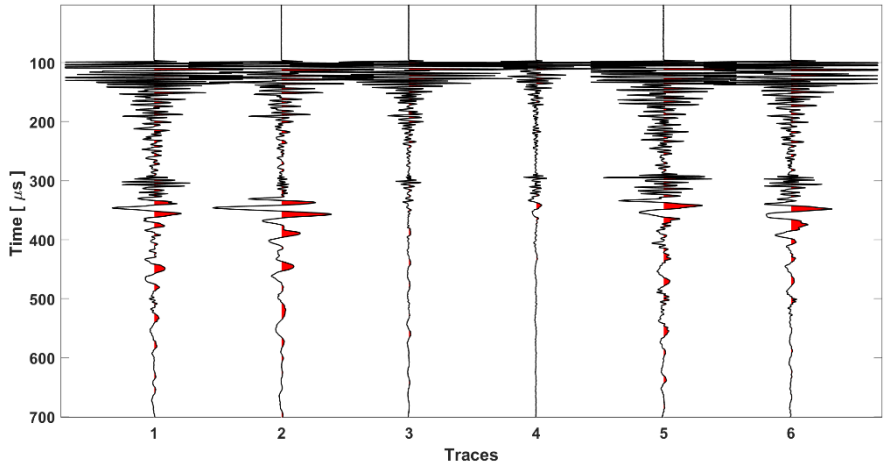

Figure 91 - Seismograms concerning samples cured for 3 months (traces 1 and 2), 4 months (traces 3 and 4) and 6 months (traces 5 and 6).

Having analysed graphically Figure 91 (focusing on traces 1 and 2) in the first instance and having secondly got a proof after the data processing, a perfect data overlap between the sample cured for 3 months with the previous test campaign was spotted. Traces 3 and 4 again highlighted the practical difficulties concerning the recording of S-waves and in fact these waves were not recognisable. Eventually, after the data processing, no significant variations could be spotted comparing traces 1 and 2 with traces 5 and 6. In other words, no significant variations in terms of the geophysical parameters were assessed between two-component samples cured for 3 and 6 months. Table 33 reports the outcomes obtained from traces 5 and 6, i.e. data related to the material cured for 6 months.

Table 33 - Geophysical parameters concerning 6 months of curing.

6 months	
v_p (m/s)	1685
v_s (m/s)	560
υ	0.44
G (MPa)	378
K (MPa)	2920
E (MPa)	1088

10.5.5 Discussion

To the best of the author's knowledge, this research is the first attempt to apply a geophysical approach to study the two-component grout used for the backfilling in tunnelling applications.

It should be underlined that the aim of the research was to estimate E, but, once the procedure had been planned and the tests scheduled, it was decided to study also all the geophysical parameters involved in the computation. This was an essential decision, given that all the parameters are connected.

However, the geophysical approach permitted a successful investigation of the two-component grout, at both short and long curing times. The advantages can be summarised in the following testing features:

- the non-destructive approach permits tests to be repeated without any limit on the number of attempts and without the need for a huge number of samples. In theory, only one sample could be enough (though it is strongly advised to have at least three samples available);
- the display that depicts the waves shape can be easily used as a check-point for the test. If something is going wrong, the displayed wave shape will signal this (weak signal, absence of signal, noise, wrong alignment between transducers during the shear wave recording, etc.);
- tests at short curing times can be successfully carried out.

On the other hand, it should be underlined that, without some familiarity with geophysics testing, it is impossible to successfully carry out the assessment. Experience in the geophysical field is required, mainly to correctly read the seismograms and the first-time waves arrivals.

Having stated these preliminary considerations, some conclusions focused on outcomes can be made. Firstly, this study has made it possible to better recognise the separation between short and long curing times. This separation can be based on the different evolution rates of the material. Considering short curing times, in a time lapse of just 9 hours both E and G increase more than tenfold ($E_{45'}/E_{9h} \simeq 13$; $G_{45'}/G_{9h} \simeq 13$), while at long curing times the material can be considered ripe (an increment of about 10% can be calculated).

However, some further clarification should be provided:

- the statement related to the achievement of a ripe state under the geophysical approach after 28 days does not mean that the material is ripe also from the mechanical point of view;
- all tested samples were cured in standard conditions, optimised to avoid dehydration or temperature shock. Further in situ analysis should be performed in order to understand if the real condition of curing affects the evolution of the final geophysics parameters;

- strictly connected with the above observations, it can be stated that the shear waves dominated all the geophysics parameters, while the compressive waves were independent and constant in time. This condition is verified in the laboratory, while at the construction site, in different curing conditions, the immutability of v_p is not ensured a priori.

Moreover, taking into account the long curing time, it can be stated that both the performed test campaigns (the first on samples cured for 1, 2 and 3 months and the second performed on samples cured for 3, 4 and 6 months) showed a good outcomes reliability. Taking into account the curing time of 3 months, the marked overlapping found was of fundamental importance because it can be considered as further proof of the reliability of the sample production (according to the established procedure) and of the curing conditions. The sensitivity of the shear wave propagation to the curing time (from 80 m/s to more than 500 m/s) and, on the other hand, the independence of the compression wave from the curing time (from 1500 m/s to 1685 m/s) indicated a behaviour completely in divergence from that of standard concrete, characterised by a relevant increase of the P-waves velocity during the curing time.

To conclude, some specific considerations can be made analysing all the computed parameters one by one.

As concerns the Poisson's ratio analysis at short curing times, it can be stated that, since the material behaviour is governed by the water (more than 70% by weight) not yet bonded in the chemical reaction, the value of 0.5 highlights the incompressible behaviour. However, with the continuation of the chemical reaction during the curing process, a decreasing trend can be observed, with a final value slightly bigger than 0.4 after 6 months of curing. It should be underscored that the samples are cured in sealed conditions, where the dehydration process is impossible. Nevertheless, in the real conditions of backfilling at a construction site, if the water is in the condition of leaving the sample, a further Poisson's ratio reduction may be expected.

Concerning G, the increasing trend recognised at short curing times follows in a good way the quick hardening reaction of the two-component material in the first minutes after mixing. As explained, the material starts to gain shear strength almost immediately after the gelation, but unfortunately this shear increase can be clearly graphically observed only after 1 h and 15 minutes (after 45' it can be observed only by analysing the outcomes with the MATLAB application).

As concerns E, the trend is governed by G and the Poisson's ratio trends. Values range between 20 and about 1000 MPa.

Regarding the bulk compressional modulus, considering the value of v_p as constant, the decreasing trend is governed by the increase of the shear modulus.

Finally, it should be noted that the data quality was not always satisfactory. At short curing times, data between 2.5 and 3.5 hours were affected by inaccuracies potentially due to the unsuitable coupling between the transducers and samples; also at long curing times, not all the scheduled tests (i.e. tests on the sample cured

for 2 months) provided the expected results. However, the main result can be recognised as the successful application of the geophysics approach on the two-component grout material, which made it possible to point out the changes of the mechanical properties during the curing time and the order of magnitude of the investigated parameters.

10.5.6 Additional information

In this paragraph, a curiosity should be underlined concerning the coupling paste commonly used between the transducers and the sample. Actually, the choice of this material was crucial and must be made carefully.

During the test campaign at short curing times, a special non-toxic / water soluble / organic substance characterised by a very high viscosity was used in order to ensure the transmission of the shear waves in the sample. Unfortunately, the supply of this special coupling paste ran out, and consequently, for the long curing time test campaign, another paste was preliminarily adopted. Only after many unsuccessful attempts, it became clear that the new coupling paste was expressly designed for compressive waves such that the transmission of shear waves was blocked. Tests were only able to go ahead after the first kind of coupling paste became available again.

10.6 Final consideration on the elastic modulus

In this chapter a double approach was tested with the aim of assessing the elastic modulus of the two-component grout. In order to better explain the concepts, the following nomenclature is introduced:

Elastic modulus computed under "the concrete rules"	E static	E_s
Elastic modulus computed under "the geophysical approach"	E dynamic	E_d

To the best of the author's knowledge, concerning the requirements usually expressed by tunnelling designers on the technical specification of the construction sites, the provision pertaining to E_s mainly relates to short curing times.

In this work, the same two-component grout was studied (in terms of the mix design used, the procedure for the component A production, procedure for the samples casting and curing time conditions) both under the standard approach for concrete and under the geophysics approach. E_s was successfully assessed for long curing times, specifically after 1 (28 days), 2, 3 and 5 months. E_d was assessed at short curing times, i.e. between 45 minutes and 9 hours, and at long curing times, specifically after 1, 3, 4 and 6 months. Considering the overlapping testing period (between 1 and 5 months), a comparison between the moduli can be made.

First, it should be underlined that in the scientific literature, the comparison and the final correlation between E_d and E_s concerning standard concrete is not a new topic. Agrò et al. (2009) highlighted how E_d is always bigger than E_s, considering the same curing time of the concrete, while Neville (1987) stated that the ratio E_s/E_d is not fixed in time. However, the technical rules n.195 drafted by the CNR (Italian National Central of Research) provide an equation that allows E_s to be estimated as 90% of E_d. Similar equations are provided in Philleo (1955) and Lee et al. (1977).

Taking into account the outcomes in terms of E obtained in this research, in the chart in Figure 92, both functions are reported. Only the overlapping time has been considered as the time domain. Concerning E_d, a good interpolation of the trend can be drawn assuming $E_d \simeq 1000$ MPa while, concerning E_s, although the trend envisaged was parabolic, the outcomes related to the tested times do not define a parabolic trend, so a linear function has been used to interpolate the data.

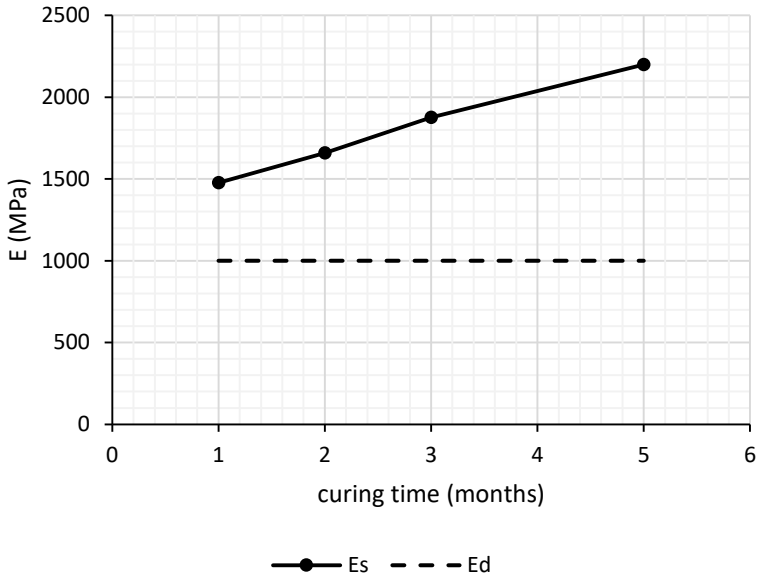

Figure 92 - E_s and E_d outcomes as a function of the curing time.

In conclusion, considering the overlapped period, it can be stated that:

- E_s is always bigger than E_d. This consideration is completely opposite to that reported in the scientific literature concerning standard concrete;
- only according to the geophysics approach, the two-component grout is ripe after 1 months. Indeed, considering E_s, it is evident that the evolution of the material continues also after 1 month;
- considering the impossibility of obtaining values of E_s at short curing times, a useful project tool for tunnelling designers could be the E_d;
- at long curing times, the estimation of E_s is preferable to E_d. The dynamic parameter is not able to accommodate further mechanical improvements;

- as reported in the scientific literature, the ratio E_s/E_d is not fixed in time. Table 34 reports the ratio values, having considered $E_d = 1000$ MPa for all the times corresponding to the E_s determinations.

Table 34 - E_s/E_d as a function of the curing time.

Curing time (months)	E_s/E_d
1	1.48
2	1.66
3	1.87
5	2.20

A final question: why is the geophysics approach not able to read the further evolution of the material after 1 month of curing? It may be presumptuous to answer this in this framework, considering the very poor state of the art. However, a starting point can be found by investigating the difference between standard concrete and the two-component grout. It is clear that the w/c ratio affects this phenomenon: since the two-component grout is mainly composed of water, the water leads the compressional waves, for the whole life of the material. Consequently, the concrete barely participates in the increase of the compression waves' velocity. It could be speculated that the P-waves "watch" only the water located in the sample, and consequently, after the asymptote of the shear modulus has been reached after 1 month, the E_d values plotted in time describe a flat function. On the other hand, the standard approach for concrete is based on a mechanical solicitation. In this case, the test is able to "watch" the improvements of the elastic modulus (due to the cement reaction) and consequently the outcomes also reflect this trend.

With reference to the state of the art reported in the initial part of the present chapter, both Thewes & Budach (2009) and Càmara (2018) listed requirements pertaining to the elastic modulus of the two-component grout without specifying if the parameter is intended as static or dynamic. Actually, Thewes & Budach (2009) did not specify either the reference time. However, in the light of the experimental results obtained, it can be deemed that the listed numerical values are compatible with E_d of the two-component grout, at short curing times.

The static approach is hard to discuss due to the impossibility of successfully performing tests at short curing times.

Actually, given that these authors intended the elastic modulus as E_s, the only one idea that could be pursued, in my opinion, is to execute a UCS test campaign and then, during the data analysis, try to recognise the slope of the linear part of the function σ - ε. In any case, further investigations are strongly necessary in order to understand which type of elastic modulus can be obtained according to this procedure. In Todaro et al. (2019), the computed E values following exactly the last described approach (i.e. assessing the slope of the σ - ε function of samples produced according to mix designs very similar to that reported in Table 21) were presented and, after 28 days of curing, the assessed order of magnitude

for E was 100 MPa. It clearly results that there is an order of magnitude of difference between the E values obtained with the slope of the σ - ε function and the E_s, so it is reasonable to think about a potential correlation, though clearly further investigations are necessary.

As concerns the result presented by Mähner and Hausmann (2017), probably the fly ash, after just 24 hours of curing, produced a material that was able to be successfully tested with the static approach.

10.7 Key concept

KEY CONCEPT 10: The elastic modulus (Young's modulus - E) is a parameter that has recently been increasing in importance in the two-component grout characterisation. It can be assessed following two different procedures that lead to E_s and E_d, called also the static elastic modulus and dynamic elastic modulus respectively. E_s cannot be assessed before 28 days of curing, but describes successfully the evolution of the elastic behaviour as a function of the curing time. E_d highlights the evolution of the grout at very short curing times, but is not able to recognise the further evolution of the material after 1 month of curing.

Given that stakeholders are strongly interested in short curing times, the geophysical approach applied to the two-component grout is suggested as a reliable engineering instrument. It turns out to be reliable and relatively simple, with the exception of the data analysis, which should always be performed by an expert in the geophysical field.

Chapter 11

Durability

The last question of the previous chapter still remained unsolved. Can the two-component grout really be considered mature after 1 month of curing? The E_s was in contrast with this statement, so it was decided that investigating the UCS of the material, after 28 days of curing, could help to clarify ideas.

Furthermore, more generally, another topic was answered: the durability of the two-component grout. In other words, the questions concerning the durability could be summarised in two points:

- if the two-component grout is cured in perfect conditions, are the mechanical properties constant in time? Does the material continue to improve its mechanical performance? Or maybe there is an impairment? Is it possible to investigate E_s after 5 months of curing?
- what can happen if the curing is performed under conditions different from the project ones (where the project curing condition means the laboratory environment)?

In this chapter, some aspects of the durability of the two-component grout are analysed.

11.1 State of the art

Durability is defined as the ability of a material to preserve its properties during the designed lifetime, without requiring excessive maintenance operations or repairs.

Concerning the two-component grout, the first reference to durability can be found in Pelizza et al. (2010). The authors highlighted that the durability of the "gel" which fills the annulus is guaranteed in the normal humidity condition of the ground. Furthermore, it is underscored that no valid proof of the future behaviour of an injected two-component grout exists, although, as an example, the case

history of the Metro Lines in Singapore is reported, where the authorities verified the good condition of the injected grout related to constructions built 10 years earlier. It is eventually stated that if the water will not leave the grout, the material will always remain stable.

Peila et al. (2011), confirming the statements expressed previously by Pelizza et al. (2010), added a key concept for the durability, concerning the impermeability of the ground that embeds the annulus. If the permeability is lower than 10^{-8} m/s, the dehydration of the two-component grout can be avoided, and hence the mechanical properties maintained. In this research, also the results of a laboratory test campaign were presented. Cylindrical samples were cored from a bigger layer of two-component grout and cured under a certain type of soil. Unfortunately, the nature of the soil and its natural water content were not provided. However, the UCS showed a parabolic increasing trend until the last testing time, i.e. after 6 months of curing.

Peila et al. (2015) reported outcomes concerning a long curing time test campaign, related to the UCS. Samples of two-component grout were cured under a dry soil (a sand, but no more information is provided) or under a soil conditioned with a water content of 5, 10 and 15%. The results highlighted that, for the studied two-component grout, there were no significant UCS changes as a function of the different humidity of the curing condition.

11.2 The issue

This issue of the durability is very wide and has not been explored yet, a statement also confirmed by the poor available information in the scientific literature.

In this research, three different aspects were considered and their effects on the two-component grout's durability were investigated:

- the ageing (and the curing modalities);
- the air;
- the water.

11.3 Ageing effect

11.3.1 The idea

The basic idea is to assess if, and with what magnitude, the action of time can affect the two-component grout, by using the UCS as the testing parameter.

Once the preliminary test campaign had been programmed, planning the curing in water, it was decided to take into account also different curing conditions: a common fluvial sand was selected as the medium for embedding samples, and was then conditioned using water, foreseeing two different moisture

contents. In this way, three different conditioning environments (herein also called "curing modalities") were available.

Tests were performed until 3 years from the samples production. The first assessments were planned with a higher frequency, while after 1 year of curing, an annual testing frequency was adopted.

11.3.2 **Material and test procedure**

11.3.2.1 Apparatus and material

All the tests were performed using the Wykeham Farrance compression testing machine. Tests were carried out using both the comprimitor and the frame for the three-point flexural test depicted in Figure 43 respectively for the assessment of the UCS and the indirect tensile strength.

Concerning the sand used to embed the samples during the curing phase, Figure 93 reports the relative grain size distribution.

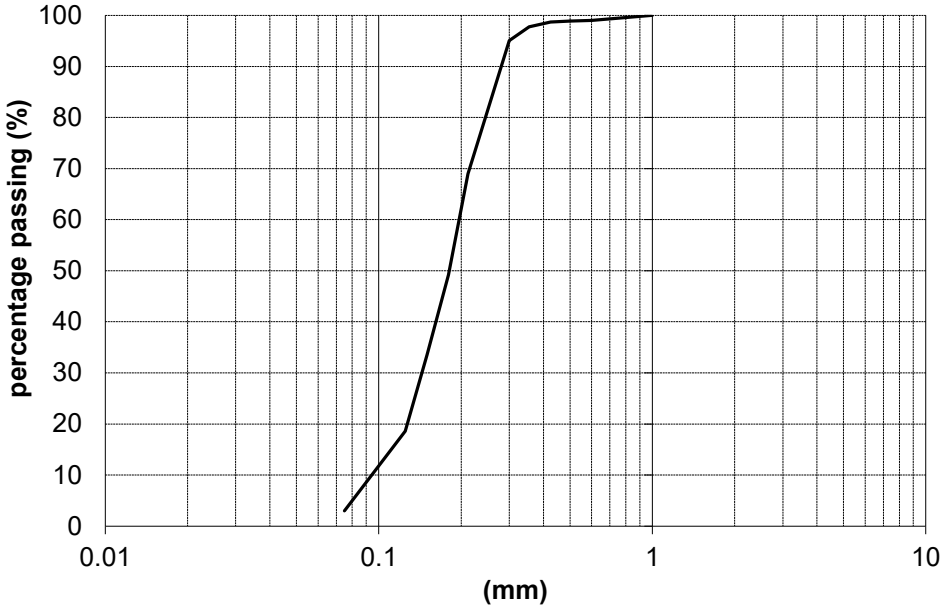

Figure 93 - Grain size distribution of the sand used for embedding and curing the samples.

The sand was a fluvial type, from a quarry on the Po River. This material was selected taking into account:

- the specific surface (the grain dimensions), able to ensure a good humidity of the two-component grout sample and embed the prisms perfectly;
- the ease and rapidity to obtain quickly a homogeneous material with a a certain moisture content (just 5 minutes of mixing in the bowl).

11.3.2.2 Summary of the technical standard and procedure

Tests were performed according to the procedure reported in paragraphs 7.3.4 and 7.3.4.3. The technical standard EN 196-1:05 allows the assessment of the UCS and the tensile strength (R_t) according to Equation 5 (which is reported again here for completeness) and Equation 15 respectively.

$$UCS = \frac{F_{p-press}}{1600}\ (MPa) \qquad 5$$

$$R_t = \frac{1.5 * F_{p-press} * l}{b^3}\ (MPa) \qquad 15$$

In Equation 15:

- R_t is the tensile strength, expressed in MPa;
- $F_{p\text{-}press}$ is the peak force recognised on the force–displacement graph, expressed in Newton;
- l is the distance between the two lower supports of the three-point flexural test frame (in our case l is equal to 100 mm).
- b is the length of the square shape prismatic sample, in our case equal to 40 mm.

Although EN 196-1:05 suggests performing the three-point flexural test applying a load control equal to 50 ± 10 N/s, the same modality as for the compression test was applied (in displacement control mode, with a displacement rate of 0.5 mm/min).

11.3.2.3 Samples manufacturing and curing modalities

The component A used for the sample manufacturing was produced according to the procedure reported in paragraph 7.2. The mix design used is reported in Table 21. Samples were produced according to the procedure reported in paragraph 7.3.3.

For each scheduled testing time, three samples for each curing modality were produced (nine samples for each scheduled testing time). After 24 hours from the casting, samples were demoulded and put in water or in sand. Previously, a sufficient quantity of sand had been conditioned with enough water to ensure a moisture content of 5% and 10% respectively for the two different condition modalities. Figure 94 depicts the burial of the samples in sand. Tanks with a volume of 25–30 L were used. After putting a centimetre layer of sand on the bottom of the tank (roughly calculated, just for ideally positioning the samples in the tank centre), the samples were placed vertically, ensuring good contact by gently pressing the samples into the sand. Before long, the samples were covered up to half of their height, after which the sand was gently pressed on their surfaces. Finally, the specimens were completely covered and, after the final manual compacting of the sand, the tanks were sealed.

Due to the large number of samples needed, different batching phases were scheduled and performed for the component A production. Usually, nine samples were successfully cast and collected for each batching phase. Concerning the punctuality of the assessments, a very strict margin of fluctuation (hours) was tolerated for tests performed on samples cured for less than 1 year, while for tests performed after 2 and 3 years of curing the tolerance was slightly greater (± 3 days).

Regarding the curing temperature, for the water the reference to paragraph 7.3.3 remains valid (23 ± 2 °C). However, considering that all the sand tanks were stored in the same environment, the same curing temperature value can be applied with marginal error also to the samples cured in sand.

Figure 94 - Samples cured in sand. Photos of the burial phase.

11.3.3 **Results**

After each testing time, the water contents of both sands were assessed in order to verify the successful sealing of the tanks. All the computed water contents were successfully verified as close to the original values (± 0.1%).

To provide the best visualisation of the work performed, each result was plotted in the relevant chart. Consequently, for each curing time, all the broken samples were represented as a cloud of points (indicated on the chart as x). Different charts were drawn up for each curing modality: the first for the UCS and the second for the R_t assessment. On these graphs, the continuous lines indicate the average trend of the calculated stresses.

Figure 95 and Figure 96 refer to the test campaign performed on samples cured in water.

Figure 97 and Figure 98 refer to the test campaign performed on samples cured in sand with a moisture content of 5% (w = 5%).

Figure 99 and Figure 100 refer to the test campaign performed on samples cured in sand with a moisture content of 10% (w = 10%).

Considering the high general level of data dispersion, a statistical analysis was performed in order to calculate the average of each strength value and the standard deviation. Figure 101 reports the comprehensive statistical analysis.

Finally, two charts (Figure 102 and Figure 103) depict the average functions of UCS and R_t related to the curing modalities studied.

It should be recalled that the curing time of 1 month refers to a standard curing time of 28 days. For longer curing times, 1 month is considered as 30 days.

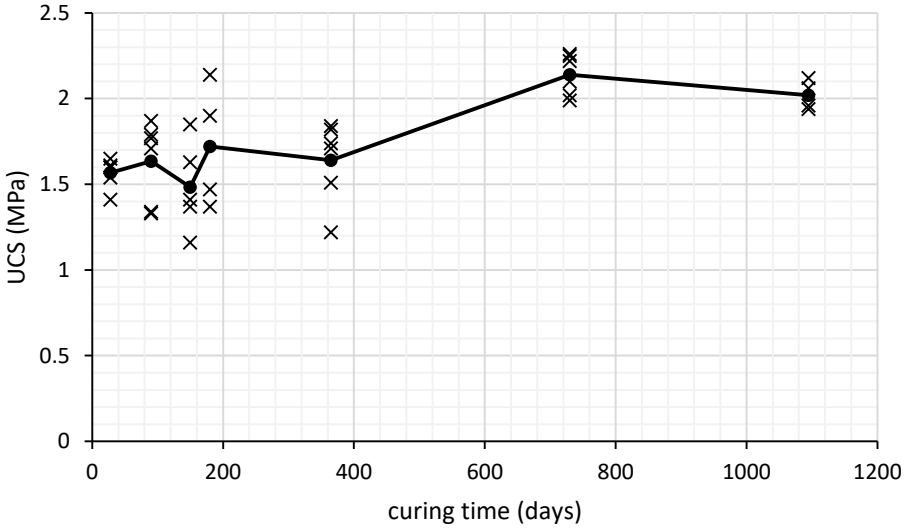

Figure 95 - UCS concerning samples cured in water.

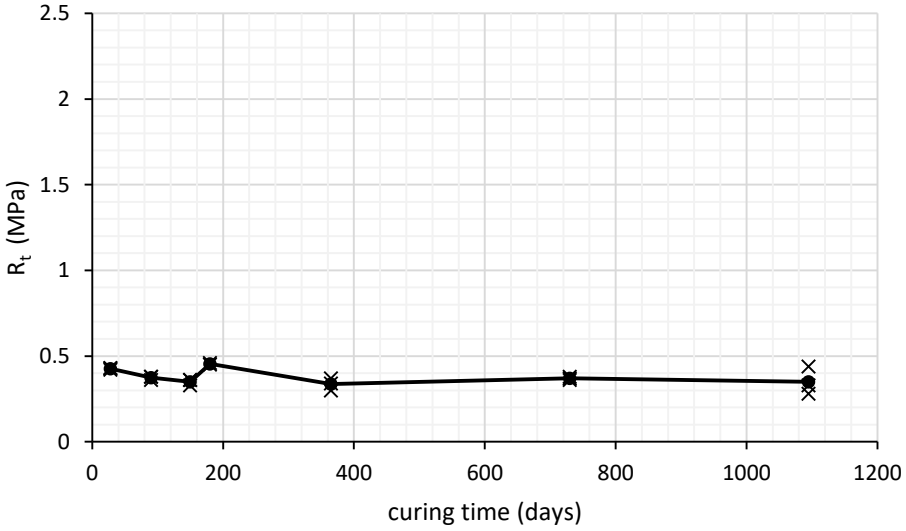

Figure 96 - R_t concerning samples cured in water.

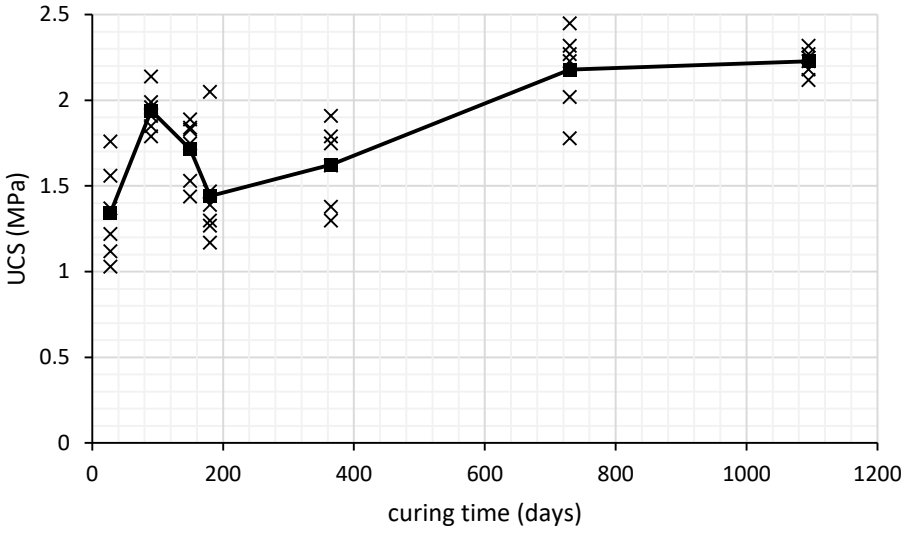

Figure 97 - UCS concerning samples cured in sand with a moisture content of 5%.

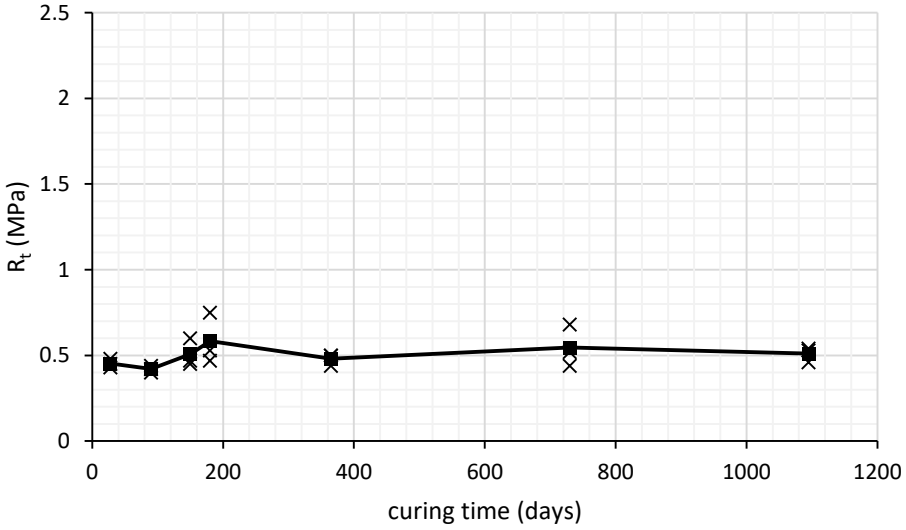

Figure 98 - R_t concerning samples cured in sand with a moisture content of 5%.

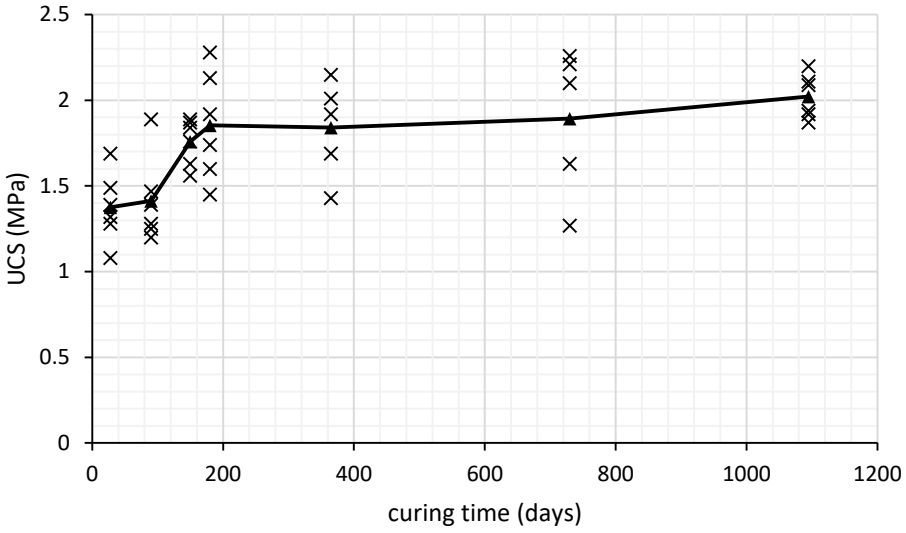

Figure 99 - UCS concerning samples cured in sand with a moisture content of 10%.

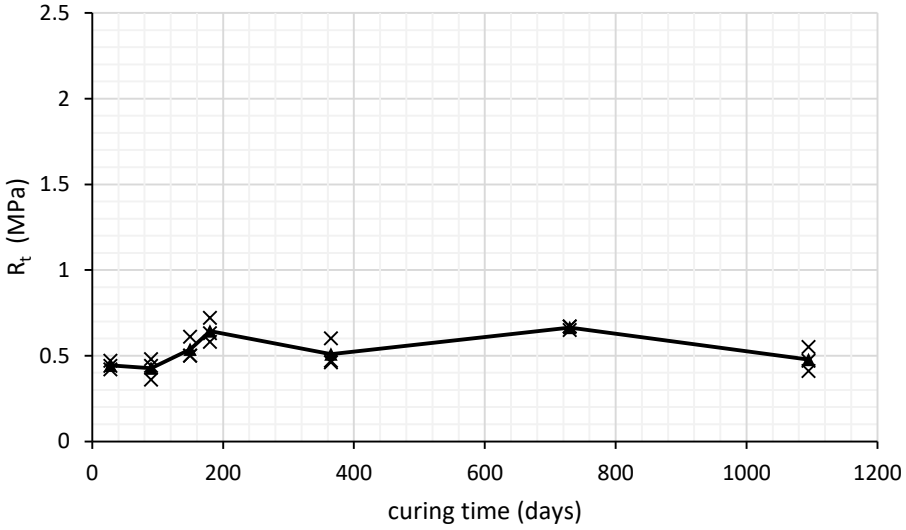

Figure 100 - R_t concerning samples cured in sand with a moisture content of 10%.

water	1 month		3 months		5 months		6 months		1 year		2 years		3 years	
	Rt	UCS	Rt	UCS	Rt	UCS	Rt	UCS	Rt	UCS	Rt	UCS	Rt	UCS
	0.43	1.65	0.38	1.34	0.36	1.85	0.45	2.14	0.37	1.22	0.37	1.99	0.28	2.12
		1.54		1.87		1.37		1.47		1.84		2.22		2.06
	0.43	1.61	0.36	1.33	0.36	1.41	0.46	1.37	0.3	1.71	0.38	2.02	0.33	1.96
		1.41		1.79		1.16		1.9		1.82		2.25		1.94
	0.42	1.6	0.38	1.77	0.33	1.63	/	/	0.34	1.74	0.36	2.1	0.44	/
		1.6		1.71		/		/		1.51		2.26		/
avarage	0.43	1.57	0.37	1.64	0.35	1.48	0.46	1.72	0.34	1.64	0.37	2.14	0.35	2.02
variance	2.22E-05	6.05E-03	8.89E-05	4.72E-02	2.00E-04	5.57E-02	2.50E-05	9.84E-02	8.22E-04	4.68E-02	6.67E-05	1.19E-02	4.47E-03	5.40E-03
standard deviation	0.005	0.08	0.01	0.22	0.01	0.24	0.005	0.31	0.03	0.22	0.01	0.11	0.07	0.07

w = 5%	1 month		3 months		5 months		6 months		1 year		2 years		3 years	
	Rt	UCS	Rt	UCS	Rt	UCS	Rt	UCS	Rt	UCS	Rt	UCS	Rt	UCS
	0.45	1.37	0.42	2.14	0.47	1.84	0.47	2.05	0.5	1.62	0.68	2.45	0.53	2.23
		1.22		1.79		1.83		1.47		1.91		2.23		2.12
	0.48	1.56	0.4	1.85	0.45	1.89	0.53	1.27	0.5	1.38	0.44	2.02	0.54	2.18
		1.03		1.91		1.53		1.17		1.75		1.78		2.27
	0.43	1.76	0.44	1.99	0.6	1.75	0.75	1.3	0.44	1.79	0.52	2.27	0.46	2.25
		1.12		1.96		1.44		1.39		1.3		2.32		2.32
avarage	0.45	1.34	0.42	1.94	0.51	1.71	0.58	1.44	0.48	1.63	0.55	2.18	0.51	2.23
variance	4.22E-04	6.41E-02	2.67E-04	1.24E-02	4.42E-03	2.84E-02	1.45E-02	8.28E-02	8.00E-04	4.83E-02	9.96E-03	4.81E-02	1.27E-03	4.11E-03
standard deviation	0.02	0.25	0.02	0.11	0.07	0.17	0.12	0.29	0.03	0.22	0.10	0.22	0.04	0.06

w=10%	1 month		3 months		5 months		6 months		1 year		2 years		3 years	
	Rt	UCS	Rt	UCS	Rt	UCS	Rt	UCS	Rt	UCS	Rt	UCS	Rt	UCS
	0.44	1.69	0.48	1.89	0.61	1.63	0.63	1.45	0.47	2.01	0.67	1.27	0.41	1.92
		1.08		1.39		1.76		2.13		1.19		2.21		2.11
	0.47	1.28	0.44	1.2	0.5	1.87	0.72	1.92	0.46	1.43	0.67	1.63	0.55	2.09
		1.49		1.25		1.89		1.74		2.15		2.1		1.94
	0.42	1.32	0.36	1.47	0.5	1.56	0.58	2.28	0.6	1.92	0.65	2.26	0.47	2.2
		1.39		1.28		1.84		1.6		1.69		/		1.87
avarage	0.44	1.38	0.43	1.41	0.54	1.76	0.64	1.85	0.51	1.84	0.66	1.89	0.48	2.02
variance	4.22E-04	3.53E-02	2.49E-03	5.35E-02	2.69E-03	1.54E-02	3.36E-03	8.38E-02	4.07E-03	5.37E-02	8.89E-05	1.47E-01	3.29E-03	1.40E-02
standard deviation	0.02	0.19	0.05	0.23	0.05	0.12	0.06	0.29	0.06	0.23	0.01	0.38	0.06	0.12

Figure 101 - Statistical analysis of the ageing test campaign. Stress values are expressed in MPa.

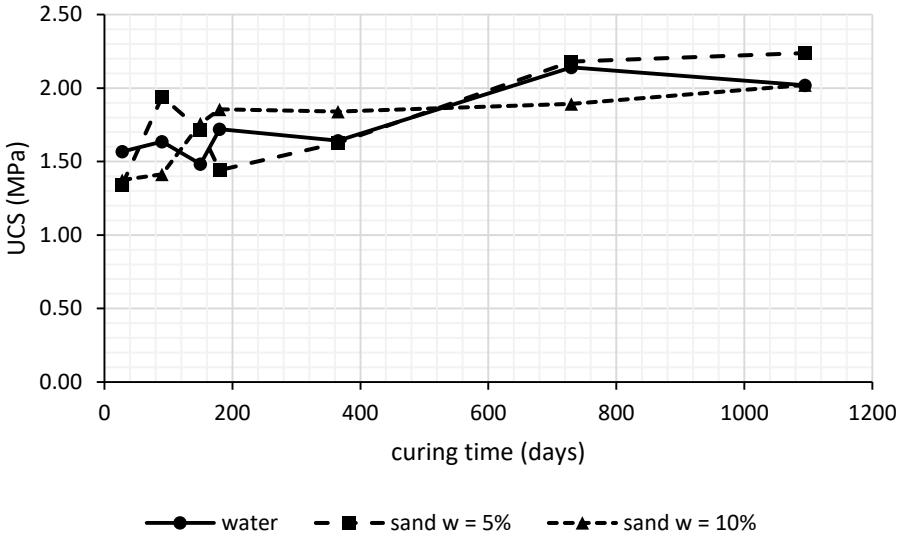

Figure 102 - UCS concerning the average of each curing modality.

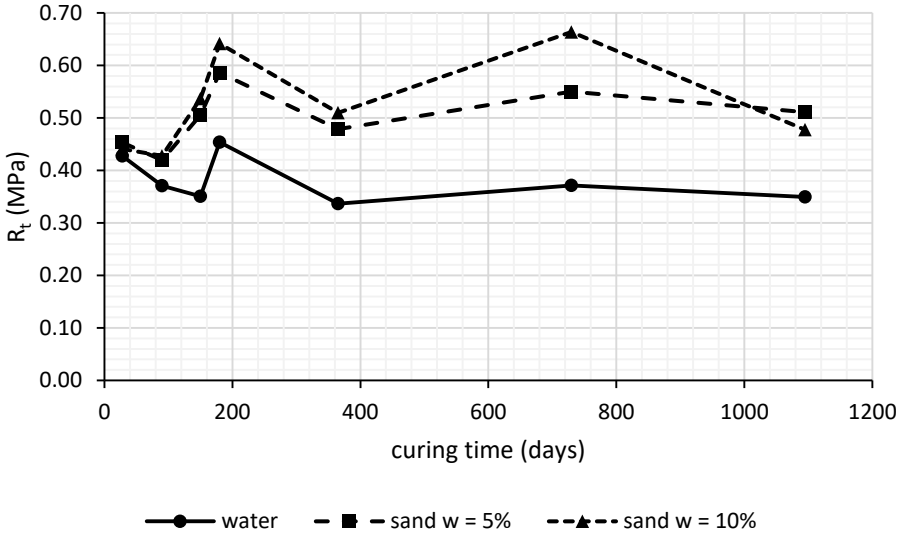

Figure 103 - R_t concerning the average of each curing modality.

11.3.4 **Discussion**

In this paragraph, the obtained outcomes are analysed. In the first part each curing modality is analysed separately, while at the end a comprehensive conclusion is presented, considering the overall information obtained from the ageing test campaign.

The standard deviation is also abbreviated with “s”.

11.3.4.1 Curing in water

Concerning the curing in water, the UCS trend is an overall increase; nevertheless two trend inversions of the average function are seen for curing times of 5 months and 1 year. The curing time of 6 months is characterised by the biggest data dispersion, with a standard deviation of 0.31. Generally, with the exception of the outcomes related to curing times of 1 month, 2 and 3 years ($s \leq 0.11$), all measurements related to other curing times are scattered, characterised by standard deviations higher than 0.2.

It can be underlined that a UCS higher than 2 MPa is reached at close to 2 years of curing.

As concerns R_t, the inversion trend of the average function is confirmed for the curing time of 5 months. The precision is comprehensively better in the UCS campaign: excluding 3 years ($s = 0.07$), the standard deviation is always equal or equal or lower than 0.03. The average function does not indicate a growing trend. More correctly, a range between 0.34 and 0.46 MPa can be identified as the domain of the average R_t function.

It can be speculated that the samples cured in water for 5 months suffered unforeseen stresses during the curing period that contributed to weakening them.

It is worth noticing that the UCS/R_t value has an increasing trend, starting from about 3.7 at 1 month to about 5.8 at 3 years.

11.3.4.2 Curing in sand with a moisture content of 5%

Concerning the curing in sand with a moisture content of 5%, the UCS trend is increasing overall, but a peak of the average function is nevertheless seen for the curing time of 3 months. However, this UCS value is characterised by a small standard deviation, equal to 0.11. Nevertheless, also the UCS average function value for the curing time of 5 months is above the forecast, but the standard deviation is in this case slightly bigger ($s = 0.17$).

Generally, excluding the determination for a curing time of 3 years, which is the most accurate ($s = 0.06$), all the determinations for this curing modality are characterised by a standard deviation ranging between 0.11 and 0.25. For the determination pertaining to 6 months of curing, the highest value of standard deviation, equal to 0.29, is again confirmed.

It can be underlined that the UCS higher than 2 MPa is again reached at close to 2 years of curing.

As concerns R_t, the average function is calculated starting from fairly scattered measures. The standard deviation of each curing time is bigger than for the samples cured in water, with the exception of samples cured for 1 and 3 years. The average function does not indicate a growing trend. More correctly, a range between 0.42 and 0.58 MPa can be identified as the domain of the average R_t function. It can be observed that the range of the strength is slightly higher than the range pertaining to samples cured in water.

It is worth noticing that the UCS/R_t value has an increasing trend, starting from about 3 at 1 month to about 4.4 at 3 years.

11.3.4.3 Curing in sand with a moisture content of 10%

Concerning the curing in sand with a moisture content of 10%, the UCS average function trend is increasing overall (it is the only one without singularities between the studied curing modalities). Excepting the determinations concerning 5 months and 3 years (s = 0.12), all the other curing times are characterised by high scattered values of UCS ($0.19 \leq s \leq 0.38$). In particular, the measurements relating to 2 years of curing time are strongly scattered, characterised by a standard deviation of 0.38 (20% of the corresponding UCS average).

It can be underlined that the UCS of 2 MPa is reached only after 3 years of curing.

As concerns R_t, the average function is calculated starting from fairly scattered measures. The standard deviation of each curing time is bigger than those for samples cured in water. The average function does not indicate an increasing trend. More correctly, a range between 0.43 and 0.66 MPa can be identified as the domain of the average R_t function.

It is worth noticing that the UCS/R_t value has an increasing trend, starting from about 3.1 at 1 month to about 4.2 at 3 years.

11.3.4.4 General discussion

The information gained can be summarised as follows:

- it was confirmed that the two-component grout is a material susceptible to the casting phase (Peila et al., 2015). In the light of the outcomes, it can be stated that, although the number of tested samples was tripled compared to Peila's research, six samples were not enough to find a reliable value of UCS for a certain curing time. The standard deviation values found often exceeded 0.1 MPa, underlining a low value of accuracy. Probably, the great care taken during the casting phase was not enough, or maybe simply a bigger number of sample is needed, due to the nature of the sample manufacturing (high turbulence between the two components and the high probability of embedded air bubbles);
- samples cured for 6 months were characterised by scattered measurements of UCS, independently of the curing modality. Something probably went wrong during the component A production or the casting phases of these nine samples;
- considering the 3 UCS average functions, it can be stated that the two-component grout continues to improve the UCS strength also after 28 days of curing, independently of the curing modality;

- samples cured with low water content (sand characterised by 5% of moisture content) seem not to suffer different curing conditions from other samples cured differently. Conversely, considering 2 and 3 years of curing time, samples cured in sand with w=5% showed the highest UCS values (this 5% probably respects the condition of "normal humidity" introduced by Pelizza et al., 2010).
- the tensile strength average functions show a trend that is hard to consider as growing, being basically horizontal. It can be speculated that the R_t value is independent of the curing time, but depends only on the mix design or the curing modality. Another possibility is that the flexural test is not suitable for assessing the tensile strength of the two-component grout.
- the UCS/R_t trend increases as a function of the curing time. The values are smaller than those for standard concrete (UCS/$R_t \simeq 10$).
- with reference to Peila et al. (2015), a numerical comparison has no sense because of the different mix designs used. However, the increasing trend with time is confirmed.

11.3.5 Additional information

The doubt about the validity and the suitability of the three-point flexural test for the two-component grout was a strong statement. It should be noticed, however, that all the prismatic samples broken on the three-point frame showed a brittle behaviour, as expected. Meanwhile, another type of test (Brazilian test) for the tensile strength assessment was taken into account. This topic is analysed in one of the next chapters.

11.4 Air impact

11.4.1 The idea

The idea was to assess how the dehydration process caused by the action of air affects the two-component grout.

In order to maximise the dehydration process without damaging the grout, it was planned to cure the two-component grout samples simply without protection, in the laboratory. Three different samples were cast, after which the weight assessments started immediately. The plan consisted in different weight determinations, in order to quantify the amount of water lost due to the evaporation/dehydration process.

Tests were performed until the samples became completely reduced to powder (an unexpected result). In the first phase, the weights were measured hourly, in a second phase daily, and finally weekly.

11.4.2 Material and test procedure

The component A used for the samples manufacturing was produced according to the procedure reported in paragraph 7.2. The mix design used is reported in Table 21. Samples were produced according to the procedure reported in paragraph 7.3.3.

Concerning the equipment used, a precision scale (p = 0.01 g) was used for the weight assessment. Samples were placed in three suitable plastic containers, raised a few millimetres from the bottom of the tanks by means of small wood cylinders. In this way, the air was able to act also on the lower surfaces of the samples.

During the curing period, the three containers with the samples were kept in a protected area (protected from direct sun rays and from air flows). The curing environment was chosen expressly without climate control, although the air's relative humidity (RH %) and temperature (°C) were measured for every sample weight assessment. This controversial choice was made in order to verify if variations of temperature and relative humidity might affect the dehydration process.

Once the scheduled time arrived, samples were weighed without moving them from the container. This precaution was taken due to the anticipated crumbling phenomenon. The relative humidity (RH %) and temperature (°C) of the air were recorded.

11.4.3 Results

Figure 104 summarises all the data recorded during the test campaign. The three samples started from an average weight of 298.33 g and finished with an average weight of about 100 g.

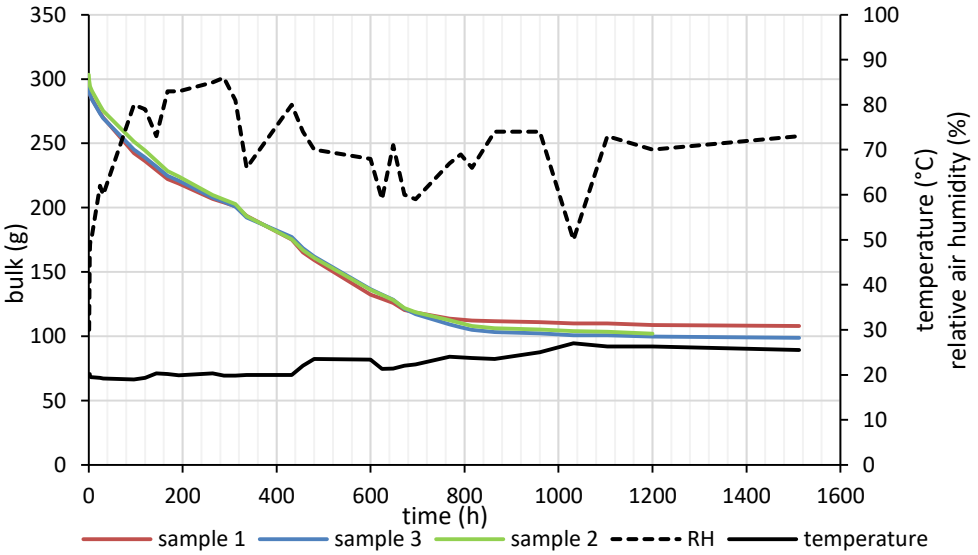

Figure 104 - Outcomes pertaining to the "air impact" test campaign.

Figure 105 depicts the percentage weight loss function, hereinafter also called the “bulk function”, which describes the decreasing of the weight of the two-component grout under the influence of the environmental air.

The bulk function values are expressed in percentage and were computed considering the average of the sample weights measured at a certain time of testing on the average of the initial weight of the samples. The last assessment was carried out after 63 days of curing.

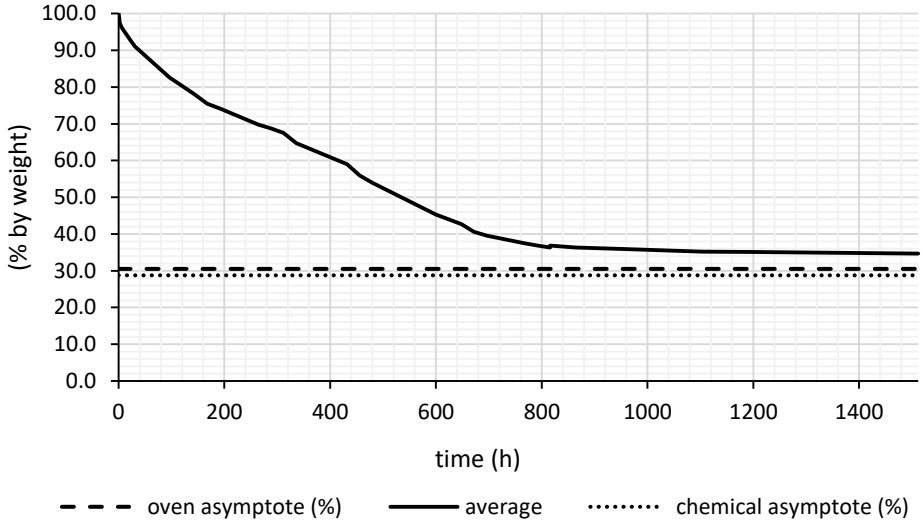

Figure 105 -Bulk function and asymptotes.

After different simulations, the experimental function was best fitted by using two different equations, a second-order polynomial for the first part ($0 \leq t \leq 800$ h) and a line for the second part $800 < t \leq 1512$ h. Two different asymptotes were drawn. The “oven asymptote” was calculated by drying the two-component material in an oven ($40 \leq T°C \leq 80$) and measuring the weight of the residual material. The “chemical asymptote” was computed as the ratio between the water and the weight of all the mix design ingredients (by weight).

Figure 106 - Samples after 28 days of curing.

Figure 107 - Samples after 63 days of curing.

11.4.4 Discussion

Taking into account Figure 104, the three samples show a very similar trend concerning the mass reduction as a function of the curing time. In the complete absence of a medium that could inhibit the dehydration process, the samples lose water from the first hours after the casting till about 1000 hours.

The environmental curing temperature ranges between 19 °C and 27 °C, with an average value equal to 22 °C. The RH ranges between 30% and 86%, with an average value of 67%. Generally, although strong fluctuations of the relative humidity and slow temperature variation were recorded during the test campaign, the mass decreasing functions seem to be independent of these environmental parameter variations. It should be highlighted, however, that the strongest RH variation, equal to 24%, occurred when the dehydration of samples was at an advanced stage.

Concerning the visual checking, after 28 days (Figure 106) the samples appeared fragmented and cracked, while after 63 days of curing, the test campaign stopped because, firstly, no further weight decrease had been recorded and secondly, the samples appeared completely powdered (Figure 107).

Figure 105 depicts the bulk function and asymptotes. The function tends to the oven asymptote for a curing time longer than 2800 hours; however, it is not correct to use this equation also to forecast curing times longer than those tested. Actually, the bulk function will never reach the oven asymptote, not even for $t \to \infty$. Considering that the oven asymptote was calculated after drying the two-component material in the oven with a temperature up to 80 °C, it can be speculated that also hygroscopic water, usually linked to the concrete matrix, left the material. In conclusion, the oven asymptote is not the real one of the bulk function. Thus, the real asymptotic value should be recognised as between 30.5% (the oven asymptote) and 35% (the bulk function values for the longer tested curing times).

Concerning the chemical asymptote, it was reported on the chart in order to note that the water is the main ingredient of the two-component grout (71.2% by weight). However, the asymptote drawn is partially wrong because it underrates the real water content of the material. In order to compute the real water content of the two-component grout, also the water present in component B should be taken into account. Unfortunately, the percentage of the silicate solution is an industrial secret.

Finally, it can be stated that:

- according to Pelizza et al. (2010) and Peila et al. (2011), it was proved that the two-component grout does not preserve its properties if the normal humidity condition of the ground is not guaranteed;
- the bulk function can be approximated with the following two equations, valid strictly only in the studied curing range:

$$\begin{aligned} bulk\ (\%) &= 7 * 10^{-5}\ t^2 - 0.1334\ t + 100 \quad \text{if} \quad 0 \leq t \leq 800\ \text{h} \\ &= -29 * 10^{-4}\ t + 38.816 \qquad\quad 800 < t \leq 1512\ \text{h} \end{aligned} \tag{16}$$

- Equation 16 has specific value for the studied grout (the studied mix design) and for the specific curing environment adopted. It permits us to calculate the residual weight of the material for a certain curing time;
- the trend drawn from Equation 16 could be successfully considered for all the two-component grouts based on the standard mix design (without innovative ingredients; see paragraph 5.2);
- in the case of a tunnel realised in a medium where the water content could be close to 0 (a dry medium), the phenomenon of the dehydration process should be taken into account during the backfilling project phase. Special additives are available on the market

that can strengthen the grout against dehydration although, in the author's experience, none of the encountered mix designs foresaw this peculiarity.

11.4.5 Additional information

The first program conceived for the above-described test campaign foresaw also performing uniaxial compression tests on the samples, at scheduled curing times, in order to assess also the changes in strength of the material. Unfortunately, it was very difficult to handle the samples, including after just a few days of curing, because of their weakness due to the dehydration process. Consequently the UCS assessment was abandoned.

Considering the bulk function, an attempt was made to approximate the experimental values by using only one fitting line, exactly one function of the second order. This possibility was discarded because the R^2 value obtained was less than the adopted solution.

A further consideration concerns the durability of grout cured in a controlled environment and subject only in a second phase to the action of air, such as in the case of tunnelling realised on the edge of a groundwater boundary and hence subject to fluctuations as a function of the seasons. A specific test campaign to pursue this issue has not been developed. However, the simple visual checking of broken samples belonging to other test campaigns (samples cured in water or in sand, then broken and collected) underlined how the dehydration process strongly affected the material, causing pulverisation of the samples in less than 28 days, even though the material had previously been cured in water for another 28 days.

Another approach allows the results to be read in terms of the water content. Considering the geotechnical definition of the water content w (%):

$$w\ (\%) = \frac{m_{water}\ (g)}{m_{dry}\ (g)} * 100 \qquad 17$$

it is possible to calculate $w(\%)_i$ at time i, where:

- $(m_{sample})_{i=0}$ is the initial sample's average weight;
- m_{dry} is the dry mass of the sample;
- $(m_{sample})_i$ is the average weight sample at time i.

Consequently:

$$w(\%)_i = \frac{(m_{water})_i}{m_{dry}} * 100 \qquad 18$$

$$w(\%)_i = \frac{\left[\left(m_{sample}\right)_{i=0} - m_{dry}\right] - \left[\left(m_{sample}\right)_{i=0} - \left(m_{sample}\right)_i\right]}{m_{dry}} * 100 \quad 19$$

$$w(\%)_i = \frac{\left(m_{sample}\right)_i - m_{dry}}{m_{dry}} * 100 \quad 20$$

The only problem is to define m_{dry}. In this case, the same approach that is valid for the asymptotes is valid, i.e. it could be an "oven" value, a "chemical" value, or the "real" value. In this framework, the oven value was taken as the reference value; hence, the initial water content can be computed and, consequently, all the w(%) values are summarised in Figure 108.

$w(\%)_{i=0\ -\ oven} = 228\%$

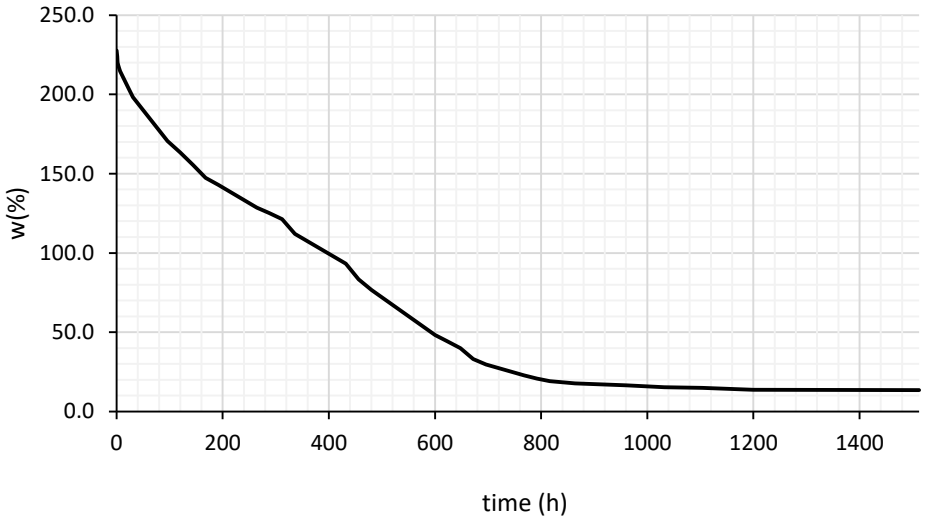

Figure 108 - Water content of the two-component grout as a function of the curing time.

11.5 Water flow effect

The impact of water on the two-component grout is a controversial issue.

In the scientific literature, almost all authors underlined that the two-component grout exhibits anti-wash-out properties (Guglielmetti et al., 2007; Reschke & Noppenberger, 2011; Pelizza et al., 2010, 2012; Peila et al., 2011; Dal Negro et al., 2014b, 2017; Càmara, 2018) but tests have never been designed or performed for this topic. The only research available in the literature was performed by Youn & Breitenbücher (2014), who studied the dewatering by using an expressly modified filter press; however, the tests were performed on a different kind of mono-component grout.

11.5.1 The idea

The aim of this section of the research was to estimate if and with what effect water can interact with the two-component grout.

In particular, considering the backfilling system of a shielded machine, the injection is performed independently of the presence of water in the excavated medium. Considering that the injection pressure is always higher than the front face pressure, and considering that the front face pressure is computed taking into account also the groundwater pressure, it can be stated that the backfilling grout, during the injection, pushes the water to fill the void. Plainly, if the water does not move, its presence is a favourable condition for the durability. But what happens if the water moves?

The idea was to design a specific apparatus to be able to apply a fixed water action, in terms of water velocity, on samples of two-component grout. Only short curing times were investigated. After a certain time of flow, the samples were tested in order to check if the action of the water had washed out part of them.

11.5.2 Material and test procedure

A specific apparatus and two-component grout samples were realised for the purpose. The basic idea was to apply a flow of water channelled inside holes expressly created in the specimens of two-component grout. The water, characterised by a constant speed, flowed through the hole for a scheduled time. After the flow phase, the diameters were tested in order to verify if the water had washed out part of the grout, enlarging the original diameter. The diameter assessment was performed indirectly.

To better understand the test structure, two different test phases can be distinguished:

- the flow phase;
- the sample testing phase.

11.5.2.1 Apparatus

A plexiglass container was used as sample holder.

The container was designed to contain a number of specimens between 1 and 8. For each sample slot, the container was drilled with a hole of 10 mm (8 holes were realised in a quincunx pattern). Each sample, with height (h), was located centrally in the designed positions (centrally on its hole) surmounted by a water table (Δh). Samples were centrally pre-drilled (ϕ) and linked with a watertight paste at the container bottom before starting the test. A pump feeds the water flow on the container and a drain guarantees a fixed water table action on the samples surface. The inlet water flow that feeds the system does not act directly on the samples: a plexiglass slab (slightly smaller than the container, 10 mm in length

and depth), raised on 4 screws, protects samples from the potential generated turbulence, acting as a water diffuser. Under the sample holder, a water storage tank holds the flowed water that has crossed the samples, running in their inner holes.

Figure 109 depicts a photo of the developed device (left) and a schematic drawing of the system (right). In Figure 110, a photo taken from a frontal point of view gives a better depiction of the details of the designed apparatus.

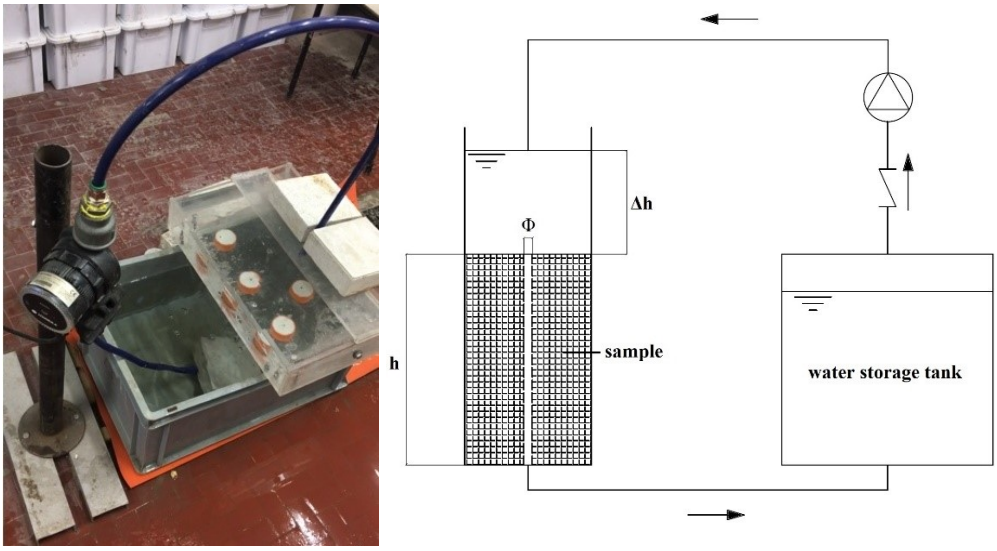

Figure 109 - Photo of the developed device (left) and schematic drawing of the plant (right).

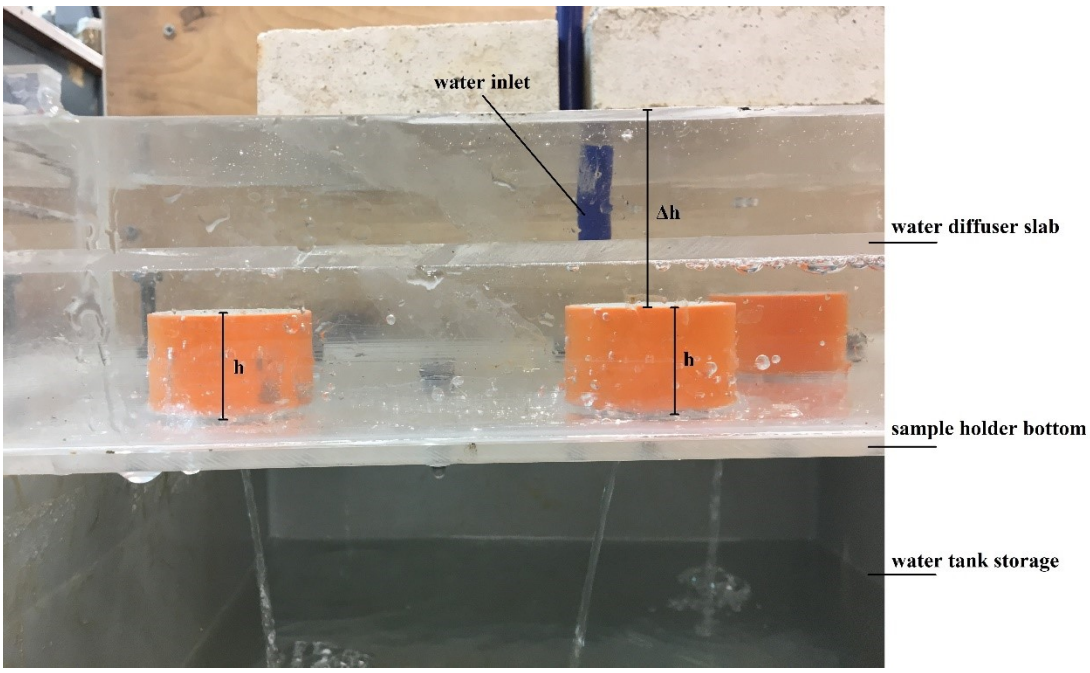

Figure 110 - Photo of details of the designed apparatus.

11.5.2.2 Samples manufacturing

The component A for the two-component grout was produced according to the procedure described in paragraph 7.2. The mix design used is reported in Table 21.

Concerning the casting and the curing modality, the procedure described in paragraph 7.3.3 was followed with the exception of the sample shape.

The sample production was the most sensitive phase of the procedure. Since the test was designed to assess the two-component grout's wash-out resistance at short curing times, there was plainly a need to handle samples that were not yet completely hardened.

The moulds were fashioned from a commercial plastic tube. Each sample was characterised by an inner hole, located in the centre. The geometrical dimensions of the sample are reported in Table 35.

Table 35 - Geometrical dimensions of produced samples.

Diameter (mm)	43.7
Height (mm)	30.2
Inner hole diameter ϕ (mm)	2.7
Inner hole (mm^2)	5.72

Due to the weakness of the material that was being tested, it was impossible to drill the samples after casting. Therefore, it was planned to cast the sample foreseeing a cylindrical solid in the centre. Common iron spikes were used for this purpose, with the only requirement being a suitable diameter, a perfectly smooth lateral surface and a length higher than the sample. A polystyrene support was

shaped in order to hold the sample moulds on the one hand, and to fix the iron spikes steadily on the other (Figure 111).

Figure 111 - Polystyrene support used for the samples production.

The verticality of the spikes was accurately measured using a spirit level. The spikes' heads were carefully covered with a plastic layer to prevent grout leakage (before gelation, the two-component grout is still fluid and leakages can potentially lead to an incomplete mould filling). Before long, a thin layer of oil was painted on the spikes, in order to simplify their removal just before starting the test. After the preparation of the polystyrene support as described, the moulds were glued centrally with respect to the spikes. After the glue had set (not more than 15 minutes), samples were cast and after just one minute the spikes were pulled out slightly for a distance that allowed perfect levelling of the cast surface using a spatula. About 15 minutes after casting, the spikes were gently completely removed. The samples, still held in their moulds (making it possible to handle them without damage), were gently removed and located in the plexiglass sample holder slots, taking care to ensure the correspondence among the samples holes and the bigger ones of the slots (each sample hole must be concentrically aligned with the hole of the container slot). Before long, the moulds were glued on the bottom of the container (a quick-setting silicone was used for this purpose) and the samples were covered with a plastic layer on their free surface (the casting surface of the samples), in order to prevent dehydration.

11.5.2.3 Flow phase: testing procedure and parameters

After the scheduled curing time, the samples were uncovered (only the plastic layer of the casting surface was removed) and the pump was switched on. The samples were tested without demoulding.

All tests were performed according to the following testing parameters:

- $\Delta h = 48.4$ mm
- $v_b \simeq 1.2\ m/s$

where Δh is the height of the water table applied on the samples' top surface and v_b is the water velocity on the bottom of the samples.

The decision to calibrate the apparatus according to this value of water speed was as a compromise between the maximisation of the potential wash-out phenomenon and the choice of velocity values comparable to a real hydraulic conductivity. It was decided to simulate the test in a gravel context, simulating a very high value of hydraulic conductivity.

A daily visual check was performed during the whole flow phase. Every 7 days, a water volume check was performed (simply watching the water level inside the water tank storage). If needed, the water was topped up to replace any water loss.

11.5.2.4 Sample testing phase: testing procedure

The sample testing phase occurred only after the flow phase. The samples (still held in moulds) were removed from the sample holder and put in another tank, under water, in order to prevent dehydration.

Assessment of the hole variations was performed indirectly, as the hole dimensions were too small to estimate using a calliper. Furthermore, it was not guaranteed that the hole diameter variation was constant along the sample height. Consequently, the Marsh cone was considered a suitable device for the purpose, being well established and known to engineers involved in tunnelling backfilling.

The sample testing phase procedure is described in the following. Apart from the Marsh cone and its specific container, a gasket and a support able to bear the sample were required, leaving the sample hole free and centred on the tank positioned below. Concerning the gasket, its dimensions must be able to perfectly seal the tail of the cone with the sample surface, avoiding leakage. It is strictly discouraged to use rigid gasket models. Soft ones can warp and change shape as a function of the sample surface (which, despite all precautions, will never be perfectly smooth).

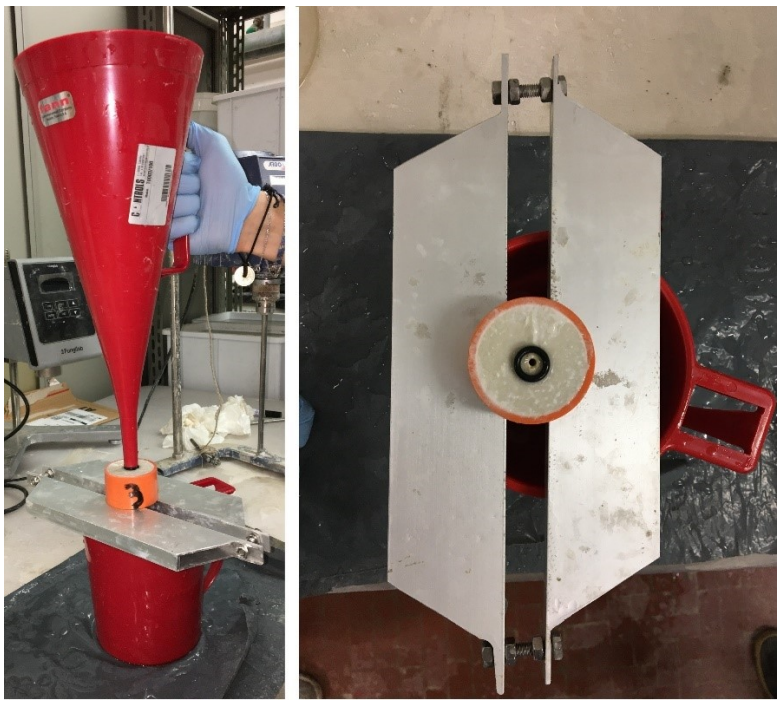

Figure 112 - Photo of the arrangement for the sample testing phase.

Previously, the sample had been positioned on the support and the gasket had been positioned concentrically with the sample hole. Initially, the cone was manually pressured on the gasket. Particular care had to be taken in checking that the system composed of the sample, the gasket, and the cone nozzle was perfectly aligned (Figure 112). After that, the lower hole of the sample was closed with one finger by the same operator who was managing the cone, while a second operator had to fill the cone with water up to the cone notch. Before long, the time count started when the cover from the hole was removed. According to the Marsh cone procedure, the time count was stopped when a level of 1 litre was reached in the container.

At least three different assessments had to be performed on each sample. Finally, the average time was compared with the values pertaining to a special sample, realised with a hole that was expressly uniform in diameter and perfectly smooth.

11.5.3 **Results**

In the following, the outcomes are presented. Unfortunately, due to Covid-19, only preliminary results can be presented. Table 36 reports data related to the tests performed on samples cured for 3–3.5 hours and then treated with a flow phase of 28 days.

It was decided to start from the least demanding situation (considering a short curing time), namely after a curing time of 3–3.5 hours. The original plan foresaw tests treated with a flow phase of 28 days but previously cured for 3 hours, 1 hour and 0.5 hour or less, compatibly with the duration of the testing preparation procedure.

Table 36 - Outcomes pertaining to the preliminary test campaign.

Curing time (h)	3 - 3.5
Flow phase (days)	28
Marsh cone reference time (s)	85.3
Marsh cone average time (s)	78.7
Δ (s)	6.7
Δ (%)	8

11.5.4 **Discussion**

The outcomes highlighted a slight reduction of the flow time, equal to 8%. This reduction is directly correlated with the increase of the hole diameter. It should be underlined that the new hole, bored for the water flow, was purportedly not constant along all the sample depth. Unfortunately, in the absence of other comparison data it is not possible to comment decisively on the obtained value of 8%. However, it can be stated that the studied curing time is considered a "short curing time" and furthermore that $v_b \simeq 1.2\ m/s$ is a very high velocity value, which rarely occurs in tunnelling work beneath the ground water.

However, according to the theory that was speculated, the erosion phenomenon due to the water flow is concentrated in the first hours of the flow phase. According to the fast growth of the two-component grout strength (UCS, SCS, shear strength), it can be reasonably speculated that also the grout's washing-out resistance increases with the curing time, and consequently that the water wear action decreases with time. The outer layer of the material is worn out in the first instance by the water flow, while with extension of the time, the action of the water flow has less impact. However, in order to prove this theory, further tests are required, varying parametrically the flow phase and the curing time of the material before the action of the water flow.

11.5.5 **Additional information**

Before adopting the Marsh cone as a device for indirectly assessing the wash-out action of the water, attempts were made to estimate the diameter variation using a calliper. The results were not reliable because the hole outer diameter measured on the samples surfaces was frequently very large (due to the geometrical concentration of the flow action) and not consistent with the real inner measurement.

Also the apparatus used and described is the third version of different failed attempts.

In conclusion, a lot of time was spent in order to optimise the apparatus, the flow phase and the testing phase, but unfortunately very poor results were obtained.

11.6 Final consideration on the durability

The whole durability test campaign on the two-component grout was very important, considering the lack of information regarding this topic and considering the spreading of this technology all around the world.

Generally speaking, it can be stated that the two-component grout exhibits a very good resistance and preservation of strength in terms of UCS if minimum values of the moisture content of the curing environment are guaranteed. A minimum moisture content of 5% guarantees a continuous increase of the compression strength with time, and consequently the good durability of the material is ensured.

Very good results in terms of durability were confirmed also when the curing was done under water. Considering the preliminary result pertaining to the resistance to the water washing-out action that is potentially present in the case of groundwater filtration flows, no particular criticalities need to be signalled.

Particular attention should be taken concerning tunnelling projects realised in dry geographical areas. In this case, a laboratory durability test campaign is strongly advised. Furthermore, specific mix designs should be developed and tested, possibly foreseeing the addition of specific ingredients to component A, to improve the resistance of the material also in curing conditions drier than with 5% of moisture content.

Concerning the deepening of the elastic modulus investigation after 5 months of curing taking the approach under the concrete rule, no useful information was added to the existing knowledge. A specific test campaign should be performed expressly to investigate this aspect.

In conclusion, the two-component grout technology is more vulnerable to the effect of air than of water.

11.7 Key concept

KEY CONCEPT 11: The curing of two-component grout implies the improvement of mechanical performance as long as a minimal water content is ensured in the embedding medium. The dehydration phenomenon must be absolutely avoided, as it can reduce the two-component grout to powder in just 2 months. The water flow that could slide on the outer surface of the material, according to preliminary outcomes, should not have a major impact.

Chapter 12

Durability: chapter 2

In the previous chapter, first investigations on the durability of two-component grout were described, and the outcomes were shown and discussed. However, all the work was performed in the laboratory. The new question is: what happens at the construction site? How does the two-component grout behave on the real scale?

This chapter is still focused on the durability, but the investigations are focused on the comparison between the construction site and laboratory environments. The realisation of this investigation was possible only thanks to Prof. Peila and his wide circle of friends involved in the tunnelling construction sites.

For NDA, in this context the name of the construction site, the raw materials supplier companies and all details strictly linked to the work have been completely anonymised.

12.1 The issue

Unfortunately, it was not possible to obtain samples of the two-component grout from the construction site where the mix design studied in this thesis was used (Table 21). However, another construction site gave us the opportunity to study samples obtained from a real curing condition.

The change of mix design implied the need to repeat also the basic characterisation (unit weight, bleeding, flowability, gel time and UCS), in order to "familiarise" ourselves with the new material and understand the new range values of the studied parameters.

However, there was no possibility of choice: a new construction site was selected, the preliminary test campaign aimed at the basic characterisation was performed in the laboratory, whereupon a comparison between the two-component grout extracted after a partial tunnel demolition (hence cured in real site conditions) and the one produced in the laboratory was performed.

12.2 The idea

The basic idea was to compare samples taken directly from the construction site and samples produced in the laboratory with the same mix design and cured for the same duration by using the UCS test and the Brazilian test.

The material from the construction site, characterised by 7 months of curing, was picked after a partial tunnelling demolition (linings were removed in order to widen a safety road). Thereby, the two-component grout was removed and sent to the laboratory. For obvious practical reasons, it was impossible to core prismatic samples from the bulk coming from the job-site, so samples with a cylindrical shape were core-drilled. In order to estimate also the tensile strength, the Brazilian test was studied and successfully applied.

12.3 Preliminary laboratory test campaign

A preliminary laboratory test campaign, following the model introduced in paragraph 7.4, was carried out in order to understand the range of validity for each of the assessed parameters.

It was considered fundamental to know the new mix design better before starting the comparison of the curing conditions. The procedures introduced in paragraphs 7.2, 7.3 and 7.4 were followed.

12.3.1 Mix design

The mix design used in this new research is reported in Table 37. Hereinafter, this new mix design is called “MIX S”.

Table 37 - Mix design S.

Mix design	Dosage
Cement (kg)	315
Bentonite (kg)	35
Water (kg)	819
Retarding/fluidifying agent (kg)	4
Accelerator (kg)	89.05

The water-cement ratio (weight by weight) and the percentage of the accelerator per cubic metre (volume by volume, computed considering the unit weights) are reported in Table 38.

Table 38 - W/c ratio and accelerator percentage per 1 m^3 (by volume).

W/c	2.6
Accelerator (%)	6.5

In the following, results concerning the unit weight (Table 39), flowability (Table 40), bleeding (Table 41), gel time (Table 42) and UCS (Table 43) are presented.

Table 39 - Unit weight of the mix design S.

Mix design	Unit weight (kg/L)
S	1.25

Table 40 - Flowability assessed on the fresh mortar and on mortar tested after 24, 48 and 72 hours from the batching of the mix design S.

	Flow time (s)			
Mix design	Fresh mortar	24 h	48 h	72 h
S	33.0	32.0	32.0	33.4

For the bleeding assessment, the test performed after 1 h was added with respect to the standard reference procedure.

Table 41 - Bleeding values assessed after 1, 3 and 24 hours from the batching pertaining to the mix design S.

	Bleeding (%)		
Mix design	1 h	3 h	24 h
S	0.20	1.02	1.00

Table 42 reports the datum related to the component B percentages foreseen by the mix designs (Table 37). Figure 113 reports the gelling function.

Table 42 - Gel time pertaining to the mix design S.

Mix design	Gel time (s)
S	7

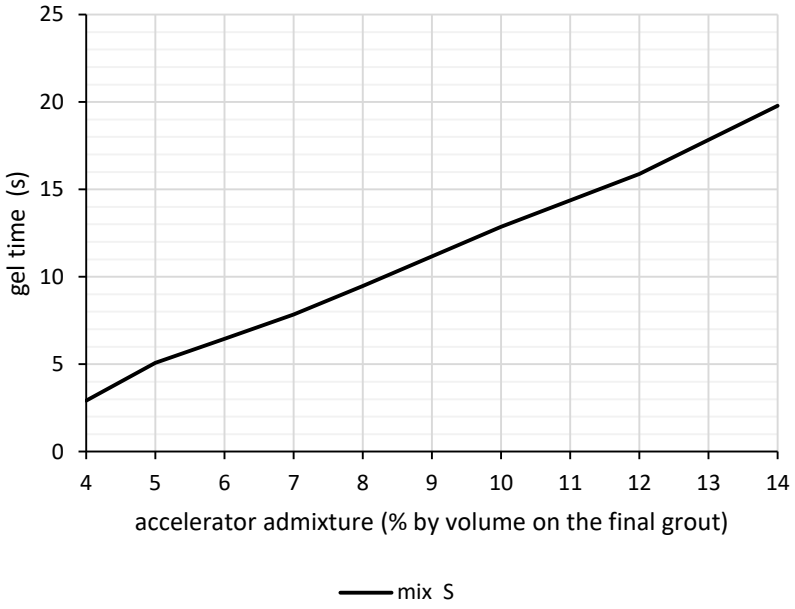

Figure 113 - Gelling function of the mix design S.

12.3.2 **Uniaxial compression strength**

It was not possible to perform the UCS tests after 3 hours of curing. However, the UCS tests performed at 7 days of curing were added to the standard procedure.

In Table 43 and in Figure 114 the outcomes are reported.

Table 43 - Average values of the uniaxial compression strengths assessed after 24 hours, 7 and 28 days of curing time for the mix design S.

	UCS (MPa)		
Mix design	24 hours	7 days	28 days
S	1.21	1.89	2.02

Concerning the measurement precision, a standard deviation of 0.04–0.05 MPa was computed for tests performed at 24 hours and 7 days of curing. Pertaining to tests carried out at 28 days of curing, the outcomes were more scattered with a standard deviation of about 0.2 MPa.

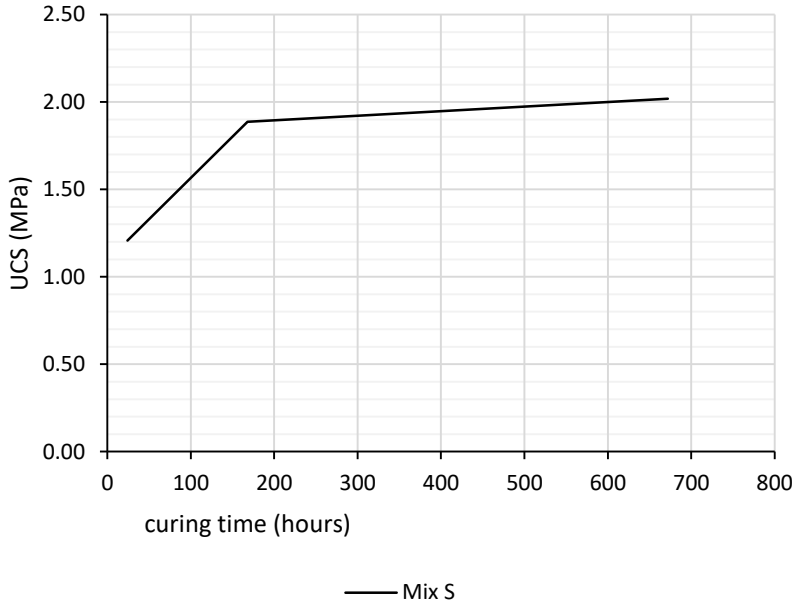

Figure 114 - UCS of the mix design S.

12.3.3 **Comments**

Mix design S is characterised by a w/c equal to 2.6, a value 1 point lower than the previous studied mix design (Table 21) but exactly aligned on the mean of the studied case histories (Table 3). The w/c ratio is strictly correlated with the unit weight, which also exhibits a higher value than that of the previously studied mix.

However, despite the strong cement content, the component A exhibits an amazing stability, with a bleeding value after 24 hours assessed as equal to 1%. Also concerning the flowability, the outcomes highlighted a substantial stability, with all values close to 32–33 seconds. The gel time of 7 seconds was aligned with the common values.

The mix S two-component grout exhibits a higher UCS value than the previously studied mix. This growth in strength is due to the higher silicate percentage (0.5% by volume higher) and the higher cement content.

Finally, it can be stated that the mix design S was perfectly designed and set up: high strength parameters are perfectly balanced with a component A stability, the perfect situation for a construction site.

12.4 Material and test procedure

12.4.1 **Apparatus**

All tests were performed using the Wykeham Farrance compression testing machine, equipped with a load cell of 5 kN. Tests were carried out using the press depicted in Figure 43 for the assessment of the UCS. For the Brazilian test, two steel flat platens were used. A cutting die with a diameter of 52 mm and a height

of 130 mm was used for shaping the material. A manual press was used during the sample trimming phase.

12.4.2 **Summary of the technical standard**

UCS tests were performed according to ASTM D2166/D2166M-16.

Although this standard was previously introduced in paragraph 7.3.4.1 as a standard for the short curing time assessment, on this occasion it was applied also at the long curing time. This is due to the impossibility of applying EN 196-1:05, because it is impossible to trim prismatic samples with such large dimensions (160*40*40 mm).

Nevertheless, the requirements of a minimal diameter of 30 mm and a height-to-diameter ratio ranging between 2 and 2.5 were respected, as well as the ratio of the applied strain suitable for accomplishing tests in 15 minutes (rate of strain equal to 0.5 mm/min). The axial strain was not taken into account, while the UCS (MPa) was computed according to Equation 21.

$$UCS = \frac{F_{p-press}}{A}\ (MPa) \qquad 21$$

where:

- $F_{p\text{-}press}$ (N) is the peak force identified on the strength–displacement chart;
- A (mm) is the sample section.

Concerning the tensile strength, ASTM C496/C496M-17 (splitting tensile strength of cylindrical concrete specimens) was not used for the required dimensions of the samples, as these were unachievable in our conditions (minimum diameter of 100 mm). However, ASTM D3967-16 was followed. This technical standard is used to assess the splitting tensile strength of intact rock core specimens. Recently, Akin and Likos (2017) assessed that this technical standard can also be successfully applied on compacted clay. The specimens have to be cylindrical, with a thickness-to-diameter ratio (t/ϕ) between 0.2 and 0.75. At least 10 samples should be tested and each test should have a duration ranging between 1 and 10 minutes. The standard regulation, once the peak force has been recorded (the load that generates a central crack able to split the sample in two parts), specifies computing the splitting tensile strength according to Equation 22, which is valid for the Brazilian test carried out with flat platens:

$$\sigma_t = \frac{2\,P}{t\,\Phi\pi}\ (MPa) \qquad 22$$

where:

- P is the peak force (N)
- t is the sample thickness (mm)

- ϕ is the sample diameter (mm).

12.4.3 Samples manufacturing

12.4.3.1 Samples obtained from the construction site material

The two-component grout delivered from the construction site consisted of three main shapeless bulks, with centimetre dimensions (Figure 115).

Figure 115 - Two-component sample from the construction site.

Unfortunately, the material was not tightly sealed before shipment, so after a preliminary visual check the material looked damaged, mainly on the external surface. Consequently, it was decided to extract the cylindrical samples only from the core of the bulks, removing all the dried part. By following this criterion, the dimension of each block was reduced to a minimum volume able to guarantee a sample suitable for testing. Different quantities were cut away. Figure 116 depicts the main phases of the trimming operation.

Figure 116 - Main phases of the trimming operation.

As a result, three samples for the UCS test (ϕ = 38.11 mm; h = 76.22 mm) and three samples for the Brazilian test (ϕ = 38.11 mm; 21 mm ≤ h ≤ 25 mm) were obtained. Despite best efforts, it was not possible to obtain a better result in terms of the number of samples. The requirement of ASTM D3967-16 concerning a minimal value of 10 tested samples was thus not respected.

12.4.3.2 Samples produced in laboratory

Taking into account that the samples obtained from the construction site grout had been trimmed, in order to reproduce possible disturbances caused by the realisation, it was planned to follow the same procedure also for the laboratory samples, i.e. to produce bigger samples that then needed to be trimmed.

Thereby, cylindrical samples (ϕ = 52 mm; h = 130 mm) were cast following the procedure described in paragraphs 7.2 and 7.3.3, with the exception of the shape. Considering that the construction site curing conditions were unknown, it was scheduled to cure the cast samples according to the three different modalities described in paragraph 11.3.2.3. The idea was to indirectly understand, by comparison of the strength performances, the construction site curing conditions.

In the end, unfortunately, a problem arose and the original plan was changed: once the curing period had elapsed and the samples demoulding operation had been performed, it was impossible to successfully trim the specimens. They exhibited such high resistance that the cutting die was irreparably destroyed. Consequently, the UCS and Brazilian tests were rescheduled, foreseeing samples with the original dimensions (ϕ = 52 mm; h = 130 mm), without trimming.

12.4.4 **Testing parameters**

According to the standard analysed above, the testing phase consisted in performing firstly the UCS and secondly the Brazilian tests. To better understand the testing plan, Table 44 summarises the general information.

Table 44 - General testing information.

		Laboratory samples	Construction site samples
UCS	ϕ (mm)	52.00	38.11
	h (mm)	130.00	76.22
	v (mm/min)	0.5	0.5
Brazilian test	ϕ (mm)	52.00	38.11
	t (mm)	21.37	22.56
	v (mm/min)	0.5	0.5
Curing	Time (months)	7	7
	Modality	Water, sand w=5%; sand w=10%	Construction site condition (unknown)

Concerning the sample depths (t) reported in the table above, the value is the average of all the tested samples.

Before the samples were broken, particular care was taken with the geometrical measurements and the unit weight assessments.

12.5 Results

Table 45 summarises the outcomes of the tests on samples trimmed from the material cured at the construction site, while Table 46 summarises the outcomes for samples produced and cured in the laboratory.

Table 45 - Outcomes concerning samples trimmed from the material cured at the construction site.

	UCS (MPa)	σ_t (MPa)	UCS/σ_t
Construction site curing condition	0.65±0.13	0.06±0.01	10.80
Density (kg/L)	1.18		

Table 46 - Outcomes concerning samples produced and cured in the laboratory

	UCS (MPa)	σ_t (MPa)	UCS/σ_t
Curing in water	2.46	/	/
Curing in sand w=5%	2.85	0.31	9.20
Curing in sand w=10%	2.45	/	/
Density (kg/L)	1.23		

For the outcomes presented in the form A±B, A is the average value and B is the standard deviation. For the strengths reported in Table 46, the statistical analysis is not available.

Unfortunately, tensile stress assessments for samples produced and cured in the laboratory in water and under sand with w=10% were not performed. The number of samples, scheduled exactly in order to perform the required tests (the starting raw ingredient amounts were limited), was greatly reduced after the failed trimming attempts (after which the samples were irredeemably damaged). Before destroying all the samples uselessly, it was decided to stop shaping the samples, and the “survivors” were tested as they were.

12.6 Discussion

A first analysis that can be carried out takes into account the UCS results.

The first aspect to point out is that no UCS values computed on laboratory samples can be absolutely comparable with the UCS values of samples cured at the construction site. However, in order to set up a comparison, samples cured in sand with a moisture content of 5% were chosen as representative (this being the only curing modality where the σ_t value was assessed). Consequently, two-

component grout produced and cured in the laboratory exhibited UCS and σ_t values about 4.5–5 times higher than those of the grout injected by the machine and cured in the real construction conditions.

This marked difference could be explained taking into account four different aspects:

1 the sample dehydration process;
2 the sample fracturing;
3 the trimming factor;
4 the mixing/casting process (scale factor).

Concerning point 1, a time lapse of 15 days (at least) passed between the construction site sampling and the laboratory shaping, without any covering or protection for the material. In this period, a dehydration process occurred, as underlined by the density difference of 0.05 kg/L (calculated between the average density of both sets of samples). Considering Equation 16, an order of magnitude of the residual bulk can be estimated as equal to 60%. Of course, the limitation of this assumption should be underlined and taken into account, i.e. Equation 16

- was obtained from studying another mix design;
- was obtained studying the dehydration process from the gelling instant.

Consequently, it could appear that the use of this equation is forced. However, it is the only control instrument currently available, and it can be successfully used for obtaining a first indication of the order of magnitude of the phenomenon.

Furthermore, it should also be considered that the samples were obtained from the two-component blocks from the construction site only after the removal of some centimetres of dried material. Consequently, the bulk of the two-component grout could be higher than the 60%, considering that the dehydration process ideally did not affect the core of the original bulk of the material (the tested samples were shaped from the core). Finally, at the state of the art there does not exist any relation that permits computation of the reduction of the strength performance as a function of the bulk reduction; thus, point one is not quantifiable.

As concerns point 2, the wide fracturing of the two-component grout material sent from the construction site was clear at the first visual check. All the obtained samples (Figure 117) were characterised by a web of fractures that were not created by the trimming process. Before testing, lower results in terms of both UCS and σ_t were expected. However, the question is: why was the two-component grout from the construction site so particularly fractured? First of all, these fractures were unlikely to have been caused by the dehydration process. It should be underlined that the nature of the fractures of the samples of the test campaign described in paragraph 11.4 was completely different. While fractures

due to dehydration affect the material bulk concentrically (from the surface in contact with the air, where they are very dense, to the core, usually intact or slightly fractured) and are usually geometrically linear, in this case the fractures affected the whole of the bulk, covering it without any recognisable geometrical scheme. Furthermore, the fractures were not homogeneous on the sample: very dense fractured areas could be seen alternating with more intact ones.

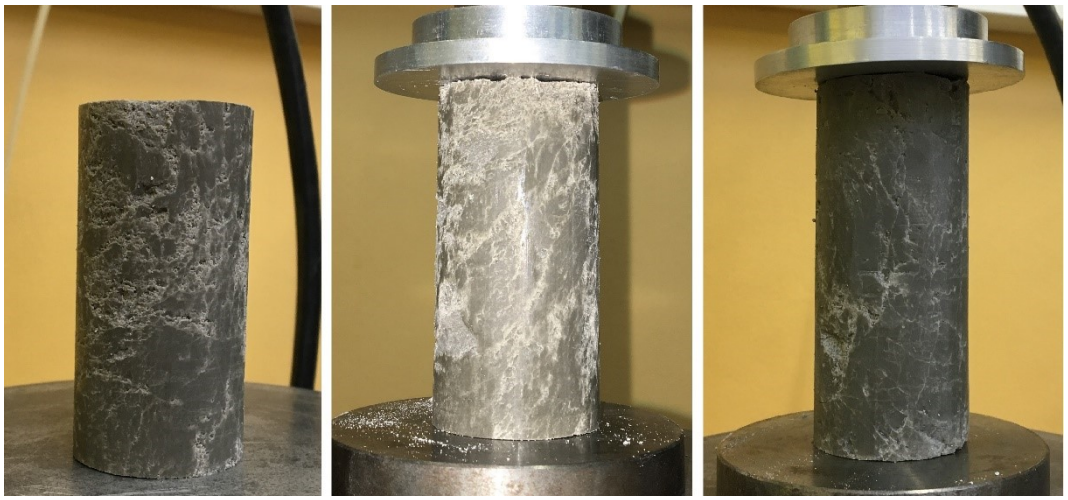

Figure 117 - Samples obtained from the two-component grout from the construction site. The fracturing is clearly visible on every sample.

The fracturing of the two-component grout could be interpreted as the result of the new equilibrium of the "excavated medium–linings" system, created at a short curing time after the injection of the backfilling material. It should be underlined that the task of the backfilling material is, among others, to bear the load of the machine backup during the advancement and to homogenise the final punctual loads. In order to satisfy these requirements, it is unthinkable that the two-component grout could fulfil its tasks without a certain degree of stress and, consequently, strains (especially considering that the incompressible bubble status is actually hard to achieve).

However, according to Antunes (2012), the real stress state of the two-component grout after the injection is triaxial; hence the presence of fractures does not strictly imply a collapse.

Pertaining to point 3, experience suggests that a trimming factor always affects experimental tests performed on weak materials. This was perfectly known before starting the test campaign, and the tests were originally scheduled taking care to avoid this drawback, by foreseeing the trimming of the laboratory samples to homogenise the dimensions of the whole sets. Unfortunately, it was not possible to avoid the scale factor, for the reason explained above.

Finally, concerning point 4, this is the only aspect that should produce a reduction of the mechanical performance in the samples cast in the laboratory, compared with real two-component grout obtained from the construction site. It has been well explained in the previous chapters how the "casting" at the construction site occurs at very high pressure and turbulence, while in the

laboratory the procedure foresees completely different mixing and casting modalities.

Thus, it can be stated that the marked difference between the outcomes for material from the construction site and the material created in the laboratory is a combination of all four of the analysed aspects. Unfortunately, no more material was available in order to continue the study.

Concluding, this study highlighted that the comparison between the two sets of samples should not be done only numerically, but it is crucial to take into account the construction site framework. Although both sample sets were made up of the same material, the bulk coming from the construction site had a past tension path that occurred probably in the short curing time after the injection. Samples cast and cured in laboratory, instead, are virgin.

Recalling the concepts expressed by Pelizza et al. (2010, 2012):

- "it is necessary to inject a fluid that does not harden instantaneously, but that becomes a gel quickly and progressively [..] creating an incompressible ball [..] the gel has to be as homogeneous as possible in order to mitigate the external loads";
- "the measurement of the compressive strength on cores extracted in situ is the most reliable and significant".

Some further information can be added, in light of the above results. Since the two-component grout aims to bear the external load at short curing times, it should always be designed with a proper strength, paying attention to the short curing time. The backfilling material will be loaded just a few hours after the injection, and it must be carefully planned in order to bear this load. Strains and fractures will affect the material; however, if the mix design is correct, limited tunnel displacements or surface subsidence will occur.

Moreover, tests on cores extracted in situ are undoubtedly more reliable and significant. However, it is very important to indicate also the exact position from which the core has been extracted. Specimens drilled from the crown could be significantly different from those extracted at the inverter. As pointed out in this research, the potential presence of fracturing does not imply construction problems (in the construction site involved, no problem was signalled due to abnormal movements of rings), but it could be interpreted as the result of the load path applied on the material.

Thus, the research should be extended also to other construction sites. Increasing the data could enable a better understanding of a phenomenon that has now been addressed for the first time.

12.7 Key concept

KEY CONCEPT 12: The two-component grout curing modalities have a strong effect on the mechanical performance of the grout. The curing in the real

environment, i.e. in the annulus in the context of a construction site, is characterised not only by the medium's moisture content, the temperature or the presence/absence of the groundwater table, but also involves a strength path that is applied to the grout. After the injection, the passages of the linings for the next rings firstly and the heavy backup (40–400 tons) secondly are loads that undoubtedly stress the young two-component grout. In conclusion, the fracturing recognised in samples obtained from the construction site could be due to this stress path but not necessarily involve stability problems.

Chapter 13

Tensile strength

In this chapter, the results of the Brazilian test campaign performed on the two-component grout are presented, in terms of indirect tensile strength. Before continuing, I wish to express doubts I have had about the possibility of publishing this chapter or, alternatively, avoiding it and forgetting about these outcomes. The reason is the incompleteness of the originally programmed research path. In other words, a lot of scheduled tests could not be performed because of the lock-down due to Covid-19. Not only did the impossibility of accessing the university laboratory cause the loss of several months of work, but much more seriously, samples that had been previously cast and were curing were irremediably damaged because of the uncontrolled curing condition. The result was that a large part of the work became trash. However, I eventually decided to present as well as possible the poor data obtained, hoping that this was the right choice according to my readers.

Only the curing modality in water was investigated. A correlation factor between the indirect tensile strength assessed with the flexural test and the Brazilian test was obtained. Furthermore, as additional information, a brief analysis pertaining to the potential correlation between the UCS and the tensile strength is presented (with a view to trying to find a relation similar to the one valid for standard concrete).

13.1 State of the art

Tensile strength is another mechanical parameter that is usually assessed for the mechanical characterisation of materials such as rock or concretes, although it has never been used for two-component grout, where the UCS is the only diffusely considered strength.

Concerning the study of rock and concrete, for reasons basically due to the difficulty of preparing suitable testing samples, the indirect approach is widely used. Different authors investigated the indirect tensile strength. Concerning the

Brazilian test, the first work was published in 1943 (Carneiro, 1943), where the invention of the "Brazilian testing method" for the "splitting tensile strength" of concrete is introduced. Li & Wong (2012) summarised all the historical evolution of this indirect approach and the tensile strength investigation was contextualised also with different laboratory case histories, highlighting how the Brazilian approach usually overestimates the tensile strength of rocks. Furthermore, the authors underlined that, despite this deviation, the Brazilian test is still popular today thanks to the easier sample preparation and easier testing procedure compared with direct uniaxial tensile tests.

As concerns the three-point flexural test (or simply flexural test), this further indirect tensile strength test used for rocks and concrete can be successfully performed, but these tests do not provide constantly a correct evaluation of the real tensile strength of a given material (Biolzi et al., 2001).

The list of authors that have studied and published works on this topic is long, but it is not the object of this research to deepen the intricate issue related to the best method for assessing tensile strength. Anyway, useful information for introducing the next topic is successfully summarised by the standard ASTM C496/C496M-17; namely, the real tensile strength of a concrete (direct tensile strength) is lower than the splitting tensile strength (Brazilian test), which is lower than the flexural strength (flexural test).

13.2 The issue

The critical issue was highlighted in section 11.3.5: the outcomes of tests of the flexural strength highlighted its independence from the curing time. Since this result is strongly innovative, it was decided to look for a proof of the invariability of the tensile strength in time by performing Brazilian tests.

13.3 The idea

Samples of two-component grout were manufactured and cured in water.

The tensile strength of materials with the same curing was assessed according to the flexural test approach and the Brazilian test. The outcomes were compared in order to understand the real trend of the tensile strength as a function of the curing time.

Secondly, new results and old outcomes (presented in paragraph 11.3) were assembled and presented together in order to provide a complete overview of the undrained mechanical parameters of the two-component grout. Starting from this point, the potential connection between the two indirect tensile test approaches was determined and discussed.

13.4 Material and test procedure

13.4.1 Apparatus

Tests were performed using the Wykeham Farrance compression testing machine, equipped with a load cell of 5 kN. Tests were carried out using two steel flat platens. Cylindrical moulds with an inner diameter of 52 mm and a height of 130 mm were used for the samples production.

13.4.2 Testing procedures

The Brazilian test was performed according to ASTM D3967-16. The main information regarding this technical regulation was discussed in paragraph 12.4.2.

13.4.3 Sample manufacturing

The component A for the two-component grout was produced according to the procedure described in paragraph 7.2. The mix design used is reported in Table 21. The procedure described in paragraph 7.3.3 was followed with the exception of the sample shape for casting and the curing modalities.

After the scheduled curing time, the specimens, originally 130 mm high, were gently cut, taking care to obtain samples with a thickness ranging between 10.4 and 39 mm. After that, all the new specimens were carefully measured and weighed. Those that exhibited a density value plainly lower than the expected value were removed from the set.

Although the original number of samples was planned foreseeing some spare ones, in this case again it was not possible always to respect the technical regulation requirement pertaining to the minimum number of 10 broken specimens. Therefore, 11 samples were tested for a curing time of 24 hours, and 8 for curing times of 1 month and 1 year.

By way of example, Figure 118 (left) depicts samples cured for 1 year and prepared according to ASTM D3967-16e. On the right, the end of a Brazilian test is shown, where the central specimen crack is clearly visible.

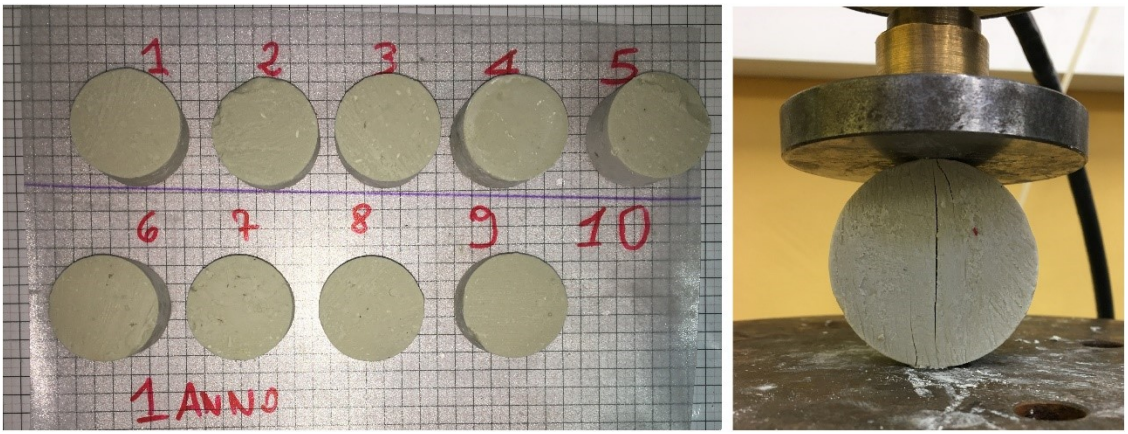

Figure 118 - Complete set of suitable samples for the Brazilian test (left) and ending of a Brazilian test (right). Curing time of 1 year.

13.5 Results

13.5.1 Splitting tensile strength as a function of the curing time

Figure 119 reports all the outcomes concerning the Brazilian test campaign. Each point on the chart represents one test. The average value (one for each studied curing time) can be identified from the continuous line.

Table 47 summarises the related statistical analysis.

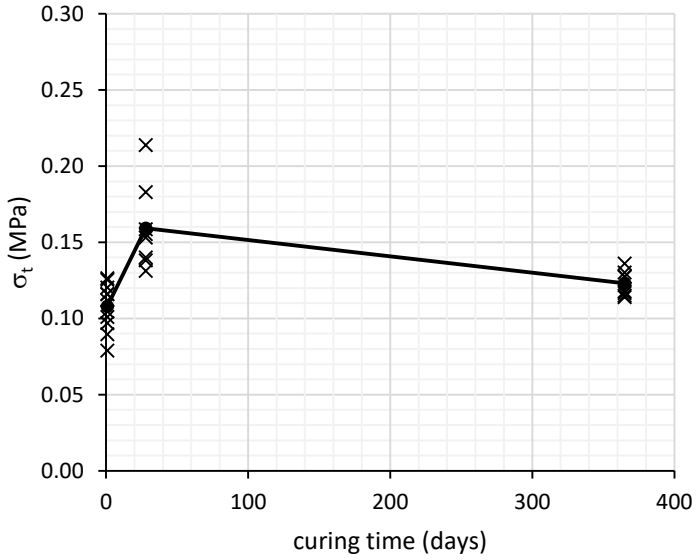

Figure 119 - σ_t as a function of curing time.

Table 47 - Statistical analysis of the test campaign concerning the indirect tensile strength according to the Brazilian procedure.

	Curing time		
Curing modality: water	1 day	1 month	1 year
	σ_t (MPa)	σ_t (MPa)	σ_t (MPa)
	0.12	0.14	0.14
	0.09	0.15	0.12
	0.10	0.18	0.13
	0.11	0.16	0.13
	0.13	0.16	0.11
	0.12	0.13	0.12
	0.08	0.14	0.12
	0.12	0.21	0.13
	0.10	/	/
	0.10	/	/
	0.13	/	/
Average	0.11	0.16	0.12
Standard deviation	0.01	0.03	0.01

13.5.2 **Relation between the tensile strengths**

Table 48 reports the ratios between the tensile strengths assessed according to the flexural approach (R_t) (Figure 101) and the Brazilian approach (σ_t).

The curing time of 24 hours was not analysed because it was not possible to successfully apply EN 196-1:05, so the related value of R_t was not available.

Table 48 - Ratio values computed between the flexural tensile strength and the splitting tensile strength for curing time of 1 month and 1 year. Curing modality: in water.

	Curing time	R_t/σ_t
Curing modality: water	1 month	2.7
	1 year	2.7

13.6 Discussion

Before starting to analyse the outcomes obtained in this chapter, the hypothesis speculated at the end of paragraph 11.3 should be recalled, and specifically the last point argued in the "General discussion": "the R_t value is independent of the curing time, and it depends only on the mix design or on the curing modality".

Other information that should be added to our framework is the analysed curing time, which in that context ranged between 1 month and 3 years.

Now taking into account the chart depicted in Figure 119, the first achievement that should be underscored concerns the data obtained also for a curing time of 1 day: the Brazilian test permitted the expansion of the curing time analysed. Focusing on the trend of the average values, it was possible to identify a slight increase of the σ_t in correspondence to the curing time of 1 month. Nevertheless, this peak should be contextualised with the higher standard deviation, three times greater with respect to the other two studied curing times. Therefore, it can be deemed that the splitting tensile strength (σ_t) is constant in time, relative to the investigated curing time ranging between 1 day and 1 year. For this time lapse, an average value of σ_t equal to 0.13 MPa can be computed.

Considering Table 48, for the curing times of both 1 month and 1 year the ratio between R_t and σ_t is equal to 2.7. This value is very important and can be used as a conversion factor for predicting one value of the indirect tensile strength starting from another one. Concluding, considering the standard C496/C496M-17 for concrete valid for our context, the relation $R_t > \sigma_t > T_0$ has been confirmed for the first two members of the inequality (having indicated with T_0 the real tensile strength of the grout). Furthermore, if the statement of Li and Wong (2012) is coherently considered valid, allegedly the T_0 of the analysed two-component grout should be lower than 0.13 MPa.

13.7 Additional information

13.7.1 Undrained mechanical parameters of the two-component grout cured in water: the tensile strength and the UCS

In the light of the new information obtained in this chapter, the tensile strength is assumed constant for the curing times ranging between 24 hours and 1 year. Table 49 gives an overview concerning the undrained mechanical parameters of the studied two-component grout.

The specification “undrained” is reported in order to highlight the difference between this kind of test and the drained tests assessed for drawing the failure envelopes τ - σ’ (paragraph 9.6.2).

The acronym n.a. stands for “not available”.

Table 49 - Overview of the undrained mechanical parameters of the studied two-component grouts. The curing was carried out in water. For the computation, the average value of σ_t = 0.13 MPa was used.

Curing modality: water	1 day			1 month			1 year		
Strength	R_t (MPa)	σ_t (MPa)	UCS (MPa)	R_t (MPa)	σ_t (MPa)	UCS (MPa)	R_t (MPa)	σ_t (MPa)	UCS (MPa)
Average	n.a.	0.11	1.04	0.43	0.16	1.57	0.34	0.12	1.64
Standard deviation		0.014	n.a.	0.01	0.02	0.08	0.03	0.01	0.22

The values of splitting tensile strengths obtained were added to the data concerning the uniaxial compression strength and flexural strength already presented in paragraph 11.3.

Considering the value of σ_t constant in time and equal to 0.13 MPa, the trend of the ratio UCS/σ_t in time is governed by the UCS trend. Table 50 summarises the numerical relation between the uniaxial compression strength and the tensile strength.

Table 50 - UCS/σ_t and UCS/R_t as a function of the curing time.

Curing time	UCS/σ_t	UCS/R_t
1 day	≃ 8	/
1 month	≃ 12	≃ 32.5
1 year	≃ 12.5	≃ 33.7

And for longer curing times? It can be speculated that the UCS/σ_t ratio tends slowly to increase, in accordance with the slow UCS increase. By using the correlation factor between σ_t and R_t, the ratio UCS/ R_t can be simply computed for the curing time of 1 month and 1 year (last column of Table 50).

In conclusion, it should be highlighted that all the above-mentioned results should be considered as numerically valid only for the studied mix design and for the curing modality used. Nevertheless, they could be considered as a valid starting point in order to calibrate the proper test campaign of a specific mix design, different from the one used in this research. Furthermore, all the presented outcomes form a valid, albeit poor, data base concerning the two-component grout technology and the order of magnitude of the relation between the compression and the tensile strength.

13.7.2 Second mix design

The original plan for this section foresaw the comprehensive study of another mix design (mix design S), and potentially also Brazilian tests on our common mix design (Table 21) performed after 6 months, 2 and 3 years of curing were planned (enough samples were cast and were curing in water). Concerning the mix S (Table 37), Brazilian tests were programmed on samples cured for 1 day, 1 month and 1 year. Unfortunately, from all the program, only the Brazilian tests performed on samples produced according to the mix design S and cured for 1 month in water were successfully performed. I decided to put these outcomes in this session, rather than forget them.

Each point in Figure 120 represents one test. The average value can be identified from the black circle.

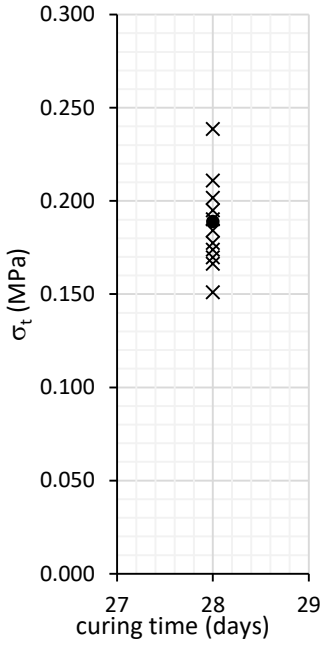

Curing modality: water	1 month
	σ_t (MPa)
	0.20
	0.18
	0.15
	0.17
	0.19
	0.18
	0.17
	0.19
	0.21
	0.17
	0.24
	0.21
Average	0.19
Standard deviation	0.02

Figure 120 - σ_t related to 1 month of curing time (left) and statistical analysis (right). Mix design S. Curing modality: water.

Moreover, for equal curing times, a test campaign according to EN 196-1:05 was also performed on samples produced, cured and tested in compliance with procedures described in paragraphs 7.2, 7.3.3 and 7.3.4. A complete overview of the outcomes is summarised in Table 51.

Table 51 - Statistical analysis concerning the undrained mechanical parameters of the two-component grout related to the mix design S. The curing was carried out in water.

Curing modality: water	1 month			
	R_t (MPa)	UCS (MPa)	σ_t (MPa)	
	0.60	2.29	0.17	0.20
		1.78	0.19	0.18
	0.47	1.85	0.21	0.15
		1.93	0.17	0.17
	0.49	2.21	0.24	0.19
		2.07	0.21	0.18
Average	0.52	2.02	0.19	
Standard deviation	0.06	0.19	0.02	

Concluding, in Table 52, the R_t/σ_t ratio is computed.

Table 52 - Ratio values computed between the flexural tensile strength and the splitting tensile strength for curing time of 1 month in water. Mix design S.

	Curing time	R_t/σ_t
Curing modality: water	1 month	2.7

Exactly as for the other studied mix design (Table 48), a value equal to 2.7 was obtained. It can consequently be stated that, also when changing the mix

design, for a curing time of 1 month the ratio between the two different tensile strengths is constant and close to 2.7.

13.7.3 The Eurocode 2

As always occurs when a new topic concerning two-component grout is studied for the first time, the first step was to consult the standard regulation on concrete. In this case, Eurocode 2 (BS EN 1992-1-1:2014 + A1:2014) was consulted in order to find useful information about potential empirical equations able to forecast the tensile strength from the UCS.

Paragraph 3.1.2 clearly explains how the development of tensile strength with time is strongly influenced by the curing and drying conditions as well as by the dimensions of the structural members. Some equations are then provided in "Table 3.1 - Strength and deformation characteristics for concrete".

Considering that:

- f_{cm} is the mean value of concrete cylinder compressive strength at 28 days;
- f_{ck} is the characteristic compressive cylinder strength of concrete at 28 days;
- f_{ctm} is the mean value of axial tensile strength of concrete at 28 days;

the following equation is suggested in order to compute f_{ctm}, in the case of a class of resistance lower than 50/60:

$$f_{ctm} = 0.3 * f_{ck}^{\frac{2}{3}} \; for \; C \leq 50/60 \qquad 23$$

The f_{ck} is the needed parameter. Hence, still in Table 3.1, the following equation is provided:

$$f_{ck} = f_{cm} - 8 \; (MPa) \qquad 24$$

It should be underlined that the output of a common uniaxial compressive strength test campaign performed according to EN 196-1:05 consists in an average value of UCS, computed on samples that should be roughly considered cubic with lateral dimensions of 40 mm. It cannot be claimed that the samples shape is perfectly cubic because only two dimensions are univocally fixed from the sample size and the compression press geometries, while the third dimension could fluctuate close to 40 mm. Consequently, the required f_{cm} cannot be easily obtained using the common cylinder/cube conversion factor for concrete (equal to 0.83), but an express test campaign should be planned in order to investigate this issue. However, also speculating on being able to compute a reliable value of f_{cm}, it is undoubtedly clear that Equation 24 is inapplicable, since the mean value of two-component cylinder compressive strength at 28 days is certainly lower than 8 MPa. In conclusion, consulting the Eurocode was useless.

13.8 Key concept

KEY CONCEPT 13: The tensile strength of the two-component grout is independent from the curing time or, alternatively, the Brazilian test and the flexural tests are not able to determine its variation in time. Assessments performed in compliance with both the flexural test regulation and the Brazilian one showed an almost constant value as a function of the curing time. The Brazilian approach permits assessment of the indirect tensile strength also for curing times shorter than 28 days. For the studied grout, a correlation factor of 2.7 between the R_t and σ_t was computed related to curing times of 1 month and 1 year, in water. Tests on another mix design confirm this value for a curing time of 1 month. With reference to 1 month and 1 year of curing in water, a preliminary attempt to correlate the UCS and the tensile strength of the two-component grout underlined once again the difference of this grout with respect to the standard one (value of UCS/R_t for the two-component grout equals about to 3 fold the value of the standard concrete)

Chapter 14

Bentonite in the two-component grout application

The content of this chapter is slightly different from the others presented up to this point. Specifically, no further investigations on the two-component grout as a whole have been run, but more depth is given on the role of one of the ingredients involved in the backfilling technology: the bentonite.

The chapter frame is aligned with the previous ones: after a preliminary paragraph to summarise the main scientific productions on the topic of bentonite as applied to two-component grout technology, the issue/lack identified is presented, whereupon the developed idea is illustrated. The results and their discussion lead readers to the conclusion.

14.1 State of the art

In paragraph 5.1.3 bentonite was introduced and the main concepts concerning its chemical constitution and its lamellar structure were explained. Furthermore, it was highlighted that the role of this ingredient for the two-component technology is mainly bounded by the stability of component A, i.e. it can control the bleeding phenomenon (Mesboua et al., 2018).

The first information that contextualises the use of bentonite in the two-component technology was provided by Pellegrini & Perruzza (2009), who underlined that the use of bentonite is intended to stabilise component A, reducing bleeding and increasing the viscosity. Another interesting aspect that should be reported concerns the strength exhibited by the grout after 1 hour of curing, which, according to the authors, depends on the dosages of cement and sodium silicate (the bentonite was not considered to be involved in the development of the grout strength). Basically the same concepts are reported in Pelizza et al. (2010, 2012) and Peila et al. (2011), with the introduction also of aspects linked to the

increasing of the waterproofing capacity and the bentonite's help in the gelation phase. Dal Negro et al. (2010) stated that the right bentonite and its appropriate dosage facilitate bleeding control. The introduction of the differentiation between different kinds of bentonite is an innovation that must be highlighted. For the first time, the potential issue of the right choice and the right dosage of a certain type of bentonite is introduced. Ivantchev & Dal Rio (2015) highlighted the experimental approach adopted for the choice of the best bentonite, compatible with their construction site needs. They explained the comparison done between common and high performance bentonite, using as comparison parameters less flaking during the mix, less bleeding and the lower viscosity (a statement contrary to Pellegrini & Perruzza, 2009). Unfortunately, no more details were provided.

Structured research concerning the influence of the kind of the bentonite and its dosage on the bleeding and the flowability can be found in Youn et al. (2016). This interesting research was based on three different bentonites, but, unfortunately, the only information on the types of bentonite concerns their dominant element (sodium) and the final addition of polymer to the chemical matrix. No bentonite parameters were introduced in order to forecast or estimate the magnitude of the bleeding or flowability variability.

14.2 The issue

The lack clearly spotted by analysing the information available in the scientific literature concerns the absence of specific investigations on the role of bentonite in other aspects of the two-component technology, apart from the bleeding phenomenon.

Let us suppose, just for a moment, that also after the gelation the two-component grout continues to be fluid (an enormously viscous fluid): in this way, the gelled material should continue to require the "stability" provided by the bentonite. Assuming the validity of this hypothesis, some questions could be asked: could the bentonite be involved also in the strength performance of the grout at short curing times? Could grouts made with different bentonites exhibit different performance in terms of strength at short curing times? Could the activation modality of the bentonite affect the strength of the grout?

Meanwhile, also hoping to experimentally prove the role played by bentonite in other fundamental two-component parameters, there is in any case a need to find an engineering instrument, a procedure, a parameter, able to guide tunnelling engineers in the choice of the best bentonite for the requirements proper of a specific project.

14.3 The idea

Three different commercial bentonites, used for two-component grout applications in three different construction sites, were considered for the study.

One mix design was established as valid for all the research: the dosage and the commercial type of each ingredient (bentonite kind excluded) were kept equal for the whole test campaign.

The procedure for the component A production was modified. Specifically, the phase related to the bentonite activation was parametrically changed in time duration: 0 minute (no activation), 2, 4 and 7 minutes of bentonite activations were tested. Thereby, four different components A for each kind of bentonite were obtained and, consequently, four complete component A characterisations were performed for each bentonite. This first research step was developed in order to verify the impact of the activation time on the component A parameters (bleeding, gel time and flowability).

A second step concerned the production of two-component samples that were tested at the curing times of 1 and 3 hours (short curing time). This second research phase aimed to highlight the role of bentonite in the surface compression strength (SCS).

Finally, the swell index and Atterberg's liquid limits were chosen as basic parameters for characterisation of the bentonites. In the discussion, the potential relations between the swelling index, the limit liquid, the component A parameters and the SCS strength are highlighted and discussed.

14.4 Material and test procedure

Bentonite "activation" is a jargon expression, common for figures involved in engineering applications where bentonite is used. In this context, "activation" means the process of hydration, which permits the bentonite particles to incorporate the water, increasing their volume. The activation of the bentonite can be obtained naturally, by leaving the bentonite in water and waiting long enough (as in the case of the swell index assessment) or forcedly, by increasing the turbulence of the water–bentonite suspension.

14.4.1 Sample manufacturing and curing condition

The mix designs used for first the component A production and then the two-component grout were the usual ones, reported in Table 21. All the dosages were kept constant. Three kinds of bentonite were used, each of them metered according to the amount foreseen from the mix design (30 kg/m^3).

For commercial reasons, in this context the industrial names of the bentonites and the names of the production companies have been anonymised, so hereinafter the different bentonites have just been numbered from 1 to 3.

The component A was produced according to the procedure described in paragraph 7.2 with the exception of the duration phase of the bentonite activation. More specifically, considering Table 6, the second step of the procedure (adding the bentonite while increasing the propeller speed at a constant rate) had a comprehensive duration of 7 minutes; this duration was varied: 0 minute (the right amount of bentonite and cement were added together), 2, 4 and 7 minutes were

used as reference times for the bentonite activation phase. Concerning the sample production, the procedure described in paragraph 7.3.3 was followed.

14.4.2 Summary of the technical standard and procedure

The complete characterisation of the component A was assessed according to the procedure described in paragraph 7.3.1.

Specifically, the unit weight was assessed according to the procedure described in paragraph 7.3.1.1. Concerning the flowability, the procedure described in paragraph 7.3.1.2 was taken as reference with the exception of the scheduled testing time: the determinations were performed only on the fresh grout. Bleeding tests were performed in compliance with the procedure described in paragraph 7.3.1.3. However, in order to better investigate the first minutes after the component A production, the frequency of the determinations was increased. Therefore, bleeding reads were carried out after 0 min, 10 min, 20 min, 30 min, 40 min, 50 min, 60 min, 90 min, 120 min and 180 min from the component A preparation. The procedure described in paragraph 7.3.3 was followed for the gel time.

Regarding the determination of the surface compression strength (SCS) performed on hardened samples, the procedure described in paragraph 8.3.2 was followed.

The only new procedures to be introduced concerned the assessment of the swell index and Atterberg's liquid limit.

Concerning the first one, ASTM D5890-18 was followed. This test method permits the evaluation of the swelling properties of a clay mineral. The procedure can be summarised as follows:

- at least 100 g of bentonite shall be available, with particle dimensions less than 150 μm;
- dry the clay specimen (12–16 h) at 105 ± 5 °C;
- cool the material in a desiccation unit; assess the bentonite water content;
- weigh 2.00 ± 0.01 g of clay onto a weighing paper;
- add 90 mL of distilled water in a clean 100 mL cylinder;
- take 0.1 g of bentonite and dust it in the cylinder over a period of 30 seconds. No funnel must be used. After 10 minutes, another 0.1g of bentonite is added to the water in the cylinder. Continue in this way till the entire 2 g has been added;
- add distilled water to reach the 100 mL level in the cylinder;
- place the cap on the cylinder. Wait at least 16 hours before carrying out the measurement. Record the volume, in mL, at the top of the settled and swelled clay deposited on the cylinder bottom;
- record the temperature of the hydrated clay mineral;
- compute the swell index (SWI) as the ratio between the swelled bentonite volume and the amount of 2 g (Equation 25)

$$SWI = \frac{V(mL)}{2\,(g)} \qquad 25$$

As an example, Figure 121 depicts the observed swelling phenomenon 20 hours after the last bentonite addition (bentonite 1).

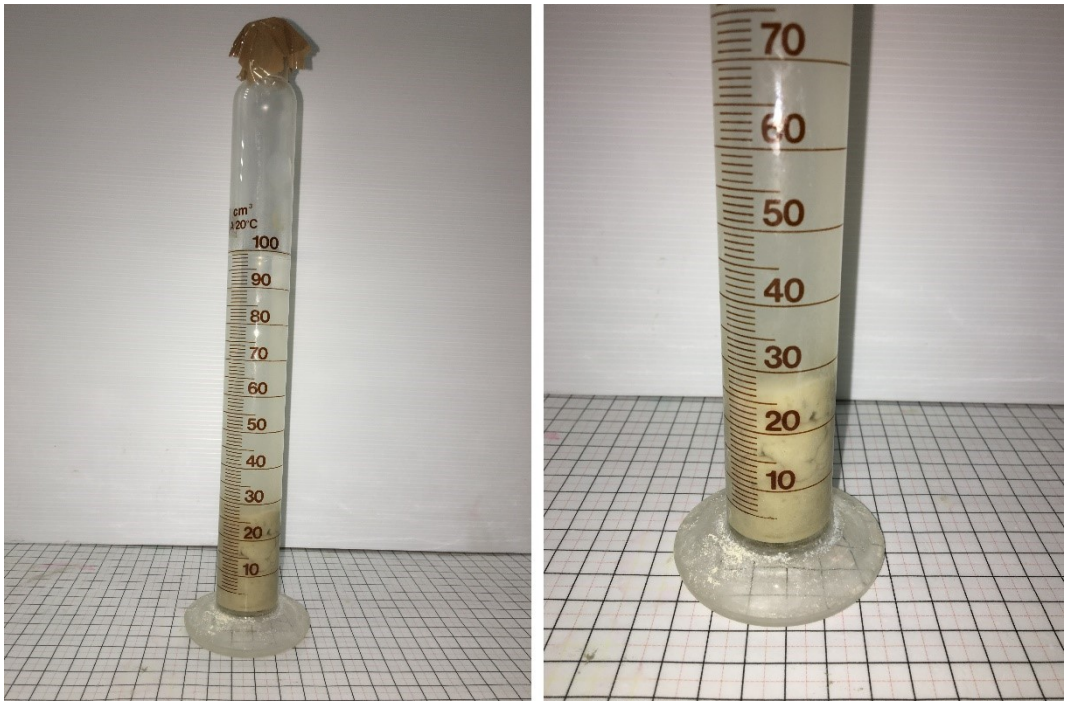

Figure 121 - Bentonite swelling phenomenon. Photo taken 20 hours after from the last bentonite increment. Bentonite 1.

For the assessment of the liquid limit, BS 1377-2: 1990 was followed as reference and the Casagrande apparatus with the specific grooving tool was used.

The main difference from the standard regulation consisted in the pre-hydration of the samples: about 300 g of powdered dry bentonite (in exactly the same state as that provided at construction sites) was put in a tank and hydrated using distilled water. This step was taken in order to deal with the very slow hydration process of the bentonite, longer than 10 minutes (i.e. the duration prescribed by the standard). Hydration of the bentonite in 10 minutes may be reached only by using mechanical energisation. However, this option was discarded, preferring to avoid accelerated operations. The amount of the added water has been computed foreseeing a first test with 50 blows. In the following the laboratory procedure is briefly summed up:

- a layer of wet bentonite is spread on the cup of the Casagrande apparatus, taking care to avoid air bubbles being trapped inside the material (Figure 122, left);
- by using an appropriate grooving tool, a groove is created, splitting the material into two parts (Figure 122, right);
- switch on the Casagrande apparatus to count the number of blows;

- record the number of blows corresponding to the creation of a contact interface of a length equal to 13 mm and collect a part of the sample close to the contact interface (about 10 g) to use for the water content determination;
- repeat all the above-listed operations after drying the sample by just moving and continuously mixing it with a spatula for enough time. No forced dehydration method is used (e.g. adding dry material or application of warm air flow).

Once four blow values (preferably equally distributed between 15 and 35) and their corresponding water contents are obtained, the flow curve can be obtained by plotting on a semi-logarithmic chart the water content as ordinates and the number of blows as abscissa on the logarithmic scale. The moisture content corresponding to 25 blows is the liquid limit (w_L).

Figure 122 - Casagrande apparatus with the cup filled with a sample of bentonite 1 and grooving tool (left). Casagrande apparatus with the groove in the centre, just before starting the test (right).

14.5 Results

The outcomes are presented in the following. In order to make the work performed clearer to the reader, three different sections are presented. The first is dedicated to the data obtained concerning component A and the second is related to the SCS assessments. Finally, the outcomes concerning the swell index and Atterberg's liquid limit are presented.

14.5.1 Component A

Table 53 presents an overview of the outcomes concerning the characterisation of the different components A produced, in terms of flow time,

gel time and unit weight. It should be noted that the flow time was assessed only on the fresh mortar.

Figure 123, Figure 124 and Figure 125 are charts related to the bleeding assessment respectively for bentonite 1, 2 and 3. In each chart, the four trends related to the different bentonite activation times are drawn.

Table 53 - Overview of outcomes concerning the components A characterisation in terms of flow time, gel time and unit weight.

		Bentonite activation time (min)			
		0	2	4	7
Bentonite 1	Flow time (s)	27	30	34	35
	Gel time (s)	6	7	7	8
	Unit weight (kg/L)	1.17	1.18	1.18	1.18
Bentonite 2	Flow time (s)	29	30	32	31
	Gel time (s)	7	6	5	8
	Unit weight (kg/L)	1.19	1.17	1.17	1.17
Bentonite 3	Flow time (s)	33	36	36	35
	Gel time (s)	6	6	6	6
	Unit weight (kg/L)	1.17	1.16	1.17	1.17

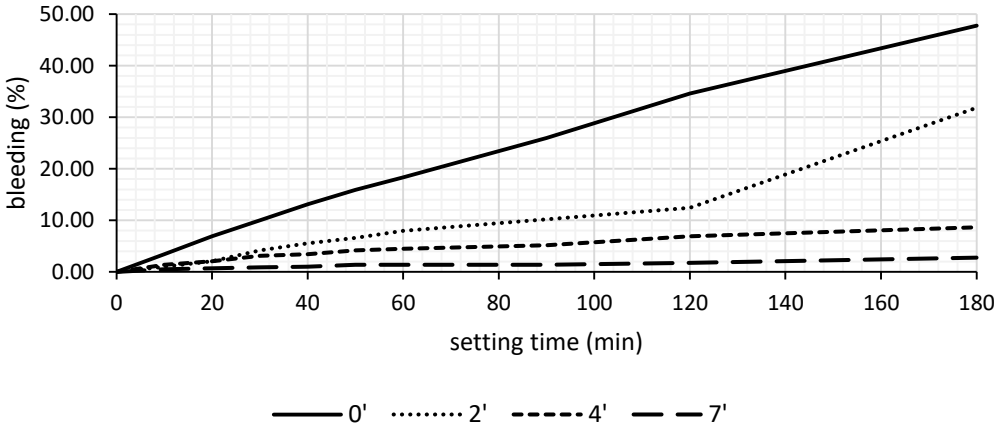

Figure 123 - Bleeding outcomes concerning the bentonite 1. Different activation times.

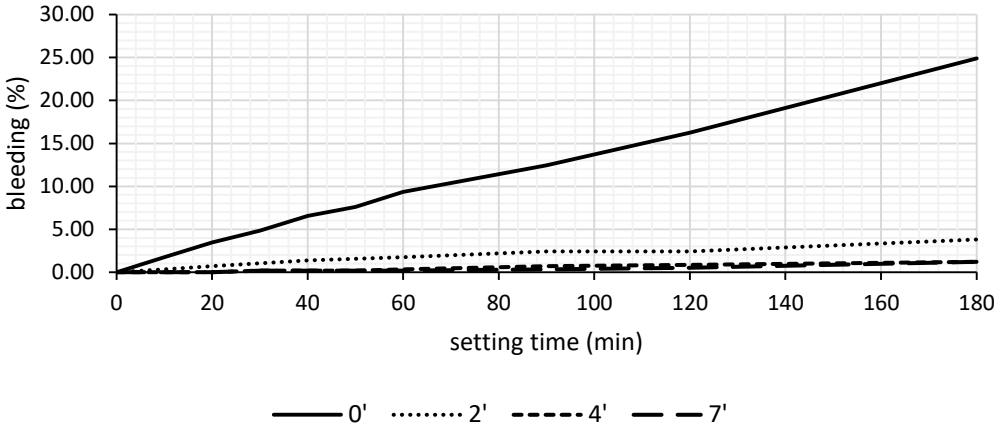

Figure 124 - Bleeding outcomes concerning the bentonite 2. Different activation times.

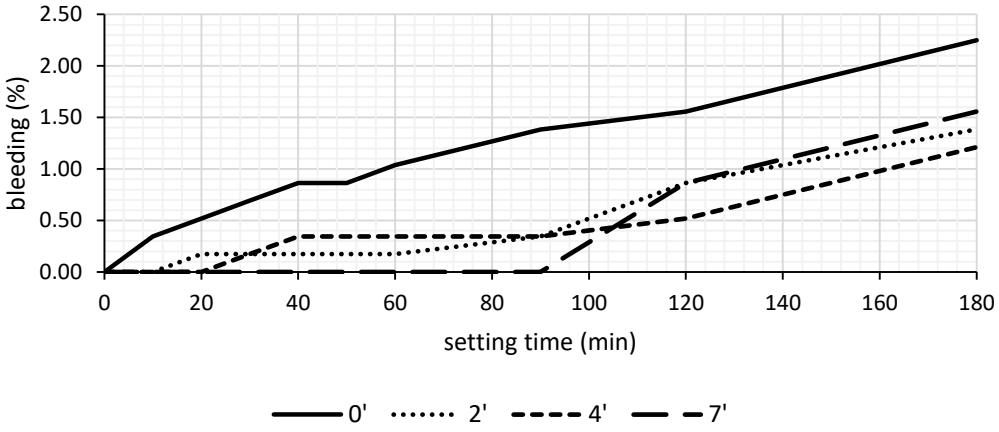

Figure 125 - Bleeding outcomes concerning the bentonite 3. Different activation times.

14.5.2 SCS as a function of the bentonite activation

Figure 126 and Figure 127 report the overviews concerning the SCS outcomes obtained from tests carried out at 1 hour and 3 hours of curing respectively. Each type of bentonite used (1, 2 and 3) is characterised by four columns, one for each bentonite activation time (0 min, 2 min, 4 min and 7 min). Each value is the average of the measurements performed.

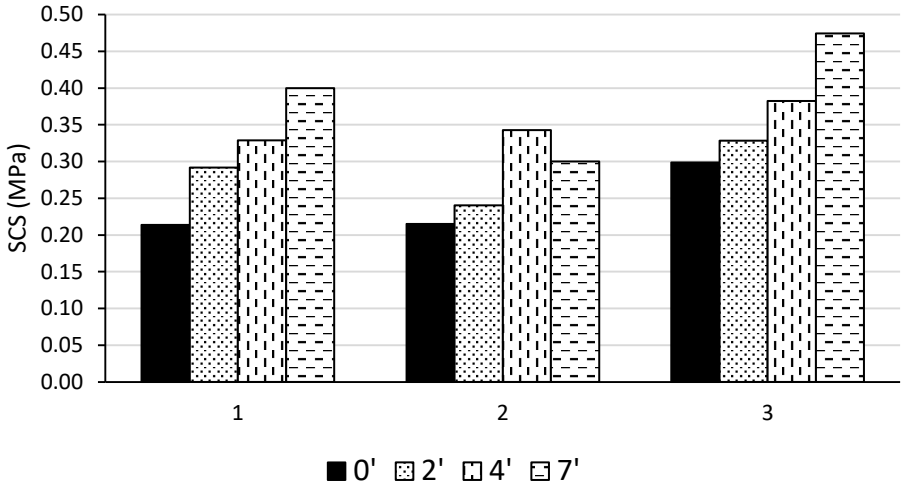

Figure 126 - SCS after 1 hour of curing pertaining to the three studied bentonites. Different activation times.

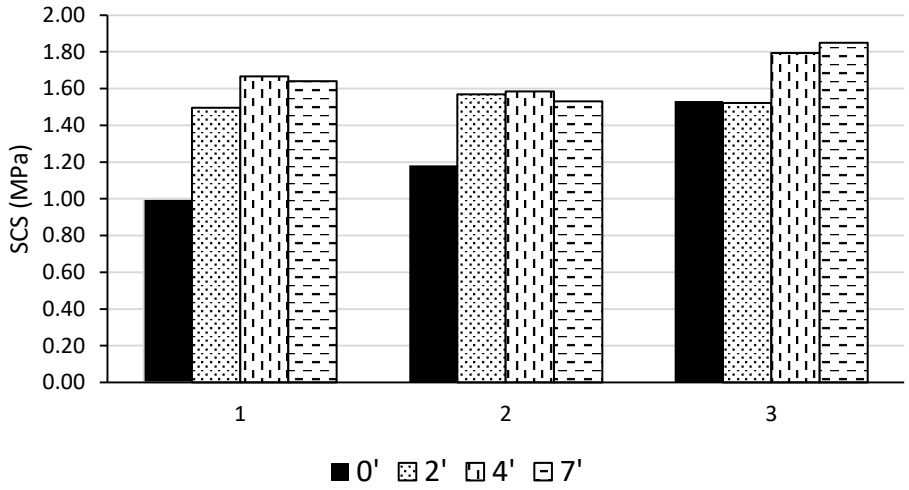

Figure 127 - SCS after 3 hours of curing pertaining to the three studied bentonites. Different activation times.

The standard deviation of the assessed SCS values is lower than 0.1 MPa.

14.5.3 Swell index (SWI)

The obtained data pertaining to the swell index assessment are summarised in Table 54. Measurements were carried out 20 hours after the last addition of bentonites in the cylinders.

The raw materials were provided by the suppliers powdered and dry, in the same condition as usually supplied to construction sites. In Table 54 w(%) indicates the natural water content of the material as provided by the suppliers. This assessment confirms that a certain moisture content different from 0 always characterises the raw materials.

Table 54 - Outcomes related to the swell index test campaign.

Bentonite	w (%)	T slurry (°C)	SWI
1	10.73	22.2	14
2	12.65	22.4	13
3	10.98	22.7	23

14.5.4 Liquid limit

The data obtained for Atterberg's liquid limits are summarised in Table 55.

Table 55 - Outcomes related to the liquid limits of the tested bentonites.

Bentonite	Liquid limit (%)
1	427
2	525
3	445

14.6 Discussion

14.6.1 Components A

Before proceeding with discussion of the outcomes, a brief reflection on the accuracy of tests should be given. As discussed in paragraph 7.4.7, taking into account the flowability and the gel time assessments, a fluctuation of ±1 second is not meaningful if all the determinations have been performed by the same operator. Similarly, if different operators have performed tests due to unforeseeable circumstances, a larger fluctuation, equal to ±2 seconds, should likewise not be considered meaningful. This second scenario reflects the real working conditions of tests that are going to be discussed.

Taking into account Table 53, the first parameter considered is the gel time. The component A produced with the bentonite 3 unequivocally exhibits a gel time independent of the bentonite activation time, with a value equal to 6 s for each determination. A constant trend can be identified also in the case of bentonite 1, with a measurement range of 2 s. The component A manufactured using bentonite 2 exhibits more scattered measurements. The fluctuation range is equal to 3 s and the gel time seems to decrease from 7 s to 5 s and eventually settles close to 8 s as a function of the increasing activation time. This set of data is plainly not accurate because, in the author's experience, the gel time trend can be managed only by changing the mutual volume percentage between components A and B; also, an inversion of the gel time as a function only of a change of the bentonite activation time makes no sense. It can consequently be speculated that slight weighing errors were made when preparing the amounts of components. In conclusion, also the

gel time trend for the component A produced with the bentonite 2 can be deemed constant, with an average value of 7 s.

From another point of view, by considering each bentonite activation time individually, it can be observed that all the measurement ranges (max value – min value) are between 1 s and 2 s (Table 56). This result highlights that the component A exhibits the same gel time, independently of the kind of bentonite used.

Table 56 - Range of gel time measurements for the four bentonite activation times.

Bentonite activation time (min)	Min value (s)	Max value (s)	Range (s)
0	6	7	1
2	6	7	1
4	5	7	2
7	6	8	2

Independently of the bentonite used and of the activation time, a constant specific weight of 1.17–1.19 kg/L was observed. The density was very stable.

As concerns the flow time assessed on the fresh mortar, it was not possible to recognise a unique trend for the three bentonites as a function of the activation time, although a general growing tendency could be identified. The component A produced with bentonite 1 showed a clearly and regularly rising trend: from 27 s for 0 min of activation to 35 s for 7 min. Also the component A manufactured with bentonite 3 exhibited a growing trend, although there was a step of 3 s between 0 min and 2 min, after which the flow time was closely aligned with values of 35–36 s. Also concerning the component A produced with bentonite 2, a slight increase of the flow time could be observed.

The parameter markedly influenced by the bentonite activation time is bleeding. The first interesting aspect that can be pointed out concerns the strong bleeding reduction that can be obtained by increasing the activation time. In Table 57, for each bentonite, the proper bleeding values assessed without activation and with 7 min of activation are reported. According to the procedure in 7.3.1.3, 3 hours of setting was selected as the reference value for the comparison.

Table 57 - Decrement in percentage of the bleeding value computed between 0 min and 7 min of bentonite time activation. Assessment performed after 3 hours of setting.

	Setting time = 3 hours		
Bentonite	Bleeding value with 0 min of bentonite activation (%)	Bleeding value with 7 min of bentonite activation (%)	Δ (%)
1	47.75	2.77	94.2
2	25.00	1.20	95.2
3	2.25	1.50	33.3

Components A produced with bentonites 1 and 2 exhibit a reduction of bleeding close to 95%, while bentonite 3 shows a lower percentage reduction, close to 33%.

Meanwhile, the charts depicted in Figure 123, Figure 124 and Figure 125 described completely different trends. For the comparison, the limit bleeding value (b_L) equal to 1.5% is considered. This value corresponds on average to the bleeding exhibited by component A, which is used in practice on construction sites, after 3 hours of setting.

The component A produced with bentonite 1 (Figure 123) exhibits the highest bleeding values between the studied cases. The value close to 50% for the inactivated bentonite is the highest of all the test campaigns. There is a bleeding reduction as a function of the increasing of the activation time, but on no occasion were bleeding values lower than b_L reached.

Concerning the component A manufactured with bentonite 2 (Figure 124), the value close to 25% obtained without activation is strongly reduced to less than 5% by activating the bentonite for just 2 min. Furthermore, bentonite activated for 4 min and 7 min exhibits a bleeding value after 3 hours that is lower than b_L.

The component A produced with bentonite 3 (Figure 125) is the most stable. Without activation, a bleeding slightly more than 2% is reached. Furthermore, by activating the bentonite (2 min, 4 min or 7 min) bleeding values smaller than b_L are reached.

Finally, from the analysis of the component A, it can be summarised that by modifying the bentonite activation time no marked variations of unit weight and gelling time can be observed. The flowability could increase, so it is always advised to verify the flow time experimentally. Undoubtedly, the parameter most strongly linked to the bentonite activation is bleeding. By increasing the activation time, without changing the mix design or the kind of bentonite, better results in term of bleeding, i.e. stability, can be obtained for the component A. Different bentonites exhibit different performances.

14.6.2 SCS as a function of the bentonite activation

The role played by the bentonite in the strength of the two-component grout in the first hours after casting has opened a new line of research that is potentially able to increase the importance of the bentonite.

Beforehand, it should be signalled that the precision of each value of the average SCS was characterised by a standard deviation lower than 0.1 MPa, perfectly aligned with the standard deviation obtained in the test campaign described in Chapter 8.

Considering the outcomes depicted in Figure 126, the increasing of the SCS as a function of a longer bentonite activation time is plainly represented, independently of the type of bentonite. In Table 58, the computed increment of SCS (%) between 0 min and 7 min of activation is reported.

Table 58 - SCS increment between 0 min and 7 min of bentonite activation concerning two-component grouts produced with different bentonites. 1 hour of curing.

	Curing time = 1 hour		
Bentonite	SCS for 0 min of bentonite activation	SCS for 7 min of bentonite activation	Δ (%)
1	0.21	0.40	87
2	0.22	0.30	40
3	0.30	0.47	59

However, a trend inversion can be seen for bentonite 2: the forecast SCS value for an activation time of 7 min was higher than the previous activation times but the results did not confirm expectations. This inconsistency should be ascribed to mismanagement of the sample casting phase. From a general comparison, the two-component grout produced with bentonite 3 exhibits the highest SCS values (with a value for 7 min of activation equal to 0.47 MPa), while bentonite 1 is found to be the most sensitive to the activation process (almost doubling the SCS from 0.21 to 0.40 MPa).

Taking into account data reported in Figure 127 for 3 hours of curing time, the increasing of the SCS as a function of longer bentonite activation times is not regular as in the case of 1 hour of curing and, furthermore, the magnitude of the phenomenon is more moderate. Table 59 reports the computed increment of SCS (%) between 0 min and 7 min of activation.

Table 59 - SCS increment between 0 min and 7 min of bentonite activation concerning two-component grouts produced with different bentonites. 3 hours of curing.

	Curing time = 3 hours		
Bentonite type	SCS for 0 min of bentonite activation	SCS for 7 min of bentonite activation	Δ (%)
1	1.00	1.64	64
2	1.18	1.53	29
3	1.53	1.85	21

For bentonites 1 and 2, activating the bentonite for 2 min, 4 min, or 7 min led to SCS values close to 1.6 MPa.

A different trend can be seen for bentonite 3: two different SCS values can be identified. For this bentonite, a negligible difference is recognised between not activating the bentonite and with an activation time of 2 min, while a marked rise in the SCS occurs for the activation time of 4 min (a step of 0.2 MPa), with a final SCS close to 1.8 MPa. As in the case of 1 hour of curing, bentonite 3 exhibits the highest SCS value, with 1.85 MPa obtained with 7 min of bentonite activation time. Again confirming the data for 1 hour, bentonite 1 has the greatest sensitivity to the activation time.

14.6.3 **Swell index (SWI)**

The swell index test campaign indicated that all the determinations were performed on material originally characterised by a very similar moisture content, ranging between 10% and 13%. It should be underlined also that although the

bentonites were provided by suppliers as “dried”, the assessment of the moisture content revealed different hydration conditions. As concerns the final temperature of the slurries, the values are noticeably similar, in the range of 22–23 °C.

Concerning the swell index, bentonites 1 and 2 exhibited very similar values, exactly 14 and 13 respectively. Bentonite 3, instead, was characterised by a markedly different value of SWI, 10 points higher than the other ones.

14.6.4 Liquid limits

The test campaign to assess the liquid limits highlighted very high values, over 400% for all bentonites. Specifically, bentonite 2 exhibited the highest value (525%) while the lowest value was for bentonite 1 (427%). The liquid limit of bentonite 3 was in between the other two, with a value of 445%.

It should be highlighted that, despite the good familiarity with the test procedure, the assessment of the liquid limit on bentonites was very hard to perform. The main difficulty was encountered in obtaining a uniform sample during the manual dehydration process. More specifically, it often occurred that after a successful determination of the number of blows, the subsequent test exhibited a number of blows that was higher than the previous one, although the mixing and intrinsic dehydration should have led to a lower number of blows. This not so rare situation could be explained by the non-uniform moisture content of the tested samples. When this drawback occurred, both test outcomes (tests with the growing trend of blows) were removed from the data record.

14.6.5 Final considerations

Bentonite has a crucial importance in the two-component grout technology and influences the behaviour of both the component A and the hardened grout.

Before providing an overview of the results obtained, some comments on the information available in the scientific literature and introduced at the beginning of this chapter are appropriate. The author does not intend to reflect badly on the past work, but a few thoughts are needed in order to integrate the present knowledge and carry on the study of the bentonite in the two-component backfilling grout context.

Considering Pellegrini & Perruzza (2009), the role of bentonite in the stabilisation of the component A and its effect on reducing the bleeding and increasing the viscosity were plainly confirmed. However, concerning the compression strength after 1 hour of curing, the role of the bentonite should be clearly recognised (with the cement and the accelerator) as one of the main factors. Concerning Pelizza et al. (2010, 2012) and Peila et al. (2011), the statement on “the bentonite helping in the gelation process” is not clearly understood. According to the results obtained, it can be clarified that, for a fixed mix design (fixed dosages), the kind of bentonite does not play a key role in the gelling time. Similarly, the bentonite activation time’s influence on the gel time is negligible.

Dal Negro et al. (2010), Ivantchev & Dal Rio (2015) and Youn et al. (2016) are the precursors of this research: these papers clearly underline the key concept related to the choice of the right bentonite as a function of the predetermined purpose.

The outcomes obtained in this part of the research are completely in compliance with the statement of those authors: it is decisively proved that different kinds of bentonite or different bentonite activation times may lead to different results in terms of SCS or bleeding. Taking into account the swell index (SWI), it is possible to assert that high values of SWI correspond to high SCS. In the specific case of bentonite 3, characterised by the highest SWI, the test campaign carried out on the two-component grout samples provided the highest values of SCS at both 1 and 3 hours of curing. It should, however, be underscored that the best performance of the grout obtained with bentonite 3 in terms of SCS is more evident at 1 hour of curing rather than 3 hours.

The gel time, unit weight and flowability assessed on the fresh mortar are parameters that are not considered to be a function of the SWI.

A more complex scenario was observed for the bleeding phenomenon. Although also for this aspect the bentonite with the highest SWI was confirmed as the best performing (also with a null activation time the bleeding for the mortar produced with bentonite 3 was lower than 2.5%), the mortar manufactured by using bentonite 2 also exhibited a bleeding value lower than b_L, by just applying a medium (4') activation time of the bentonite. Considering that the SWI of bentonite 2 is substantially equal to that of bentonite 1 and that the respective bleeding performances are markedly different, it is evident that another bentonite-dependent parameter should be taken into account: the liquid limit. Indeed, considering that bentonite 2 has a higher liquid limit than bentonite 1, it can be stated that a higher liquid limit leads to a lower value of bleeding, for a certain constant testing procedure and for an equal value of SWI. Hence, concerning the bleeding, the limit liquid should also be considered in addition to the SWI.

To conclude, a high value of SWI is a necessary but not sufficient condition for choosing a suitable bentonite, from both the strength and bleeding points of view. A high SWI corresponds to a high level of SCS, but if different bentonites exhibit the same SWI, the assessment of the liquid limit can determine the choice of the better bentonite also from the bleeding point of view.

In the light of all the work carried out, it can be deemed that a suitable tool for the preliminary choice of the best bentonite for two-component grout applications has been identified. In the mix design project phase, the SWI could be successfully used for a preliminary selection, followed by the assessment of the liquid limit in order to take into account also the bleeding phenomenon. In any case, in the case of a final choice between two bentonites with the same value of SWI, it is strongly advised to perform a laboratory test campaign similar to the one described in this chapter, aiming to verify the SCS.

Finally, a reflection on the economic aspect is of value. Different types of bentonites are available on the market and the cost range for this product is wide. Concerning the two-component backfilling applications, once the grout targets

have been established, it should be considered that a bentonite with a high SWI may satisfactorily fulfil the requirements with a lower dosage than a bentonite with a lower SWI. Consequently, as suggested by Ivantchev & Del Rio (2015), an expressly scheduled test campaign should always be performed at the construction site, in order to verify the influence of the bentonite on the two-component grout, to optimise the batching station and to verify the behaviour of the bentonite also at the real scale. Furthermore, staying in the construction site field, a last aspect should be discussed: if a bentonite with a suitable SWI value has been chosen, the possibility of obtaining good performance in terms of bleeding and SCS also without a complete activation process of the bentonite is an interesting option that could be of paramount importance in the critical case of an immediate demand for component A over the mean. Also, in the case of reducing or completely cutting the bentonite activation time during the component A production, the manufactured product might still ensure the minimal required parameters for a satisfactory backfilling operation. On the other hand, if a certain bentonite does not satisfy the construction site requirement for minimal fluctuations of values, engineers should know that, by increasing the duration of the activation phase, there is room for improvement of both the SCS and the bleeding, maybe enough to satisfy the provisions.

14.7 Additional information

In this chapter the importance of the bentonite in the two-component technology has been discussed, recognising also its important role in the mechanical strength in the first hours of curing. However, the impact of bentonite inactivation was not studied at long curing times. Consequently, the study on the bentonite time activation ended with the final test campaign, aiming to assess the UCS at 28 days of curing, on samples produced without bentonite activation.

The mix design used is reported in Table 21. The component A production was carried out in compliance with the procedure described in paragraph 7.2 with the exception of the bentonite activation phase, which has been cut (the cement and bentonite were added together). Concerning the samples production and the curing modality, the procedure described in paragraph 7.3.3 was followed.

Table 60 reports the outcomes and the statistical analysis.

Table 60 - Statistical analysis concerning samples cured in water for 28 days, with component A produced without bentonite activation.

Curing modality: water	1 month	
	R_t (MPa)	UCS (MPa)
	0.30	1.06
		1.11
	0.51	1.96
		1.76
	0.54	1.88
		1.84
Average	0.45	1.60
Variance	1.16E-02	1.36E-01
Standard deviation	0.107	0.37

Considering the average R_t and UCS values equal to 0.45 and 1.60 MPa, these results are close to those obtained when producing the component A according to the standard procedure (Table 6) reported in Figure 101, i.e. 0.43 and 1.57 MPa. It should be underscored that the standard deviation in this case is bigger than in the previous tests. It is evident that the first sample was markedly weaker than the others. Without considering it in the statistical analysis computation, both the R_t and UCS increase, reaching values higher than the corresponding ones listed in Figure 101.

In the light of this additional research, an addition to the knowledge gained about the use of bentonite in two-component grout applications is that, at long curing times, there is no evidence of the "activation process" of the bentonite. It could be speculated that, in the long term, the strength of the grout is a function only of the water/cement ratio and of the kind of cement.

14.8 Key concept

KEY CONCEPT 14: Bentonite plays an active role in the stability of the component A and in the SCS of the hardened grout. In order to choose the right bentonite for the backfilling application in compliance with the given construction site technical requirements, the SWI is the main parameter that should be assessed. The higher the SWI, the higher is the performance of the bentonite. In the case of bentonites with similar values of SWI, Atterberg's liquid limit can help to identify the best one also from the bleeding point of view. However, after a preliminary investigation leading to the final choice between only 2 bentonites, a test campaign is strongly advised in order to put in evidence all the peculiarities of the materials. The test campaign should be composed of:

- bleeding assessment with different bentonite activation times;

- SCS assessment at 1 and 3 hours of curing;

- SWI assessment;

- liquid limit assessment.

In Figure 128 the above-described steps aiming at the choice of the most suitable bentonite for a two-component grout application are summarised.

Furthermore, if during the work advancement (after the launch of the machine) the technical construction site requirements are not reached (which can happen for various reasons), it should be remembered that a certain degree of improvements in terms of bleeding and SCS can be reached by increasing the duration of the activation process of the bentonite. The modification of the bentonite activation duration has no bearing on the UCS at long curing times.

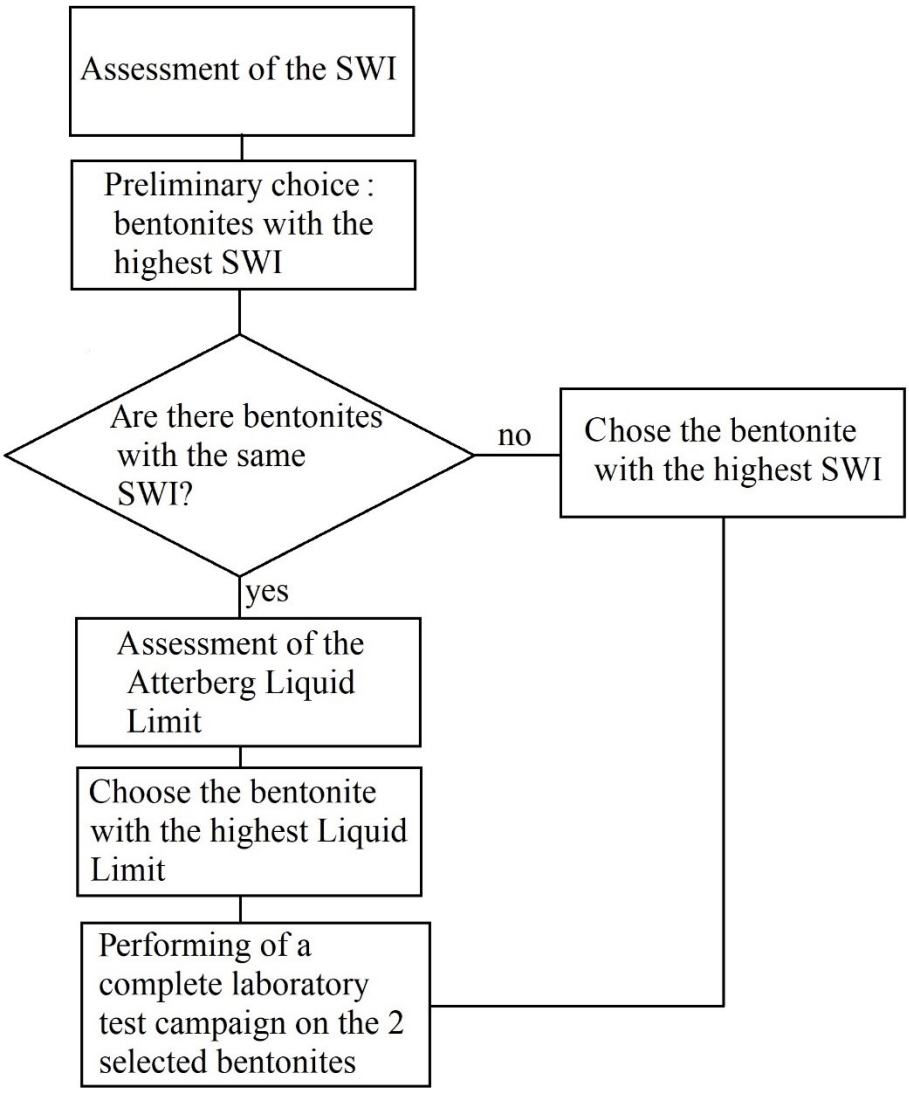

Figure 128 – Flow chart for the choice of the most suitable bentonite for a two-component grout application.

Chapter 15

New frontiers: the two-component grout 2.0

In this chapter, an innovative raw material used in the two-component grout technology is presented and tested. Although the two-component grout technology is relatively young compared with other backfilling techniques, a time-lapse of 3 years (the duration of the PhD research) was long compared to the fast process of research and development that currently characterises the market for the raw materials involved in tunnelling construction. In other words, before finishing the experimental tests on the standard two-component grout, and before sharing the new results obtained with the scientific community, a new product able to completely replace the bentonite in the component A has been created in the laboratory of a chemical enterprise. Thanks to the strong and long-lasting collaboration, a sample of this innovative product has been made available for a preliminary characterisation. Thereby, I had the pleasure to introduce in this research this innovative ingredient and I have consequently used the title "two-component grout 2.0" for this chapter in order to highlight the innovation introduced with this new raw ingredient, which is able to replace one of the cornerstones of the affirmed technology.

15.1 The issue and the idea

Bentonite is a natural material, but not naturally available in all parts of the world. On the other hand, tunnels are necessary in all parts of the world, so if a project foresees the use of the two-component grout technology for backfilling, the problem of the bentonite provision must be faced. Generally speaking, if the transport lines are well structured, the problem does not arise. But, in the case of a construction site that is not easily accessible, the cost of the bentonite can significantly rise, even becoming unsustainable.

In order to overcome this potential issue, a new ingredient was developed for the two-component backfilling technology that can replace the bentonite. In this context, the product is named “stabiliser polymer” or SP.

A test campaign was performed to assess the real potential of this new ingredient, by first producing a component A and then a two-component grout and checking the properties of both the mortar and the gelled/hardened grout.

15.2 Material and test procedure

15.2.1 Apparatus and material

All the tests were performed using the Wykeham Farrance compression testing machine, equipped with a load cell of 5 kN. Tests were carried out using both the comprimitor and the frame for the three-point flexural test depicted in Figure 43 respectively for the assessment of the UCS and the indirect tensile strength.

SP is a natural liquid-phase polymer, with a colour between brown and black. It has been expressly chemically designed to be eco-friendly. Used as an ingredient in the component A production, it replaces the bentonite and the retarding/fluidifying agent.

15.2.2 Technical standard and procedure

Component A was produced according to the procedure described in paragraph 7.2. Obviously, the procedure used for the component A production listed in Table 6 was modified due to the absence of the bentonite (no activation time needed) and the uselessness of a retarding/fluidifying agent. Consequently, instead of the usual 12 minutes, the component A was produced in only 8 minutes. Details of the new procedure steps are reported in Table 61.

Table 61 - Procedure for the component A production modified for the SP use.

Operation	Impeller rotation speed (rpm)	Duration (min)
Fill the tank with water and start the mixer	800	/
Add the SP, increasing the propeller speed at a constant rate	from 800 to 2000	0.5
	2000	4.5
Add the cement	2000	3

The procedure for the characterisation of the two-component grout described in paragraph 7.3 was followed. Paragraph 11.3.2.2 can be taken as reference for the flexural test assessment. SCS tests were performed in compliance with the procedure described in paragraph 8.3.2.

15.2.3 Samples manufacturing and curing condition

Samples were manufactured and cured according to the procedure described in paragraph 7.3.3. The mix design used is reported in Table 62 and, for simplicity, hereinafter the mix is called “mix SP”.

Table 62 - SP mix.

	Ingredients	Dosage (kg/m^3)
Component A	Water	861
	SP	7
	Cement Buzzi CEM I 52.5 R	230
Component B	Accelerator Mapei Mapequick CBS 3	81

The presented mix design is the result of a long preliminary trial phase to calibrate the ingredient dosages in order to obtain a bleeding value after 24 hours of curing typical of construction sites’ technical specifications, i.e. lower than 6–7% (another four different mix designs were tested without obtaining satisfactory results).

15.3 Results

In the following, results concerning the unit weight (Table 63), the flowability (Table 64), the bleeding (Table 65), the gel time (Table 66), the SCS (
Table 67) and the UCS/R_t (Table 68) are presented.

As concerns the SCS, UCS and R_t assessments, the outcomes are presented in the form of A±B, where A is the average value and B is the standard deviation.

Table 63 - Unit weight of the mix design SP.

Mix design	Unit weight (kg/L)
SP	1.15

Table 64 - Flowability assessed on the fresh mortar and on mortar collected 24, 48 and 72 hours from the batching pertaining to the mix design SP.

	Flow time (s)			
Mix design	Fresh mortar	24 h	48 h	72 h
SP	30	33	32	32

For the bleeding assessment, the test performed after 1 h was added to the standard reference procedure.

Table 65 - Bleeding values assessed 1, 3 and 24 hours after the batching of the mix design SP.

	Bleeding (%)		
Mix design	1 h	3 h	24 h
SP	0.17	0.69	5.73

For the gel time results, Table 66 reports the datum related to the component B percentages foreseen from the mix deigns (Table 62). The gelling function has not been drawn.

Table 66 - Gel time pertaining to the mix design SP.

Mix design	Gel time (s)
SP	12

Table 67 - SCS assessed after 1 and 3 hours of curing time pertaining to the mix design SP.

	SCS (MPa)	
Mix design	1 h	3 h
SP	0.23±0.01	0.77 ± 0.03

Differently from the procedure described in paragraph 7.3, UCS tests after 3 hours of curing were not carried out. The only UCS value reported in Table 68 pertains to the curing times of 1 and 28 days.

Table 68 - Uniaxial compression strengths assessed after 1 and 28 days of curing time pertaining to the mix design SP. Flexural strength related to 28 days of curing.

	UCS (MPa)		R_t (MPa)
Mix design	24 h	28 days	28 days
SP	0.55	0.85	0.2

Concerning the measurement precision, a standard deviation close to 0.03 MPa was computed for all curing times.

15.4 Discussion

The use of SP highlighted how the two-component backfilling grout technology can successfully work also without using bentonite.

In order to better discuss the obtained results, a comparison with the characteristics of the standard mix (Table 21) should be performed. First, a consideration concerning the water/cement ratio is due in order to establish if it makes sense to compare such different mixes. Actually, the w/c ratio of our usual mix design is close to 3.71, while the w/c ratio of the mix SP is about 3.74. This difference of less than 1% comes from the different water dosages, equal to 853 and 861 kg/m^3 respectively. Anyway, considering the recommendation of EFNARC (2005) reported in paragraph 3.2.1 and the information on a real case history reported in Càmara (2018), this value is well within the precision range

that the batching stations of the construction site need to ensure during the work. Consequently, it can be deemed that both the considered mix designs have the same w/c ratio and that a comparison therefore does make sense.

The value of the specific weight of 1.15 kg/m^3 is slightly low compared with other unit weights reported in Table 53. It was perfectly forecast, considering that bentonite ($2.5<\rho<2.8$ kg/L) was replaced by SP and water ($\rho \simeq 1$ kg/L).

The obtained flowability values of 30–32 seconds and their constancy up to 72 hours highlighted a paramount level of stability. Taking into account all the developed tests, such a low flow time has never been measured after 24 hours of setting time.

As concerns the bleeding value, it should be underscored that the data obtained were the results of the trial test campaign to calibrate the mix design. The bleeding limit of 6% was reached with an SP dosage of 7 kg/m^3. However, smaller values could be easily reached by just increasing the SP dosage. Generally speaking, once the bleeding target is fixed, the SP dosage should be the lowest possible to satisfy the requirement, for economic reasons.

The gel time is the first parameter that is strongly different from the expectations. If the values reported in Table 53 are taken into account, it can be observed that the computed gel time, equal to 12 seconds, is nearly doubled. Assuming that mismanagement has not occurred during the gel time testing phase, it could be speculated that the SP stretches the gelling time, slightly retarding the gel reaction.

The SCS values assessed after 1 hour of curing are aligned with those of bentonite 1 and 2 without activation (Figure 126). Tests carried out on samples cured for 3 hours show, for grout produced with the SP, values lower than the corresponding values assessed on grouts produced with bentonite (Figure 127).

Considering the UCS for samples cured for 24 hours, the average value of 0.55 MPa is about 50% less than the one potentially obtained by using the bentonite (considering an average of 1 MPa). The same decreasing percentage is confirmed also for the UCS and the R_t strengths assessed after 28 days of curing.

This test campaign indicated the good results that could be obtained by using SP. A virtually perfect component A was produced, but the strength performance is still lower than expectations. However, the results should be contextualised as the first attempt at experimentation with this innovative product, and it is undoubtedly clear also that small dosage adjustments can lead to higher performance.

15.5 A further thought on the role of bentonite

In the light of the results obtained by testing the mix design with the bentonite replaced by the SP but keeping the w/c constant, it was possible to identify further details concerning the role of the bentonite in the UCS of the two-component grout.

As can be plainly deduced by comparing the outcomes reported in Table 68 with the results reported in Table 60 and Figure 101, considering 28 days of curing in water, the UCS and the R_t strength of the grout produced with the bentonite are about twice those for the grout without bentonite. In conclusion, it can be stated that the bentonite indisputably plays an active role in the strength performance of the two-component grout, at both short and long curing times.

15.6 Key concept

KEY CONCEPT 15: In the case of difficulties in the provision of bentonite and in the case of confirming the usage of the two-component grout as backfilling technology in a certain construction site, specific products already available on the market allow the replacement of the bentonite. These innovative raw materials used in the component A production lead to a mortar and a hardened grout of high quality. Special care should be taken with the gel time, which, all things being equal, could become longer. Pertaining to the mechanical strength, preliminary outcomes highlighted the requirement for a higher cement or silicate dosage, in order to reach a strength result comparable to the one commonly obtained by using bentonite.

Bentonite plays an active role in the development of the mechanical compression strength at both short and long curing times.

Chapter 16

Conclusions

This research concerns two-component grout, the most frequently used technology for annulus filling in tunnelling applications based on the use of full face shielded machines.

The aim of the study was to deepen the knowledge of this material, providing engineering tools for all parts involved in the backfilling field, that can be used to better calibrate the grout design phase with a view to the real operative context, at the construction site scale. The research path was defined according to the great number of questions raised by engineers involved in the two-component world: the main issues that have been faced in the last decades without a clear and unique approach were taken into account and the search for answers became the real "engine" of this research work.

The first step was to set up a laboratory procedure focused on the component A production, the mixing of components, the casting and the curing. The choice of identifying univocally a procedure allowed two-component grout samples to be obtained that were constant in their properties for the whole duration of the research. The proposed procedure was drawn with the purpose of obtaining a resulting product as similar as possible to the one obtained at construction sites, and it can be considered as the "cornerstone" of all the research work. Chronologically in parallel, a compliance protocol based on tests related to the component A, the gel time and the hardened grout was established, taking into account as far as possible the standard regulations currently available. Sometimes, the peculiarities of the material required changes to the technical standards.

Once the procedure was established, one mix design was chosen for the whole of the research path.

Consultation of the situation-specific technical requirements highlighted the need to investigate the strength exhibited by the hardened grout at short curing times. The study was developed by using in parallel a laboratory compression testing machine and a pocket penetrometer. The use of the penetrometer was investigated in more depth, a testing procedure for its use was defined and the

surface compression strength (SCS) was introduced as a different quantity with respect to the uniaxial compression strength (UCS). The tested two-component grout exhibited UCS values ranging between 0.08 and 0.33 MPa related to a curing time between 1 and 3 hours; moreover, a correlation factor close to 5 was computed between the SCS and UCS ($SCS = 5\ UCS \quad 1h \leq t \leq 3h$). This relation can be used in order to promptly assess the order of magnitude of the UCS at the construction site, starting from a faster, simpler and less cumbersome testing modality.

The study of the shear strength made it possible to assess, under drained conditions, the evolution of the two-component grout as a function of the curing time. The Mohr–Coulomb failure envelope criterion obtained highlighted the increase of the grout performance in terms of cohesion and friction angle, although these do not increase linearly. It should be underlined that for the curing time of 1 hour it was not possible to successfully approach the study under the drained condition.

The elastic modulus was studied taking a double approach. The static approach pertained to two-component grout samples cured for more than 28 days. Tests were performed according to the technical standard applicable for samples of common mortar. The outcomes highlighted a growing trend of the E value, starting from 1478 MPa at 28 days and reaching 2199 MPa after 5 months of curing. Unfortunately, the test campaign was not continued beyond 5 months because of the impossibility of correctly reading the strains. In the geophysical approach, tests were performed at both short curing times (between 45 minutes and 9 hours of curing) and long curing times (from 1 to 6 months), in compliance with the well-established technical standard and by using a direct transmission scheme. The study of the short curing time highlighted the clear increasing trend of the geophysical parameters. The elastic modulus evolved from 24 to 312 MPa, the shear modulus from 8 to 105 MPa, and the bulk modulus and Poisson's ratio decreased from 2703 to 2570 MPa and from 0.5 to 0.48 respectively. It should be highlighted that the P-wave velocity was constant for all the determinations and that consequently all the measured parameter variations are a function exclusively of the growing S-wave velocity. Tests performed on samples cured for long times highlighted a ripe behaviour, i.e. the geophysical approach is not able to sense the evolution of the material.

The study of the durability was focused on the aspects of ageing, and the action of both air and the water flow. Concerning the ageing, samples were cured from 1 month to 3 years following three different curing modalities. Although not linearly, the UCS trend increased as a function of the curing time, while the flexural strength remained at almost constant values. The mechanical properties of the grout were preserved if a minimal moisture content of the curing environment was ensured (5% in our case); otherwise, critical issues can occur in a relatively short time. In order to investigate this issue in more depth, the worst laboratory condition was planned, i.e. samples of grout were left under the action of air. The results showed that 2 months are sufficient to completely reduce the grout to powder. Unfortunately the study of the reduction of the strength performance due

dehydration could not be performed, but this aspect could be the starting point for future investigations. In any case, the risk of weakening of the two-component grout in the case of a tunnel embedded in a completely dry medium should be taken into account during the design phase of the mix design. The study of the durability was completed by setting up an innovative apparatus to assess the capacity of a certain hardened grout to resist the action of a water flow. Unfortunately only the descriptions of the procedure and the apparatus could be provided, but the poor preliminary outcomes highlighted a strong resistance of the material against the wearing action of the water. Finally, it should be signalled that although in the laboratory the mechanical performance can be guaranteed in time just by ensuring a certain moisture content of the curing environment, at the construction site the situation is completely different. Collecting samples of grout from a construction site for testing, one should not be surprised if the material exhibits very low performance compared to the expected one. As a function of the sampling area (top or bottom of the ring) in the tunnel, the two-component grout could have been stressed during its lifetime and been fractured, but without causing stability problems for the tunnel. More details were not obtained, but this issue too could be a starting point for further investigations.

The last two-component grout mechanical parameter that was investigated was the tensile strength. The Brazilian test was successfully applied to the material and the constant trend as a function of the time, already evident from the ageing campaign, was confirmed for curing times ranging between 1 day and 1 year. Furthermore, a correlation factor of 2.7 ($R_t = \sigma_t * 2.7$) was assessed between the two modalities of indirect tensile strength computation.

The last part of the research concerned the study of bentonite in the two-component grout applications. Differently from the information available in the scientific literature, bentonite is involved in the strength of the hardened grout at both short and long curing times. The activation process (the hydration of the bentonite accelerated mechanically) can increase the component A performance in terms of reducing the bleeding and increasing the SCS. By increasing the activation time from 0 to 7 minutes, the bleeding phenomenon assessed after 3 hours of setting could be reduced by as much as 95%. Pertaining to the SCS, particularly after 1 hour of curing, values obtained after 7 minutes of bentonite activation were double those obtained without activation. These performances are a function of the kinds of bentonite and their properties, and it is precisely on this subject that the swelling index (SWI) was identified as the main parameter responsible for good performance in terms of the stability and SCS. In a preliminary phase, bentonites with the highest values of SWI should be taken into account even if, in the case of similar SWI values, Atterberg's liquid limit can help in the choice linked to the bleeding phenomenon. At long curing times, for a certain bentonite the activation time has no influence on the UCS. In the case of using an innovative polymer expressly designed and realised to replace the bentonite, preliminary results highlighted the excellent quality of the component A, although it should be underlined that the UCS values after both 24 hours and

28 days could exhibit a marked reduction, up to 50% less than the values potentially obtained using the bentonite.

References

Agrò, G., Lo Giudice, E., Sacco, M.M. (2009). Il modulo elastico statico e dinamico del calcestruzzo. *Conferenza AIPnD – Associazione Italiana Prove non Distruttive Monitoraggio Diagnostica*.

Antunes, P. (2012). Testing Procedures for Two-Component Annulus Grouts. *North American Tunneling Proceedings,* April 10.

ASTM C403/C403M. (2016). *Standard test method for time of setting of concrete mixtures by penetration resistance.* American Society for Testing and Material International.

ASTM C496/C496M. (2017). *Standard test method for splitting tensile strength of cylindrical concrete specimens.* American Society for Testing and Material International.

ASTM C597. (2016). *Standard test method for pulse velocity through concrete.* American Society for Testing and Material International.

ASTM C939. (2010). *Standard Test Method for Flow of Grout for Preplaced-Aggregate Concrete (Flow Cone Method)*. American Society for Testing and Material International.

ASTM D2166/D2166M. (2016). *Standard test method for unconfined compressive strength of cohesive soil.* American Society for Testing and Material International.

ASTM D2573/D2573M. (2018). *Standard Test Method for Field Vane Shear Test in Saturated Fine-Grained Soils.* American Society for Testing and Material International.

ASTM D3967. (2016). *Standard test method for splitting tensile strength of intact rock core specimens.* American Society for Testing and Material International.

ASTM D5890. (2018). *Standard test method for swell index of clay mineral component of geosynthetic clay liners.* American Society for Testing and Material International.

Aydin, A. (2014). Upgraded ISRM suggested method for determining sound velocity by ultrasonic pulse transmission technique. *The ISRM Suggested*

Methods for Rock Characterization, Testing and Monitoring: 2007–2014, pp. 95-99. https://doi.org/10.1007/978-3-319-07713-0_6.

Barnett, P. (2008). Construction of bored tunnels in urban areas - Essential techniques for success. Retrieved from http://wiryanto.files.wordpress.com/2011/07/makalah_9.pdf.

Basu, A. & Aydin, A. (2006). Evaluation of Ultrasonic Testing in Rock Material Characterization. *Geotechnical Testing Journal,* 29(2), 117-125. https://doi.org/10.1520/GTJ12652.

Bezuijen, A., Van der Zon, W.H., Talmon, A.M. (2005). Laboratory testing of grout properties and their influence on back fill grouting. *Underground Space Use: Analysis of the Past and Lessons for the Future*. ISBN: 0415374529.

Biolzi, L., Cattaneo, S., Rosati, G. (2001). Flexural/Tensile Strength Ratio in Rock-like Materials. *Rock Mechanics and Rock Engineering,* 34(3), 217-233. DOI: 10.1007/s006030170010.

Bollettino Ufficiale CNR N.195 (2000) – Norme Tecniche – parte IV.

Boscaro, A., Barbanti, M., Dal Negro, E., Plescia, E., Alexandrowicz, M. (2015). The first successful experience in Poland of tunnel excavation with EPB for the Metro Warsaw. In *Proceedings of the ITA WTC World Tunnel Congress 2015*, May 22-28, Dubrovnik (HR).

BS 1377-2. (1990). *Methods of test for soils for civil engineering purposes – Part 2: Classification tests.* British Standards Institution. London, United Kingdom.

BS EN 1008. (2002). *Mixing water for concrete. Specification for sampling, testing and assessing the suitability of water, including water recovered from processes in the concrete industry, as mixing water for concrete.* British Standards Institution. London, United Kingdom.

BS EN 12390-13. (2013). *Testing hardened concrete. Part 13: Determination of secant modulus of elasticity in compression.* British Standards Institution. London, United Kingdom.

BS EN 12504-4. (2004). *Testing concrete. Determination of ultrasonic pulse velocity.* British Standards Institution. London, United Kingdom.

BS EN 197-1. (2011). *Cement. Composition, specifications and conformity criteria for common cements.* British Standards Institution. London, United Kingdom.

BS EN 1992-1-1:2004+A1. (2014). *Eurocode 2: Design of concrete structures.* British Standards Institution. London, United Kingdom.

BS EN ISO 17892-10. (2018). *Geotechnical investigation and testing – laboratory testing of soil. Part 10: Direct shear tests.* British Standards Institution. London, United Kingdom.

Càmara, R.J. (2018). Use of two-component mortar in the precast lining backfilling of mechanized tunnels in rock formations. In *Proceedings of the ITA WTC World Tunnel Congress 2018*, April 20-26, Dubai (UAE).

Carneiro, F.L.L.B. (1943). A new method to determine the tensile strength of concrete. In *Paper presented at the Proceedings of the 5th meeting of the*

Brazilian Association for Technical Rules (Associação Brasileire de Normas Técnicas—ABNT), 3rd section.

Dal Negro, E., Boscaro, A., Barbero, E., Darras, J. (2017). Comparison between different methods for backfilling grouting in mechanized tunneling with TBM: technical and operational advantages of the two-component grouting system. In *Proceedings of the AFTES International Congress 2017*, November 13-16, Paris (FR).

Dal Negro, E., Boscaro, A., Plescia, E. (2014a). Two-component backfill grout system in TBM. The experience of the tunnel "Sparvo" in Italy. In *Proceedings of the Tunnelling in a Resource Driven World Conference (TAC)*, October 26-28, Vancouver (CA).

Dal Negro, E., Boscaro, A., Schulkins, R. (2010). Two-component backfill grouting on Rome's Line C. *Tunnels & Tunnelling International*.

Dal Negro, E., Boscaro, A., Schulkins, R. (2012). Buenos Aires settlement control. *Tunnels & Tunnelling International*.

Dal Negro, E., Schulkins, R., Boscaro, A., Pediconi, P. (2014b.) Two-component backfill grout system in double shield hard rock TBM. The "Legacy Way" tunnel in Brisbane, Australia. In *Proceedings of the WTC World Tunnel Congress 2014*, May 9-14, Foz do Iguaçu (BR).

Deniz Akin, I. & Likos, W. (2017). Brazilian Tensile Strength Testing of Compacted Clay. *Geotechnical Testing Journal,* 40(4), 608-617. https://doi.org/10.1520/GTJ20160180.

DIN 4094-4. (2002). *Subsoil – Field testing – Part 4: Field vane test*. Deutsche Institut für Normung.

EFNARC. (2005). Specification and guidelines for the use of specialist products for mechanized tunneling (TBM) in soft ground and rock.

EN 196-1. (2005). Methods of testing cement – Part 1: Determination of strength. European Committee for Standardization, Brussels (B).

ETC5–ISSMGE. (1998). *Recommendations of the ISSMGE for geotechnical laboratory testing.* Beuth Verlag GmbH, Berlin.

Flores, A.Q. (2015). Physical and mechanical behavior of a two component cement-based grout for mechanized tunneling application. *PhD thesis*.

Green, R.E. (1991). Introduction to Ultrasonic Testing. A.S. Birks, R.E. Green, and P. McIntire, Eds. American Society for Nondestructive Testing, Metals Park, Ohio, pp.1–21.

Guglielmetti, V., Grasso, P., Mahtab, A., Xu, S. (2007). *Mechanized tunnelling in urban areas*. ISBN: 978-0-415-42010-5. Taylor & Francis.

Hashimoto, T., Brinkman, J., Konda, T., Kano, Y., Feddema, A. (2005). Simultaneous Backfill Grouting, Pressure Development in Construction Phase and in the Long-Term. *Tunnelling. A Decade of Progress*. GeoDelft 1995-2005. Adam Bezuijen, Haike van Lottum, CRC Press.

Hirata, T. (1989). Study on behavior of cohesive soil in type shield tunneling work and on construction technique. *Doctoral Thesis*, Kyoto University.

Home, L. (2014). ITACET Training session on Mechanized Tunnelling. Mexico (MX). June 26-27.

https://doi.org/10.1016/j.tust.2014.05.021.

ISRM. 1977. *Suggested methods for determining sound velocity*. International Society for Rock Mechanics: Commission on Standardization of Laboratory and Field Test. (USD 5).

ITAtech. (2014). ITAtech Guidelines on Best Practices For Segment Backfilling. In *ITAtech Publications*.

Ivantchev, A. & Del Rio, J. (2015). Two-component Backfill Grouting for Double Shield TBMs. In *Proceedings of the ITA WTC World Tunnel Congress 2015*, May 22-28, Dubrovnik (HR).

Khan, Z., Cascante, G., El Naggar, M.H. (2011). Measurement of dynamic properties of stiff specimens using ultrasonic waves. *Canadian Geotechnical Journal*, 48(1), 1-15. https://doi.org/10.1139/T10-040.

Lee, K.-M., Kim, D.-S., Kim, J.-S. (1997). Determination of dynamic Young's modulus of concrete at early ages by impact resonance test. *Journal of Civil Engineering*, 1, 11-18.

Li, D. & Wong, L.N.Y. (2012). The Brazilian Disc Test for Rock Mechanics Applications: Review and New Insights. *Rock Mechanics and Rock Engineering,* 46(2). DOI:10.1007/s00603-012-0257-7.

Liu, H., Xie, X., Sato, M. (2012). Accurate thickness estimation of a backfill grouting layer behind shield tunnel lining by CMP measurement using GPR. In *Proceedings of the 14th International Conference on Ground Penetrating Radar (GPR)*, Shanghai, pp. 137-142.

Mähner, D. & Hausmann, M. (2017). New Development of an Annular Gap Mortar for Mechanized Tunnelling. In *Proceedings of the AFTES International Congress 2017*, November 13-16, Paris (FR).

Maidl, B., Herrenknecht, M., Maidl, U., Wehrmeyer, G. (2013). Mechanised shield tunnelling. Wilhelm Ernst & Sohn, Verlag für Architektur und technische Wissenschaften GmbH & Co. KG, Berlin (DE). ISBN: 978-3-433-60105-1.

McCann, D.M., Forde, M. (2001). Review of NDT methods in the assessment of concrete and masonry structures. *NDTE International*, 34, 71-84.

Mesboua, N., Benyounes, K., Benmounah, A. (2018). Study of the impact of bentonite on the physico-mechanical and flow properties of cement grout. *Cogent Engineering*, 5(1), 1446252. https://doi.org/10.1080/23311916.2018.1446252

Mitchell, J.K., Soga, K. (2005*). Fundamentals of soil behavior*. John Wiley & Sons, Hoboken, NJ (USA).

Neville, A.M., Brooks, J.J. (1987). *Concrete technology*. Second edition. Pearson. ISBN: 978-0-273-732219-8 (pp. 210–211).

Novin, A., Tarighazali, S., Akhondi, M. (2012). Two component grout admixtures planning in Line 7 of Tehran Metro Project (E-W lot). In *Proceedings of the ITA WTC World Tunnel Congress 2012*, May 18-24, Bangkok (TH).

Novin, A., Tarighazali, S., Foroughi, M., Fasihi, E., Mirmehrabi, S. (2015). Comparison between simultaneous backfilling methods with two components and single component grouts in EPB shield tunneling. In

Proceedings of the ITA WTC World Tunnel Congress 2015, May 22-28, Dubrovnik (HR).

Peila, D., Borio, L., Pelizza, S. (2011). The behaviour of a two component backfilling grout used in a Tunnel Boring Machine. *Acta Geotechnica Slovenica,* 2011(1), 5-15. ISSN 1854-0171.

Peila, D., Chieregato, A., Martinelli, D., Oñate, C., Shah, R.P., Boscaro, A., Dal Negro, E., Picchio, A. (2015). Long term behavior of two component back-fill grout mix used in full face mechanized tunneling. *Geoingegneria Ambientale e Mineraria*, Year LII (1), 57-63.

Pelizza, S., Peila, D., Borio, L., Dal Negro, E., Schulkins, R., Boscaro, A. (2010). Analysis of the performance of two-component back-filling grout in tunnel boring machines. In *Proceedings of the ITA World Tunnel Congress 2010*, May 14-20, Vancouver (CA).

Pelizza, S., Peila, D., Sorge, R., Cignitti, F. (2012). Back-fill grout with two component mix in EPB tunneling to minimize surface settlements: Roma Metro – line C case history. In *Geotechnical Aspects of Underground Construction in Soft Ground*. ISBN 978-0-415-68367-8.

Pellegrini, L. & Perruzza, P. US Society for Mining, Metallurgy, and Exploration (2009). Sao Paulo metro project - control of settlements in variable soil conditions through EPB pressure and bicomponent backfill grout. In *Proceedings of the 19th Conference of Rapid Excavation and Tunneling*, Las Vegas (USA), pp. 1137-1153.

Philleo, R.E. (1955). Comparison of results of three methods for determining Young's modulus of elasticity of concrete, *Journal of the American Concrete Institute*, 51(1), 461-469.

Popovics, J.S. (2003). NDE techniques for concrete and masonry structure. *Progress in Structural Engineering and Materials*, 5, 49-59. https://doi.org/10.1002/pse.146.

Reschke, A. & Noppenberger, C. (2011). Brisbane Airport Link earth pressure balance machine two component tailskin grouting - a new Australian record. In *Proceedings of 14th Australasian Tunnelling Conference 2011: Development of Underground Space*, March 8-10, Auckland (NZ).

Robbins brochure. Tunnel Segment Backfilling with Double Shield TBMs.

Schulkins, R. (2020). Backfill grout. Master lesson of Tunnelling and Tunnel Boring Machines, 2nd level Specializing Master. Politecnico di Torino.

Schulte-Schrepping, C. & Breitenbücher, R. (2019a). Two-component grouts with alkali-activated binders. In *Proceedings of the ITA World Tunnel Congress 2019*, May 3-9, Naples (IT).

Schulte-Schrepping, C. & Breitenbücher, R. (2019b). Development of a test setup for the simulation of the annular gap grouting on a semi technical scale. In *Proceedings of the ITA World Tunnel Congress 2019*, May 3-9, Naples (IT).

Shah, R. (2017). A numerical study on back-filling of the tail void with two-component grout based on laboratory tests. *PhD thesis, Politecnico di Torino*

Shah, R., Lavasan, A.A., Peila, D., Todaro, C., Luciani, A., Schanz, T. (2018). Numerical study on backfilling the tail void using a two-component grout. *Journal of Materials in Civil Engineering*, 30(3), Article number 04018003.

Sturrup, V.R., Vecchio, F.J., Caratin, H. (1984). Pulse Velocity as a Measure of Concrete Compressive Strength. *In-Situ Non-Destructive Testing of Concrete*. American Concrete Institute, Detroit, 82, 201-227.

Thewes, M. & Budach, C. (2009). Grouting of the annular gap in shield tunneling – an important factor for minimisation of settlements and production performance. In *Proceedings of the ITA-AITES World Tunnel Congress 2009*, May 23-28, Budapest (HU).

Thewes, M. (2013). Backfilling grout. In *Proceedings of the Seminar on Mechanized Tunneling 2013*, April 26-27, Sao Paulo (BR).

Todaro, C., Bongiorno, M., Carigi, A., Martinelli, D. (2020a). Short term strength behavior of two component backfilling in shield tunneling: comparison between standard penetrometer test results and UCS. *Geoingegneria Ambientale e Mineraria*, Year LVII (1), 33-40.

Todaro, C., Bongiorno, M., Martinelli, D. (2021). Two component backfilling technology: a comparison study between laboratory and job site testing procedures. In *Proceedings of the AFTES 2020.* Accepted for publication.

Todaro, C., Godio, A., Martinelli, D., Peila, D. (2020). Ultrasonic measurements for assessing the elastic parameters of two-component grout use in full face mechanized tunnelling. *Tunnelling and Underground Space Technology,* 106, 103630.

Todaro, C., Peila, L., Luciani, A., Carigi, A., Martinelli, D., Boscaro, A. (2019). Two component backfilling in shield tunneling: laboratory procedure and results of a test campaign. In *Proceedings of the ITA WTC World Tunnel Congress 2019*, May 3-9, Naples (IT).

UNI 11152. (2005). *Sospensioni acquose per iniezioni a base di leganti idraulici - Caratteristiche e metodi di prova.* Ente nazionale italiano di unificazione.

Ye, G.-L., Hashimoto, T., Shen, S.-L. Zhu, H.-H., Bai, T.-H. (2015). Lessons learnt from unusual ground settlement during Double-O-Tube tunnelling in soft ground. *Tunnelling and Underground Space Technology*, 49, 79-91, ISSN 0886-7798. https://doi.org/10.1016/j.tust.2015.04.008. http://www.sciencedirect.com/science/article/pii/S0886779815000644.

Youn, B. & Breitenbücher, R. (2014). Influencing parameters of the grout mix on the properties of annular gap grouts in mechanized tunneling. *Tunnelling and Underground Space Technology*, 43, 290-299.

Youn, B., Schulte-Schrepping, C., Breitenbücher, R. (2016). Properties and Requirements of Two-Component Grouts in Mechanized Tunneling. In *Proceedings of the ITA WTC World Tunnel Congress 2016*, April 22-28, San Francisco (USA).

Zarei, Y., Uromeihy, A., Reza Nikoodel, M., Fathollahy, M. (2019). A testing procedure for determining ultrasonic wave velocity. *Bollettino di*

Geofisica Teorica ed Applicata, 60(3), 433-442. DOI 10.4430/bgta0272 433.

Zarrin, A., Zare, S., Jalali, S.M.E. (2015). Backfilling grouting with two-component grout - Case study Tehran metro line 7 east-west lot. In *Proceedings of the ITA World Tunnel Congress 2015*, May 22-28, Dubrovnik (HR).